CompTest 2004

Department of Aerospace Engineering

Composites Testing and Model Identification

Book of Abstracts

21st–23rd September 2004
University of Bristol, U.K.

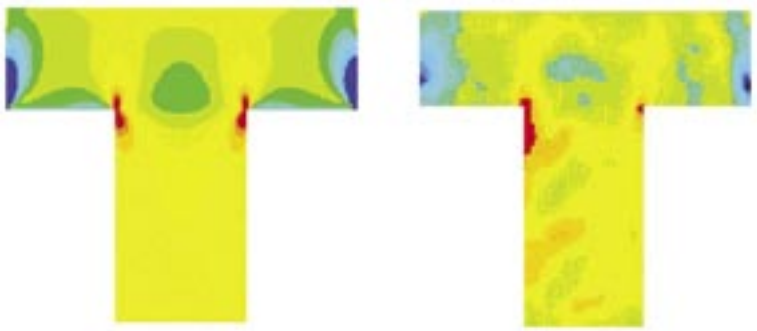

Sponsored by:

AIRBUS

University of BRISTOL

2ND INTERNATIONAL CONFERENCE ON COMPOSITES TESTING AND MODEL IDENTIFICATION

21 - 23 September 2004
University of Bristol, UK

SESSION PROGRAMME

TUESDAY 21 SEPTEMBER

08.30-08.45	**Conference Opening and Welcome to Bristol**	
08.45-10.25	**Session 1 – Structures** Chair: Dr Peter Davies, IFREMER, France	**Page no. 1**
10.25-11.10	**COFFEE + POSTER SESSION 1**	**Page no. 9**
11.10-12.50	**Session 2 - Scaling Effects and Notches** Chair: Prof. Paul Curtis, dstl, UK	**Page no. 29**
12.50-14.00	**LUNCH**	
14.00-15.40	**Session 3 – Testing** Chair: Dr Ivana Partridge, Cranfield University, UK	**Page no. 35**
15.40-16.25	**COFFEE + POSTER SESSION 2**	**Page no. 41**
16.25-18.05	**Session 4 - Fatigue and Durability** Chair: Prof. Olivier Allix, Laboratoire de Mecanique et Technologie, France	**Page no. 59**
18.30-20.00	**Reception at Bristol Industrial Museum**	

WEDNESDAY 22 SEPTEMBER

08.30-10.35	**Session 5 - Full Field Techniques I** Chair: Prof. Fabrice Pierron, ENSAM, France	**Page no. 69**
10.35-11.15	**COFFEE + POSTER SESSION 3**	**Page no. 77**
11.15-12.55	**Session 6 - Full Field Techniques II** Chair:Dr Bill Broughton, National Physics Laboratory, UK	**Page no. 97**
12.55-14.00	**LUNCH**	
14.00-15.40	**Session 7 - Identification of Damage Models** Chair: Dr Kevin O'Brien, U.S. Army Research Laboratory	**Page no. 103**
15.40-16.20	**COFFEE + POSTER SESSION 4**	**Page no. 111**

16.20-18.00 **Session 8 – Fabric Composites** **Page no. 133**
Chair: Prof. Stepan Lomov,
Katholieke Universiteit Leuven, Belgium

19.30-22.30 **Conference Dinner on SS Great Britain**

THURSDAY 23 SEPTEMBER

08.30-10.35 **Session 9 – Novel Methods and Residual Stresses** **Page no. 141**
Chair: Prof. Anoush Poursartip,
University of British Columbia, Canada

10.35-11.15 **COFFEE + POSTER SESSION 5** **Page no. 147**

11.15-12.55 **Session 10 – Fracture** **Page no. 167**
Chair: Dr. Pedro Camanho, DEMEGI, Portugal

12.55-14.00 **LUNCH**

14.00-16.05 **Session 11 - Properties** **Page no. 175**
Chair: Dr Jonas Neumeister,
Royal Institute of Technology, Sweden

COMPOSITES TESTING AND MODEL IDENTIFICATION

21 - 23 September 2004
University of Bristol, UK

FULL PROGRAMME

TUESDAY 21 SEPTEMBER

08.30-08.45 **Conference Opening and Welcome to Bristol**

SESSION 1 – STRUCTURES **PAGE NO. 1**
Chair: Dr Peter Davies, IFREMER, France

08.45-09.10 *Large Scale Composite Testing at AUK (Paper No. 109)*
R Ferguson, Airbus UK

09.10-09.35 *Experimental Measurement and Finite Element Analysis of Load Distribution and Strength in Multi-Bolt Composite Joints with Variable Bolt Hole Clearances (Paper No. 43)*
M A McCarthy, V P Lawlor, W F Stanley, G S Padhi, C T McCarthy
University of Limerick/ University College Dublin, Ireland

09.35-10.00 *Characterisation of the Rotational Stiffness and Strength of Web-Flange Junctions of Pultruded GRP WF-Sections via Web Bending Tests (Paper No. 3)*
G.J. Turvey and Y. Zhang, University of Lancaster, UK

10.00-10.25 *Towards a Standard Qualification Plan (SQP) for Composite Materials (Paper No. 96)*
M R L Gower, G D Sims, National Physical Laboratory, UK

10.25-11.10 Coffee + POSTER SESSION 1 **PAGE NO. 9**

Testing of Glass-Fibre Reinforced Polymer Composites (Paper No. 1)
N K Sookay, C J von Klemperer, V E Verijenko, University of Natal, South Africa

Transverse cracking and stiffness in hygrothermal aged cross-ply laminates (Paper No. 2)
Pr Adda Bedia, A Tounsi, K H Amara, S A Meftah, Universiti de Sid Bel Abbhs, Algeria

Strain Fields in the Picture Frame Test (Paper No. 5)
S V Lomov, T Stoilova, I Verpoest, Katholieke Universiteit Leuven, Belgium

A 3-D Micromechanical Model for Predicting the Elastic Behaviour of Woven Fabrics (Paper No.6)
M V Donadon, J M Hodgkinson, B G Falzon, L Ianucci, Imperial College, UK

Identification of Elastic Properties in Stiffened Composite Shells (Paper No. 7)
R Rikards, H Abramovich, O Ozolinsh, E Skukis, S Ruchevskis, Riga Technical University, Latvia/Institute of Technology, Haifa, Israel

Modelling Damage Development in Off-Axis Plies of Laminated Composites (Paper No. 13)
M Kashtalyan, C Soutis, University of Aberdeen/ University of Sheffield, UK

POSTER SESSION 1 (Cont.)

Evaluation of the Exchange Magnetic Coupling in Nanocomposite Magnetic Materials (Paper No.14)
M-H Phan, H-X Peng, M R Wisnom, S-C Yu, N Chau, University of Bristol, UK/ Chungbuk National University, Korea/National University of Hanoi, Vietnam

Design and Failure of Materials Systems under Multi-Axial Loads (Paper No. 15)
J Cook, C Williamson, QinetiQ, UK

Using 3D Fabric on Light Glider Fuselage (Paper No. 16)
J Juracka, J Splichal, Brno University of Technology, Czech Republic

Prediction of Impact-Induced Fibre Damage in Circular Composites Plates (Paper No. 21)
J Lee, C Soutis, University of Sheffield, UK

Tomography Based Approach for Finite Element Modelling of Particle Reinforced Metal-Matrix Composites (Paper No. 22)
P Keensei, H Biermann, A Borbely, Eotvos Lorand University, Hungary/Technische Universitat Freiburg, Germany

Modelling of a Steel Reinforced Thermoplastic Pipe (Paper No.23)
M P Kruijer, L Warnet, R Akkerman, University of Twente, Netherlands

The Effects of Stiffness Variability on the Observed Flexural Performance of a Composite Box-Section Beam under Three Point Bending - a Statistical Approach (Paper No. 25)
N Papadakis, N Reynolds, University of Warwick, UK

SESSION 2 - SCALING EFFECTS AND NOTCHES **PAGE NO. 29**
Chair: Prof. Paul Curtis, dstl, UK

11.10-11.35 *Size Effects in Unidirectional and Quasi-isotropic Composites Loaded in Tension (Paper No. 65)*
B Khan, K Potter, S R Hallett, M R Wisnom, University of Bristol, UK

11.35-12.00 *Strength Scaling Mechanics of Polymer Composites (Paper No. 37)*
T K Jacobsen, B F Sorensen, LM Glasfiber, Riso National Laboratory, Denmark

12.00-12.25 *Tensile Scaling Effects in Notched Composites (Paper No. 19)*
B Green, M R Wisnom, S R Hallett, University of Bristol, UK

12.25-12.50 *Mesh Independent Modelling and Moire Interferometric Examination of the Accumulation of Damage in Composites with Open-Holes (Paper No. 61)*
D Mollenhauer, E Iarve, R Kim, US AFRL/University of Dayton Research Institute, USA

12.50-14.00 **LUNCH**

SESSION 3 – TESTING **PAGE NO. 35**
Chair: Dr Ivana Partridge, Cranfield University, UK

14.00-14.50 **Invited Lecture 1**
Testing of Marine Composites: From Materials to Structures
Dr Peter Davies, IFREMER, France

14.50-15.15 *A Tensile Setup for the IDNS Composite Interlaminar Shear Test (Paper No. 73)*
K Petterson, J M Neumeister, Royal Institute of Technology, Sweden

15.15-15.40 *Influence of a Near Free Edge on the Impact of Thick CFRP Panels (Paper No. 30)*
C Breen, F Guild, M Pavier, University of Bristol, UK

15.40-16.25 Coffee + POSTER SESSION 2 **PAGE NO. 41**

Probabilistic Method to Define a Development Test Campaign in the Engineering Process (Paper No. 26)
C Ramos Gutiérrez, School of Aeronautical Engineering, Madrid, Spain

An Image Analysis Approach for the Structural Characterisation of Pyrocarbons (Paper No. 29)
J P da Costa, C Germain, P Baylou, M Cataldi, ENSEIRB, ENITAB, France

Strength Evaluations for Stitched CFRP Laminates (Paper No. 32)
Y Iawahori, S Horikawa, M Yamamoto, T Ishikawa, H Fukuda, Japan Aerospace Exploration Agency/ Tokyo University of Science, Japan

A Screening Method for Investigating Fibre Composite Residual Strength after Impact (Paper No. 33)
A Jarneteg, CSM Materielteknik AB, Sweden

Transverse Evolution of the Residual Stresses in Notched Epoxy Cylinders using the OLCR Technique and Embedded FBG Sensors (Paper No. 38)
F Colpo, L Humbert, J Botsis, Swiss Federal Institute of Technology

Computational Modelling of Fatigue-Driven Delamination (Paper No.39)
U Galvanetto, P Robinson, Imperial College, UK

The Video Gauge - A New Tool for Simple and Accurate Measurement of Complex Composite Properties (Paper No. 41)
K Potter, C Setchell, University of Bristol and Imetrum Ltd, UK

Modelling of Effective Dielectric Properties of Composites using Expansion into Fourier Series and Finite Element Method (Paper No. 44)
F Moravec, I Krakovsky, University of West Bohemia/Charles University, Czech Republic

The Effect of Ply Orientation on the Peak and Delamination Threshold Loads of CFRP Composite Plates (Paper No. 45)
O S David-West, D H Nash, W M Banks, University of Strathclyde, UK

POSTER SESSION 2 (Cont.)

Effect of Thermal Cycling on Stiffness and Strength Degradation of Polymeric Composite Materials (Paper No. 46)
G C Papanicolaou, T C Theodosiou, T V Kosmidou, University of Patras, Greece

Fatigue Damage Analysis of a Steel-Composite Hybrid Pin (Paper No. 47)
A Avanzini, G Donzella, A Mazzu, V Zacche, University of Brescia, Italy

Bending Characteristics of Carbon Fabric-Polymeric/Metallic Foam Sandwich Structures (Paper No. 62)
Seong Sik Cheon, Tae Seong Jang, Seung Hwan Chang, Kongju National University/Satellite Technology Research Center/Chung-Ang University, Korea

Synthesis of Al2O3/Al Co-continuous Composite by Reactive Melt Infiltration (Paper No. 116)
C.M.L. Wu and G.W. Han, City University of Hong Kong

SESSION 4 - FATIGUE AND DURABILITY **PAGE NO. 59**
Chair: Prof. Olivier Allix, Laboratoire de Mecanique et Technologie, Cachan, France

16.25-16.50 *Methods of Monitoring Fatigue Damage under Variable Amplitude Loading in CFRP Composites (Paper No. 20)*
M Bourchak, I R Farrow, I P Bond, University of Bristol, UK

16.50-17.15 *On the Relation between Crack Densities, Stiffness Degradation, and Surface Temperature Distribution of Tensile Fatigue Loaded Glass-Fibre Non-Crimp-Fabric Reinforced Epoxy (Paper No. 70)*
A Gagel, D Lange, K Schulte, Technical University Hamburg/Harburg, Germany

17.15-17.40 *Off-Axis Fatigue Behaviour of Plain Woven Carbon/Epoxy Laminates at Room and High Temperatures (Paper No. 77)*
M Kawai, T Taniguchi, University of Tsukuba, Japan

17.40-18.05 *Durability of Glass Fibre Reinforced Composites Experimental Methods and Results (Paper No. 40)*
H Cuyperes, J Wastiels, E de Bolster, G Moselmans, M Alshaaer
Vrije University of Brussels, Belgium

18.30-20.00 **Reception at Bristol Industrial Museum**

WEDNESDAY 22 SEPTEMBER

SESSION 5 - FULL FIELD TECHNIQUES I **PAGE NO. 69**
Chair: Prof. Fabrice Pierron, ENSAM, France

08.30-09. 20 **Invited Lecture 2**
Full-field Optical Methods for Mechanical Engineering: Essential Concepts to find One's Way
Prof Yves Surrel, CNAM, Paris

09.20-09.45 *Experimental Investigation of Composite Patches with a Full-Field Measurement Method (Paper No. 11)*
J-D Mathias, X Balandraud, M Grediac,
French Institute for Advanced Mechanics/LERMES, Blaise Pascal University, France

09.45-10.10 *Quantitative Thermoelastic Stress Analysis of Laminated Composite Components (Paper No. 90)*
J S Earl, J M Dulieu-Barton, University of Southampton, UK

10.10-10.35 *Use of Full Field Strain Measurements to model the behaviour of CFRP woven ply laminates (Paper No. 10)*
C Bordreuil, C Hochard, N Lahellec, F Mazerolle, LMA/CNRS, France

10.35-11.15 Coffee + POSTER SESSION 3 **PAGE NO. 77**

A Continuum Damage Model for the Simulation of Delamination under Variable Mode Ratio in Composite Materials (Paper No. 48)
A Turon, P P Camanho, J Costa, C G Davila, Universitat de Girona, Spain/ Universidade do Porto, Portugal/NASA Langley, USA

Analysing the Flexural Strength Properties of Unidirectional Carbon/Epoxy Composites (Paper No.50)
Z Racz, Z L Simon, L M Vas, Budapest University of Technology and Economics, Hungary

Intralaminar Fracture in CFRP Laminates (Paper No.51)
N Vrellos, S L Ogin, P A Smith, N Balthi, F J Guild, B W Drinkwater, University of Surrey, University of Bristol, UK

Deformation and Fracture of Unidirectional GFR Composites at High Strain Rate Tension (Paper No. 52)
G Makarov, W Wang, R A Shenoi, University of Southampton, UK

A Digital Image Analysis for Determining Mode I and Mode II Stress Intensity Factors (Paper No.55)
S M'Guil, N Bahlouli, C Husson, S Ahzi, Universite Louis Pasteur/CNRS, France

Square Grid Analysis for Intraply Shear in Thermoformed Thermoplastic Composites (Paper No. 57)
G F Nino, O K Bergsma, H E N Bersee, TU Delft, Netherlands

A Mixed Numerical-Experimental Identification Method for Evaluating the Constitutive Parameters of Composite Laminated Shells (Paper No. 58)
J Cugnoni, T Gmur, A Schorderet, Swiss Federal Institute of Technology

POSTER SESSION 3 (Cont.)

Flexure Tests for Determining Tensile and Compressive Modulus (Paper No. 59)
F Mujika, I Mondragon, EUP, Spain

Comparison of Moire Inteferometry and Image Correlation Deformation Measurement Techniques (Paper No. 60)
D Mollenhauer, J Tyson, US AFRL/Trillion Quality Systems, USA

Development of Design System for FRP Gears for Power Transmissions (Paper No.64)
T Hirogaki, E Aoyama, T Katayama, K Sugimura, Y Yagura, Doshisha University/ Ishida Co Ltd, Japan

Impact Damage and CAI Strength of MR50K/PET15 Carbon/Tough-Polyimide Composite Material (Paper No.69)
H Katoh, T Shimokawa, A Ueda, Y Hamaguchi, Japan Exploration Agency/Tokyo Metropolitan Institute of Technology

The Application of the Interphase Model for the Description of the Filled Composite Properties with Nanoparticles. Identification of the Parameters of the Model (Paper No.71)
S A Lurie, N P Tuchkova, V I Zubov, Dorodicyn Computing Centre of the Russian Academy of Science, Russia

Thermal Fatigue Behavior of SiCp/ Al Composite Synthesized by Metal Infiltration (Paper No. 117)
C.M.L. Wu and G.W. Han, City University of Hong Kong

SESSION 6 - FULL FIELD TECHNIQUES II **PAGE NO. 97**
Chair: Dr Bill Broughton, National Physics Laboratory, UK

11.15-11.40 *Non-homogenous CFRE Strain Field Monitoring with the Electronic Speckle Pattern Interferometry Technique (Paper No. 49)*
J-P Bouquet, A H Cardon, SABCA/Vrije Universiteit Brussel, Belgium

11.40-12.05 *Use of Phase-Stepping Photoelasticity to Measure Interfacial Shear Stress in Single Fibre Model Composites (Paper No. 56)*
F M Zhao, S A Simon, E A Patterson, R J Young, F R Jones
University of Sheffield/ UMIST, UK

12.05-12.30 *Identification of the Through-thickness Elastic Constants of Thick Laminated Tubes using the Virtual Fields Method (Paper No. 89)*
R Moulart, S Avril, F Pierron, LMPF-ENSAM, France

12.30-12.55 *Application of the Open Hole Tensile Test to the Identification of the In-Plane Characteristics of Orthotropic Plates (Paper No. 115)*
J Molimard, R Le Riche, A Vautrin,
SMS/MeM, GDR CNRS & URA CNRS, France

12.55-14.00 **LUNCH**

SESSION 7 - IDENTIFICATION OF DAMAGE MODELS **PAGE NO. 103**
Chair: Dr. Kevin O'Brien, U.S. Army Research Laboratory

14.00-14.25 *Experimental Identification of a Damage Model for Composites using the Grid Technique Coupled to the Virtual Fields Method (Paper No. 88)*
H Chalal, F Meraghni, S Avril, F Pierron, ENSAM, France

14.25-14.50 *Identification of a Delay-Damaged Mesomodel for the Localization and Rupture of Composites: Feasibility and Identification Strategy (Paper No. 104)*
P Feissel, O Allix, P Thevenet
Laboratoire de Mecanique et Technologie, France

14.50-15.15 *Extracting Matrix Creep Parameters for Modelling the Consolidation of Matrix-Coated Fibre Composites (Paper No. 12)*
H-X Peng, M R Wisnom, F P E Dunne, P S Grant, B Cantor
University of Bristol /University of Oxford /University of York, UK

15.15-15.40 *Identification of Parameters in Nonlinear Viscoelastic,Nonlinear Viscoplastic Material Model (Paper No. 112)*
J Varna, L-O Nordin, Lulea University of Technology, Sweden

15.40-16.20 Coffee + POSTER SESSION 4 **PAGE NO. 111**

Microscopic Observation of Tow Deformation for Carbon Fabric-PVC Foam Sandwich Structures during Forming (Paper No. 63)
Seung Hwan Chang, Chung-Ang University, Korea

Experimental Determination of Composite In-Plane Shear Properties (Paper No. 72)
L N Melin, J M Neumeister, Royal Institute of Technology, Sweden

An Investigation of the Pull-Out and Shear-Out Processes in Z-Pin Reinforced Laminates (Paper No. 74)
M Fert, P Robinson, D Hitchings, Imperial College, UK

Off-Axis Creep Rupture Behaviour of Unidirectional CFRP Laminates at Elevated Temperature (Paper No. 76)
M Kawai, Y Masuko, T Sagawa, University of Tsukuba, Japan

Experimental Analysis of RC Beams in Flexure Reinforced with CFRP Sheets (Paper No. 79)
Z J Wu, M Xylouri, P Nedwell, UMIST, UK

The Behaviour of Uncured Prepreg (Paper No. 82)
C Langer, K D Potter, University of Bristol, UK

Optimisation of the Mechanical Test Procedure for Testing of Unidirectional Carbon Fibre/Peek Specimens (Paper No. 83)
J Kilroy, P McDonnell, C O'Bradaigh, Composites Testing Laboratory, Ireland

Modelling the Thermoelastic Properties of Short Fibre Composites with Anisotropic Phases (Paper No. 17)
P Hine, C D Price, A M Cuhna, I M Ward, University of Leeds, UK/ Universidade Do Minho, Portugal

Composite Deformation Controlled with a Source of Heat (Paper No. 84)
H Drobez, G L Hostis, F Laurent, B Durand, G Meyer, CETIM/CRNS Mulhouse, France

POSTER SESSION 4 (Cont.)

Multiscale Modelling of the Strain Rate Dependent Damage in Sheet Moulding Compound Composites (Paper No. 85)
F Meraghni, Z Jendli, J Fitoussi, D Baptiste, ENSAM Chalons en Champagne/ENSAM Paris, France

Neural Network Metamodelling for Optimisation of Negative Poisson's Ratio Chiral Honeycomb (Paper No. 86)
T L Lew, F Scarpa, K Worden, University of Sheffield, UK

Damage Extension and Failure Behaviour of CFRP Specimens in Open Hole Compression Tests and Analytical Simulation (Paper No. 91)
T Kato, T Ishikawa, Y Hamaguchi, N Shikata, G Ben, Japan Aerospace Exploration Agency/ Nihon University, Japan

Modelling of Left over Strength in Drilling of Composite Laminates (Paper No. 92)
S K Malhotra, R Ktishnamurthy, J Ramkumar, IIT Madra/IIT Kanpur, India

SESSION 8 – FABRIC COMPOSITES **PAGE NO. 133**
Chair: Professor Stepan Lomov, Katholieke Universiteit Leuven, Belgium

16.20-16.45 *3D Finite Element Damage Analysis of a Twill-weave Lamina Subjected to In-Plane Shear (Paper No. 81)*
G Baruffaldi, E Riva, G Nicoletto, Universita di Parma, Italy

16.45-17.10 *Failure and Impact Modelling of Braided Fabric Reinforced Composites (Paper No. 27)*
M Fouinneteau, A K Pickett, Cranfield University, UK

17.10-17.35 *Progressive Damage Characterization of Stitched, Bi-Axial, Multi-ply Carbon Fabric Composites (Paper No. 78)*
M Vettori, T Truong Chi, S V Lomov, I Verpoest
University of Parma, Italy/ Katholieke Universiteit Leuven, Belgium

17.35-18.00 *Measurement of Meso-scale Deformations for Modelling Textile Composites (Paper No. 75)*
P Potluri, D A Perez Ciurezu, UMIST, UK

19.30-22.30 **Conference Dinner on SS Great Britain**

THURSDAY 23 SEPTEMBER

SESSION 9 – NOVEL METHODS AND RESIDUAL STRESSES **PAGE NO. 141**
Chair: Prof. Anoush Poursartip, University of British Columbia, Canada

08.30-09.20 **Invited Lecture 3**
Novel Methods for Testing and Modelling Composite Materials and Laminates
Prof CT Sun, Purdue University, USA

09.20-09.45 *Characterization of Manufacturing Residual Stresses in Wound Composite Tubes (Paper No. 95)*
P Casari, F Jacquemin, P Davies, GeM, Nantes, France

09.45-10.10 *Tests to Measure the Material Properties Relevant to the Modelling of Process Induced Deformations of Composite Parts (Paper No. 42)*
N Ersoy, T Gartska, K Potter, M R Wisnom, University of Bristol, UK

10.10-10.35 *Residual Strain Development in Laminated Thermoplastic Composites Measured using Fibre Bragg Grating Sensors (Paper No. 53)*
L Sorensen, T Gmur, J Botsis, Swiss Federal Institute of Technology

10.35-11.15 Coffee + POSTER SESSION 5 **PAGE NO. 147**

Damage Monitoring in Woven Composites Laminates Using the DC Electrical Method (Paper No. 80)
E Riva, M Vettori, G Nicoletto, Universita di Parma, Italy

Industrialised Shearography Testing on Aircraft Composites in Combination with 3D Imaging and Defect Location (Paper No. 98)
J Collrep, R Berger, Interferometry, Steinbichler Optotechnik GmbH

Mechanical Response of a Fiber Bragg Grating Sensor in a Non-uniform Stress Field (Paper No. 99)
P Casari, X Chapeleau, D Leduc, GeM, Nantes, France

Effect of Local Constraint on Measured Bearing Stress in Carbon/Epoxy Laminate (Paper No. 100)
R Ferguson, Airbus UK

Experimental Investigation into the use of Penetrant Enhanced X-ray Techniques for the Evaluation of Fatigue Damage Around an Open-hole in 4mm Thick Carbon Fibre Composite Panels (Paper No. 101)
N J Rooney, T M Young, University of Limerick, Ireland

Identification of the Elastic Constants of Composite Materials using Deflectometry (Paper No. 102)
S Avril, M Grédiac, F Pierron, Y Surrel, E Toussaint, LMPF/LERMES/CNRS-LM3, France

Identification of Elastic Properties of a Ceramic-based Joint using Kinematic Fields determined by Digital Image Correlation (Paper No. 103)
M Puyo-Pain, F Hild, J Lamon, Universite Bordeaux/Universite Paris, France

Non-Destructive Evaluation of Prosthetic Carbon Fiber Feet (Paper No. 106)
R Unnporsson, University of Iceland

POSTER SESSION 5 (Cont.)

Multi-instrumented Technological Demonstrator: a Multiscale Study of Composite Structures (Paper No. 107)
M Mulle, F Collombet, B Trarieux, J-N Périé, Y-H Grunevald, LGMT/DDL Consultants, FRANCE

Generation of Design Allowables for Composite Materials at Airbus UK (Paper No. 110)
S J Hallett, Airbus UK

Strain Monitoring of Smart Concrete Cylinders with Overwrap Composite Materials using Fibre Optic Sensors (Paper No. 111)
J S Leng, D Winter, R A Barnes, G C Mays, G F Fernando, Cranfield University, Shrivenham, UK

Investigation of Parameters Dictating Damage Characteristics in Composite Honeycomb Sandwich Panels (Paper No. 113)
G Zhou, M Hill, N Hookham, Loughborough University, UK

Identification of Residual Strain and Stress in Cross-ply Laminate by using Embedded Fibre Bragg Sensor (Paper No. 114)
S Vacher, J Molimard, H Gagnaire, A Vautrin, Université Jean Monnet, France

SESSION 10 – FRACTURE **PAGE NO. 167**
Chair: Dr. Pedro Camanho, DEMEGI, Portugal

11.15-11.40 *Measurement of Fracture Energy for Kink-Band Growth in Sandwich Specimens (Paper No. 24)*
W C Jackson, J G Ratcliffe, US Army Research Laboratory

11.40-12.05 *An Experimental Study of the Fracture Behaviour of Stitched RFI Composites – Evaluation of the Damage Process Zone to Calibrate a Strain-softening Model (Paper No. 94)*
J Mitchell, A Poursartip, University of British Columbia, Vancouver, Canada

12.05-12.30 *Modelling Delamination in an Explicit FE Code using 3D Decohesion Elements (Paper No. 93)*
S Pinho, L Iannucci, P Robinson, Imperial College, London, UK

12.30-12.55 *Development and Evaluation of Self Repairing Concepts for Composite Materials (Paper No. 9)*
J Pang, I P Bond, University of Bristol, UK

12.55-14.00 **LUNCH**

SESSION 11 - PROPERTIES **PAGE NO. 175**
Chair: Dr Jonas Neumeister, Royal Institute of Technology, Sweden

14.00-14.25 *Mechanical Properties Balance in Novel Z-pinned Sandwich Panels (Paper No. 67)*
A I Marasco, D D R Cartié, I K Partridge and A Rezai, Cranfield University/ BAE SYSTEMS ATC Sowerby, Bristol UK

14.25-14.50 *Failure Criteria for Prediction of Transverse Matrix Cracking in Composites (Paper No. 4)*
P P Camanho, C G Davila, DEMEGI, Portugal

14.50-15.15 *Analytical Models for Assessing Environmental Degradation of Unidirectional and Cross-Ply Laminates (Paper No. 66)*
W R Broughton, M J Lodeiro, National Physical Laboratory, UK

15.15-15.40 *Fibre Orientation Measurements in Composite Materials (Paper No. 28)*
R Blanc, J P da Costa, Ch Germain, P Baylou, M Cataldi, ENSEIRB, ENITAB, France

15.40-16.05 *Modelling the Thermoelastic Properties of Short Fibre Composites with Anisotropic Phases (Paper No. 17)*
P Hine, C D Price, A M Cuhna, I M Ward, University of Leeds, UK/ Universidade Do Minho, Portugal

16.05 **Conference Closes**

SESSION 1 – STRUCTURES

Chair: Dr Peter Davies
IFREMER, France

Tuesday 21 September
08.45-10.25

LARGE SCALE COMPOSITE TESTING AT AUK

R Ferguson
Composite Research, Airbus UK, Building 07C, Golf Course Lane, Filton, Bristol BS99 7AR

INTRODUCTION

Over the last 25 years, the use of composite materials on Airbus aircraft has been progressively increased. Early uses such as fairings, spoilers and rudders for the A300/A310 have been steadily expanded and in-service applications for the A320 family, A330 and A340 now include primary structure such as the fin, horizontal tailplane, rear pressure bulkhead and keel beams. At its entry into service in 2006, the A380-800 will include a carbon composite rear pressure bulkhead, tail cone, fin, horizontal tailplane, ribs and centre wing box.

Demonstration of structural performance is essential for aircraft certification by the Airworthiness Authorities. Full scale testing of aircraft components therefore forms a key part of certification activities. As composites have become more significant and more widely used in Airbus aircraft, so the scale and complexity of research and certification tests has increased. This paper describes large scale composite component test activities at Airbus UK, and examines past, present and future test activities.

TESTING OF COMPOSITE STRUCTURAL COMPONENTS AT AIRBUS UK

Airbus UK's primary area of technical expertise is in the design, manufacture and assembly of wings for the Airbus family of aircraft. Research into the use of composite materials for wingbox structure started in 1995 with the initiation of the Composite Wing Project, the precursor to the current Composites Research team. Recent work has produced several large scale test articles that are the subject of this paper.

HLIE (High Load Input Element) is a full scale partial wingbox for evaluating structural response to cantilever bending and engine pylon loading. It has been subjected to a number of tests including static loading, vibration testing, pressurisation and fatigue cycling.

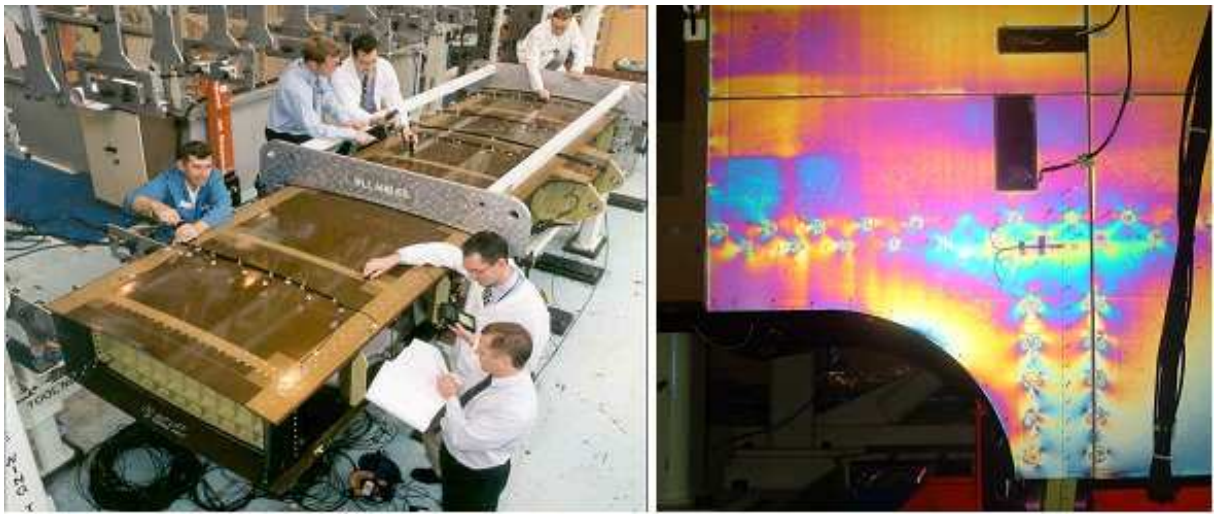

Figure 1: HLIE under construction (left); photoelastic image of skin at pylon area under load (right)

In the TANGO project, the lateral wingbox assembly is complete and it is being equipped and instrumented ready for testing to commence in June 2004.

Figure 2: TANGO wingbox in assembly

In addition to the full scale outer wingbox test article, the TANGO project has provided several significant supporting test articles including spar web shear, spar flange joint and spar mid span interface tests.

Fig 3: TANGO spar web shear test - main test (left); photoelastic under load (top right); failure (bottom right)

Other supporting research projects include BOJCAS (complex full-scale bolted joint arrays) and composite lower cover.

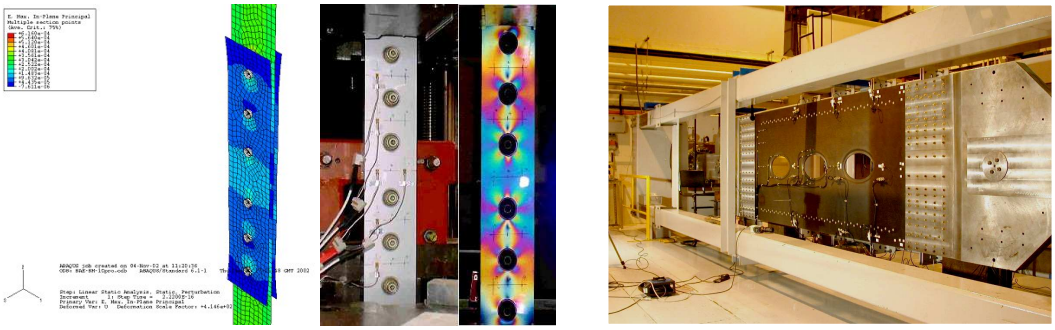

Figure 4: BOJCAS FEA model, test and photoelastic response (left); lower cover tension test (right)

EXPERIMENTAL MEASUREMENT AND FINITE ELEMENT ANALYSIS OF LOAD DISTRIBUTION AND STRENGTH IN MULTI-BOLT COMPOSITE JOINTS WITH VARIABLE BOLT HOLE CLEARANCES

M.A. McCarthy[a]*, V.P. Lawlora, W.F. Stanley[a], G.S. Padhi[a], C.T. McCarthy[b]
[a]Composites Research Centre, Dept. Mechanical and Aeronautical Engineering,
University of Limerick, Ireland
* Corresponding Author, Fax: +353-61-202944, email: michael.mccarthy@ul.ie
[b]Materials Ireland, Department of Mechanical Engineering, University College Dublin, Dublin 4, Ireland

The analysis of multi-fastener composite joints is typically done in two steps: firstly a determination of oad distribution between fasteners; then a more detailed analysis of the bearing-bypass loads at the most critical location to ensure a safety margin for all modes of failure. Load distribution analyses are typically done with quite simple models, e.g. spring models or two-dimensional finite element models. These models generally assume idealised conditions such as neat-fit bolt-hole clearances and finger-tight torque conditions, and very little has been published regarding the effects of variations from these idealised conditions.

This paper presents a study of the effects of variable bolt-hole clearance in multi-bolt composite joints on load distribution and quasi-static strength. The effects of clearance in multi-bolt joints were studied previously by Fan and Qiu [1] in a purely analytical study. They studied a four-fastener, single-shear joint made of carbon-fibre laminates. They found quite significant effects. For example, when the inner two bolts had a 60 μm clearance, with the outer two bolts being neat-fit, the inner bolts together took only about 25% of the load. However no experimental verification was performed.

The present study involved single-shear and double-shear, three-bolt specimens, with six different clearance conditions, as shown in Table 1. In the first four cases, the clearance was varied in Hole 1 only from neat-fit up to a maximum of 240 μm - with neat-fit clearances in the other two holes. In the remaining two cases, the clearance varied in the middle hole as well.

For the single-shear specimens, load distribution was measured using specially manufactured instrumented bolts, while for the double-shear joints strain gauges across the width of the specimen were used, as shown in Fig. 1. The advantages and disadvantages of both methods will be discussed in the presentation. The laminates were made from carbon-fibre/epoxy (HTA/6376) with a balanced, symmetric, quasi-isotropic stacking sequence. The bolts used were aerospace grade fasteners of a protruding head configuration, made from a Titanium alloy, with nominal diameter 8 mm, to an f7 ISO tolerance.

The variable bolt-hole clearances were obtained by using (nominally) constant diameter bolts and variable hole diameters. The tooling used for drilling the holes was manufactured specially for the project by an aerospace supplier. Four different sized reamers used to finish the holes were manufactured to a tight (h6) tolerance. Several precision jigs had to be designed and manufactured for accurate positioning and drilling of the holes, and assembly of the joints; these will be described in the presentation. The 160 um clearance in Table 1 represents the upper range of clearances found in aerospace structures according to Di Nicola and Fantle of United Technologies-Sikorsky Aircraft [2]. The 240 μm clearance was studied to examine an out of tolerance situation.

Results

Both load measurement techniques worked well, and results were verified with three-dimensional finite element analyses that will be described in the presentation. The strain gauge method is considerably cheaper and consequently tests can be performed to failure, which is not economically feasible with the instrumented bolts. The strain gauge method is also simpler to use, but it cannot easily be applied to single-shear joints. The calibration process for the instrumented bolts was quite lengthy and will be described in the presentation. Figure 2 illustrates some results from the double-lap joints. In the "C1_C1_C1" case (all holes neat fit), for the tested configuration the highest loads are taken by the outer bolts. However, on introducing clearance into the first two holes ("C3_C3_C1" case), the entire load is initially taken by Bolt 3. As load increases, the other bolts pick up load, but most of the load is still taken by Bolt 3. Another advantage of the strain gauge method illustrated in Fig. 2 is that the results pattern is clearly interrupted when the first significant failure event occurs in the joint (bearing failure at one or more holes). From this it can be seen that clearance had a highly significant effect on this first failure event (occurred at a joint load of 37 kN instead of 50 kN). However, looking at the ultimate load we can see that clearance had little effect (unchanged at about 70 kN). The main effects of clearance were thus found to be on load distribution and initial joint failure.

Acknowledgements

This work was partially funded by "BOJCAS - Bolted Joints in Composite Aircraft Structures" which is a RTD project partially funded by the European Union under the European Commission GROWTH programme. Key Action: New Perspectives in Aeronautics, Contract No. G4RD-CT99-00036.

Table 1 Nominal Joint Clearances

Case Code	Nominal Clearance (μm) Hole 1	Hole 2	Hole 3
C1_C1_C1	0	0	0
C2_C1_C1	80	0	0
C3_C1_C1	160	0	0
C4_C1_C1	240	0	0
C1_C3_C1	0	160	0
C3_C3_C1	160	160	0

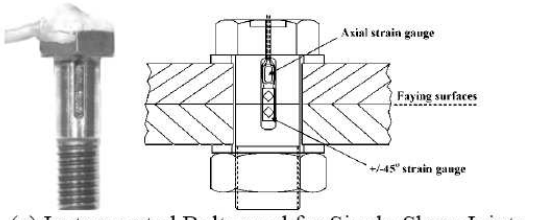

(a) Instrumented Bolts used for Single-Shear Joints

(b) Strain Gauges used for Double-Shear Joints

Figure 1 Load Distribution Measurement

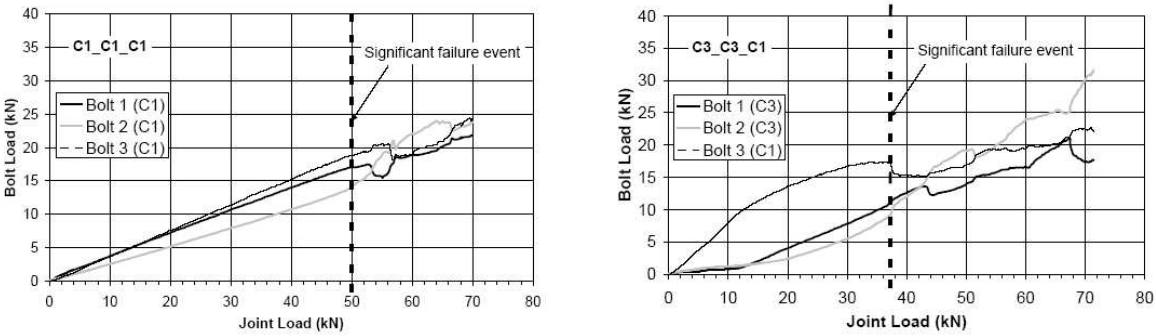

Figure 2 Load Distribution Results from Strain Gauges on Double-Lap Joints

References

1. Fan WX, Qiu CT. Load Distribution of Multi-Fastener Laminated Composite Joints. International Journal of Solids and Structures 1993; 30(21): 3013-3023.
2. DiNicola AJ, Fantle SL. Bearing strength of clearance fit fastener holes in toughened graphite/epoxy laminates. Composite Materials: Testing and Design Vol. 11, ASTM STP 1206, pp. 220-237, 1993.

CHARACTERISATION OF THE ROTATIONAL STIFFNESS AND STRENGTH OF WEB-FLANGE JUNCTIONS OF PULTRUDED GRP WF-SECTIONS VIA WEB BENDING TESTS

G.J. Turvey* and Y. Zhang
Engineering Department, Lancaster University, Bailrigg, Lancaster, LA1 4YR, UK
* Corresponding author's contact details:-
Tel.: +44 (0) 1524 593088; Fax:+44 (0) 1524 381707; Email: g.turvey@lancaster.ac.uk

During the course of the past decade there has been a considerable research effort directed towards the development of knowledge and understanding of the buckling response of pultruded GRP (Glass Reinforced Plastic) beams and columns. This research effort has been in response to the increasing use of fibre-reinforced polymeric composite materials in infrastructure.

Buckling response is of particular interest, because the strength to stiffness ratios of GRP composites are much higher than those of conventional structural materials such as steel and aluminium, and because buckling is one of the more common modes in which these structural elements become unserviceable. It is, perhaps, for this reason too that much less research has been carried out on the ultimate failure response of pultruded GRP beams and columns. To date only a handful of studies [1 – 3], which were partly or solely concerned with beam failure, have been reported. It appears too that research on column failure is scant [4 – 6]. From the limited information that is available, it is clear that GRP beams and columns fail in a brittle manner. However, the collapse mechanisms are not yet fully understood, but often appear to involve failure of the web-flange junction(s). Moreover, the few attempts to model the collapse behaviour of pultruded GRP beams have assumed that the failure strengths of the web-flange junctions of pultruded GRP profiles are the same as those obtained from tests on coupons cut out of web and/or flange material (see [2 &3]).

It is the authors' view that such an assumption is likely to be unconservative, because web and flange coupons will have a more uniform fibre architecture. The architecture of the web-flange junction is different in a number of respects. Firstly, there is a triangular shaped *core* of rovings at the centre of the junction. Secondly, the curvature of the fibre architecture is both zero and finite within the junction region, whereas the curvature of the fibre architecture in the coupon is zero. And thirdly, there is more evidence of wrinkling of the CFM (Continuous Filament Mat) in web-flange junctions than in flat coupons. These differences constitute the principal reasons why it is important to characterise the strengths of web-flange junctions of pultruded GRP profiles. Only through the acquisition of such strength data will it be feasible to develop accurate and reliable numerical models for predicting the failure of pultruded GRP beams and columns. These models are required to underpin future developments of limit state design codes such as EUROCOMP [7], which will grow in importance as the use of structural pultrusions in infrastructure increases.

About two years ago the authors recognised the need to embark on a programme of research to try to characterise the stiffness and strength of web-flange junctions subjected to a number of basic types of load. Their first research investigation was to quantify the tensile strengths of the web-flange junctions of two sizes of pultruded GRP WF (Wide Flange) profile. The results of this study were reported recently [8]. This was followed by a second study [9], which was concerned with quantifying the shear strengths of the web-flange junctions of the same two sizes of WF profile.

The present study represents an extension of the earlier work reported in [8] and [9] and is concerned with quantifying the rotational stiffness and strength of the web-flange junction of the larger WF profile used in the previous two studies. A test rig has been developed for testing the cross-section of the WF profile as a beam in three point bending with clamped or simply supported flanges. Details of the test rig are presented. The instrumentation of the WF test specimens and the test procedure are also described. A simple analytical model, based on a semi-rigidly supported beam with a point load applied at mid-span is introduced. The model is used to analyse the data obtained from 12 tests on cross-section specimens of a 203 x 203 x 9.5mm WF profile and to derive the rotational stiffnesses and strengths of their web-flange junctions and the transverse elastic moduli of their webs. The junction strengths are shown to be much lower than the tensile and bending strength values given in the manufacturer's design manual [10] for the same pultruded GRP profile. In contrast, the transverse moduli values are significantly higher than the minimum values given in [10].

References

1. Mottram, J.T., 'Structural properties of a pultruded E-glass fibre-reinforced polymeric I-beam', Proceedings of the 6^{th} *International Conference on Composite Structures*, Elsevier Applied Science, 1991, 1-28.

2. Bank, L.C., Nadipelli, M. and Gentry, T.R., 'Local buckling and failure of pultruded fiber-reinforced plastic beams', *Journal of Engineering Materials Technology*, **116** (2) 1994, 233-237.
3. Bank, L. and Yin, J., 'Analysis of progressive failure of the web-flange junction in post-buckled pultruded I-beams', *Journal of Composites for Construction*, **3** (4) 1999, 177-184.
4. Pecce, M, Lazzaro, F. and Cosenza, E., 'Local buckling of FRP profiles: experimental results and numerical analyses'. In *ECCM-8 (European Conference on Composite Materials): Science, Technologies and Applications*, Crivelli Visconti I. (ed.), Woodhead Publishing Ltd, Cambridge, 1998, **II**, 331-338.
5. Stubbs, D., *Buckling tests on pultruded GRP short columns in axial compression*, Final Year Project Report, Engineering Department, Lancaster University, 1998, pp.159.
6. Yates, R., *Buckling Tests on Pultruded HF Short Columns in Axial Compression*, Final Year Project Report, Engineering Department, Lancaster University, 1999, pp.94.
7. Clarke, J.L. (ed.), *Structural Design of Polymer Composites – EUROCOMP Design Code and Handbook,* E. & F.N. Spon, London, 1996.
8. Turvey, G.J. and Zhang, Y., 'Tearing failure of web-flange junctions in pultruded GRP profiles', Proceedings of the *DFC-7 Conference on Deformation and Fracture of Composites*, 22nd – 24th April 2003, University of Sheffield, Sheffield, UK.
9. Turvey, G.J. and Zhang, Y., 'Shear failure strength of web-flange junctions in pultruded GRP profiles', Proceedings of the *2nd International Conference on Advanced Composites in Construction (ACIC 2004)*, 20th - 22nd April 2004, University of Surrey, Guildford (to appear).
10. Anon., *EXTREN Fiberglass Structural Shapes Design Manual*, Strongwell, Bristol, Virginia, 1989.

TOWARDS A STANDARD QUALIFICATION PLAN (SQP) FOR COMPOSITE MATERIALS

Michael R L Gower and Graham D Sims
NPL Materials Centre, National Physical Laboratory
Teddington, Middlesex, TW11 0LW, UK

Both composites suppliers and end-users are affected by the high cost of composite materials qualification. Qualifying a product against different user specifications, introducing new materials and finding data for materials selection and preliminary design can all be prohibitively costly due to repetition of testing. For example, one qualification programme for a new product cost £2 million to repeat ten times for different customers, rather than £130,000 if one qualification could have been accepted by all. An estimate of a 40% increase in design cost was also given due to the delayed availability of design data.

The National Physical Laboratory (NPL) has formulated a Standard Qualification Plan (SQP) that is aimed at reducing the substantial costs involved in qualifying materials on behalf of suppliers, designers and end-users of fibre-reinforced plastic composite materials. The SQP is aimed at satisfying the minimum common requirements necessary to allow initial material selection, quality control and preliminary design to be undertaken. Further qualification requirements, not met by the minimum SQP, are included in an Extended Qualification Plan (EQP). The SQP/EQP does not constitute a full qualification programme, but is intended to act as a building block forming the initial stage of a qualification or certification programme and is considered suitable for covering coupon level testing.

The recent publication of a test plate manufacture standard (ISO/FDIS 1268), a suite of harmonised ISO test methods (mechanical, thermal and physical) and a data-sheet database standard (ISO 10350-2) has made the realisation of the SQP feasible. To determine which test methods should be included in the SQP/EQP, a survey was carried out by requesting several organisations in the composites industry (material suppliers, end-users, designers and certification bodies e.g. the Civil Aviation Authority (CAA)), to rank individual test methods with regard to their importance in materials qualification. The survey was performed using a detailed questionnaire followed by a number of 'follow-up' industrial visits in order to ensure that the SQP had a suitable content and format to be readily accepted and used by industry. These requirements were compared with existing qualification initiatives (or those currently being developed) mostly driven by aerospace industry certification requirements in order to determine a suitable content, format and style for the SQP. The best-known publicly available procedures are given in MIL-HDBK-17-1E, and are based on testing 30 specimens from 5 batches of material. Companies such as Airbus Industries also have well-developed material qualification documentation. In the USA, the Advanced General Aviation Transport Experiments (AGATE) consortium have recently

released a document under the title of 'Material Qualification and Equivalency for Polymer Matrix Composite Material Systems', with the purpose of providing information and procedures for producing repeatable base composite material properties for primary and secondary aircraft structures. The AGATE consortium is a cost-sharing industry-university-government partnership initiated by the National Aeronautics and Space Administration (NASA) to create the technological basis for revitalisation of the US general aviation industry. It has more than 70 members from industry, universities, the Federal Aviation Administration (FAA), and other government agencies. The AGATE report considers a reduced, 18 specimen qualification plan (6 panels x 3 specimens) and an extended 55 specimen approach that uses alternatively 5 and 6 repeat sets of specimens from a total of 5 batches x 2 panels each.

The approach set out in the SQP procedure is somewhat similar to that used in the AGATE initiative, but is based on measurements of 30 specimens (3 batches x 2 panels x 5 specimen sets). It does not prescribe a full materials qualification programme, nor is it solely intended for use by the aerospace industry. For all properties, where available and suitable, the preferred test methods are ISO standards. Some of the 'building block' test methods in the EQP are not ISO standards, but are ISO new work items (NWI) being led and validated by the National Physical Laboratory (NPL) on behalf of the UK (e.g. open and filled-hole tension/compression, pin bearing etc.). In other cases, such as the compression-after-impact (CAI) test, there are no standardised versions of the test method available. This is currently an area of work under the G7/8 VAMAS (Versailles Project on Advanced Materials and Standards) international pre-standards programme. As the SQP is initially intended to be used for carbon fibre preimpregnated material systems, the conditioning and test temperatures/relative humidities are typical of material applications. The test temperatures and conditioning regimes selected (room temperature and/or 1000 hours at 70°C/85% relative humidity), are typical of those used for aerospace qualification requirements but have been chosen to be in-line with standard ISO test temperatures. Several of the test methods included in the SQP have been validated through round-robin exercises and the SQP procedure is freely available to industry.

POSTER SESSION 1

TESTING OF GLASS FIBRE-REINFORCED POLYMER COMPOSITES

NK Sookay, CJ von Klemperer, VE Verijenko
School of Mechanical Engineering, University of Natal, Durban, 4041, South Africa

Introduction

Polymer composite components are being used in an increasing number of environments across the world. The material is thus exposed to previously untested environments in which the change in physical or mechanical properties has not been clearly established. Natural exposure testing in the expected working environment remains the most reliable method to determine predominant degradation modes as well as change in physical and mechanical properties. Dexter (i) has reported on an extensive outdoor testing programme spanning America, Europe and New Zealand. Similar tests have been undertaken by Chester and Baker (ii), and Fukuda (iii) in Australia and Japan respectively. There are presently no reported natural exposure tests of polymer composites in Southern Africa. The present work aims to identify predominant degradation modes and quantify changes in mechanical properties of laminates with time.

Exposure

Two types of woven glass reinforcements were used. An eight harness satin-weave was used as reinforcement in the epoxy 1 prepreg and the remaining of the laminates were reinforced with a 2×2 twill weave. Matrices tested include two aerospace grade epoxies (epoxy 1 was prepreg), a vinylester, an isophthalic polyester and an orthophthalic polyester. The non-prepreg laminates were prepared by wet lay-up using nine layers of fibre reinforcement and processed as per manufacturer's instructions with the appropriate post cure. Initially unprotected laminates were exposed, with laminates protected by gel coats being exposed at a later date. Specimens with dimensions 150×50mm were mounted on exposure racks inclined at 30° (approximate latitude of the region) to the horizontal and facing North. The exposure frames are set-up to ensure the specimens receive maximum solar irradiance. Exposure frames are presently placed at six locations in South Africa, representing the full range of different South African climates ranging from hot and dry to cool and wet.

Results

Examination and characterisation of exposed laminates was performed using optical microscopy, Scanning Electron Microscopy and compression testing. Figure 1 overleaf shows an image that has been captured using a Scanning Electron Microscope. Loose fibres, on the transverse weave of epoxy 1, are visible on the upper most layers of fibres. Fibres on the cross-sectional weave have begun to come loose. Figure 2 overleaf shows the average compressive strength of epoxy 2 laminates, tested to ASTM D3410, at various locations after 5 months of exposure. Laminates exposed at Irene, characterised by a warm, moderate rainfall environment, appear to be the most effected by exposure while laminates exposed in the Karoo, characterised by a hot, dry environment, appear to have retained their strength. Unlike the epoxy systems tested, vinylester and polyester laminates showed no signs of fibre prominence after 11 months of exposure.

Discussion

Matrix erosion, as observed on figure 1, resulting in fibre prominence is most noticeable on the prepreg laminate. Fibre debonding similar to that noticed by Zhang e*t al* (iv) has also been observed on epoxy 1. Fibre prominence is thought to be due to the high fibre volume fraction of the prepreg laminate resulting in minimal protection of the fibres closest to the surface. Matrix erosion on laminates was observed at all test locations. There appears to be no damage to the underlying matrix material. After 5 months of exposure, laminates exposed at Irene appear to be the weakest in compression. The environment at Irene, with the highest combination of rainfall and total solar radiation of test sites examined, appears to be the most detrimental to the polymer laminates at this stage. Although fibre prominence has been observed on laminates exposed at the Karoo, the overall effect of the environment on the laminates appears to be minimal during the exposure period. The most detrimental variable responsible for the loss of compressive strength appears to be radiation as laminates exposed at Durban experienced greater rainfall and lower radiation when compared to Irene but do not show as much strength loss/reduction.

Laminates with gel coats have been added to the exposure panels. Examination of these laminates will assist in identifying degradation mechanisms and improve understanding of the progression of damage within the laminate. Laminates with a painted surface will be exposed during 2004.

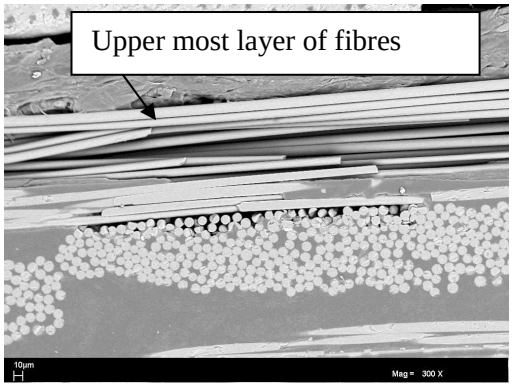

Figure 1 – Cross-section of Epoxy 1

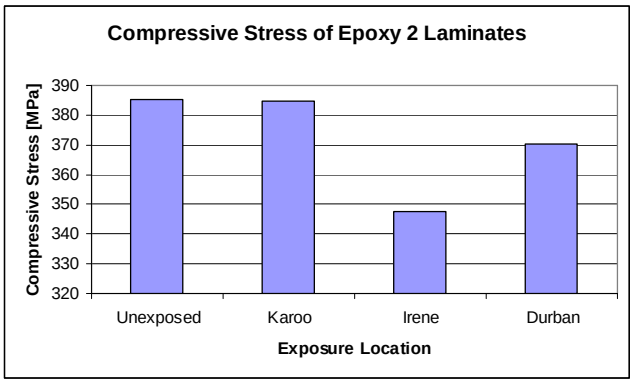

Figure 2 – Compressive Stress of Epoxy 2

Conclusion

Outdoor exposure tests have been initiated in Southern Africa to determine the predominant degradation mechanisms and the rate of change of mechanical properties. Total solar radiation appears to be the most detrimental environmental parameter to the laminates exposed, resulting in mechanical property deterioration.

References

[i]Dexter HB; Long-term environmental effects and flight service evaluation of composite materials; NASA Technical memorandum 89067; January1987
[ii]Chester RJ and Baker AA; Environmental durability of F/A-18 GR/EP Composites; Proceedings of ICCM-10, 1995; pp239-246
[iii]Fukuda H; Five years outdoor exposure of advanced composite materials; Proceedings of the International Colloquium held in Brussels, Belgium August 1990; pp 428-436
[iv]Zhang S, Karbhari VM, Lin-Ye and Mai Y; Evaluation of property retention in E-glass/Vinylester Composites after exposure to salt solution and natural weathering; Journal of reinforced plastics and composites, Vol. 19, No. 09/2000

TRANSVERSE CRACKING AND STIFFNESS LOSS IN HYGROTHERMAL AGED CROSS – PLY LAMINATES

EA. Adda-Bedia, A. Tounsi, KH. Amara, S.A Meftah
Laboratoire des Matériaux et Hydrologie, Université de Sidi Bel Abbes, BP 89 Cité Ben M'hidi 22000 Sidi Bel Abbes, Algérie.

The aim of this study is to characterise the damage development in graphite/epoxy cross – ply laminates subjected to tensile loading by taking into consideration the reduction of the elastic moduli of materials due to the variation of temperature and moisture within this latter, before applying the mechanical loading. It is well known that in the case of static loading, cracks are initiated on the edges of test specimens and cross instantaneously the whole width of the specimens.

In this work a systematic study will be made of the influence of transverse matrix cracking on the evolution of both the longitudinal Young's modulus and the Poisson's ratio in the hygrothermal aged cross – ply laminates. Both complete parabolic shear – lag analysis and progressive shear model are used with some modifications to predict the effect of transverse cracks on the stiffness degradation of composite laminates. First, general expression for longitudinal modulus reduction versus transverse crack density is obtained by introducing the stress perturbation function. Good agreement is obtained comparing prediction with experimental results. This latter is also modified by introducing the stress perturbation function. In the second part of this investigation, the hygrothermal effect on the material properties of the laminate is taken into account to evaluate the stiffness loss in cross – ply laminates containing transverse cracks. It is well known that during the operational life, the variation of temperature and moisture reduces the elastic moduli and degrades the strength of the laminated

material. The obtained results illustrate well the dependence of the degradation of elastic properties on the cracks density and hygrothermal conditions.

Keywords: Transverse cracking; Hygrothermal aged cross–ply laminates; Stress perturbation function; LongitudinalYoung's modulus.

REFERENCES

1. Groves S.E., Harris C.E., Highsmith A.L., Allen D.H., Norvell R.G., "An experimental and analytical treatment of matrix cracking in cross – ply laminates" Experimental Mechanics, Vol 27, pp. 73 – 79, 1987.
2. Berthelot J.M, Leblond P, El Mahi A, Le Corre J.F "Transverse cracking of cross – ply laminates. Part 1: analysis" Composites, 27A: 989 – 1001 (1996).
3. Berthelot J.M "Analysis of the transverse cracking of cross – laminates: a generalized approach" J of Composite Materials, 31: 1780 – 805 (1997).
4. Smith P.A, Wood J.R "Poisson's ratio as a damage parameter in the static tensile loading of simple cross – ply laminates" J of Composites Science and Technology, 38: 85, (1990).
5. Joffe R, Varna J "Analytical modelling of stiffness reduction in symmetric and balanced laminates due to cracks in 90° layers" J of Composites Science and Technology, 59: 1641, (1999).
6. Shen C.H, Springer G.S "Environmental effects in the elastic moduli of composite material", Environmental Effects on Composite Materials, Springer G.S., Ed., Technomic Publishing Company, Inc., Westport, CT, pp. 94 – 108, 1981.
7. Adams D.F., Miller A.K., "Hygrothermal microstresses in a unidirectional composite exhibiting inelastic materials behaviour", J of Composite Materials, 11: 285 – 299 (1977).
8. Bowles D.E., Tompkins S.S., "Prediction of coefficients of thermal expansion for unidirectional composites", J of Composite Materials, 23: 370 – 381 (1989).
9. Shen H.S., "The effects of hygrothermal conditions on the postbuckling of shear deformable laminated cylindrical shells", J of Solids and Structures, 38: 6357 – 6380 (2001).
10. Megueni A, Tounsi A, Bouiadjra B.B, Serier B "The effect of a bonded hygrothermal aged composite patch on the stress intensity factor for repairing cracked metallic structures" International Journal of Composite Structures, 62 (2): 171 – 176 (2003).
11. Tounsi A., Adda-Bedia EA, "Simplified Method for Prediction of Transient Hygroscopic Stresses in Polymer Matrix Composites with Symmetric Environmental Conditions", J of Applied Composite Materials, 10: 1- 18 (2003).
12. Tounsi A., Adda Bedia. E.A., "Some observations on the evolution of transversal hygroscopic stresses in laminated composites plates: Effect of anisotropy", International Journal of Composite Structures, 59: 445 – 454 (2003).
13. Adda-Bedia E.A., Tounsi A., Sereir Z., "A quantitative study on the influence of anisotropy on the hygrothermal behaviour of the laminated composite plates", Eighth International Conference on Composite Engineering ICCE8, August 5-11, 2001, Tenerife, Spain, 71.
14. Benkeddad A., Grediac M., Vautrin A., "Computation of transient hygroscopic stresses in laminated composite plates", J of Composites Science and Technology, V 56, pp 869 – 876, 1996.

STRAIN FIELDS IN THE PICTURE FRAME TEST

S.V.Lomov, T.Stoilova*, I.Verpoest
Department MTM, Katholieke Universiteit Leuven, Kasteelpark Arenberg, 44, Leuven, B-3001, Belgium
*Technical University Sofia, Bulgaria

The characterisation of the shear resistance is needed for accurate prediction of the fabric draping during forming of a 3D-shaped composite part. Reliable virtual prototyping of this process is extremely important for cost-effective design and production of composite parts. The available software packages for the forming simulation include material model of non-linear shear resistance, with the input data recommended to be obtained via the picture frame test, which is *de facto* standard for characterisation of shear resistance of composite reinforcements. It is believed to provide most reliable information of the fabric behaviour for a wide range of shear angles, up to 45…60°, sometimes even up to 75°. A "competitor", tensile test in bias direction, is also widely used, but the stress-strain state of the fabric in this test is much more complex and the simple shear resistance may be blurred by other factors. To be a true characterisation of the fabric shear behaviour, the test must provide dependency of the shear force on the average shear angle of the *fabric.* Due to the complications

of the gripping discussed above, one cannot be sure that it is the same as the shear angle of the frame. One of our aims is to estimate the difference between them and provide a correction technique (Fig.1). Another requirement for the picture frame measurement is uniformity of the strain of the fabric. Our second aim is to study this uniformity and estimate errors introduced when one assumes it to be perfect (Fig.2).

Full field methods of registration of the strain field in the picture frame test is an ideal tool to study the behaviour of the fabric during the test. The ARAMIS system was used for the strain registration. The measurements show that the difference between the shear angle of the frame and average shear angle of the fabric can reach 10°; the variations of the shear angle over the fabric surface are limited to 5% of the average shear angle. Measurements of three cycles of the shear loading highlight the major influence of the (pre)strain of the fabric on its shear resistance.

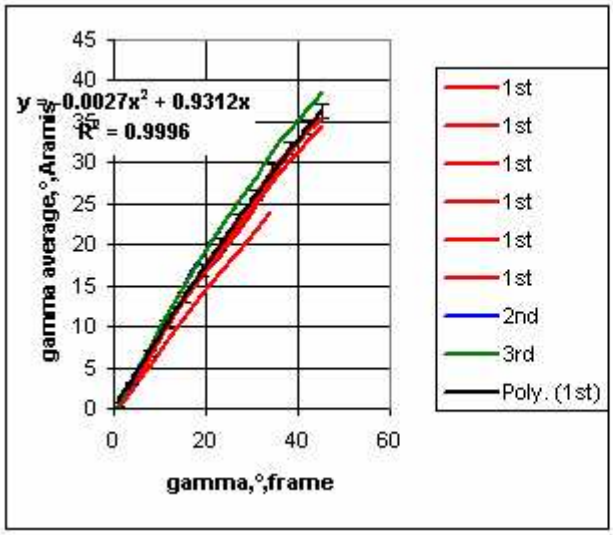

Fig.1 Average shear angle vs frame shear angle.

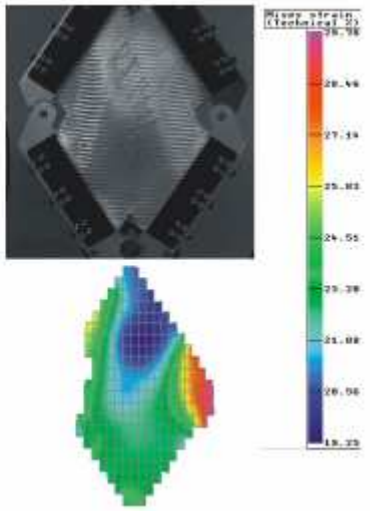

Fig.2 Typical strain-mapping results. Shear strain, %.

A 3-D MICROMECHANICAL MODEL FOR PREDICTING THE ELASTIC BEHAVIOUR OF WOVEN FABRICS

Mauricio V. Donadon, John M. Hodgkinson, Brian G. Falzon, Lorenzo Iannucci
Department of Aeronautics, Imperial College London, South Kensington, London SW7 2AZ, U.K.

In recent years, researchers and industrial companies worldwide have become increasing aware of the potential of fabric architectures for reinforcement, such as Woven and Non-Crimp Fabrics (NCF) over conventional unidirectional pre-pregs. Enhancement in the interlaminar shear strength [1] and improvements in the damage tolerance and impact resistance [2] have also been observed. They also can provide more balanced properties in the fabric plane than unidirectional laminae. Furthermore, woven fabrics due their ease of handling and greater drapability have become prime candidates for reinforcement materials in low-cost manufacturing processes; such techniques are based on resin infusion technologies, e.g. RIFT.

In this context, this paper presents an analytical model for the prediction of the elastic behaviour of plain-weave fabrics [3]. The 3-D micromechanical model presented in this paper is an extension of the 2-D model proposed by Naik and Shembekar [4]. The fabric is assumed to be a hybrid plain weave with different materials and undulations in the warp and weft directions (Fig.1). The derivation of the effective material properties is based on the Classical Laminate Theory (CLT) [5].

The theoretical predictions have been compared with experimental results and predictions using similar models available in the literature. A good correlation between theoretical and experimental results for the prediction of in-plane properties was obtained and some issues regarding the limitations of the existing models based on Classical Laminate Theory (CLT) for predicting the out-of-plane mechanical properties are presented and discussed.

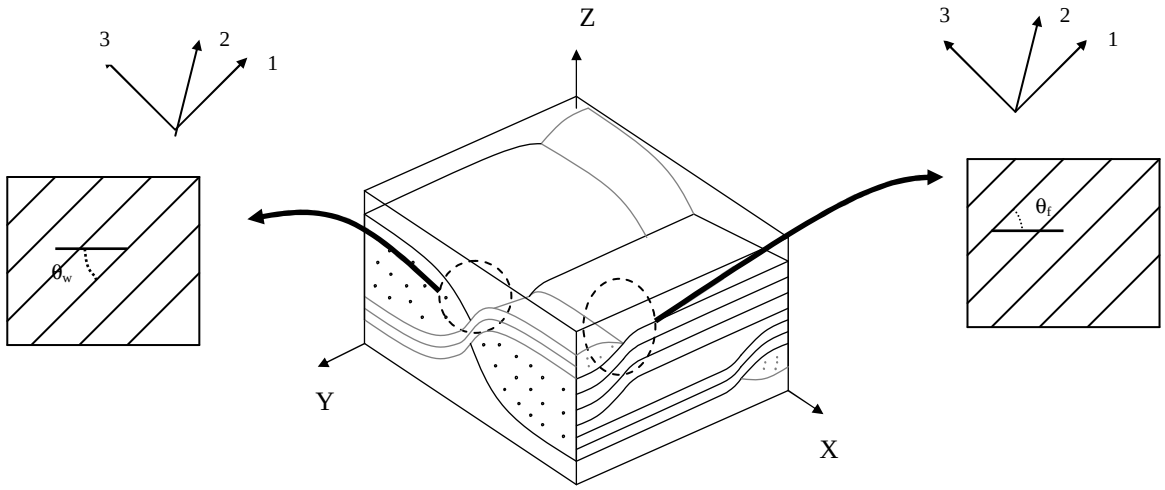

Figure 1: Unit Cell Geometry

[1] Matthews ST, Hill BJ, McIlhagger AT, McIlhagger R. Investigation into through the thickness yarns in carbon fibre epoxy composites. *Proceedings of the Sixth International Conference on Automated Composites*, Bristol; September 1999. pp. 195-201.

[2] Mohamed MH, Bogdanovich AE, Habil, Dickinson LC, Singletary JN, Lienhard RB. A new generation of 3D woven fabric performs and composites. *SAMPE J.;* May/June 2001. pp 8-17.

[3] Donadon, M.V., The Impact Behaviour of Composite Structures Manufactured using Resin Infusion, *Internal Report, Department of Aeronautics, Imperial College London*, 2003.

[4] Naik, NK, Shembekar PS, Elastic behaviour of woven composites: II-Laminate analysis. *Journal of Composite Materials*, 26(15), 1992.

[5] Jones, R.M, Mechanics of composite materials, Taylor & Francis, Inc., USA, 2nd edition, 1999.

IDENTIFICATION OF ELASTIC PROPERTIES IN STIFFENED COMPOSITE SHELLS

R. Rikards*, H. Abramovich**, O. Ozolinsh*, E. Skukis*, S. Ruchevskis*
*Institute of Materials and Structures, Riga Technical University, Latvia
**Faculty of Aerospace Engineering, Israel Institute of Technology, Haifa, Israel

For design of stiffened composite shells, for example aircraft fuselage, it is important to know actual laminated composite properties. Conventional way is testing the coupon specimens, which are manufactured with similar technology as the real large structure. Employing such method still is open the question, whether the material properties obtained from the coupon tests are the same as in the large structure. In the present paper comparative study of three methods is performed. Material properties of laminated carbon/epoxy composite were obtained from conventional static tests, from vibration tests of the flat plates and from vibration tests of the small panel with one stiffener. The small panel was cut from the large stiffened composite panel, which before was tested for post-buckling. The method of identification is based on solution of inverse problem. For this experimental and numerical frequencies are employed in identification functional, which is defined as squared discrepancies between the measured and numerical frequencies. Approximation of the functional was obtained using method of experimental design and response surface approach [1, 2]. The results for elastic properties obtained employing the first (static tests of coupons) and second (vibration tests of flat plates) method are in good agreement. The results obtained from the vibration tests of the small panel cut from the real structure are with some differences. This can be explained so, that single ply thickness, material density, layer angles of the real structure is slightly different from the nominal values. These differences should be taken into account in design of real structures by choosing safety factors, calculating the limit and the collapse loads of composite stiffened structures.

References

1. Rikards R., Auzins J., Response surface method for solution of structural identification problems. *Inverse Problems in Science and Engineering*, **12** (1) (2004) 59-70.
2. Rikards R., Abramovich H., Green T., Auzins J., Chate A., Identification of elastic properties of composite laminates. *Mechanics of Advanced Materials and Structures*, **10** (4) (2003) 335-352.

MODELLING DAMAGE DEVELOPMENT IN OFF-AXIS PLIES OF LAMINATED COMPOSITES

Maria Kashtalyan*, Costas Soutis**
*College of Physical Sciences, University of Aberdeen, Fraser Noble Building, Aberdeen AB24 3UE,
**Aerospace Engineering, University of Sheffield, Sir Frederick Mappin Building, Mappin Street, Sheffield S1 3JD, UK

When a multidirectional composite laminate is subjected to in-plane tensile or thermal loading, matrix cracks parallel to the fibres appear in the off-axis plies long before catastrophic failure. Matrix cracking significantly reduces the laminate stiffness and triggers development of other harmful resin-dominated damage modes such as delaminations.

Observations of sequential damage accumulation in off-axis plies of multidirectional laminates have been reported for balanced (Marsden et al, 1999; Varna et al, 1999), unbalanced (Crocker et al, 1997) and quasi-isotropic (Tong et al, 1997a,b) glass/epoxy laminates under quasi-static and fatigue tensile loading. Concurrent matrix cracking in the adjacent off-axis plies is an extremely complex problem to model analytically and has been therefore analysed using finite elements method (Tong et al, 1997). Analytical models have been developed recently to predict stiffness degradation due to matrix cracking in off-axis plies (McCartney, 1996; Zhang and Herrmann, 1999; Kashtalyan and Soutis, 2000).

The present paper is concerned with theoretical modelling of damage development in off-axis plies of general symmetric laminates subjected to in-plane tensile loading. The approach employs the Equivalent Constraint Model (ECM) of the damaged laminate to predict strain energy release rates for off-axis ply cracking and crack-induced delaminations.

Strain energy release rates for matrix cracking and crack-induced delaminations can be calculated efficiently if instead of the damaged laminate one considers an ECM laminate, in which the damaged ply is replaced with a homogeneous equivalent constraint layer with degraded stiffness properties. For matrix cracking, the in-plane stiffness matrix $[\overline{Q}]_\theta$ of the equivalent constraint layer is a function of the relative crack density $D^{mc} = h_2 / s$ and can be determined from the micromechanical analysis developed by the authors (Kashtalyan and Soutis, 2000). The total strain energy release rate G^{mc} for matrix cracking is found as

$$G^{mc}(\bar{\varepsilon}, D^{mc}) = -h_2 \{\bar{\varepsilon}\}^{\mathrm{T}} \frac{\partial [\overline{Q}]_\theta}{\partial D^{mc}} \{\bar{\varepsilon}\} \sin\theta$$

where $\bar{\varepsilon}$ is the applied strain, and θ is ply orientation angle of the damaged ply.

Due to shear-extension coupling, damage development in the off-axis plies of general symmetric laminates always occurs under mixed mode conditions. Contributions of Mode I and Mode II into the total strain energy release rate will be identified.

Dependence of the Mode I, Mode II and total strain energy release rates on the crack density and ply orientation angle will be examined and discussed for carbon /epoxy and glass/epoxy laminates. It will be then applied to predict cracking onset strain in a glass/epoxy $[0/\theta]_s$ laminate using a mixed mode fracture criterion.

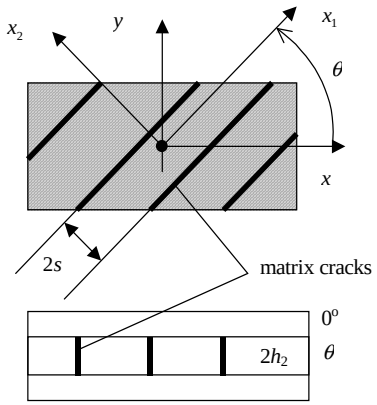

Figure 1. Front and edge views of an unbalanced symmetric $[0/\theta]_s$ laminate with off-axis ply cracks. Matrix cracks are assumed to span the full width of the laminate and full thickness of the θ-layer and be spaced uniformly at a distance $2s$.

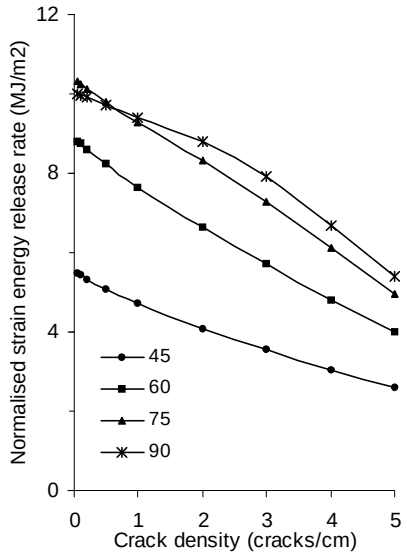

Figure 2. Normalised strain energy release rate $G^{mc}/\bar{\varepsilon}_{xx}^2$ for matrix cracking in a glass/epoxy $[0/\theta]_s$ laminate as a function of crack density in the θ-layer.

References

Kashtalyan M, Soutis C (2000) Modelling stiffness degradation due to matrix cracking in angle-ply composite laminates. *Plastics, Rubber and Composites* 29, 482-488

McCartney LN (1996) Stress transfer mechanics for angle-ply laminates. Proceedings of the *7th European Conference on Composite Materials*, 14-16 May 1996, London, UK

Marsden WM, Guild FJ, Ogin SL, Smith PA (1999) Modelling stiffness-damage behaviour of $[\pm 45/90]_s$ and $[90/\pm 45]_s$ glass fibre reinforced polymer laminates, *Plastics, Rubber and Composites* 28, 30-39

Tong J, Guild FJ, Ogin SL, Smith PA (1997) On matrix crack growth in quasi-isotropic laminates. – I. Experimental observation, *Composites Science and Technology* 57, 1527-1535

Tong J, Guild FJ, Ogin SL, Smith PA (1997) On matrix crack growth in quasi-isotropic laminates. – II. Finite element analysis, *Composites Science and Technology* 57, 1537-1545

Varna J, Joffe R, Akshantala NV, Talreja R (1999) Damage in composite laminates with off-axis plies. *Composites Science and Technology* 59, 2139-2147

Zhang J, Herrmann KP (1999) Stiffness degradation induced by multilayer intralaminar cracking in composite laminates, Composites Part A: Applied Science and Manufacturing 30, 683-706

EVALUATION OF THE EXCHANGE MAGNETIC COUPLING IN NANOCOMPOSITE MAGNETIC MATERIALS

Manh-Huong Phan, Hua-Xin Peng, Michael R. Wisnom
Department of Aerospace Engineering, Bristol University, Queen's Building, University Walk, Bristol, BS8 1TR, United Kingdom
Seong-Cho Yu
Department of Physics, Chungbuk National University, Cheongju, 361-763, Korea
Nguyen Chau
Center for Materials Science, National University of Hanoi, 334 Nguyen Trai, Hanoi, Viet Nam

The discovery of Finemet-type nanocomposite magnetic materials with a composition of $Fe_{73.5}Si_{13.5}B_9Cu_1Nb_3$ provided some new insights into the science and technology of soft magnetic materials [1]. This kind of materials, routinely obtained by some appropriate heat treatment of a amorphous precursor, exhibits excellent magnetic properties due to its unique microstructure, namely, ultrafine nanocrystalline α-Fe(Si) grains embedded in an amorphous matrix. This is directly depending on the exchange magnetic coupling between the grains through the amorphous boundaries. However, the exchange magnetic coupling is not thoroughly understood.

Fortunately, several recent studies on the giant magnetoimpedance (GMI) effect in amorphous soft magnetic ribbons/wires subject to heat treatment [2,3] showed some insights into the nature of the exchange magnetic coupling between these grains through the amorphous boundaries in Fe-based nanocrystalline materials. Because of the fact that the two-phase Fe-based nanocrystalline alloy has two distinct Curie temperatures, one for the nanocrystalline grains and the other belonging to the amorphous phase, the roles of the two magnetic phases in the intergrain magnetic coupling can be taken apart in a sufficiently high temperature region.

In this context, we report here, the results of a detailed study of the effect of annealing on GMI profiles in Fe-based amorphous alloys. The GMI profiles were measured in the amorphous samples annealed at different temperatures ranging from 350 to 650 ^{0}C in vacuum and for 1 hour. It is shown that the GMI profile increased with increasing annealing temperature from 350 up to 500 ^{0}C. The largest GMI profile has been found to occur in the alloy annealed at 540 ^{0}C. With further increasing annealing temperatures, the GMI profile decreased. In view of the experimental results, it is reasonable to claim that the nanocrystalline grains in the nanocrystalline alloys are strongly coupled through exchange magnetic interactions, and the local magnetocrystalline anisotropies of grains are averaged out. Meanwhile, the intergranular amorphous phase plays an important role because the exchange coupling can only be conveyed through it. Therefore, any variation in the magnetic nature of the amorphous phase will change the intergrain exchange coupling, hence alter the magnetic softness and the effective anisotropy and finally modify the GMI features.

For the as-cast amorphous alloy, the amorphous phase is ferromagnetic and maintains the exchange coupling. When the amorphous sample was annealed at temperatures up to ~500 ^{0}C, which is far below the onset crystallization temperature (~530 ^{0}C, determined by differential scanning calorimetry diagram), the combination of the stress release and the magnetocrystalline anisotropy decrease in the amorphous phase softens the ribbon magnetically, thus enhances the GMI effect. The maximum of GMI observed in the sample annealed at 540 ^{0}C is likely due to the presence of ultrasoft magnetic materials (i.e. a nanocomposite soft magnetic alloy). When the annealing temperature (~600 ^{0}C) is close to the crystallization temperature of the hard magnetic Fe-B phase, an overwhelming decrease of GMI is observed. This is because that the Fe-B phase has a soft magnetic phase of α-Fe(Si) and suffers a ferromagnetic to paramagnetic transition. It becomes incapacitated in conveying the intergrain magnetic exchange coupling. These results coincide with the annealing-temperature dependence of the magnetostriction saturation and the effective anisotropy constant evaluated by a separate magnetization measurements. It is believed that the temperature-dependent GMI profile is useful to further understand the exchange magnetic coupling between these grains through the amorphous boundaries in Fe-based nanocrystalline materials.

References:

[1] Y. Yoshizawa, S. Oguma, K. Yamauchi, J. Appl. Phys. **64**, 6044 (1988).
[2] J. L. Coasta-Kramer and K. V. Rao, IEEE Trans. Magn. **31**, 1261 (1995).
[3] Y. K. Kim *et al.*, J. Appl. Phys. **83**, 6575 (1998).

DESIGN AND FAILURE OF MATERIALS SYSTEMS UNDER MULTI-AXIAL LOADS

J Cook and C Williamson
QinetiQ, Farnborough, UK

Polymer composite materials are being increasingly used in a wide variety of industrial applications, but there are difficulties in applying these materials in ways that exploit their full potential. The main reason for this is that these materials are more complex than other engineering materials such as metals. The number of options allowed by composites confers a number of design freedoms but at the same time leads to greater difficulties in applying these materials efficiently. One important aspect of this complexity is the behaviour of composites under multi-axial loading. For metals, the rules covering multi-axial behaviour are reasonably well established, but for composites the situation is far more complex, partly as a result of their anisotropy and partly due to the multiplicity of their failure modes. Nevertheless, the understanding of the behaviour of composites under multi-axial loading is of great practical significance, since bi- or even tri-axial loading regimes are the norm in real engineering structures.

In order to rectify this situation, a programme has been set up under the DTI's Measurements for Materials Systems (MMS) initiative. The specific programme addressing failure under multi-axial loading, termed MMS5, commenced in September 2002 and will run for three years. It is being run by a team consisting of QinetiQ, AEA Technology, Nottingham University, UMIST (ARP), NPL and Netcomposites, and the objective is to address the widest possible range of UK industry needs in this important area of technology. It is anticipated that large benefits will accrue to both industrial suppliers and to users of composites.

Until now, most of the work in the UK on the topic of multi-axial testing has been carried out within the defence and aerospace sectors. Within the aircraft market, it has been estimated that, on average, the composite structure used is 15% overweight due to the lack of such information and the necessarily conservative assumptions that have to be imposed by the airworthiness authorities. It is likely that similar factors apply in other industry sectors, and so a major part of the MMS5 programme is to transfer this knowledge out of aerospace arena and to disseminate it as widely as possible to other parts of industry. In the automotive sector, for example, commodity materials are generally used such as glass fibre (both continuous and chopped) within a polyester or polypropylene matrix. Although components are generally designed to achieve a specified stiffness, accurate failure data is essential. This is particularly so for structures designed for crashworthiness, where the onset of damage must be determined within structural analyses. Similar considerations apply within the marine sector, but at present the appropriate materials data is simply not available.

Many of the results from aircraft and defence-based programmes have now been published, and more is due to be released in 2005. In addition, a very comprehensive world-wide exercise dealing with the failure of composites was completed in 2003, and its findings published.

Outside the aerospace sector, there is tremendous scope for applying the knowledge gained more widely.

The diagram below depicts the situation. Currently, there is a vast body of test data on aerospace materials in the form of simple coupons and this data has been extended to cover tubes and flat panels. In some instances, this has gone as far as the bi-axial testing of 3D structural elements. All this is shown on the left of the diagram. The purpose of MMS5 (as shown on the right of the diagram) is to follow the same route for bulk usage composites.

The purpose of this programme is therefore to apply the existing multi-axial knowledge and testing techniques to a range of non-aerospace materials of wider commercial interest, and to extend the existing theoretical framework (which is substantial) to cover such materials. Individual multi-axial tests tend to be somewhat expensive, and so the theoretical backup is important in determining which tests to carry out and in extracting the maximum value from them.

Industry involvement is vital in the selection of materials of greatest interest and in defining the applications. An Industrial Advisory Group (IAG) has been set up to guide this process. This IAG is open to the companies participating in MMS5, as well as to organisations wishing to gain insight into this important topic.

The paper will describe some of the activities being carried out, and, in particular, the test results obtained to date and their significance. These results are likely to include those for woven materials with a thermoplastic matrix, multi-directional non-crimp materials, very thick composites (up to 20mm thick) and, possibly, braided tubes.

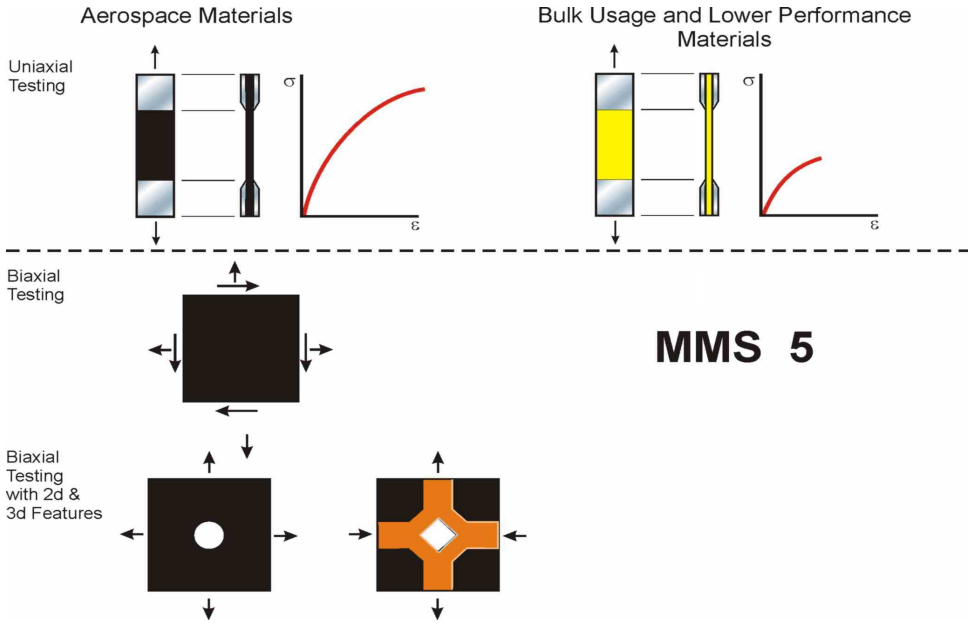

USING 3D FABRIC ON LIGHT GLIDER FUSELAGE

Jaroslav Juračka, Ph.D., Jan Splíchal
Brno University of Technology

1. Introduction

A new material, which is called the Paraglass, has been used for the development of the ultralight composite glider TST-10 Atlas, unlike usual technology of the sandwich construction. The glider TST-10 Atlas is the cantilever midwing momoplane [1] with the T tailplane. The take off engine is installed on the stow-away arm. The Paraglass is made by the Dutch company Parabeam in Helmond. The advantage of this material is very simple and cheap technology of the structure production. The material is used as middle lay of all coverings, that are skin of wing, fuselage and tailplane. The experiences of the Paraglass application on the skin of glider fuselage are specified at the following abstract.

2. Loading

Several cases are crucial for the loading of fuselage because both the bending and the twist are carried with the fuselage structure. A maximum force on the horizontal tail unit is one of the important bending cases. The resultant force, applied in the horizontal tail hinge F_{HTU}= 811 N, was determined for this case (Case 1). This force presents air load after deducting inertial effects. The second important case is the bending to a side simultaneously with the twist of fuselage (that is load from the vertical tail unit). The force F_{VTU}= 811 N and the twist moment Mx = 852.95 Nm presented load of Case2. Load cases mentioned above are limit loads. A carrying capacity was calculated with the safety factor 1.5 and the special coefficient for composites 1.5. Ultimate loads were 2.25 times bigger than limit ones.

3. Analysis

The first step of analysis was a simple calculation. The shear forces, bending moments and the torsion moment along fuselage were calculated. Then the tensile and shear flows (forces on the length unit) were calculated. The maximal size of the tensile flow q_t=38 N/mm (Case 1) and the shear flow q_s=14,7N/mm (Case 2) were determined in the area, where the fuselage was changed into a fin. These loads represent tensile or compression

stress 45 MPa and shear stress 23 MPa in the upper lay of laminates. Both values are low for achievement of strength.

However, this judgement is not sufficient for an appraisal of the carrying capacity. The effect of buckling on the fuselage has to be taken into account for the next appraisal. A similar equation, like for curved isotropic sheet, was used for the first establish of critical area and value of critical compression flow determination:

$$q_{KRc} = \left[kE\left(\frac{t}{b}\right)^2 + 0{,}3E\frac{t}{R} \right] t$$

The critical area of buckling of bending case was predicted from the ratio of critical flow and limit flow in the co-ordinate range 3.8-4.4 m from the fuselage nose. The value of a reserve factor, by which the given failure comes about, could not be defined without experimental verification at the panel or directly at the fuselage structure. he second step of analysis was FEM modelling and non-linear solution. MSC Patran/Nastran system was used for FEM analysis. By FEM analysis, the failure was established with reserve factor 2,15in the area with co-ordinates 3.8 m. The area, where fuselage is changed into fin, was determined as a critical one from an analysis of shear flow (Case 2) and its influence on structure. But from the view of the carrying capacity we could take the reserve as sufficient.

4. Testing

The results of analysis and structure carrying capacity were verified during tests. The bending test proved ability to carry the maximal horizontal tail unit force F_{HTUmax} = 1638 N that is 184% of limit load. The failure came about at the point 3.92m. But the failure area had a bad bond of both halves of the fuselage body. There was another test after the repair. It was for the definition of a further failure point, which was found at the load value F_{HTUmax} = 1946 N (ie. 219% of limit load) and the failure area moved at 3.72m. It means that the area of failure was moved by the repair effect (local reinforcing) about 200mm forward. The next critical case was Case 2. The fuselage was also tested on the twist and the bending to a side. The fuselage carried a side force on the vertical tail unit F_{VTUmax}= 1890 N and the induced rolling moment Mx = 324 Nm (ie. 240% of limit load for the Case 2 at twist). The test was stopped without failure.

5. Conclusion

Tests confirmed the expected assumptions and the ability of fuselage to carry required loading. The agreement was proved at the prediction of the failure area of structure. As we assumed there were no exact agreements at the determination of load amount, by which the failure comes about.

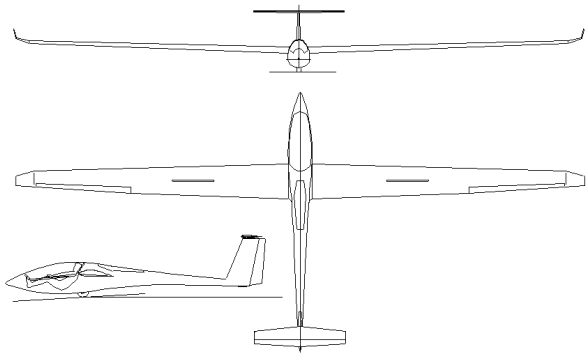

Figure 1. Sailplane TST-10

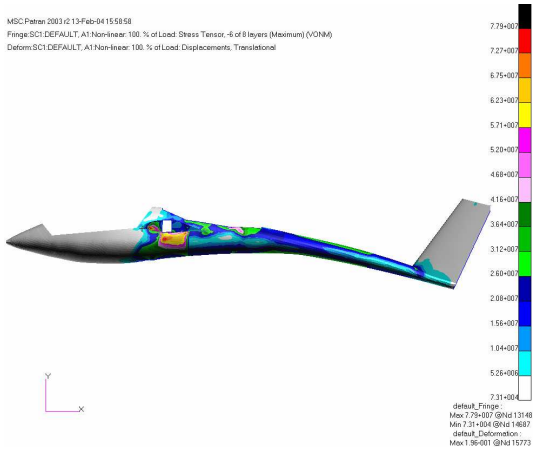

Figure 2. Result of FEM analysis

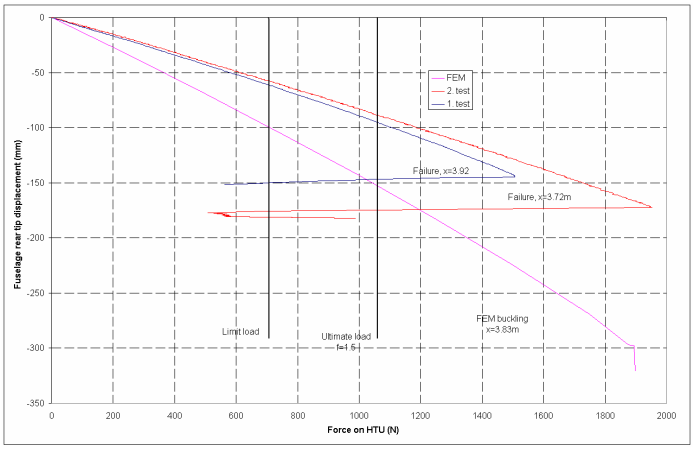

Figure 3. Fuselage rear tip displacement depending on VTU force

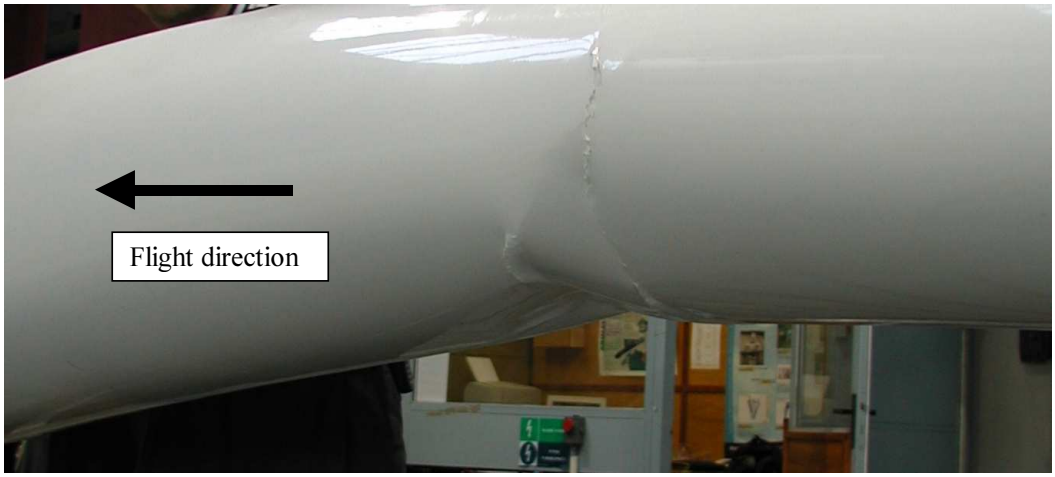

Figure 4. First failure of fuselage structure

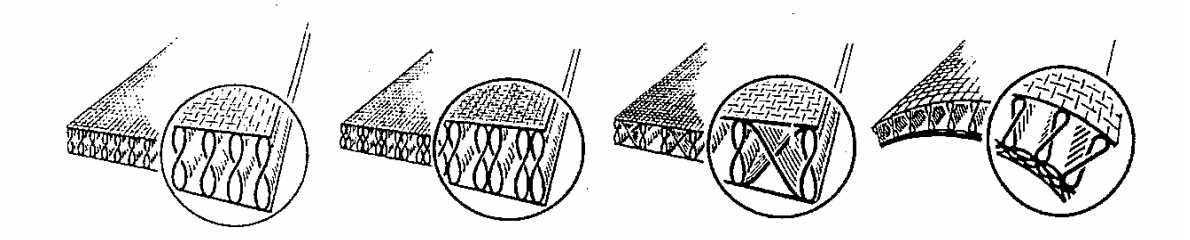

Figure 5. Types of Paraglass material

PREDICTION OF IMPACT-INDUCED FIBRE DAMAGE IN CIRCULAR COMPOSITE PLATES

J Lee and C Soutis
Aerospace Engineering, Faculty of Engineering, The University of Sheffield, Mappin Street, Sheffield, S1 3JD

An impact damage site in a composite laminate contains delaminations, fibre fracture and matrix cracking. A model to predict the damage area taking into account all these factors would be complex and take considerable time and funding to develop. It was recognised that the problem could be simplified by making some assumptions about the nature of the impact damage.

In this study a simple analytical impact damage model for preliminary design analysis excluding the time-consuming dynamic finite element analysis of the structure is developed. The analytical model uses a simple non-linear approximation method (Rayleigh-Ritz) to predict the damage area and the number of failed plies for a quasi-isotropic (assumed axisymmetric) composite circular plate subjected to a point load at its centre using large deflection plate theory. The model is based on the concept that the low velocity impact response is similar to the deformation due to a static transverse load. The damage introduced is studied by treating the response to the impact as static global bending. By neglecting the inertia forces from the plate the problem is reduced to a static equivalent one and by considering degraded stiffness in the plate with increasing loads, damage accumulation in the form of fibre breakage is introduced. A maximum strain failure criterion is adopted to predict fibre damage in each ply.

It will be shown that the present analytical model agrees well with finite element predictions and experimental data for the deflection of the undamaged elastic plate despite its simplicity (see Figure 1) and gives an idealized fibre damage shape at each ply as a circle and number of failed plies. From the theoretical analysis, fibre damage at each ply of the plate shows two types of failure patterns. When the plate thickness is quite thin (1mm thick in the current analysis), fibre damage is produced by the effect of geometrical non-linearity, i.e. membrane stretching effect due to large deflection and the maximum non-linear effect occurred at a certain inner region of each ply displaying an overall annular damage shape. For a thick circular plate (3mm thick in the current analysis), fibre damage initiates from the centre of each ply and propagates to the plate edge. In this case, the damage is dominated by the bending effect since the plate deflection does not exceed the plate thickness. However, with a large applied load, i.e. the plate deflection > the plate thickness, fibre damage initiates at a certain inner region from the top ply like the case of the 1mm thick plate. Based on the number of failed plies in the plate, degraded elastic moduli are obtained using the classic laminate plate theory.

From the outputs produced by the current analytical damage model, it is shown the possibility that CAI strength on fibre based impact damage could be predicted analytically using the equivalent hole model or a soft inclusion model proposed by Soutis and co-workers [1]. In addition, the model can save significant running time, compared with FE solutions.

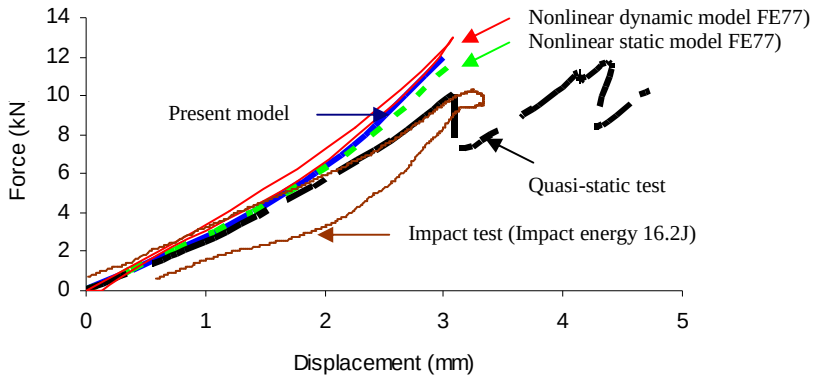

Figure 1 Comparison of force-displacement curves for a 3mm thick circular plate $(45/-45/90/0]_{3s}$ – IM7/8552)

References

Soutis C. and Curtis P. T., “Prediction of the post-impact compressive strength of CFRP laminated composites”, Composite Science and Technology, 1996, Vol. 56 (6), pp. 677-684.

TOMOGRAPHY BASED APPROACH FOR FINITE ELEMENT MODELING OF PARTICLE REINFORCED METAL-MATRIX COMPOSITES

P. Kenesei[1], H.Biermann[2] and A. Borbély
1 Eötvös Loránd University, Department of General Physics, H-1518 Budapest, POB. 32, Hungary
2 Institut für Werkstofftechnik, Technische Universität, Bergakademie, Gustav Zeuner Str., 09569 Freiberg, Germany.

3D holotomographic scans were performed at the European Synchrotron Facility in Grenoble in order to characterize the microstructure of a Particle reinforced Metal-Matrix Composite (PMMC) consisting of an AA6061-T6 aluminium alloy as matrix, and 20 vol.% of Al_2O_3 particles as reinforcements. The structure of the composite was reconstructed with a resolution of 2 □m, an average particle of equivalent diameter of 12 μm being given by about 120 voxels. The statistical evaluation of the microstructure was performed by considering the size, shape and distribution of particles, as well as the two point probability functions of the matrix and particle phases [1]. Special attention was given to those parameters, which allow building of one and multi-particle cell models appropriate for Finite Element (FE) modeling.

With this respect the local volume fraction of particles was considered, which was defined as the ratio between the particle volume and the sum of the particle volume and the volume of the matrix material adjacent to the particle. The evaluation shows that the distribution of the local volume fractions is very broad, ranging from values near to zero up to values of 40%, twice as large as the nominal value of 20%. The obtained distribution can be well described by a Gaussian function centered however, not at the nominal value of 20%, its center being shifted towards smaller values. This evaluation allows treating the composite as an ensemble of single particles, which can be modeled more easily than the real structure. The overall mechanical behavior of the composite can be obtained from the single particle cells with appropriate weighting factors under the assumptions of Reuss or Voigt [2].

The next point considered during evaluations was the determination of the *geometrically* Representative Volume Element (RVE), which can be used as a first approach in order to determine of the *physical* RVE of the composite. This evaluation was done based on the two-point probability function of the matrix, which gives the probability to find two points separated by a given distance, both situated in the matrix. This evaluation has shown that the *geometrical* RVE is an ellipsoid of revolution, aligned in the direction of the extrusion axis. It also indicates that the microstructure has statistical isotropy in the transverse direction, a property that must be fulfilled by all multi-particle models considered in the following. The size of the *geometrical* RVE is not big, the semi-axes of the corresponding ellipsoid being of about 28 μm x 23 μm x 23 μm. This size should be understood in a statistical sense, which means that the macroscopic behavior of the composite can be obtained from the average behavior of many such volumes. For FE simulations cubical volumes of 64^3 μm^3, slightly larger than the correlation volume were considered. An original volume of 2563 □m3 was decomposed into 16 different sub-volumes and displacement controlled compression stress–strain curves were calculated of each sub-volume. Modeling was done by the FE method considering J2 flow criteria for the matrix and elastic behavior for the ceramic reinforcements.

The average curve over the 16 geometrical RVEs is presented in Fig. 1 together with the curves obtained for one-particle unit cell models (UC_Voigt and UC_Reuss), and the curve describing the behavior of the large original volume. The best agreement is obtained for the latter, which approximates the experimental curve with an error less than 8%. This error is attributed to the use of trilinear interpolation functions. The larger flow stress obtained from averaging over the 16 geometrical RVEs (geom_RVE) indicates that the *geometrical* RVE is smaller than the *physical* RVE. Very bad agreement is obtained for unit-cell models in the Voigt approximation, while the Reuss approximation the leads to a good agreement.

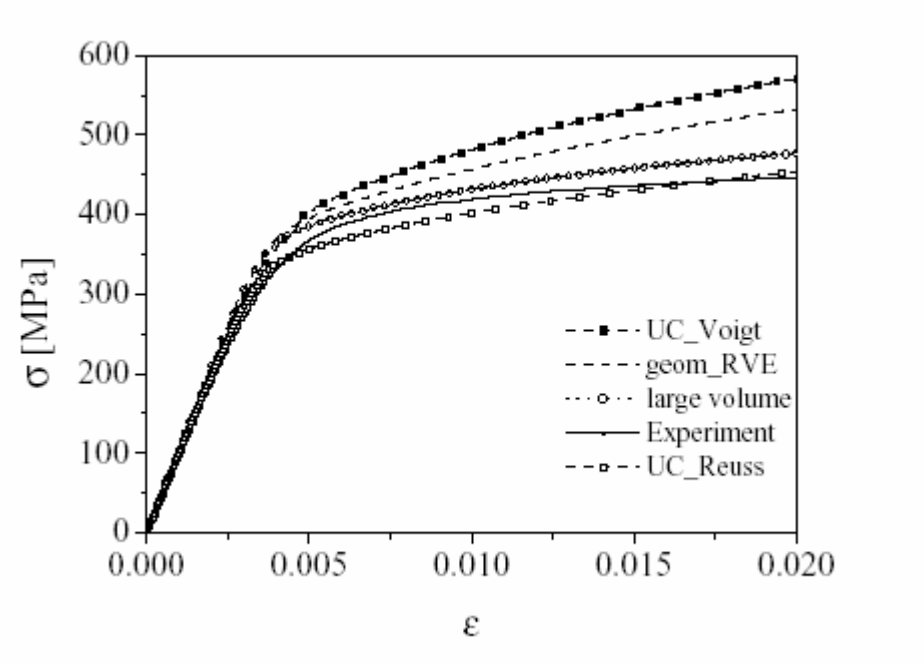

1. A. Borbély, F.F. Csikor, S. Zabler, P. Cloetens and H. Biermann, Materials Sci. Engng. A, *Article in the press.* (2004).
2. J. Llorca, C. González, J. Mech. Phys. Sol. (1998) **46** 1-28.
3. P. Kenesei, A. Borbély and H. Biermann, Proc. ICSMA-13, Budapest, 24-29 August 2003. *In the press.*

MODELLING OF A STEEL REINFORCED THERMOPLASTIC PIPE

M P Kruijer, L Warnet, R Akkerman
University of Twente, Netherlands

Steel Reinforced Thermoplastic Pipe (sRTP) is a new class of pipe that offers the benefits of Polyethylene (HDPE) at pressures up to 120 bar, whereas HDPE is limited to pressures below 16 bar. Such advantages include corrosion resistance, continuous coilable lengths and damage tolerance.

Figure 1 sRTP lay-up

s-RTP is manufactured by overwrapping a thermoplastic liner (i.e. plain HDPE pipe) with a high strength steelcord reinforced tape. The reinforced tapes consist of high strength steel cords embedded in a HDPE matrix. During production of sRTP, the liner with the tapes will be heated to weld them together, resulting in a sturdy monolithic structure.

Experiments indicated that although the cords behave linear elastic, the s-RTP shows considerable time-dependent behaviour and as a result, failure does not solely depend on the height of the load but also on time.

Objectives
The main objective is to prepare a theoretical model for s-RTP to derive the long-term deformation behaviour and time to failure for a set of frequently arising s-RTP configurations and load-cases.

Experiments
Experiments were performed with a 125 mm inner diameter prototype sRTP. With the Flexirig® (see figure 2) it is possible to subject the sRTP to combined loading of internal pressure, torsion and axial tension or compression and to measure the resulting stresses and strains simultaneously.

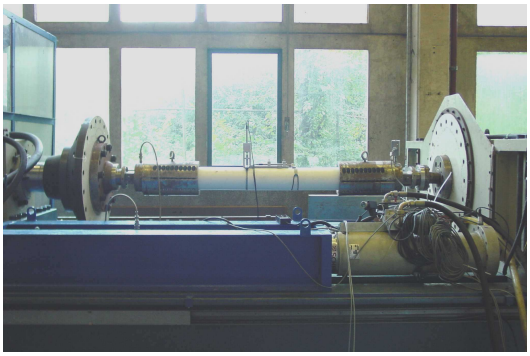

Figure 2: prototype sRTP fixed in Flexirig test facility

As indicated in Figure 3. The sRTP shows considerable time-dependent deformation behaviour when pressurised. As the load bearing capacity of the HDPE decreases in time, the load taken by the steel cords will increase in time, which can finally lead to failure of the sRTP.

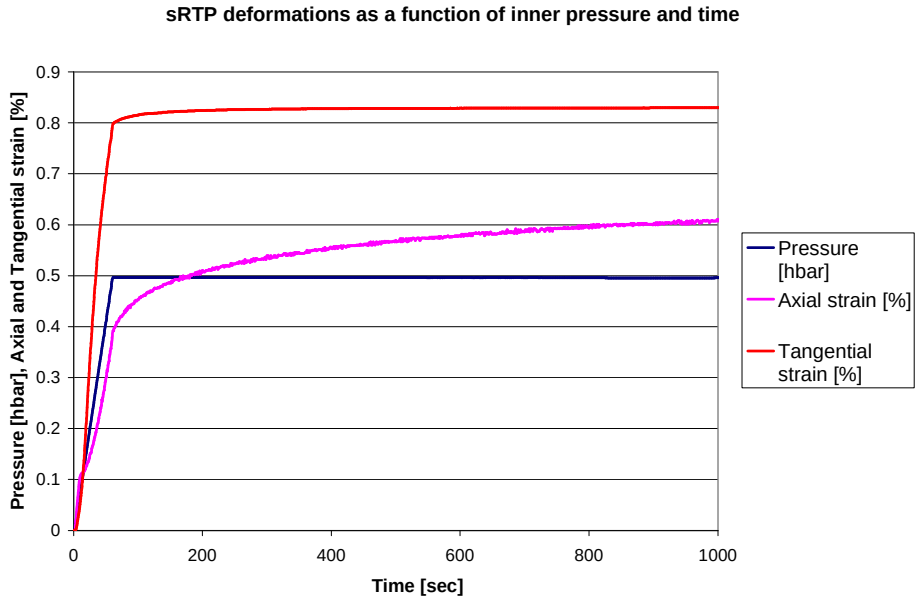

Figure 3 Experimentally measured deformations in axial and tangential direction as a function of inner pressure and time

Modelling
First the s-RTP was modelled linear elastic as a multi-layer thick cylinder, with the reinforcing cords positioned between the layers. A geometrically non-linear system is derived, taking into account the increasing inner diameter of the s-RTP and the changing angles of the reinforcement layers during deformation. The short-term deformations for the hydrostatic pressure load case are well described by the linear elastic multi-layer model. In addition, to model the long-term deformation behaviour and time to failure, the model was extended to allow for the visco-elastic properties of the HDPE.

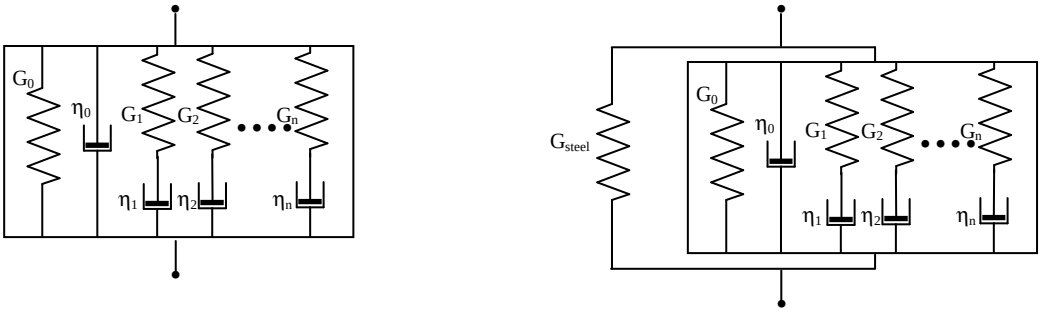

Figure 4 Generalised Maxwell model for the HDPE (left) and the steel reinforced HDPE tapes (right)

It is assumed that the HDPE behaves linear viscoelastic and that the relaxation function can be described by generalised Maxwell model. (see Figure 4) For the steel reinforced tapes a spring, which represents the stiffness of the cords, is connected in parallel with a generalised Maxwell model. It is assumed that the viscoelastic behaviour of the HDPE is only present in the deviatoric direction. Therefore, the compression modulus is assumed to be constant and is defined by a single constant K. The different parameters in the Maxwell model are found from relaxation experiments with both HDPE tensile bars (1D uniaxial stress) and thin walled HDPE pipes (2D plane stress)

At the time of writing, the model for the long-term behaviour is not completely finished, so no result is available yet. After finishing the model, the results of the long-term experiments obtained with the flexirig (see figure 2, 3) will be compared with the results obtained with the model.

References

M.P.Kruijer. 'Analysis of the properties of a Reinforced Thermoplastic Pipe', *Composites Part A*, to be published early 2004.

THE EFFECTS OF STIFFNESS VARIABILITY ON THE OBSERVED FLEXURAL PERFORMANCE OF A COMPOSITE BOX-SECTION BEAMS UNDER THREE POINT BENDING – A STATISTICAL APPROACH.

N.Papadakis, N.Reynolds
International Automotive Research Centre, Warwick Manufacturing Group (WMG)
University of Warwick, Coventry, United Kingdom

This paper discusses the effect of stiffness variability on the expected flexural performance of a composite material beam. Engineers implicit assume that the deflection under the load introduction point of composite beams under 3 point bending at a given load (in the elastic region) is a Gaussian (normal) distribution ($d \sim N(\mu_d, \sigma_d)$). Often the results deviate from the normal distribution and that is attributed to the experimental error or poor manufacturing, however the authors believe that there the probability distribution of the deflection is inherently skewed.

To test this hypothesis, a Monte Carlo methodology was used – see Figure 1. Gaussian (normal) probability density functions (pdfs) were randomly sampled to generate stiffness properties of skin and core materials of an encapsulated sandwich beam, and also for the stiffness properties of a monolithic steel and monolithic composite box beam. The generated values were introduced to the analytical expression for the deflection under the load introduction point for three-point testing (for simplicity the shear induced deflections are not included) which yield a population (1000 shots) of the deflection under the load introduction point. Then, the kernel density estimation was generated from the simulation generated deflection values.

The theoretical analysis concluded that for increasing coefficient of variance (CoV) within the material stiffness properties, the probability distribution of the deflection under the load introduction becomes increasingly biased. The estimated mean of the deflection under the load introduction point is always greater than the median value. Finally, the theoretical value of the deflection of the load introduction point based on the nominal stiffness properties was best approximated by the median instead of by the mean of the deflection kernel density estimation (see Figure 2).

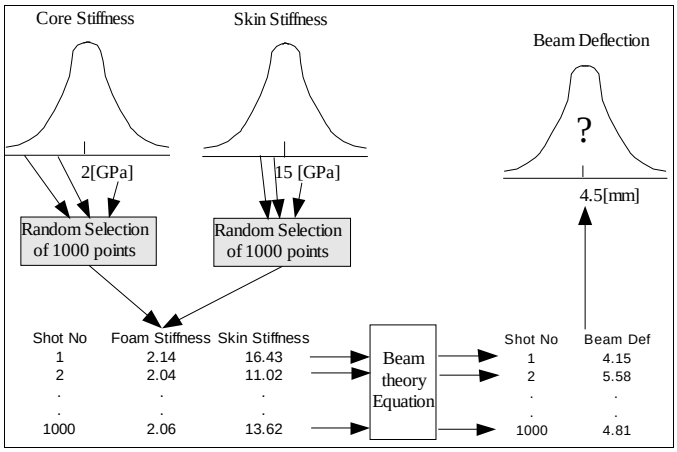

Figure 1: Monte Carlo methodology flowchart

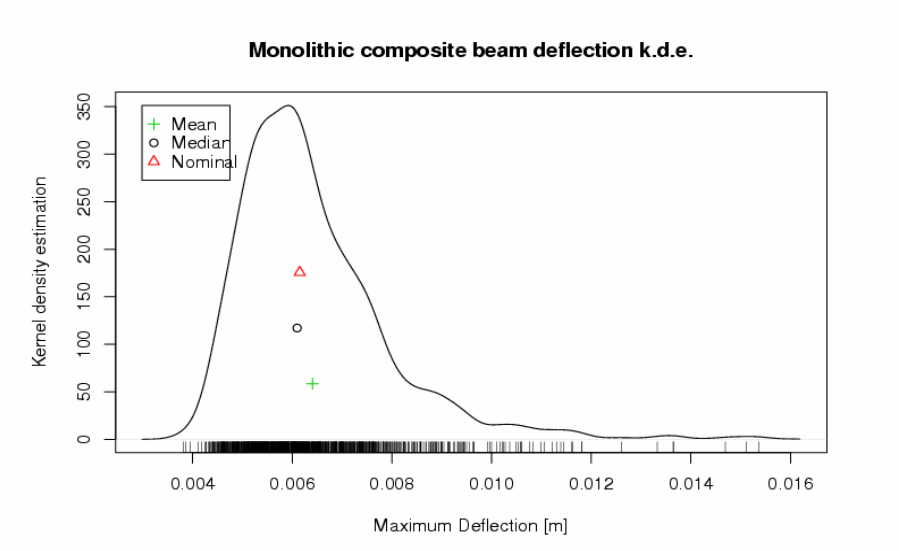

Figure 2: Flexural deflection probability density function for a monolithic composite beam.

This paper discusses the implications of the findings from an experimental/characterization and a design perspective.

SESSION 2 – SCALING EFFECTS AND NOTCHES

Chair: Prof. Paul Curtis
dstl, UK

Tuesday 21 September
11.10-12.50

SIZE EFFECTS IN UNIDIRECTIONAL AND QUASI-ISOTROPIC COMPOSITES LOADED IN TENSION

B. Khan, K. Potter, S. R. Hallett and M. R. Wisnom
Department of Aerospace Engineering
University of Bristol, University Walk, Bristol, BS8 1TR, UK.

Introduction:

It is well known that the strength of composites is inversely related to the size or volume of the specimen tested. The study of scaling in composites is important, when data from small test coupons are used for designing large structures. If these effects are not taken into account during the design, catastrophic failure could result. On the other hand if the design were highly conservative it would result in a weight penalty. This necessitates an understanding of the effect of size on the strength of the system. In the present study size effects of unidirectional composites (glass and carbon fibers) and quasi-isotropic laminates were investigated with change in volume.

Materials and specimen:

Two types of composite material were used in this experiment they are Glass fiber epoxy (E-Glass/913) and Carbon fiber-epoxy (IM7/8552). Tapered specimens with unidirectional fibers were made by interleaving dropped plies between the continuous plies. The details of the specimen configuration and the dimensional details are given in Table 1 below.

Table 1 Details of UD specimen configuration and dimensions.

Specimen ID	Number of plies at gauge section	Specimen thickness (mm)	Specimen widths (mm) for Glass; Carbon	Specimen gauge length (mm)
S-4	4	0.5	10; 5	30
S-8	8	1.0	20; 10	60
S-16	16	2.0	40; 20	120
S-32	32	4.0	--; 40	240

Quasi–isotropic (QI) specimen $(+45_m/90_m/-45_m/0_m)_{ns}$ were made with uniform thickness and were scaled in two ways namely sub-laminate and ply-level scaling. The specimen configurations are given in Table 2.

Table 2 Details of QI specimen configuration and dimensions.

Specimen ID	Number of plies	Specimen thickness (mm)	Specimen width (mm)	Specimen gauge length (mm)
QI-1	8	1	8	30
QI-2	16	2	16	60
QI-4	32	4	32	120
QI-8	64	8	64	240

Results:

In general the strength of unidirectional specimens was found to decrease with increase in volume of the specimen tested. The strength reduction for carbon specimen was found to be about 5-10% between each step change in size while glass specimens showed little reduction (<3%) Table 3. Accordingly the Weibull modulus for glass specimens was found to be about 150 while for carbon it was 40. These values are higher than reported in the literature. The quasi-isotropic ply-level scaled specimens showed a large reduction in strength with increase in ply thickness while the sub-laminate level specimens showed a slight increase in strength with increasing laminate thickness. The results from the QI tests are summarised in Table 4.

Table 3. Results obtained for unidirectional glass and carbon specimens with change in volume.

Specimen ID	Failure stress for Glass (MPa)	Failure stress for Carbon (MPa)
S-4	1512	2806
S-8	1516	2683
S-16	1471	2553
S-32	*	2347

* Specimens damaged with grip failure

Table 4. The variation of strength with thickness for the two scaled of quasi-isotropic specimens.

Thickness (mm)	Failure stress (MPa) Sub-laminate level	Failure stress (MPa) Ply-level
1	842	
2	911	670
4	929	541
8	-- --	460

Conclusion:

The strength of unidirectional composites shows a decrease with increase in size of the test sample although the variation is less for glass composites than carbon. Quasi-isotropic specimens with ply-level scaling showed a significant reduction in strength with increase in thickness of the plies although not much variation is seen for the sub-laminate level scaling. This is because the ply-level scaled samples showed an early onset of delamination and hence the failure was essentially controlled by delamination. The sub-laminate scaled samples showed a higher resistance to delamination and accordingly showed higher strength values with the final fracture showing a dominant fiber failure.

STRENGTH SCALING MECHANICS OF POLYMER COMPOSITES

Torben K. Jacobsen
Material Mechanics, LM Glasfiber A/S, Rolles Møllevej 1, 6640 Lunderskov, Denmark
Bent F. Sørensen
Risø National Laboratory, Frederiksborgvej 399, 4000 Roskilde, Denmark

The design of large-scale composite structures is typically based on design allowables established by simple coupon tests. However, it has become evident that a reliable design of large structures demands testing at all length scales. LM Glasfiber A/S applies an integrated testing methodology, which ensures that the composite components exhibit low cost and high reliability [1]. Besides low cost and high reliability it is also important that new composite materials can be qualified quickly and enter new structural designs. As shown in Figure 1, it is preferable to make most tests at small length scales, because the specimen geometry is less complex and specimens are cheap to make. So, from an industrial point of view, material qualification and development on small length scales are desirable for characterisation of fundamental material properties, before starting to make components for test. The road to success, when scaling up, is to establish how a strength property at a lower length scale controls the strength at a higher length scale.

In this paper we demonstrate how fracture mechanics characterization made at small test specimens can be used for predicting the load carrying capacity of much larger structures. Double Cantilever Beam (DCB) specimens were used for characterizing the fracture resistance of an adhesive joint. A significant part of the joint strength is due to fiber cross-over bridging. Having measured the steady-state fracture resistance, the fracture strengths of ten times larger bending-loaded adhesive joints is then predicted solely based on geometry parameters, see Figure 2.

The steady-state fracture energy is the integral of bridging stresses and crack opening displacements. The shape of the bridging law (stress-displacement) contains the information regarding which mechanisms that are active at the constituent level (fibre-matrix-adhesive interfaces). The shape of the bridging law during fibre crossover bridging is controlled by the interface strength between fibre and matrix. This interface strength is again controlled by the molecular structures that form the interphase between fibre and matrix. At the other end of the scale the external loads acting on the adhesive joint have to be calculated by a global analysis of the whole structure as the joints then will be loaded in a combination of load and displacement control depending on the flexibility of the structure. The global loads are then entered into a fracture strength surface, which depends on actual joint geometry and mixed mode fracture strength obtained from simple DCB test specimens.

References:

[1] J. Korsgaard and T. K. Jacobsen, "Integrated testing in reliable design of large wind turbine blades," European Wind Energy Conference and Exhibition (EWEC); 16-19 June 2003, Madrid, Spain.

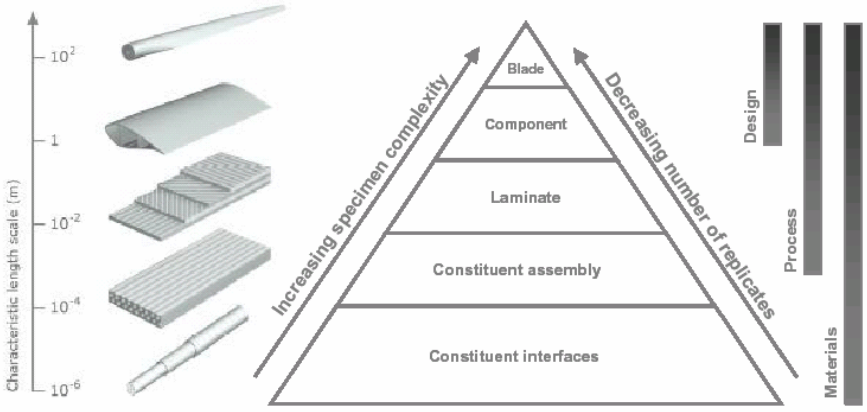

Figure 1: Length scales and levels of materials testing.

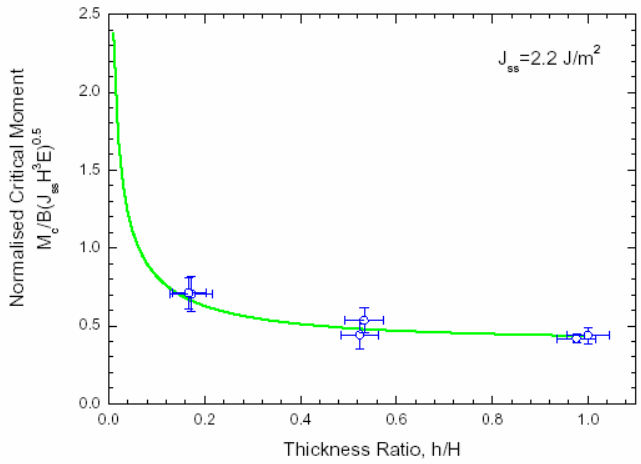

Figure 2: Strength prediction of a large bending loaded adhesive joint. Predicted (solid line) and measured values (points) of applied moment at crack growth as a function of thickness ratio, h/H.

TENSILE SCALING EFFECTS IN NOTCHED COMPOSITES

B. Green, M.R. Wisnom and S.R. Hallett
Department of Aerospace Engineering, University of Bristol, University Walk, BS8, 1TR, UK

Introduction

With the use of increasingly large composite components on aircraft comes the need for reliable design guidelines so as to be able to extrapolate data from laboratory tests with confidence to the full size components, thus reducing the need for full-scale testing. Holes are required in aircraft components for joints, access, or to allow wires to run through solid pieces. In the present project, an extensive testing program has been conducted to investigate the influence of specimen size on the notched tensile strength of composites, and the mechanisms behind variations. The results are to be
used to develop a finite element method to aid engineers in the design of large composite structures.

Testing Program

A testing program has been conducted on a quasi-isotropic lay-up with specimens containing a centrally located hole, loaded through a quasi-static tensile configuration. IM7/8552 uni-directional carbon fibre pre-preg is being used with a [45/90/-45/0]s lay-up. The testing matrix showing the scope of this investigation is shown in Figure 1. Three different types of scaling have been investigated: Thickness, in-plane and three-dimensional scaling, with scaling factors doubling with each increment to a maximum of 8. Two different scaling methodologies have also been followed: Sublaminate-level scaling, where the stacking sequence is repeated as many times as is required to achieve the correct laminate thickness, and ply-level scaling, where the thickness of each ply is increased to obtain the required thickness. The ratios of w/d and l/d have been kept constant throughout, at 5 and 20 respectively, as has the strain rate during testing.

Results

Initial results show that in all cases of scaling (thickness, in-plane and 3-D) there is a strength reduction for both ply-level and sublaminate-level scaled laminates. An increase in all three dimensions of a specimen by a factor of 8 leads to a decrease in strength of 42% for the sublaminate- level scaling method and 57% for ply-level scaling. There was also a change in failure mechanisms observed in some related series of specimens, as illustrated in Figure 2. Here, scaling the in-plane dimensions of a 8mm thick sublaminate-level scaled specimen by a factor of 8 leads to a change from a failure with extensive delamination, pull-out and splitting present, to a cracklike one.

Conclusion

A size effect has been observed in the scaling of notched composites, with various factors associated with the type of scaling affecting the extent of the phenomenon. Further tests are ongoing to complete the testing matrix shown above and thus be able to quantify the size effect as fully as possible. A program of non-destructive and interrupted testing is being conducted to investigate in detail the sequence of events leading to the different failure mechanisms observed. Various theoretical and computational analysis techniques are being used in conjunction with the results to help understand the reasons for the strength and mechanism variations observed.

t (mm)	Sublaminate-level Scaling (hole sizes in mm)				Ply-level Scaling (hole sizes in mm)			
	3.175	6.35	12.7	25.4	3.175	6.35	12.7	25.4
1								
2								
4								
8								

Figure 1 Testing matrix for experiments

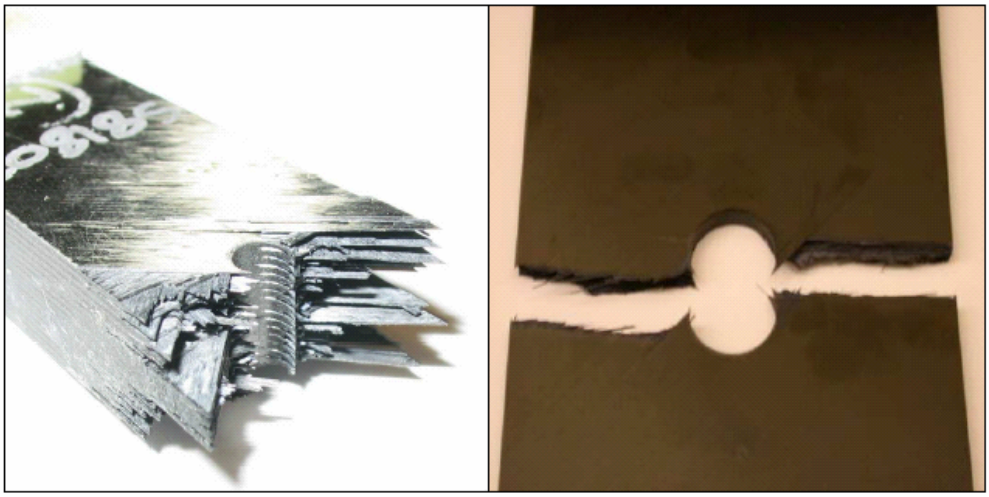

a) b)

Figure 2 Post-failure pictures of 8mm thick sublaminate-level scaled specimens with a) 3.175mm hole, and b) 25.4mm hole

MESH INDEPENDENT MODELING AND MOIRÉ INTERFEROMETRIC EXAMINATION OF THE ACCUMULATION OF DAMAGE IN COMPOSITES WITH OPEN-HOLES

D. Mollenhauer[1α], E. Iarve, [2] and R. Kim[2]
[1] U. S. Air Force Research Laboratory, AFRL/MLBC, Wright-Patterson AFB, OH 45433-7750
[2] University of Dayton Research Institute, 300 College Park Ave., Dayton, OH 45469-0168

Three-dimensional ply level modeling of multiple matrix cracking near an open hole in a quasi-isotropic composite laminate was performed. A mesh independent displacement discontinuity modeling method based on higher order shape functions was constructed for this purpose. The mesh configuration is dictated by the boundaries of the specimen, such as the presence of a hole, whereas the matrix cracking surfaces are aligned with the fiber direction in a given ply. The surface of the displacement jump associated with matrix cracking was defined in terms of the domain Heaviside function approximated by using higher order polynomial B-splines. Several matrix cracks in each ply of a $[0/45/90/-45]_s$ composite were modeled, and their effect on the fiber direction stress magnitude in the 0^0 ply was examined. Up to 35% relaxation of the of the fiber direction strain amplitude was predicted due to matrix cracking (splitting) of the 0^0 ply. Moiré interferometry was used to experimentally determine the strain and displacement fields in the surface layer of the same composite, previously prestressed beyond the damage initiation load. Good correlation between the experimental data and the stress redistribution predicted by the mesh independent damage modeling technique was observed.

α Corresponding author, tel.:01-937-255 9728, e-mail: david.mollenhauer@wpafb.af.mil

SESSION 3 – TESTING

Chair: Dr Ivana Partridge
Cranfield University, UK

Tuesday 21 September
14.00-15.40

TESTING OF MARINE COMPOSITES. FROM MATERIALS TO STRUCTURES

Peter Davies
Materials & Structures Group, IFREMER Centre de Brest, BP 70, 29280 Plouzané, France
peter.davies@ifremer.fr

Composite materials have been used by the pleasure boat industry for over 50 years. Glass fibre woven roving and mat have been the main reinforcements and polyester has traditionally been the matrix resin. Experience plays a large role in design but new safety legislation, the arrival of improved fabrication methods such as infusion, and the development of other applications (high performance craft and offshore) is resulting in increasingly large test programmes. This presentation will give an overview of marine applications of composite materials, illustrated by some examples of material and structural test programmes for four applications :

- small boats
- racing yachts
- offshore structures
- underwater vehicles

For each example the material and design requirements will be discussed, followed by a presentation of the tests performed to validate design choices.

Test developments for small boats are being influenced by a current draft ISO document (ISO/DIS 12215, Hull construction, Scantlings- Part 5 Design pressures for monohulls). This indicates required material properties and proposes a drop test for boats less than 6 metres long, Figure 1a. Racing yacht design teams are very reactive to new materials and processes and provide a test platform for innovative composite solutions, Figure 1b. Wave impact is one of the loading cases which needs to be evaluated for such structures and a simple test has been developed to evaluate sandwich materials. The requirements for offshore structures are quite varied, fire resistance is often the primary criterion and high-energy impact and blast resistance may also be critical. A demonstration test for composite floors will be described, based on a 4-ton container drop test (120 kJ impact), Figure 1c. Finally, the use of composites in pressure hull applications will be described, and results from hydrostatic pressure tests will be discussed, Figure 1d.This is an example where the loads are clearly defined by the immersion depth but biaxial compression tests are required to determine design allowables.

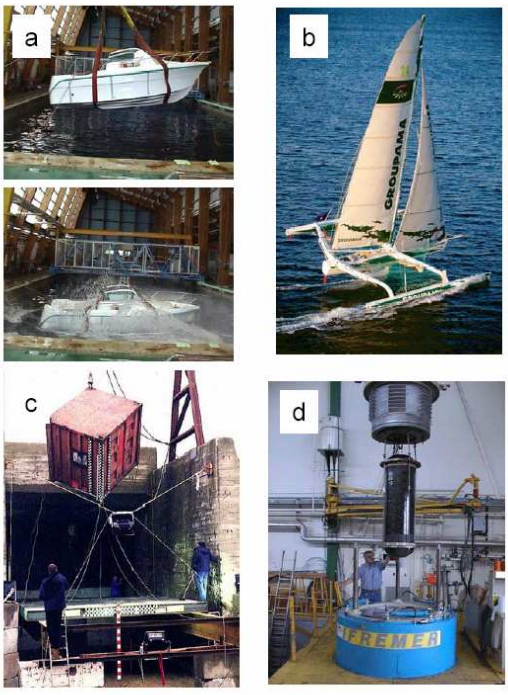

Figure 1.Examples of tests on marine structure

a) Drop weight test to check motor boat hull integrity
b) Racing multi-hull
c) 120 kJ impact on composite floor
d) Pressure test on carbon/epoxy prototype underwater vehicle.

A TENSILE SETUP FOR THE IDNS COMPOSITE INTERLAMINAR SHEAR TEST

Kaj B. Pettersson and Jonas M. Neumeister
Dept. of Solid Mechanics, KTH - Royal Institute of Technology, SE - 100 44 Stockholm, Sweden

To date, the inclined double notch shear (IDNS-) test is the best performing test method for measurement of composite interlaminar shear properties. In-situ measurements of strain fields confirm a more homogeneous shear strain state in the test region. Moreover, the IDNS-test is capable of producing higher interlaminar shear-strength (ILS-) values than other methods, a suitable benchmark when comparing shear test methods. However, it suffers from some unresolved issues which justify the further development presented here.

The original IDNS-test uses the standard DNC-specimen, which is furnished with two notches cut to the center of the specimen, one from each panel face. The test region is thereby confined to the central interlaminar layer between the two notch roots. The specimen is subjected to a combination of two load cases (Figs 1a-c): normal compression (*N*) and bending (*M*). The load case *N* is in essence the standard DNC load-case with its well known shortcomings in terms of high (compressive) stress concentrations in the vicinity of the notches. The (tensile) load case *M* is superimposed in order to counteract these severe stress concentrations. Additionally, nearly homogeneous shear stresses are obtained, c.f. Fig 1d. Correct proportions among the load-sets are chosen such that the combination of arising symmetrical mode-I stress intensity factors vanish, *i.e.*

$$K_{\mathrm{I}}^{N} + K_{\mathrm{I}}^{M} = 0$$

in a specimen were the notches are treated as sharp cracks.

With the original IDNS-test setup, the two load cases *N* and *M* are created by statically determined support reactions (*N*, *P*, and *R* in Figure 1c) from a special test fixture. Mutual proportions among these are then adjusted by inclination of the fixture relative to the external load. In this setup, specimen deformation occurs which may alter the conditions at the notches continuously throughout a test. Moreover, compressive loading of the specimen implies a potential instability of the setup.

A modified (tensile) IDNS-test setup, schematically shown in Fig. 2a–b, was proposed which dealt with the issues related to the original IDNS-loading configuration. It used the same doubly notched specimen again subjected to a statically determined combination of loads in order to minimize arising stress concentrations at the notch roots. The specimen was fixed in two special holders, c.f. Fig. 2b, which transferred a tensile load (*N* in Fig. 2b) through shear over the gripping length l_g. The counteracting bending was accomplished through the forces *N*, *P* and *R*, c.f. Fig. 2b. The forces *P* were applied *inside* the notched region ($l_P < L$, in Fig. 2b) to secure the highest shear stresses there, not in the ligament opposite to each notch. The latter would inevitably lead to premature specimen failure and should thus be avoided. A straight forward analysis of the specimen loading and geometry together with the IDNS-criterion (1) gave an expression for the specimen inclination as,

$$\alpha = \operatorname{atan}\left[\frac{b(f^{N}(l_P + L_{\mathrm{tot}} + l_l) - 3f^{M}(L + l_P))}{3f^{M} l_P (L_{\mathrm{tot}} - L + 2l_l)}\right],$$

where *b* is the specimen thickness, and f^{N} and f^{M} are shape functions for the respective stress intensity factors $\mathrm{K_I^N}$ and $\mathrm{K_I^M}$ found in handbooks. Based on analyses of the setup, the lengths l_g and l_l were chosen to 30 mm and 20 mm, respectively.

Numerical (FEA) and experimental studies were performed on a uniaxial carbon/epoxy composite. Further testing conditions such as notch distance and appropriate specimen inclination, in Fig. 2a, were specified for optimal test performance in terms of achieved shear strengths and shear strain fields. It was confirmed that the modified IDNS-setup produced ILS-values of the same magnitude as the original setup. Gripping of the specimen was critical at high loads, and knurled gripping surfaces were used to circumvent related issues. Instability of the setup was no longer an issue. However, specimen bending still occurred, but to a much smaller

extent than before. This implied that the conditions in the notched regions were essentially unchanged during a test. Thereby, load proportions chosen according to the IDNS-criterion (1) would hold throughout the entire test.

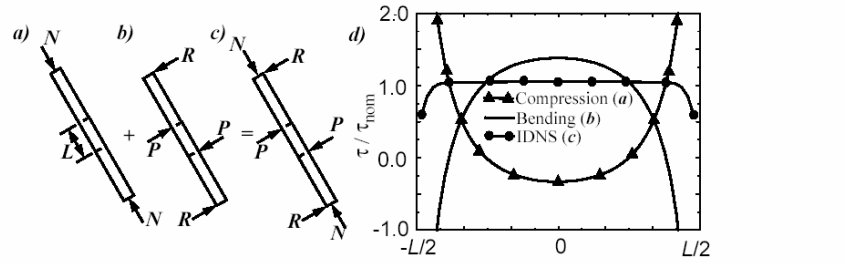

Figure 1 a–c: the original IDNS-loading configuration, and d: resulting shear stress profiles

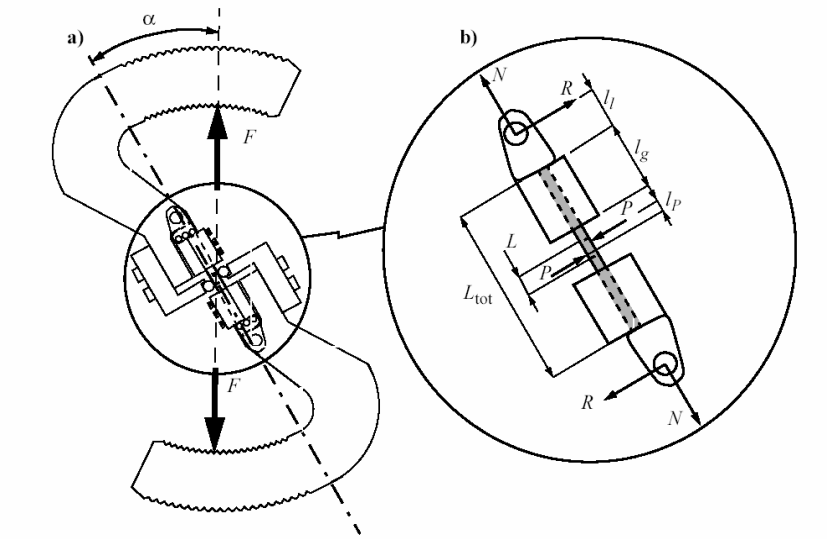

Figure 2 a: the modified IDNS-setup, and b: specimen loading.

INFLUENCE OF A NEAR FREE EDGE ON THE IMPACT OF THICK CFRP PANELS

Charles Breen, Felicity Guild and Martyn Pavier
Dept. of Mechanical Engineering, University of Bristol, UK

Carbon fibre reinforced plastic laminates of the order of 24mm thick are being considered for the wing panels of large civil aircraft. Knowledge of their properties after impact is a critical design criterion that needs to be explored fully. Further, the design of these wing panels will include access holes. The panel's impact behaviour will be considerably different when impacted close to these holes. In this paper, the effect of impact near a free edge is considered in detail. The results from a series of experiments are presented and compared with some finite element analysis.

Multidirectional carbon fibre/epoxy laminates have been manufactured using the resin film infusion process and autoclaved cured. The non-crimped fabrics used allow thick laminates to be manufactured with relative ease, and using a stacking sequence block that produces a 4mm thick laminate, plates with thicknesses 4mm, 8mm and 12mm have been produced.

A 4.3m tall, instrumented drop weight impact tower was used to impact the laminates. The impact tower is instrumented to measure the impact velocity and acceleration of the impactor, which can obtain incident impact energies up to 400J. Specimens were clamped on a steel fixture with a 200mm diameter hole. Following impact the specimens were ultrasonically non-destructively tested using a C-scanning system. This allows determination of the delamination area and depth of the major delaminations. Finally 50mm wide coupons with the impact location at their centre were cut from the panels and tested in tension and compression for residual strength measurement.

The tests have shown that the damage arising from an edge impact is significantly different compared to a central impact where the panel lay-up and materials, and impact are the same. In a central impact the damage is dominated by fibre breakage and back face splitting. In an edge impact there is much less surface visible damage, instead large delaminations that grow to the extent of the fixture, as shown in the enhanced photograph in Figure 1.

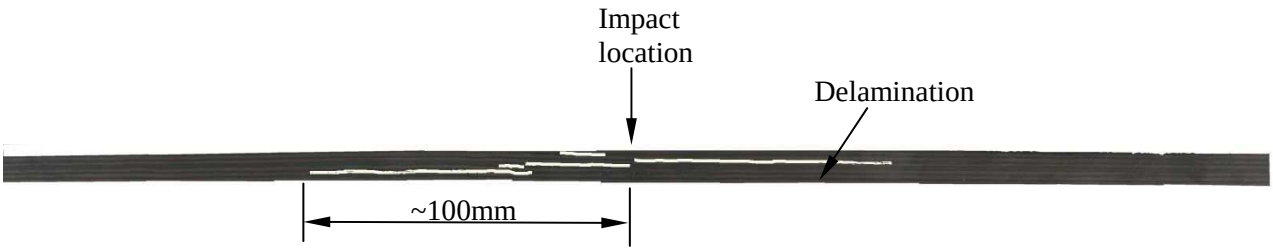

Figure 1 – Photograph of the edge of the edge impacted panel, showing delaminations

The extent of the delaminations can be seen in the C-scan results, looking at the plot of the intensity of the back face reflection shown in Figure 2. The plate was impacted twice, the dark blue area on the left the delamination due to the edge impact and the dark blue area to the right that due to a central impact. The red circle indicates the position and size of the fixture for the edge impact, the fixture clearly limiting the size of the delaminations.

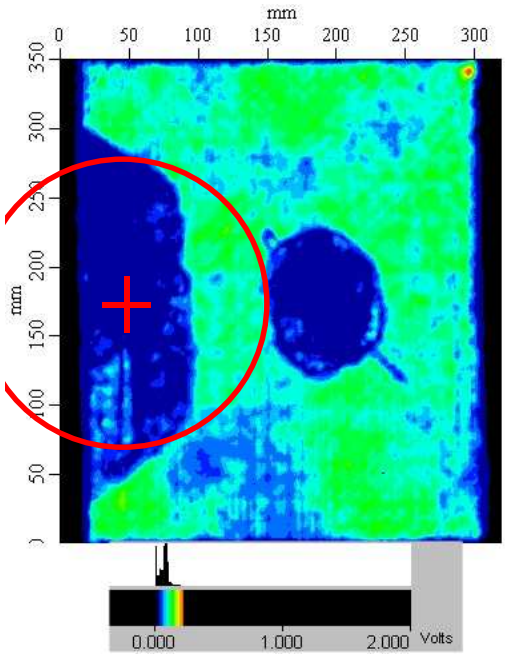

Figure 2 – C-scan plot showing back face reflection intensity for an 8mm thick plate impacted near a free edge and the centre with 200J

Subsequent residual strength tests have shown that the post impact strengths of edge and centrally impacted coupons are different. Centrally impacted laminate coupons have smaller residual tensile strength compared to the equivalent edge impacted coupon due to the greater extent of fibre breakage. The edge impacted laminate coupons have smaller residual compressive strength compared to the equivalent centrally impacted coupon due to the greater extent of delaminations. In each impact situation a different energy absorption mechanism dominates. This is vital to the aeroplane designer as the laminate's post impact behaviour is consequently also different.

POSTER SESSION 2

PROBABILISTIC METHOD TO DEFINE A DEVELOPMENT TEST CAMPAIGN IN THE ENGINEERING PROCESS

Carlos Ramos Gutiérrez
MS in Aero-Structures Engineering by Aeronautical Engineering School at Madrid
Bóreas, Ingeniería y Sistemas (Sener Group)

Design process with composite material usually requires the management of a set of activities strongly interconnected. Firstly, it is necessary a development test campaign in order to get a finest characterization both of the materials and the structural assembly itself (i.e. sandwich or laminate arrangement). It is typical either to devote too much effort trying to fit the probabilistic density function of a certain parameter (i.e. Young modulus) or devote almost nothing. Secondly, it is necessary an efficient analysis tool. Usually it is mandatory the use of extensive and comprehensive FE models in order to obtain a good validation of the proposed structural assembly. It is a common understanding from engineering community that as the number of elements in a FE model increase also the correlation between analysis and test increases. Also, in addition with the correlation procedure, there are also some "know-how" and in-house codes which apply specific rules to specific problems (i.e. no valid for the rest of the universe). It always seems that there is something lost in the middle of the process. There is an answer to this question: uncertainty. Uncertainty is not just a name, it is also something physic, actual and every engineer have to live with. Always, it have been assumed that uncertainty is something not desirable and many professionals try the hide this term in the bottom of their drawer. Why?, in the opposite, uncertainty is a powerful means to define the number of specimens required in a test campaign, it is also a good way to limit the size of the FE model and to improve the behaviour and robustness of the structure. The only thing left is to think how to manage uncertainty. This is the role of Monte Carlo simulation. Through an extensive analysis and testing campaign, using Monte Carlo processes coupled with Nastran, this paper proposes a methodology able to address issues like composite characterization and failure, FE modelling and structure optimisation. To give an example, the methodology allow to define the required number of specimens in a test campaign. It is proposed that the size of the sample depends on the uncertainty of the requirements for which the structure must be sized, also links among several features structural behaviour and material uncertainties are shown. One answer that is really important to every engineer who plans a test campaign.

AN IMAGE ANALYSIS APPROACH FOR THE STRUCTURAL CHARACTERISATION OF PYROCARBONS

J P da Costa, C Germain, P Baylou, M Cataldi
ENSEIRB, ENITAB, France

Thanks to their physical properties, carbon/carbon composites have been used in a growing number of domains e.g. aerospace industries or motor sports applications. Pyrocarbons are used in the densification process of such materials. As material properties depend on the nature of the pyrocarbon deposit, several studies have been carried out on the mechanisms involved in the deposit process [3][4][9] but few of them concern the heterogeneous phase mechanisms. High Resolution Transmission Electron Microscopy is a relevant technique to investigate the nanometric structure of such materials since, in the 002 lattice fringe imaging mode, it allows the direct visualization of graphene layers. This technique has been used in literature to access crystallographic information such as the length L_1 of a perfect fringe, the length L_2 of a distorted fringe or the number N of fringes in distorted stacks (see [6] for a recent review). In this paper, we focus on the structure of pyrocarbons obtained by Chemical Vapor Infiltration and observed by Transmission Electron Microscopy (TEM) imaging. More particularly, we present an automated approach to the quantitative description of fringe lengths and propose a simple stochastic model for fringe description which corroborates the obtained length statistical distributions.

Fringe Extraction Algorithm

Recent quantitative studies dedicated to the characterization of pyrocarbon structure by TEM imaging have been reported in literature. Germain et al. [2] focus on the multi-scale anisotropy of fringe arrangements. Their approach is based on the image orientation field and does not require the explicit extraction of the fringes. On the contrary, the structural approach of Shim et al. [8] assumes the prior extraction of fringes. Their image analysis framework provides statistics on the length, the tortuosity and the orientational order of graphene

layers. It consists in several stages including filtering, thresholding/binarization and squeletonization. Later, Rouzaud and Clinard [7] have proposed a quite similar approach where the thresholding step is improved by a top-hat topological operation.
In this paper, we present a structural approach to extract the fringes and compute length statistics. It proceeds in two steps. First of all, TEM images, obtained with a 430,000 magnification and digitalized with a resolution of 2000 dpi, are preprocessed by a smoothing filter which combines both a frequential and a directional filtering. Then, fringe identification is performed using the level curve tracking algorithm previously presented in [1]. This algorithm consists in tracking the level curves which go through a pre-defined set of seeds until they reach the extremities of the patterns i.e. until an abrupt change occurs in the orientation of the curves. It results in a set of parametric curves, called generatrices, connecting the extremities of the patterns. These generatrices are obtained from the grey level picture by a sub-pixel interpolation. This technique allows to fit better the underlying layers and avoids the drawbacks induced by the thresholding and binarization steps [8]. An example is given in Fig. 1a where generatrices are superimposed on the filtered image. Generatrices interrupted by the image border are not represented and not included in the statistics. Note that in practice, the images used to compute length statistics are much larger.

Fringe Length Statistics

Figure 1b shows examples of length distributions computed on four series of pictures. PB and PC are two materials obtained by CVI. The suffixes T and nT correspond respectively to the materials which have been subjected or not subjected to a post thermal treatment. Such statistics allow to compare different materials on the basis of their fringe lengths and also to characterize quantitatively the effect of temperature on the pyrocarbon structure. Beyond this kind of information, it can be seen that these distributions have a specific shape. They show a mode between 5 and 10 angstroms (depending on the material), a rapid fall under this maximum and a long tail for greater lengths. We have shown that the right tail of the distribution presents an exponential decrease.

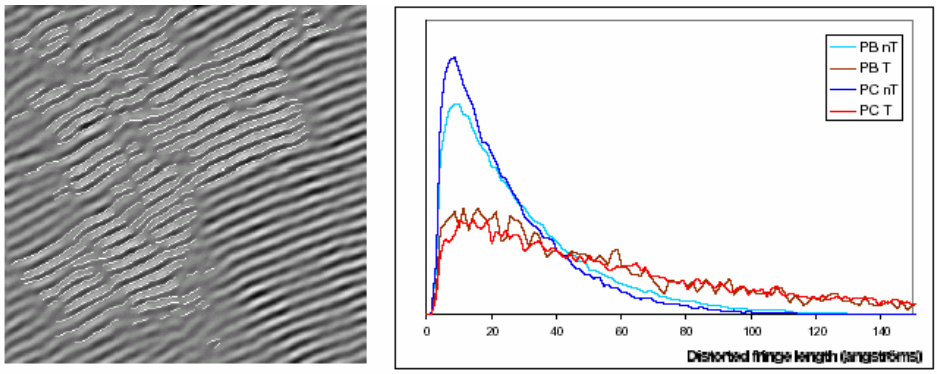

Figure 1. (a) Example of a composite material image: level curves are superimposed. (b) Fringe length histograms obtained on four different material.

A Stochastic Model for Structure Description

The results above suggest that the fringe length may fit a simple stochastic model. Inspired by recent knowledge on pyrocarbon structure [3-6,9]), we have proposed a structural model for the description of the fringes. The model, presented on Fig. 2, describes the fringes individually, without taking into account the relations between neighboring fringes. It assumes that a distorted fringe, with length L_2, arises from an arrangement of contiguous perfect (straight) fringes and that any straight fringe, with length L_t is made of aligned elementary patterns of length L_0. Despite its simplicity, this model finally corroborates the experimental distributions observed on material images, and opens new ways of progress in the knowledge of the heterogeneous phase mechanisms through possible correlation between L_0 and the size of the molecules involved in these mechanisms.

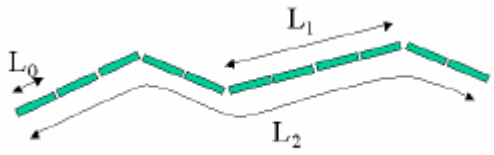

Fig. 2. Structural model for fringes

References

[1] J.P. Da Costa, C. Germain, and P. Baylou, "Level curve algorithm for textural feature extraction", *Proc of ICPR*, pp. 921-924, Barcelona, 2000.
[2] C. Germain, J.P. Da Costa, O. Lavialle, P. Baylou, "Multiscale estimation of vector field anisotropy. Application to texture characterization", *Signal Processing*, vol. 83, no 7 , pp. 1487-1503, July 2003.
[3] J. Lavenac, F. Langlais, X. Bourrat, R. Naslain, J. Phys. IV, France 11 (2001) Pr3 – 1013.
[4] H. Le Poche, "Mécanismes chimiques de CVD/CVI des pyrocarbones laminaires issus du propane: cinétique texture et composition", PhD Thesis, University Bordeaux 1, in French, 2003.
[5] A. Oberlin, in: Thrower PA (Ed.), *Chemistry and Physics of Carbon*, vol. 22, Dekker, New York, 1989, p. 1.
[6] A. Oberlin, *Pyrocarbons*, Carbon, vol. 40, 2002, pp. 7-24.
[7] J.-N. Rouzaud, C. Clinard, "Quantitative high-resolution transmission electron microscopy: a promising tool for carbon materials characterization", *Fuel Processing Technology*, vol. 77-78, 2002, pp. 229-235.
[8] H.-S. Shim, R.H. Hurt, N.Y.C. Yang, "A methodology for analysis of 002 lattice fringe images and its application to combustion-derived carbons", *Carbon*__no 38, 2000, pp. 29-45.
[9] W.G. Zhang, Z.J. Hu and K.J. Hüttinger, Carbon 40 (2002), 2529.

STRENGTH EVALUATIONS FOR STITCHED CFRP LAMINATES

Yutaka Iwahori#, Shin Horikawa##, Masataka Yamamoto##,
Takashi Ishikawa# and Hiroshi Fukuda##
#Advanced Composites Evaluation Technology Center, Japan Aerospace Exploration Agency
Osawa 6-13-1, mitaka-shi, Tokyo Japan 181-0015

##Department of Science and Technology
Tokyo University of Science, Yamazaki 2641, Noda, Chiba, JAPAN 278-8510

Carbon fiber (CF) and Kevlar stitching effects on CFRP laminates strengths have been investigated experimentally. The CFRP laminates are fabricated by RTM as low cost consolidation cure method. Figure 1 shows a picture of double cantilever beam (DCB) test for CF stitched laminate. Several broken of CF stitch threads are observed. DCB test results are shown in Figure 2 as relationships between interlaminar fracture toughness (G_I) and volume fraction of stitch thread (V_{ft}). Three types of Kevlar stitch thickness data (111, 80, 60 tex) are tested and superimposed on this graph. It is observed that CF thread stitch laminates have higher G_I than Kevlar stitch laminates on the same V_{ft}. It is suggested that CF stitched laminate shows more effectiveness in G_I increase rate than Kevlar stitched laminates.

Figure 1 Picture of CF stitched laminates in DCB test

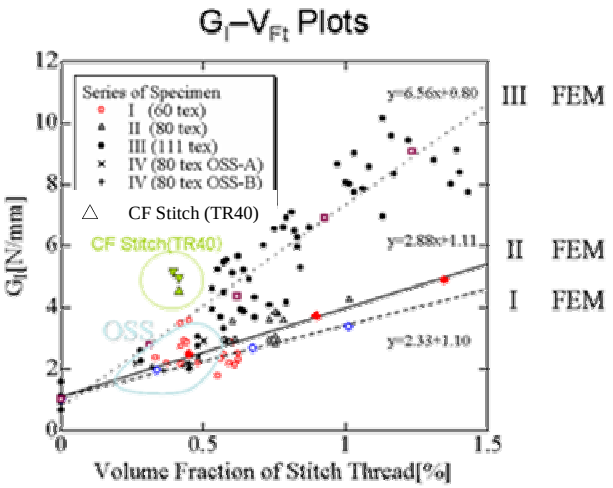

Figure 2 Relationships between Vft-GI

Double notch shear (DNS) tests are conducted for CF stitched laminates. A picture of the DNS test is shown in Figure 3 where JAXA proposed method for textile through-the-thickness composites is used. Double notches, one on each opposite face of the specimen and 6.4 mm apart, are sawed across the entire width of the specimen and centrally located along its length. The width of the notch is 1 mm and depth is 1/2 specimen thickness. The

DNS tests were conducted L and T stitch directions. Figure 4 shows the results of DNS tests for CF stitched laminates. The results are indicated that DNS strengths of L directions slightly higher than T directions. It is also found that CF stitch densities are not affected to the DNS strength results.

A part of this work has been supported by Japan Aircraft Development Corporation (JADC) and NEDO under control of METI of Japanese government. The authors also would like to thank Mr. Fujishima, Mr. Yamazaki and Mr. Ichikawa in Ishikawajima Jet Service Co., Ltd who support many tests.

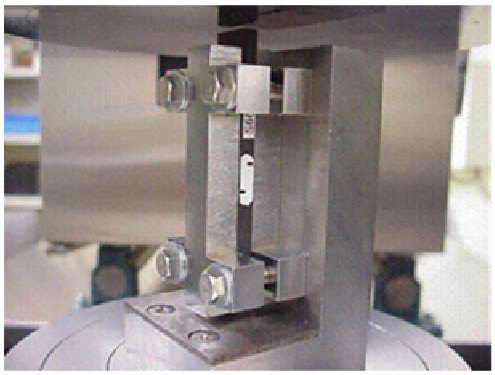

Figure 3 Picture of DNS test

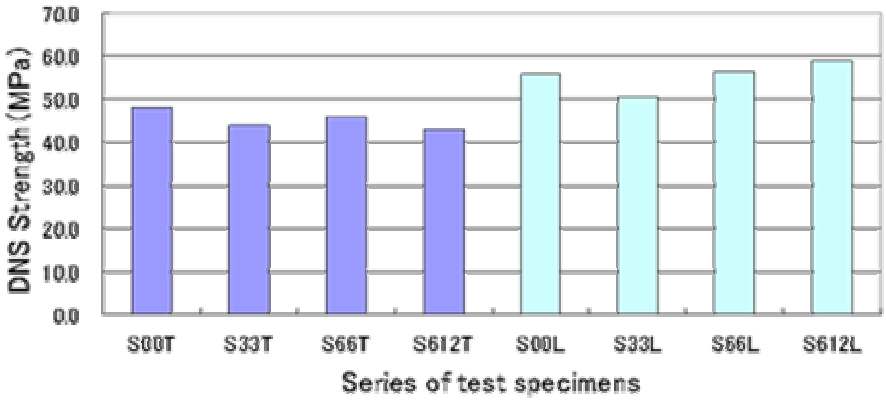

Figure 4 DNS Test Results

A SCREENING METHOD FOR INVESTIGATING FIBRE COMPOSITE RESIDUAL STRENGTH AFTER IMPACT

Anette Järneteg
CSM Materialteknik AB, Department of Polymer Composites, Sweden

One disadvantage with carbon fibre composites is its sensitivity to impact. In aircraft it is not rare that impact damages occur during maintenance or in service by collisions or other accidents, at ground or in air. The decision whether a damage is safe, or severe enough to be repaired is complicated by the nature of damage distribution in composite materials. A low-velocity impact can cause significant strength reduction although invisible on the impact side of the panel or structure. The damage zone is then gradually increasing through the thickness and is largest at the back face of the panel. A severe damage can be observed by broken fibres and the area can be repaired. When the damage is constricted to the matrix and delamination, methods such as ultrasonic testing must be used to detect the damage, which is not easily performed in an in-field situation. A good knowledge of damage distribution, the damage effect on residual strength and methods for detecting damages is therefore vital for damage resistance design.

When studying damage resistance of composite materials the residual strength is usually measured by compression testing (Compresssion After Impact, CAI) since delamination due to low-velocity impact, although

invisible, can cause a significant reduction in the compressive strength of the material. Compression testing is though very time and material consuming and great demands are made upon the testing equipment.

At CSM Materialteknik a simple method for residual strength testing has been developed. Carbon fibre laminates were impacted at different energy levels. The damage area was localized and the area distribution was measured by ultra-sonic testing. The material was then tested in 4-point-bend. By cutting the specimens with the damage zone located between one support span and the corresponding load span, the damage zone is loaded in constant shear stress, assuming a linear elastic stress state. The results were then compared to the reduction of compression strength by testing specimen with equal damage size. The sensitivity of the 4-point-bend test method was found to be twice as high compared to compression testing. For example, the strength, as measured by 4-point bend test, was reduced by 45 % when the specimen had a damage zone of app. 100 mm^2, compared to undamaged material. The residual compression strength was reduced by 25% with the same damage size. This relationship between the two different loading modes is likely to appear as long as the damage is dominated by matrix damage and delamination, and not fibre breakage.

The method is useful for comparative or screening studies of damage effects on composite materials since it is based on a standardized method, is easy to perform and cheap in material cost.

TRANSVERSE EVOLUTION OF THE RESIDUAL STRESSES IN NOTCHED EPOXY CYLINDERS USING THE OLCR TECHNIQUE AND EMBEDDED FBG SENSORS

F. Colpo, L. Humbert and J. Botsis
Laboratory of Applied Mechanics and Reliability Analysis, College of Engineering,
Swiss Federal Institute of Technology, Lausanne, Switzerland (fabiano.colpo@epfl.ch)

In this work, long gage length fibre Bragg grating (FBG) sensors and optical low coherence reflectometry (OLCR) are used to characterize the longitudinal and transversal evolution of the residual strain field arising along a glass fibre included in a polymeric material during curing and post curing processes. The studied specimens are epoxy cylinders with length of 40 mm and diameter of 25 mm, that surround a standard optical fibre. The fibre typically contains a 24-mm-long FBG, whose centre coincides with the specimen centre.

Mechanically, the glass fibre acts as a cylindrical inclusion and locally influences the development of residual stresses. The presence of a non-uniform stress field along the grating, causes a considerable modification of the FBG response. That is, for an initial uniform grating, the single Bragg peak becomes relatively broader, splits into multiple peaks and is generally accompanied with a decrease of reflectivity. The grating is said to be "chirped" and the FBG's spectra are more complicated to interpret and cannot be directly related to strain distributions along the grating length. In this case, the FBG parameters, including grating and optical periods, are functions of the position along the fibre axis. Existing techniques allow to reconstruct strain profiles from spectral amplitude measurements alone, but generally require a priori strong assumptions on the strain distribution because the phase information is not known.

Alternatively, the strain profile can be determined in time domain from FBG's impulse response. This is achieved by using a novel method developed at EPFL, which combines the OLCR technique and a back-scattering technique called layer-peeling. This method leads to direct reconstruction of the optical period and related strain profiles along the sensing length without any initial assumption. As described previously [1], it permitted to measure parabolic residual strain profiles along the grating length that are caused by the epoxy matrix shrinkage. Additionally, the modelling of the residual stresses was carried out in the whole specimen through an equivalent thermo-elastic approach by introducing a shrinkage function S_m. Assuming an axisymmetric mode of deformation, S_m was taken as a parabolic function of the axial direction z in relation to the FBG measurements and kept constant along the radial direction r. Simulated and measured strain profiles have been found to be in good agreement along the fibre core.

As an extension of the previous analysis, we aim here to describe more realistically the residual stress evolution in the radial direction of the specimen. Based on the experimental results, the r-dependency of the function S_m is also addressed. The proposed approach is based on the crack compliance method, largely diffused by Prime and co-workers [2]. This method involves incrementally introducing a circumferential notch into the specimen as depicted in the insert of the Figure 1. It releases axial stress, which is normal to the cut plane. At successive extension of the notch, resulting strain distributions are then measured along the FBG's grating. Preliminary

results are gathered in Figure 1 where the local Bragg wavelength is plotted as a function of the axial co-ordinate z, for different notch depths a. The data in Figure 1 demonstrate that the effect of the mechanically induced crack (cuts) are not significant up until crack length of 11 mm. For longer crack length, however, the FBG response is very significant indicating that the residual strain field is affected by the presence of the fibre in about 10 fibre diameters.

The strain changes resulting from such cut depth are significant and measurable. Such strain data are used in

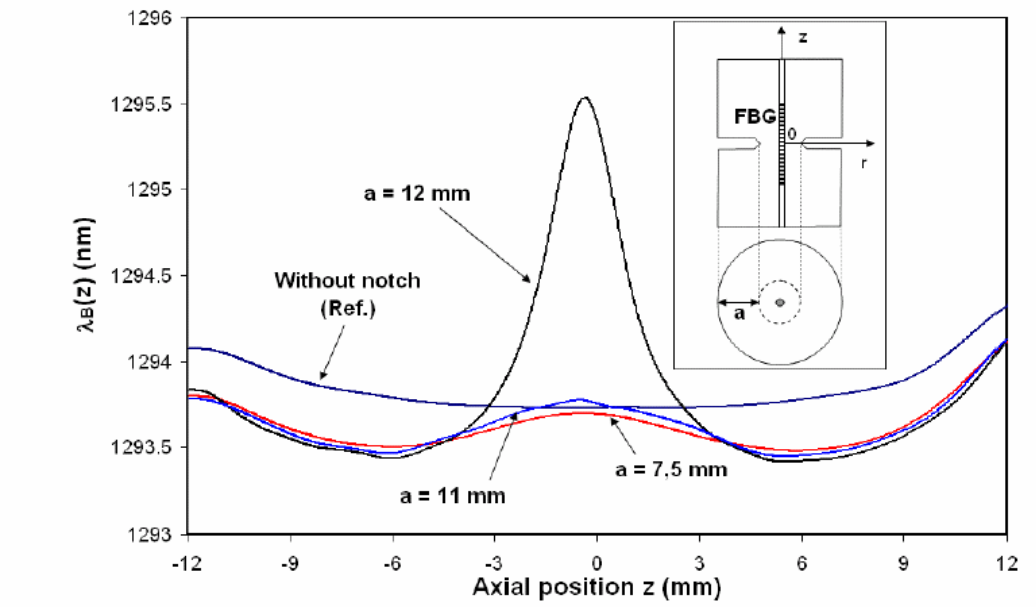

Figure 1: *Local Bragg wavelength $\lambda_b(z)$ evolution for different notch depths a*

reconstruction the residual stresses in the r-direction using the method developed in [3]. The axial residual stress variation as a function of depth is written as a series expansion whose the unknown coefficients have to be determined. This is achieved by calculating associated compliance functions for each term allowing to express the strain profile along the fibre core as a series of these previous functions with the same unknown coefficients. By a least square minimization with the experimental distribution the coefficient can be calculated. The results of this work help in reconstruction the residual stress field along z axis as well as in the radial direction. More importantly, the zone of influence of the fibre on the residual stresses of the cylinder will be obtained. The later results being important in mechanics of composite material.

ACKNOWLEDGEMENT

The authors wish to acknowledge the Financial Support of the Swiss National Science Foundation, Grant N° 2000-65277.01

References

[1] Colpo F, Giaccari P, Humbert L, Botsis J., *Residual stresses characterisation in an epoxy block by embedded FBG sensor and the OLCR technique*. Euromech 453 Internal Stresses in Polymer Composite Processing & Service Life. Saint-Etienne, France 2003.
[2] Prime, M.B. *Measuring residual stress and the resulting stress intensity factor in Compact Tension specimen*. Fatigue Frac. Engng. Mater. Struct. 22, pp.195-204, 1999
[3] Finnie I, Cheng W, *A summary of past contribution on residual stresses*. Material Science Forum, 404-407, pp. 509-514, 2002

COMPUTATIONAL MODELLING OF FATIGUE-DRIVEN DELAMINATION

Galvanetto and Paul Robinson
Department of Aeronautics, Imperial College London, UK

1. Introduction

Fibre composite structures often consist of layers that are bonded together as part of the curing process. Delamination can be caused by edge effects, impact, or other sources of significant interlaminar stresses. Delamination growth, which may result in catastrophic structural failure, can be modelled using methods based on *Linear Elastic Fracture Mechanics* (LEFM). LEFM follows from an elastic analysis of the stress field for small strains and gives excellent results for brittle materials. An alternative approach to modelling the delamination process is based on the *Cohesive-Zone Model* (CZM). CZM assumes the existence of a zone at the tip of the delaminated area where stresses are not zero and relative displacements can occur. This model combines principles of Damage Mechanics and LEFM and is successfully applied to numerical simulation by means of a particular type of finite element: the interface element. The use of interface elements for the analysis of interlaminar fracture in composite structures has been widely proposed in the literature. However, such a formulation does not account for delamination growth due to cyclic loading. In the present study the interface element formulation proposed by Crisfield and co-workers [1-2] has been further developed to allow propagation of cracks in laminated composites caused by fatigue loading. The main idea consists of coupling the long-term effect of fatigue with instantaneous delamination occurring as a result of overloads. The aim of this work is to investigate whether the modified interface element could be used to simulate the linear regime of the fatigue curve, often referred to as the linear or Paris regime. In this range the Paris power law applies:

$$\frac{da}{dN} = B(\Delta G)^m \qquad (1)$$

where a is the crack length, N the number of cycles, $\Delta G = G_{max} - G_{min}$ is the Strain Energy Release Rate range, B and m are empirical constants.

2. Interface Elements

This paper considers only two-dimensional problems although interface elements can of course be used for the simulation of three-dimensional cases. The interface is considered to be of zero thickness in the unstrained state and is modelled by *4-noded* (linear) elements An interface element is connected to the finite elements of the bulk material above and below the interface via the nodes on the upper and lower surface. The formulation of the interface elements has been presented elsewhere [1, 2]. At a generic point of the interface the relative displacement will be denoted by $\delta = [\delta 1, \delta 2]^T$ while $t = [t1, t2]^T$ will indicate the corresponding interface traction, in which subscripts 1 and 2 indicate the opening (Mode I) and sliding (Mode II) components respectively.

3. Fatigue implementation in Interface elements

Fatigue damage is a cycle-dependent reduction of strength and/or stiffness. In order to account for delamination due to fatigue the interface element formulation has been extended by including a damage law which allows the evaluation of the accumulated damage due to the cyclic application of a load.

Some assumptions were made in order to simplify the calculation process for both cases of uncoupled and coupled modes. The cyclic load that we want to simulate (in terms of applied displacement or forces) is sinusoidal, oscillating between zero and a maximum value. Since the aim of this investigation is to simulate high-cycle fatigue, it would be extremely demanding to simulate the effective relative displacement history for each pair of nodes of the interface elements. For constant amplitude loading the load numerically applied to the structure will therefore be taken as constant and equal to the maximum value of the actual cyclic load and consequently the relative displacement calculated at the interface will be considered as the envelope of its cyclic variation with time, Figure 1 and reference [3]. The number of cycles will be considered as a real-valued variable and represents the pseudo-time of the structure.

3.1. Delamination model for fatigue

In order to combine the traction/relative displacement relationship of the interface element [1, 2] with a fatigue model, the rate of damage $\overset{*}{D}$ is split into the sum of two terms:

$$\dot{D} = \dot{D}_s + \dot{D}_f \tag{2}$$

where $\overset{*}{D}_{s\ s}$ is the term related to the static delamination given in [2] and $\overset{*}{D}_{f\ f}$ is the term related to fatigue.

A law relating the rate of damage to an equivalent strain has been developed by Peerlings *et al.* [3]. Slightly modifying the law proposed in [3] a general law can be written for the delamination model as follows:

$$\dot{D}_f = \frac{\partial D_f}{\partial t} = \begin{cases} g\left(D, \dfrac{\delta(t)}{\delta_a}\right)\dfrac{\dot{\delta}(t)}{\delta_a} & \text{if} \quad \dot{\delta} \geq 0 \ \text{ and } \ f \geq 0 \\ 0 & \text{if} \quad \dot{\delta} < 0 \ \text{ or } \ f < 0 \end{cases} \tag{3}$$

where g is a dimensionless function, δa is a displacement quantity introduced for dimensional reasons and f is a damage loading function. The dimensionless function g has been taken as the following modified version of the exponential-law proposed in [3]:

$$g\left(D, \frac{\delta(t)}{\delta_a}\right) = C e^{\lambda D}\left(\frac{\delta}{\delta_a}\right)^{\beta} \tag{4}$$

where β, λ and C are parameters to be determined by means of comparison with experimental data.

The law for the growth of damage, derived in [4], is explicitly written as follows, for the case of single mode delamination:

$$D(N+\Delta N) = D(N) + \underbrace{\frac{\delta_0 \delta_c}{\delta_c - \delta_0}\left(\frac{1}{\kappa(N)} - \frac{1}{\kappa(N+\Delta N)}\right)}_{\text{static delamination}} + \underbrace{\Delta N \frac{C}{1+\beta} e^{\lambda D_\mu}\left(\frac{\delta_\mu}{\delta_c}\right)^{1+\beta}}_{\text{fatigue delamination}} \quad \text{with } \kappa(N+\Delta N) \geq \kappa(N) \tag{5}$$

where δ_0 and δ_c are the values of the relative displacement which define the static constitutive law, Figure 2. From equation (5) it is evident that the damage D is function of itself and so the value of the damage must be evaluated iteratively. To see how fatigue damage affects the constitutive model of the interface element we can consider a single interface element constrained at the bottom nodes and subjected to an initial displacement δ^*_1 at the top nodes so as to cause an initial static delamination damage $D1$, Figure 2. From point 1, if the displacement increases without fatigue, the stress-displacement locus will follow the straight line, typical of the static constitutive model, up to the maximum relative displacement δ_c, where complete debonding occurs, (path 1-2). On the contrary, if from point 1 we apply a displacement oscillating between 0 and δ^*_1, the load path will follow the line 1-2', typical of the fatigue constitutive model. In most cases we work with structures with several interface elements that operate in conditions between the two previous extreme cases (i.e. path 1-2'' in figure 2).

Finally figure 3 shows the good agreement which can be obtained with the proposed numerical method between experiments [5] and computations.

References

[1] Y. Qiu, M.A. Crisfield, G. Alfano. An interface element formulation for the simulation of delamination with buckling. *Engineering Fracture Mechanics*, 68, 1755-1776, (2001).

[2] G. Alfano, M.A. Crisfield. Finite element interface models for delamination analysis of laminated composites: mechanical and computational issues. *Int. J. Numer. Meth. Engng*, 50, 1701-1736, (2001).

[3] R. H. J. Peerlings, W.A.M. Brekelmans, R. de Borst, M.G.D. Geers. Gradient-enhanced damage modelling of highcyclic fatigue. *Int. J. Numer. Meth. Engng,* 49, 1547-1569, (2000).

[4] P. Robinson, U. Galvanetto, D. Tumino, G. Bellucci. Numerical simulation of fatigue-driven delamination using interface elements. Submitted to the *Int. J. Num. Meth. Engng*.

[5] L.E. Asp, A. Sjögren, E.S. Greenhalgh. Delamination growth and thresholds in a Carbon/Epoxy composite under fatigue loading. *J. of Composites Technology & Research*, 23, 55-68, (2001).

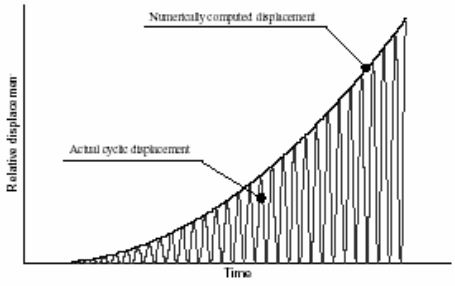

Figure 1: Cyclic load effectively applied and its envelope curve.

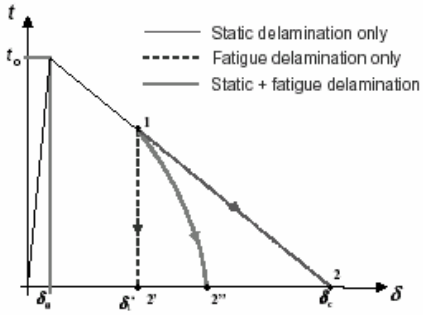

Figure 2: Constitutive model for an interface element subjected to static delamination, fatigue delamination or a mixture of both.

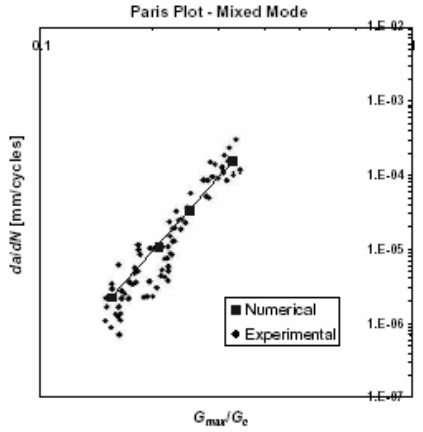

Figure 3 – Paris plot for the mixed mode with experimental and numerical results, (C=1E-4, β=2.8).

THE VIDEO GAUGE – A NEW TOOL FOR SIMPLE AND ACCURATE MEASUREMENT OF COMPLEX COMPOSITE PROPERTIES

Kevin Potter, Chris Setchell
University of Bristol and Imetrum Ltd. UK.

Composite materials and structures very often exhibit complex responses to relatively simple applied load cases and these responses can be very difficult to both measure and interpret. Video metrology techniques can be used to generate data that is very difficult to obtain in any other way and can simplify interpretation by providing unambiguous strain or deflection data.

The underlying principle embodied in the Video Gauge developments is that of pattern matching via normalised correlation algorithms. That is to say that a target is identified within a video frame and the user selects a point within that target to be taken as the reference position. The target could be a mark added to the structure being investigated or could be a natural feature of that structure. For example the hairs on a locust wing have been used as targets, as have the bolt heads on a large structure. In subsequent video frames the image is scanned for patterns that match those of the target, the best match is found and the new reference position is found and recorded.

Multiple targets can be tracked at the same time to allow a wide variety of measurements to be taken. It is important to note that there are no limitations on the sorts of features that are required as targets for this approach to image measurement. It is not necessary that the target be of a certain shape, or that it have sharply defined edges with a lot of contrast. The Video Gauge software has been shown to track targets over very wide ranges of illumination levels. It has successfully tracked targets that can barely be distinguished from the background by eye. Figure 1 shows the principle of operation schematically.

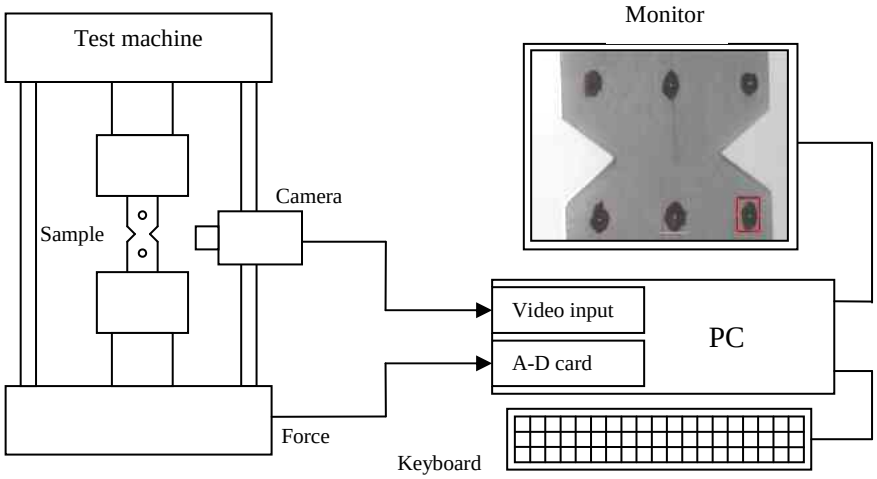

Figure 1. Schematic of the operation of the Video Gauge in testing a notched composite specimen

Video signals are taken from a camera trained on the test sample or structure and taken into a PC via an image grabber. At the same time other inputs such as load or cross-head displacement from a test machine can be taken in via an A-D converter card so that these can be compared directly with the Video Gauge data.

If two targets are used then the strain between them is readily found and for multiple targets the strain and displacement fields can be arrived at. It is clear that this approach has many advantages, such as being insensitive to the scale of the measurement - the structure being looked at could be under a microscope or be a complete aircraft wingbox. Equally the structure could be in a hot, chemically aggressive or otherwise difficult environment. So long as a video feed can be arranged, measurements can be taken.

The developments of this approach have been made possible by bringing together computer scientists and engineers experienced in materials and structural testing to ensure that developments are focussed towards real applications. Pattern matching algorithms that would enable video metrology to be carried out are well established. Imetrum has made critical improvements to those algorithms such that resolution can approach that of conventional measurement techniques such as strain gauging, in the simple cases where those techniques are usable. It is very important to note that the Video Gauge is measuring in pixels, so an absolute accuracy level cannot realistically be ascribed to it. However, the resolution in tracking a single target has been measured at better than$1/250^{th}$ of a pixel. Taking two targets initially 500 pixels apart and assuming a lower resolution of $1/100^{th}$ of a pixel the strain resolution between the two parts can be calculated at 1 part in 50000 or 0.002%.

Emphasis has been placed on ease of use and to this end we have developed a user friendly graphical interface that fits within the industry standard Windows environment and enables the Video Gauge to be used “out of the box” by inexperienced staff.

The Video Gauge is expected to be used in two different ways.

- In conventional mechanical testing such as uniaxial tensile or compression testing the Video gauge would be used to measure the strains in the sample. Both the direct and Poisson strains are available using four targets and with a larger number of targets non-uniformity in the strain field can be captured. So long as a set of targets can be identified or applied the nature of the sample does not limit the acquisition of data. Very soft and delicate samples would be as easily measured as steel samples and very high strain levels can be measured with no loss in accuracy.

- For testing structures the Video Gauge is more likely to be used as a displacement monitor than as a strain monitor and a number of targets can be monitored to build up the totality of the deformation picture. For either mechanical or structural testing the tests could be videotaped, or otherwise recorded, to permit more detailed study by sequential re-examination of multiple target sets.

The Video Gauge system has the following advantages compared to conventional mechanical measurement devices such as clip-on extensometers and strain gauges:

- minimal sample preparation required (especially compared to strain gauges)
- can allow full automation of set up and testing
- can measure complex measurement's such as Poisson's ratio, or separate out shear and bending deformations in a flexural test
- complete picture of test outputs from single piece of equipment
- flexible and scale independent;
- can track in 2 dimensions (and 3 with two cameras)
- can track multiple targets;
- can handle long elongation tests;
- can track existing features on sample;
- can operate with delicate samples that would be damaged by other techniques
- can operate in difficult environments such as corrosive chemicals or high temperatures

In addition to the uses of the Video Gauge in a materials or structure testing environment the Video Gauge approach can be used for long term structural monitoring. This has been demonstrated on long-span suspension bridges and has been shown to be a superior technique to the use of accelerometers as the inevitable baseline drift of such instruments can be avoided. For monitoring the structural deformations in aircraft an approach has been defined that would be capable, for example, of measuring the shear, bending and torsional deformations in a fuselage using a single camera and one set of targets. The Video Gauge developments are the subject of appropriate patent applications.

MODELING OF EFFECTIVE DIELECTRIC PROPERTIES OF COMPOSITES USING EXPANSION INTO FOURIER SERIES AND FINITE ELEMENT METHOD

Fanny Moraveca and Ivan Krakovskyb ,
a Department of Mechanics, Faculty of Applied Sciences, University of West Bohemia, Husova 11, 306 14 Plzen, Czech Republic
b Department of Macromolecular Physics, Faculty of Mathematics and Physics, Charles University, V Holesovickach 2, 180 00 Praha 8, Czech Republic

I. INTRODUCTION

Composite materials consist of two or more constituents which differ in physical properties. They can be prepared in many ways leading to a large variety of morphologies. The morphology of a composite has a big influence on its macroscopic behaviour. Therefore, the relation between the morphology and resulting physical (e.g., dielectric, thermal, elastic etc.) properties is of a great practical importance.
Effective dielectric constant of periodic composites, ε_{eff} of the simplest morphology (square lattice) in 2D is given by the asymptotic formula [1, 2].

$$\frac{\epsilon_{\text{eff}}}{\epsilon_a} = 1 + \frac{2\beta v_b}{1 - \beta v_b - 0.305827\beta^2 v_b^4 + \cdots}, \qquad \beta = \frac{\epsilon_b - \epsilon_a}{\epsilon_b + \epsilon_a} \qquad (1)$$

where v_b is volume fraction of inclusions, $\in_a$, $\in_b$ are dielectric constants of matrix and inclusions, respectively.

With a big progress in computer technology in recent years, morphology of composites and prediction of their macroscopic behaviour have become an attractive object for computer modelling [3, 4]. Space distribution of the dielectric constant in a periodic composite can be prescribed in two ways:

1. explicitly, i.e. $\in (x, y) = \in \varepsilon_a$ in the matrix and $\in \varepsilon(x, y) = \in \varepsilon_b$ in the inclusion,
2. and using an expansion into Fourier series.

While the former method is straightforward for composites of simple morphologies (spherical, cylindrical inclusions), the latter one can be useful in case of complex morphlogies (e.g. gyroidal). The objective of this study is an investigation of the Fourier series method for using in Finite Element Method (FEM).

II. MATHEMATICAL MODEL

Effective dielectric behaviour of periodic composites is illustrated in Fig. 1. A model 2D capacitor of the size of square elementary composite cell with edges of the length *h* is filled by matrix and inclusion of circular shape with radius *R*. Macroscopically, the single effective dielectric constant can be obtained from the electrostatic energy, W, stored in the capacitor as

$$W = \frac{1}{2}\epsilon_0 \epsilon_{\text{eff}} \left(\frac{U}{h}\right)^2 \tag{2}$$

where ϵ_0 is permittivity of free-space and U potential difference between the capacitor plates. Microscopically, the same energy can be obtained if space distribution of the electrostatic potential, $\phi(x, y)$, in the capacitor is known

$$W = \frac{1}{2}\epsilon_0 \int_\Omega \epsilon(x,y) \left(\frac{\partial \Phi}{\partial x} + \frac{\partial \Phi}{\partial y}\right)^2 \mathrm{d}x\mathrm{d}y \tag{3}$$

where $\varepsilon(x, y)$ is space distribution of dielectric constant.

Space distribution of the potential is governed by Laplace equation in conjunction with appropriate boundary conditions given in Fig. 1. Calculations in the present work were performed using FEM software package FEMLAB of company COMSOL [5].

III. RESULTS

Comparison of space distribution of dielectric constant simulated by the above methods is given in Fig. 2. At the same size of the expansion into Fourier series, including of the smoothness parameter leads to more realistic space distribution except the proximity of interphase. Fig. 3 shows the dependence of the effective dielectric constant obtained by eq.(1) and FEM using two ways of the simulation of the space distribution of dielectric constant. A systematic error is obtained when smoothness parameter is used. The method can be generalized in modeling effective properties of periodic composites with more complex morphologies in three dimensions.

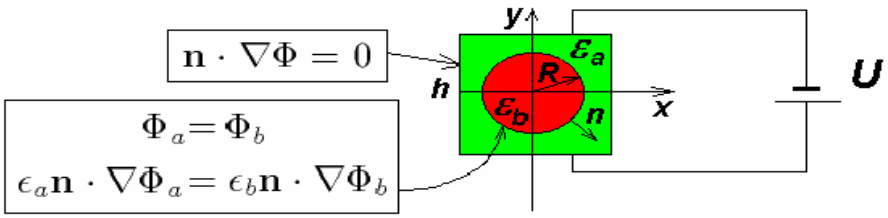

Figure 1: Model capacitor.

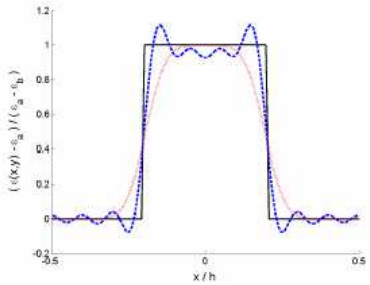

Figure 2: Space distribution of the relative dielectric constant $\frac{\epsilon(x,y)-\epsilon_a}{\epsilon_b-\epsilon_a}$ in cross-section $y = 0$ (full line) with $R/h = 0.2$, and its expansion into Fourier series (100-terms series without filter (dash line) and filtered with smoothness parameter $\sigma_0 = 0.05$ (dot line)).

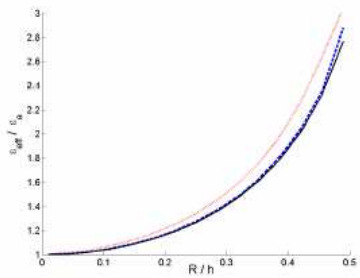

Figure 3: Effective dielectric constant v.s. the inclusion's radius with $\epsilon_b/\epsilon_a = 4$, using space distributions of dielectric constant as given in Fig. 2.

Acknowledgement

Financial support from the Grant Agency of the Czech Republic (grant GACR 203/02/0653) and Ministry of Education of the Czech Republic (project MSM 11320001) is gratefully acknowledged.

References

[1] S. Torquato, Random Heterogeneous Materials, Springer, N.Y. 2002
[2] W.T. Perrins, D.R. McKenzie, R.C. McPhedran, Proc.Roy.Soc.Lond. A 369, 207 (1979)
[3] H. Cheng, S. Torquato, Phys.Rev.B. 56, 8060 (1997)
[4] C. Brosseau, A.Beroual, Eur.Phys.J. Applied Physics, 6, 23 (1999)
[5] FEMLAB, Version 2.2., 2001

THE EFFECT OF PLY ORIENTATION ON THE PEAK AND DELAMINATION THRESHOLD LOADS OF CFRP COMPOSITE PLATES

Opukuro S David-West, David H Nash and William M Banks *
Department of Mechanical Engineering, University of Strathclyde,
75 Montrose Street, Glasgow.
* Corresponding author: Phone: 0141 5482321, Fax: 0141 5534117, E-mail: bill.banks@strath.ac.uk

Fibre composite materials are used today in a variety of structural applications. Their relatively low weight in combination with good strength and stiffness make fibre composites the preferred material in many structural applications. The phenomenon of delamination in laminated composite structures usually originates from discontinuities such as matrix cracks or the presence of free edges. Delamination, although mostly invisible on the surface, leads to reduced stiffness and strength of the structure that may lead to catastrophic failure. The ability to accurately predict damage evolution is essential for predicting the performance of composite structures and developing reliable safe designs.

Although fibre composites can carry large in-plane loads they have poor mechanical properties for transverse loading, especially when they are subjected to low velocity impacts. Such events can generate fibre, matrix and/or delamination damage inside a fibre composite laminate, which may significantly reduce the in-plane strength. The fact that these impacts may take place without leaving any visible evidence on the surface of an impacted laminate makes it even more important to account for these loading cases in the design process.

Owing to the widespread use of laminated composites in industries, the possibility of failure could be disastrous. Observations of damage due to impact on flat laminates by the present authors and past investigators have shown that delamination has a peanut-like shape and propagates along the fibre direction of the lower layer. That is as delamination takes place between two plies; it grows along the fibre direction of the lamina below taking cognisance of the sense of the impact.

The present study on the effect of ply orientation on the peak and delamination loads aims to advise composite designers on their choice of ply angles. This investigation involves changing the sense of a lamina in a composite plate through the angles 0°, 30°, 45°, 60° and 90°; and determining the delamination loads, whilst keeping other parameters constant.

The peak and delamination loads are obtained from the load history and the results and outcomes are presented herein. In addition, some guidance is given on the stacking of plies to reduce or avoid the threshold of delamination as a result of low velocity impact, hence, improving the laminate resistance to delamination.

EFFECT OF THERMAL CYCLING ON STIFFNESS AND STRENGTH DEGRADATION OF POLYMERIC COMPOSITE MATERIALS

G. C. Papanicolaou* and T. C. Theodosiou, Th. V. Kosmidou
Composite Materials Group, University of Patras, Department of Mechanical and Aeronautical Engineering, Section of Applied Mechanics, Patras – 265 00, GREECE

Thermal Fatigue (TF) is a process of damage origination and growth in machine parts and structural components. This study is focused on the degradation of the mechanical properties of FRPs when they are exposed to thermal shock conditions. Such events can occur frequently during the lifetime of a composite; e.g. during manufacturing (cooling from curing temperature to environment temperature) or during operation (external temperature of aircraft can change from -50^0C to $+150^0$C, during landing, within seconds). The residual properties studied were the elasticity modulus in bending (flexural modulus – E) and the respective maximum stress (flexural strength - σ_{max}) developed within the specimens. The experimental results are compared with the results given by a simple and approximate analytical model, developed to predict the residual properties of a material subjected to a specific damage. It was found that the model successfully quantified mechanical degradation behavior observed under thermal cycling conditions. The same model predicts, also successfully, the behavior of a system being subjected to impact, hygrothermal or thermal fatigue, erosion, etc.

* To whom all correspondence should be addressed.

FATIGUE DAMAGE ANALYSIS OF A STEEL-COMPOSITE HYBRID PIN

A. Avanzini*, G. Donzella*, A. Mazzù*, V. Zacchè**
* University of Brescia, Department of Mechanical Engineering
** SIG-Simonazzi, Parma, Italy

The aim of the work is the fatigue experimental testing and the analysis of a steel-composite hybrid pin, designed to sustain a cyclic bending load, acting as a reaction element in a pressurisation device of an automatic machine for food industrial application.

The choice of a hybrid technology for this component has been made in order to achieve the requirement of low weight, because it has to be cyclically moved by a hydraulic actuator from the not working to the working position: a mass reduction implies a reduction in the actuator power necessary to maintain the cycle time within the requested threshold.

The pin core (see figure 1) is a steel cylinder, which acts as a mandrel for the fibres winding; the composite is a Carbon Fibre Reinforced Polymer (CFRP), made up by layers with different fibres orientation; finally, the external composite surface is covered by a thin steel bush, which has the function of protecting the composite from fretting. The pin is subjected to alternate bending stress, and its target life is 3×106 cycles.

Different damage phenomena can occur simultaneously on these components: fretting and fatigue on the external steel bush due to micro–slips between the pin and the support, bush-composite debonding, fatigue in the composite.

Three points bending fatigue tests (see figure 2) were carried out in load control on ten pin specimens, in order to investigate these phenomena and to assess the fatigue life of the industrial components. Two different solution for the bush-composite coupling were also tested: in five specimens the external steel bush was press – fitted on the composite bulk; in the remaining five specimens it was bonded with an epoxy – based adhesive, chemically similar to the matrix.

During the tests, the deformations of the pin were measured by two strain gages, and the maximum deflection by a LVDT. The pin stiffness decay as a function of the cycle number was obtained from these measurements, in order to obtain an estimation about the material damage increment. The specimens with press – fitted bush failed early, due to the external steel bush cracking, but also the composite showed delamination marks; the specimens with bonded bush survived to the requested load cycles number.

FEM analyses (see the model in figure 3) were performed in order to interpret the experimental results: the models included the composite properties definition, friction between the external bush and the support, the

simulation of press – fitting or bonding of the external bush to the composite. The stress condition of the pin (in terms of the Tsai Hill criterion for the composite) resulted significantly heavier in the specimens with press – fitted bush, in agreement with the experimental results.

Finally, a model for the degradation of the elastic properties of the material during fatigue loading was applied [1], calibrating it on the basis of the calculated applied stresses and the experimental results.

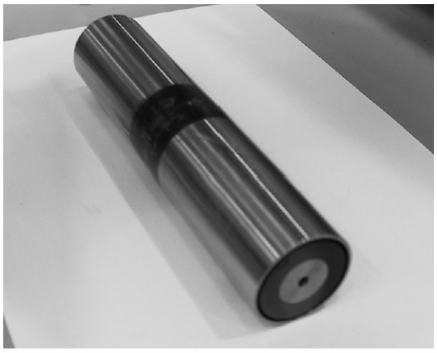

Figure 1: the pin structure

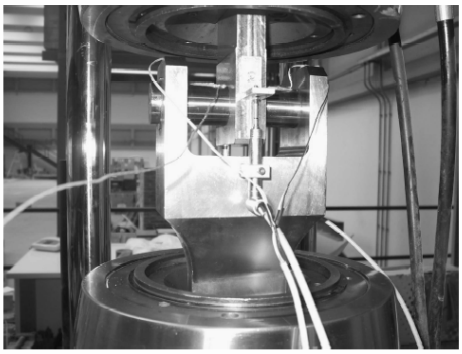

Figure 2: test rig for bending fatigue tests

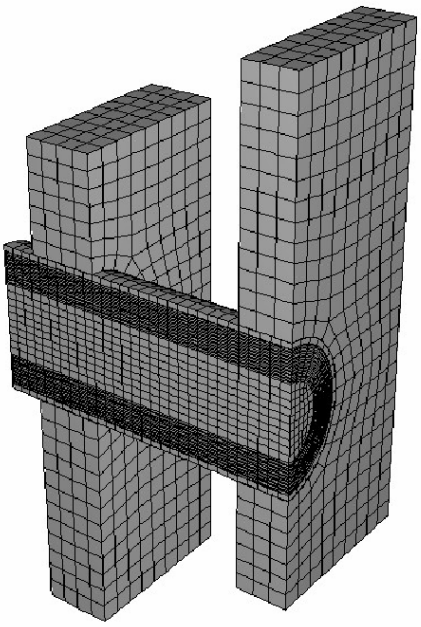

Figure 3: FEM model of the test apparatus

BENDING CHARACTERISTICS OF CARBON FABRIC-POLYMERIC/METALLIC FOAM SANDWICH STRUCTURES

Seong Sik Cheon[*], Tae Seong Jang[**], Seung Hwan Chang[***]
[*]Division of Mechanical and Automotive Engineering, College of Engineering,
Kongju National University, 182 Shinkwan-dong, Kongju, Chungnam, Republic of Korea, 314-701
[**]Structure and Thermal Control Team, Satellite Technology Research Center, 373-1, Guseong-dong, Yuseong-gu, Daejon, Republic of Korea, 305-701
[***]School of Mechanical Engineering, College of Engineering, Chung-Ang University 221, Huksuk-Dong, Dongjak-Ku, Seoul 156-756, Republic of Korea

Fibre reinforced composites have high specific stiffness (stiffness/density), specific strength (strength/density), and damping characteristics. Due to these beneficial properties, they have been used for structural materials of aircraft and space vehicles. As low cost manufacturing technologies and mass production methods for composite structures have been developed, the applications of composite materials to leisure sport goods and automotive structures are being increased nowadays. Composites will be much more useful in the near future on condition that recycling would be settled. Even though polymeric foam was traditionally used for core materials of sandwich structures, metallic foams are potentially popular from various types of industries because of their excellent material properties, weight saving effect as well as high level of crashworthiness. Even in the field of space technology and automotive engineering successful application of metallic foams was reported frequently. Among several fabrication methods of metallic foams, direct melting and gas injection, powder metallurgy route and investment castings are mainly used. The former two are for closed cell structure, the later for open cell type. Combination of these two materials, i.e. sandwich structures, has superior bending rigidity and lightweight as well, can be applied in many fields of engineering.

Plain weave carbon fabric has several key parameters such as tow interval, amplitude and crimp angle. These parameters are considered to affect mechanical properties, not to mention crashworthiness of the sandwich structure. Also, core material, i.e. polymeric or metallic foam has parameters, cell shape and relative density. They will be a major role in plateau stress as well as onset of densification of metallic foam material. In case of metallic foam, heat treatment can be considered as additional parameter. From the engineering industry point of view, these types of parameters can be a huge block to mass production or real field application unless they have proper values. In this study, sandwich structures were investigated in bending characteristics using LS-DYNA, a commercial explicit finite element analysis programme. Two types of sandwich structures, i.e. carbon fabric plate and polymer foam core material and carbon fabric plate and metallic foam core material, are studied. Polymer has 5 species, such as PVC type50, 70, 90, 110 and polyurethane. For metallic foam material, open cell type aluminium foam is considered with relative density of 10%. In case of metallic foam core material, electrically non-conductive medium is indispensable between carbon fabric and metallic foam to avoid galvanic corrosion. A sheet of glass fibre epoxy composite prepreg or adhesive film is sufficient. In FE modelling, rigid body connection between carbon fibre fabric and metallic foam core represents adhesive bonding. These connections are modelled to be broken with respect to longitudinal and shear strengths of film adhesive.

After forming analysis with respect to outer pressure, tow interval, amplitude and crimp angle can be calculated in each pressure of each material, i.e. mechanical properties of carbon fibre fabric plate can be predicted. Initial slopes, onsets of yielding and plateau stresses of polymeric and metallic foams would be obtained experimentally. Therefore, bending properties of sandwich structures can be estimated. Eventual goal of this study is to compare the properties between composite-polymeric foam and composite-metallic foam and apply the latter to the satellite body design.

SYNTHESIS OF AL_2O_3/AL CO-CONTINUOUS COMPOSITE BY REACTIVE MELT INFILTRATION

C. M. Lawrence Wu[1] and G. W. Han[1,2]
[1]Dept. of Physics and Materials Science, City University of Hong Kong, Hong Kong SAR, P.R. China
[2]Dept. of High Temperature Mater. Res., Central Iron & Steel Research Institute, Beijing 100081, P.R. China

Metal-matrix composites (MMCs) containing high volume fractions of reinforcement are attracting more and more attention because of their comprehensive properties such as low density and high stiffness for various engineering applications. The method of pressureless spontaneous liquid metal infiltration is regarded as a suitable method for mass production and the manufacture of complex shaped parts.

The pressureless spontaneous liquid metal infiltration method was further extended to synthesize ceramic/metal co-continuous composites using a sintered ceramic preform with three-dimensional fine open porosities throughout its microstructure. The co-continuous composite is expected to possess outstanding advantages such as lower coefficient of thermal expansion, higher stiffness and higher wear resistance over the MMCs with the same volume of ceramic reinforcement. It should also have higher thermal conductivity and higher fracture toughness than the ceramic matrix composite with the same volume of ductile metal as toughening phase distributed as discrete, isolated particles in the ceramic matrix. In other words, this kind of composite is expected to acquire the good properties from both the continuous ductile metal network and in the ceramic perform.

The infiltration of liquid metal into porous ceramic perform can only occur spontaneously when the wetting of the molten metal on the ceramic surface reaches a certain extent, so that a capillary action can be produced within the porosity so as to lead the spontaneous infiltration. For example, the direct infiltration of metal into a porous Al_2O_3 preform can synthesize the Al_2O_3/Al co-continuous composite. However, the resulting composite may have inherent microstructural defects as it is difficult for the ceramic surface to be wetted by a molten metal. To overcome this, many means have been studied to increase the wetting of the molten metal on ceramic surface. For example, by pre-doping Mg and Si in the aluminum alloy and using nitrogen gas environment, chemical reaction at the interface of molten metal and ceramic can be established. So, using a SiO_2 preform, the Al_2O_3/Al co-continuous composite can be synthesized via the chemical reactions of

$$3SiO_2 + 4Al = 2Al_2O_3 + 3Si$$

and metal + Al = aluminide compound .

In particular, the wetting ability of molten aluminum alloy on ceramic surface is increased. Although a certain amount of research work has been carried out on the microstructure and properties of this composite, it is still not clear what actually occurred at the front of infiltration caused by this chemical reaction.

In the present work, the microstructural change from the SiO_2 preform to Al_2O_3/Al co-continuous composite at the infiltration front was studied in depth using scanning electron microscopy, energy dispersive microanalysis and x-ray diffraction. Also, the difference in the synthesis process between this kind of Al_2O_3/Al co-continuous composite and that synthesized by direct infiltration of porous Al_2O_3 preform was compared.

It was concluded from the present results that reactive melt infiltration can occur spontaneously for the SiO_2 preform in the aluminum alloy at a high infiltration rate, and is therefore suitable to fabricate the Al_2O_3/Al co-continuous composite. The chemical reaction occurred ahead of infiltration front produced a transitional zone with a new type of continuous porosity. Molten aluminum alloy infiltrates into the porosities first and reacts with the residue SiO_2 further to produce Al_2O_3. It was also found that the Si-phase could be produced when the content of aluminum alloy is high.

SESSION 4 – FATIGUE AND DURABILITY

Chair: Prof. Olivier Allix
Laboratoire de Mecanique et Technologie, France

Tuesday 21 September
16.25-18.05

METHODS OF MONITORING FATIGUE DAMAGE UNDER VARIABLE AMPLITUDE LOADING IN CFRP COMPOSITES

Mostefa Bourchak, Dr. Ian Farrow and Dr. Ian Bond
Department of Aerospace Engineering, University of Bristol, Bristol, BS8 1TR, UK

Fatigue life prediction methods in composite materials under variable amplitude of loading such as the Palmgren-Miner's rule, are found to be unconservative. The main reason for this is the use of damage parameters in the life prediction process that fail to account for the damage events that may occur in a specimen undergoing a complex spectrum of loading such as the severity of cycle mixing in a spectrum of loading.

Damage development in a number of carbon fibre reinforced composite laminates has been studied under static, constant amplitude and different two-block fatigue loading regimes using the following online damage monitoring techniques:

- Modulus Degradation and Stiffness Degradation
- Temperature measurement
- Potential Difference measurement
- Thermal Camera and DeltaTherm Imaging
- Acoustic Emission

C-scan NDT method as well as short beam shear tests were also conducted in conjunction with the above methods.

Results showed that AE damage monitoring was found to be more superior to the other NDT/NDE methods in determining damage events, types of damage, location of damage, onset of damage and effective life of the specimen before catastrophic failure as well as the capacity to record continuously and non stop unlike the other methods.

Acoustic Emission results were found to correlate with damage indicated by ultrasonic C-scanning and short beam shear tests results, supporting the use of AE results to represent damage states in composites and consequently as a damage parameter in fatigue life prediction models under variable amplitude of loading.

ON THE RELATION BETWEEN CRACK DENSITIES, STIFFNESS DEGRADATION, AND SURFACE TEMPERATURE DISTRIBUTION OF TENSILE FATIGUE LOADED GLASS-FIBRE NON-CRIMP-FABRIC REINFORCED EPOXY

Andreas Gagel, Dirk Lange, and Karl Schulte
Technical University Hamburg-Harburg (TUHH), Germany
Polymers and Composites (5-09)

Designing lightweight components from fibre reinforced polymers requires tools that – if high safety factors should be avoided – are able to handle the mechanical degradation process of the material. In this work a textile reinforced polymer – as commonly used for structural applications – was mechanically loaded and the degradation of the material in terms of damage increase and stiffness decrease was monitored. It was focused on the onset, development and effect of non-critical inter-fibre failures in a glass-fibre non-crimp-fabric reinforced epoxy (GF-NCF-EP) under quasi-static and constant amplitude fatigue loading.

By using resin-transfer-moulding a composite was manufactured with the epoxy resin L135i/H137i (MGS GmbH) and two layers of a [0,45,90,-45] E-glass non-crimp-fabric (Seartex GmbH) with relative mass fractions of [48%,23%,6%,23%]. With coupon specimens according to EN ISO 527 quasi-static tensile tests and constant amplitude fatigue tests (R=0.1) where performed: a) continuous load until failure, and b) interrupted load until failure. In the latter case in between the load blocks the crack densities where measured non-destructively.

In Fig. 1 the density of a) ±45° cracks and b) 90° cracks are displayed versus an applied tensile strain. First inter fibre failures were found to occur at low strains between 0.2% and 0.3%. The crack densities typically show a high scatter. Nevertheless their increase with applied strain shows the usual degressive behaviour.

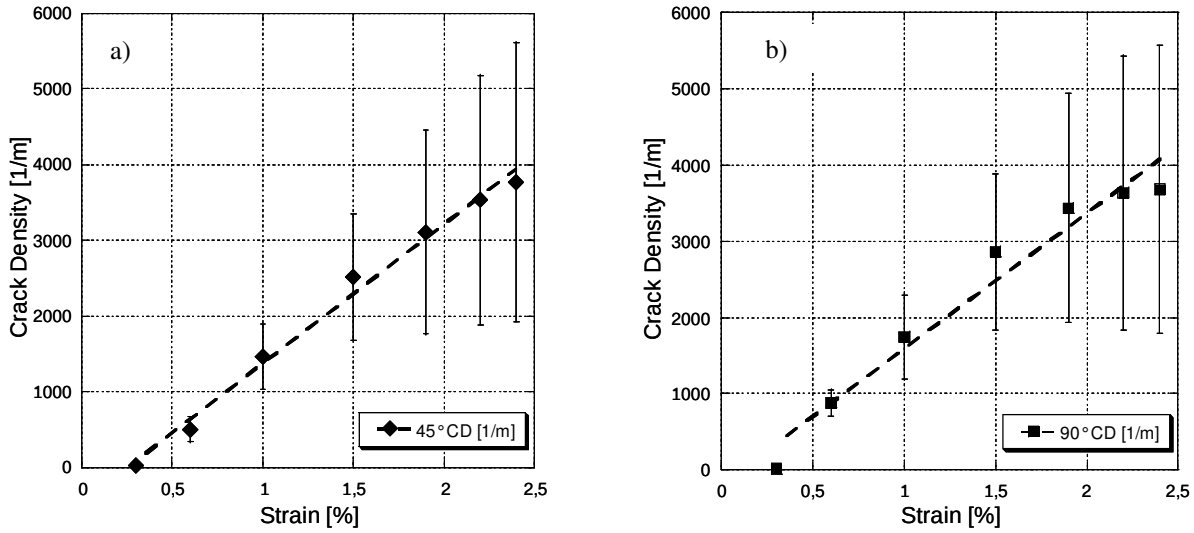

Fig. 1 Crack density vs. static tensile strain of GF-MAG-EP, a) 45° crack density, b) 90° crack density

When loading GF-NCF-EP dynamically (R=0.1, f=10Hz) without interruption the specimens mean temperature T_{glob} increases about 50°C from room temperature (RT) of 25°C at the beginning of the test to about 75°C at failure after 8000 load cycles. In Fig. 2 the difference between RT and T_{glob} as well as the difference between RT and the temperature T_{loc} is displayed. T_{loc} is the temperature of the location where finally the fatal rupture of the specimen takes place. In both cases the temperature increase can be divided into three stages: stage I of degressive temperature increase, stage II of approximately linear temperature increase, and stage III of progressive temperature increase until failure. In this special case stage I and III represent each about ¼ of the specimens life. It can clearly be recognised that T_{loc} is elevated compared T_{glob}, already in a very early stage of the fatigue life. The difference between T_{loc} and T_{glob} increases throughout the specimen fatigue life to an extraordinary high value out of the range of the thermographic camera. The also displayed relative stiffness (ratio of dynamic modulus of virgin sample and dynamic modulus while fatiguing) shows a similar stage-wise behaviour which suggests a correlation between stiffness loss and temperature increase.

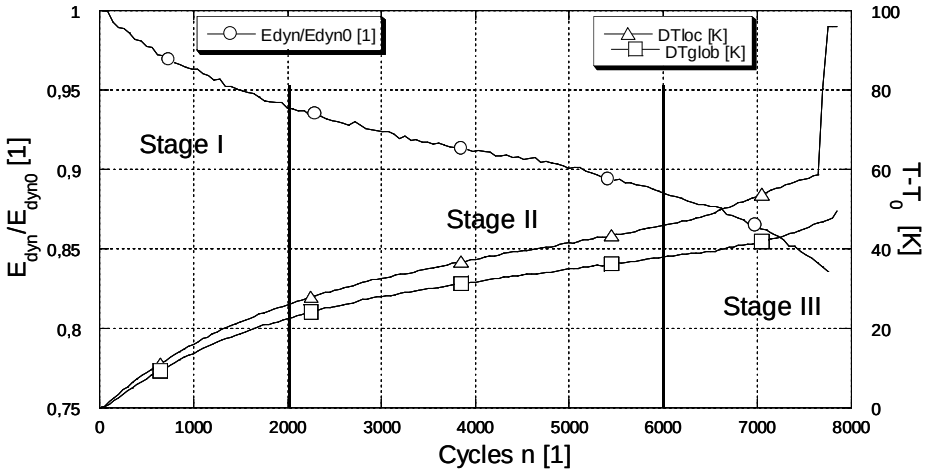

Fig. 2 Surface temperature increase and relative stiffness vs. load cycles (f=10Hz, $\sigma_{max} = 0.6 \cdot \sigma^{ut}$)

The surface temperature distribution on the specimen while fatigue loaded shows a characteristic pattern of areas with temperatures higher and lower than the mean temperature. This pattern is typically arranged along the specimen in a ±45° zigzag, such as shown in Fig. 3a). It is remarkable to see that the temperature difference between the hotter (T_{hot}) and cooler (T_{cold}) areas along the specimen axis keeps approximately constant in stage II of the fatigue life, while their values themselves as well as the specimen´s overall temperature increases.

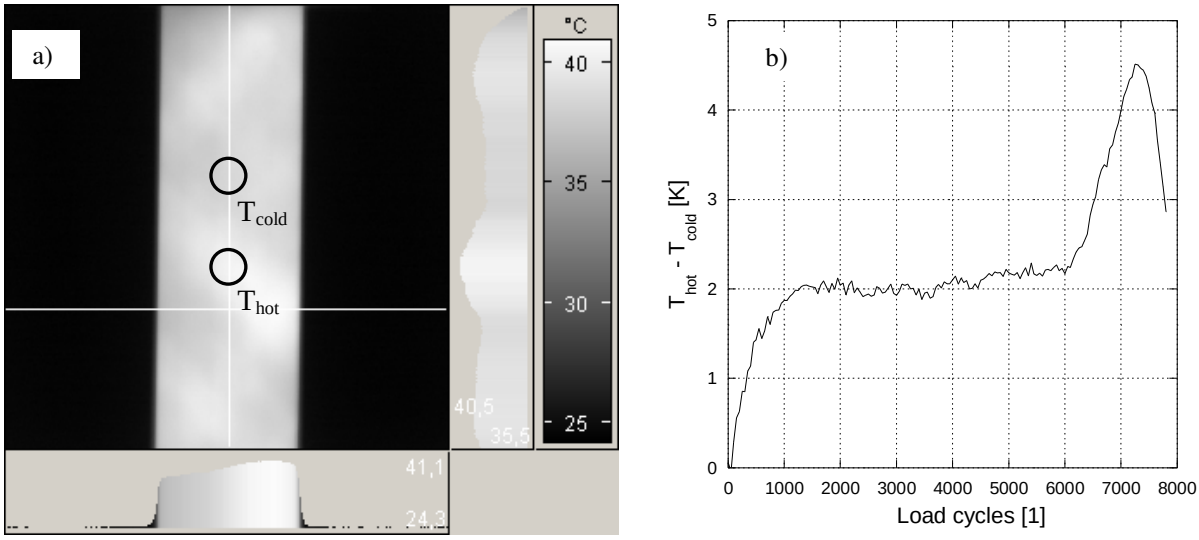

Fig. 3 a) Surface temperature distribution while fatigue loading (f=10Hz, $\sigma_{max} = 0.6 \cdot \sigma^{ut}$, n =1000)

b) Difference in surface temperature vs. number of load cycles (f=10Hz, $\sigma_{max} = 0.6 \cdot \sigma^{ut}$)

The development of the ±45° crack density in an fatigue loaded GF-NCF-EP is displayed in Fig. 4a). The upward pointing triangles denote the crack density in hotter areas; the downward pointing triangles those in the colder areas of the specimen. The line shows the mean of the crack densities in the hot and cold areas. The crack density increases in both areas grows in good approximation linearly with number load cycle number, starting at about 5100 1/m after a few load cycles (calculated from the linear curve fit) to about 6700 1/m before failure. It is remarkable to see, that no correlation can be found between local crack density and local surface temperature.

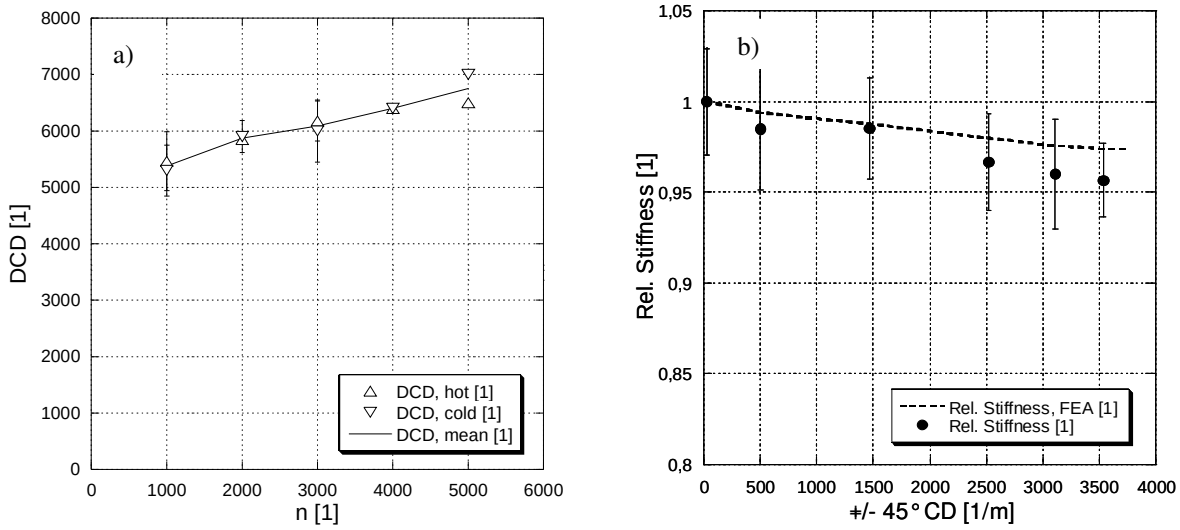

Fig. 4 a) Diagonal crack density (±45° cracks) vs. load cycles ($\sigma_{max} = 0.6 \cdot \sigma^{ut}$)

b) Relative stiffness loss vs. ±45° crack density under quasi-static tensile load

In Fig. 4b) the experimentally obtained and the – via FEA – calculated relative stiffness of cracks containing GF-NCF-EP is displayed. A good correlation between calculation and experiment could be found.

The following facts can be summarised for the analysed glass-fibre non-crimp-fabric reinforced epoxy (GF-NCF-EP):

- The onset of inter fibre failures initiates at low strains between 0,2 and 0,3%.
- While fatigue the surface temperature increase and the stiffness decrease show a similar, three-staged, behaviour.
- A characteristic zigzag shaped surface temperature pattern forms when fatigue loaded.
- The surface temperature distribution **cannot** be correlated with crack densities.

These facts lead to the following conclusions:

- The stiffness decrease of static loaded specimens **can** be correlated to crack densities. These facts lead to the following conclusions:
- The stiffness loss under mechanical load **is** related to the inter fibre failure (IFF) crack density increase *whereas*
- the location of the fatal failure (and thus the final failure) causing event **is not** related to the IFF crack density but can be located via thermography in an very early stage of the fatigue life.

The authors acknowledge the funding of this project by the DFG within the SPP1123.

OFF-AXIS FATIGUE BEHAVIOR OF PLAIN WOVEN CARBON/EPOXY LAMINATES AT ROOM AND HIGH TEMPERATURES

M. Kawai 1 and T. Taniguchi 2
1 Institute of Engineering Mechanics and Systems
University of Tsukuba, Tsukuba 305-8573, Japan
2 Graduate School of Science and Engineering, University of Tsukuba

INTRODUCTION

Owing to excellent drapeability, reduced manufacturing costs and increased resistance to impact damage, woven fabric carbon-fiber-reinforced plastics are now rapidly acquiring opportunities to be used for primary aerospace structures. The expanded need for woven fabric CFRPs necessitates understanding and modeling of their fatigue behaviors. The fatigue behavior of woven carbon fabric composites has been studied in a few experimental works [1-3]. Due to the limited amount of available data, however, understanding and modeling for the fatigue behavior of woven carbon fabric composites are still limited, especially for the effects of loading mode on the fatigue behavior.

The present study aims to examine the fatigue behavior of plain weave carbon/epoxy laminates under off-axis loading conditions and to observe effects of temperature by comparing the results at room and high temperatures. An attempt is also made to develop a fatigue failure model for plain-woven composites on the basis of the nondimensional effective stress [4] and the continuum damage mechanics. The validity of the proposed model is evaluated by comparing with experimental results.

TEST PROCEDURE

The composite laminates used in this study were made from carbon fiber plain woven roving fabric prepreg; it consists of T300H carbon fibers and thermosetting epoxy resin (#2500, T_g = 130°C). Five kinds of unnotched coupon specimen with different fiber orientations (θ = 0, 15, 30, 45, and 90°) were cut from 400mm by 400mm laminate panels. The shape and dimensions of the off-axis specimens are based on JIS K 7083.

Tension-tension fatigue tests were performed in load control with a 100 kN servo hydraulic testing machine at room temperature (RT, ~25°C) and high temperature (100°C). The stress ratio was kept at a constant value R = 0.1, and the fatigue load was applied in a sinusoidal waveform with a frequency of 10 Hz. Maximum fatigue stresses were determined so as to obtain the fatigue data within the life range from 10^3 to 10^6 cycles. The specimens were fatigue tested for up to 10^6 cycles, and then the fatigue tests were terminated.

EXPERIMENTAL RESULTS

The on- and off-axis S-N relationships (σ_{max} - logNf) at room temperature for the warp and weft directions are shown in Fig.1. The on-axis S-N curves agree with each other, and they are almost linear over the range of fatigue life up to 106 cycles. The S-N curves are shallow, and the fatigue limit cannot be identified in the tested range. For the loading in the off-axis directions, the fatigue strengths of the woven-fabric laminates becomes smaller with increasing off-axis angle from 15° to 45° and they are much lower than those in the on-axis directions. A significant reduction in fatigue strength appears in an intermediate range of fatigue life, which is followed by a plateau indicating an apparent fatigue limit. The off-axis fatigue strengths are significantly reduced as the test temperature increases.

FATIGUE DAMAGE MECHANICS MODEL

The normalized on- and off-axis S-N relationships using the maximum non-dimensional effective stress σ^*_{max} [4] which can be interpreted as a theoretical fatigue strength ratio for the off-axis fatigue loading on plain coupon specimens are shown in Fig.2. The fatigue data points clearly separate into two groups associated with the on-axis directions and the off-axis directions. This tendency implies that the fatigue failure of plain-weave fabric specimens for each of these two groups is controlled by different physical mechanisms. The data band for the latter group is very narrow, indicating that the off-axis fatigue behavior for these fiber orientations can be treated in a unified manner using the maximum value of the non-dimensional effective stress. Note that we can identify the two master S-N relationships by a single line fit of the fatigue data for each of the two groups. Fig. 3 shows a comparison between the normalized plots of the off-axis fatigue data at room temperature and at 100°C. This reveals that the off-axis fatigue strengths are much lower at a higher test temperature.

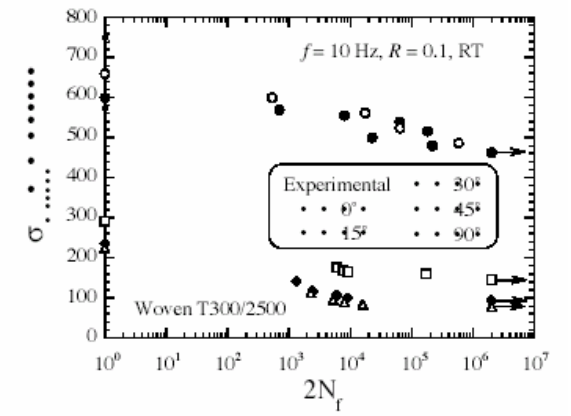

Fig.1 The S-N diagrams for all fiber orientation (R = 0.1, RT)

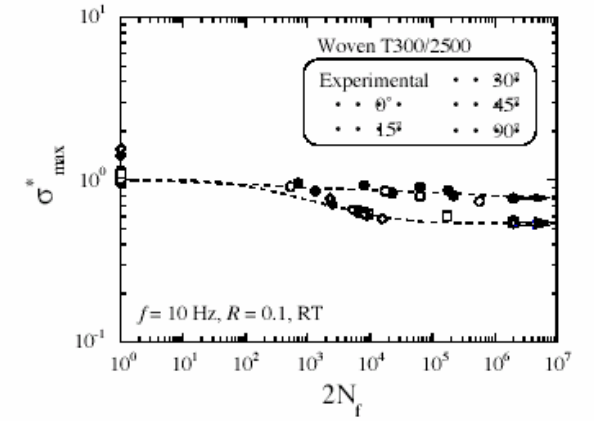

Fig.2 The normalized fatigue data for all fiber orientations (R = 0.1, RT)

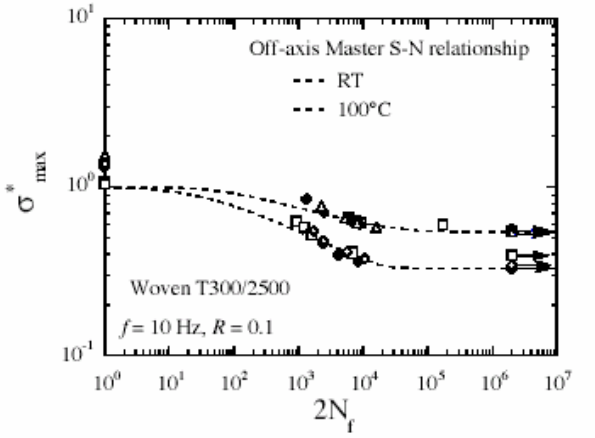

Fig.3 A comparison between the normalized off-axis S-N relationships at RT and 100°C

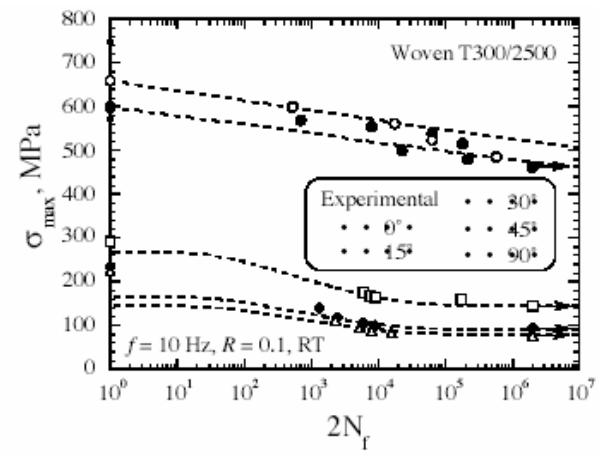

Fig.4 A comparison between the observed and predicted S-N diagrams for all fiber orientations (R = 0.1, RT)

The fatigue damage mechanics model [4] that considers the static strength dependence and the endurance limit of the off-axis S-N relationship is applied to the off-axis fatigue behavior of the plain weave fabric composite. On the basis of the observation in Fig. 2, we assume two master S-N relationships expressed as

$$N_f = \frac{1}{(1+k)K\sigma^{*\,n}_{\max}} \cdot \frac{\left\langle 1-\chi\sigma^*_{\max}\right\rangle^a}{\left\langle \sigma^*_{\max}-\sigma^*_L\right\rangle^b} \qquad (2)$$

where σ^*_i denotes the non-dimensional effective stress associated with the fatigue endurance limit. The coefficients K, k, n, a and b are material constants. If the static strength dependence is considered, x takes a

constant value of unity, otherwise it is 0. The angular bracket < > represents the Macaulay brackets: $\langle x \rangle = x$ if $x \geq 0$, otherwise $\langle x \rangle = 0$. Since the on-axis S-N relationships are almost linear, the associated master S-N relationship may be simplified as $N f = 1/ (\sigma^*_{max})^n$.

Comparisons between the theoretical and experimental S-N relationships for the fatigue loading in the on-axis and off-axis directions are shown in Fig. 4. The off-axis fatigue behavior of the unnotched plain weave CFRP composite has been adequately described using the proposed fatigue damage mechanics model.

REFERENCES

1. Miyano Y., McMurray M.K., Enyama J. and Nakada M. Journal of Composite Materials 1994; 28(13):1250-1260.
2. Kawai M., Morishita M., Fuzi K., Sakurai T. and Kemmochi K. Composites Part A 1996; 27: 493-502.
3. Khan R., Khan Z., Sulaiman A. and Merah N. Journal of Composite Materials 2002; 36(22): 2517-2535.
4. Kawai M., Yajima S., Hachinohe A. and Takano Y. Journal of Composite Materials2001; 35(76): 545-576.

DURABILITY OF GLASS FIBRE REINFORCED COMPOSITES EXPERIMENTAL METHODS AND RESULTS

H.Cuypers, J. Wastiels, E. de Bolster, G. Mosselmans and M. Alshaaer
Vrije Univeriteit Brussel, Brussel, Belgium
J. Orlowsky and M. Raupach
Reinisch-Westfälische Technische Hochschule, Aachen, Germany

Textile reinforced concrete (TRC) represents an interesting new construction material, offering several advantages compared to steel or fibre reinforced concrete. These advantages dominate in those fields of applications where thin-walled structural elements with a high load-carrying capacity are necessary. Unfortunately, even today a main topic of consideration for glass-fibre reinforced cementitious composites is the durability. Several mechanisms causing damage to glass fibre reinforcement in cementitious matrices can be distinguished1 : (1) the glass is chemically attacked (by hydroxyl ions), leading to a break-up of the Si-O-Si glass network, (2) formation of hydration products in the contact zone filament/concrete increases transversal shearing on the filaments and leads to loss of ductility and (3) during production of the fibres, flaws are introduced; these propagate under constant load and occasionally lead to delayed fracture (this effect is often referred to as static fatigue).

To protect glass fibres from chemical attack, 15-20 % zirconium is added to the conventional E-glass remaining strength, % mixture. This AR-glass (alkali resistant) improves the durability of the concrete reinforcement but does not solve the degradation problems entirely. To overcome the problem of chemical attack of the fibres by hydroxyl ions, a new cementitious material (Inorganic Phosphate Cement - IPC) has been developed at the Vrije Universiteit Brussel (Belgium), providin g a non-alkaline environment during and after hardening. The neutral environment of IPC after hardening is used to study other parameters, such as humidity, temperature and hydration product formation. AR-glass is combined with ordinary Portland cement (OPC) and both E-glass and AR-glass are used in Inorganic Phosphate Cement (IPC). For the investigation of the durability of these composites, the following techniques are used:

- Monotonic tensile testing
- Matrix crack counting
- Interpretation of limited cyclic loading
- Measurement of resonance frequencies

By application of these testing methods, determination of the evolution of different matrices, fibres and their interaction under accelerated ageing conditions (specimens kept under water at 50°C for 7, 14, 28 or 90 days) can be studied.

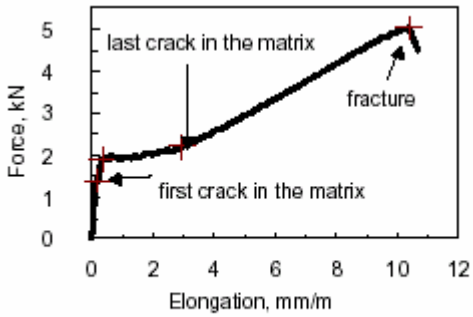

Figure 1a. Typical stress-strain curve of cementitious composite in tension

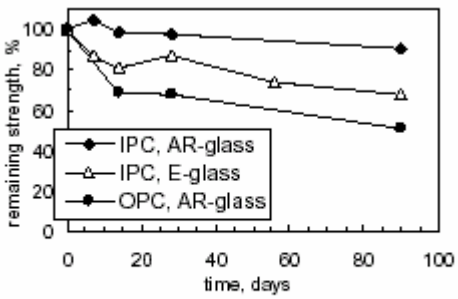

Figure 2b. Evolution initial stiffness with ageing

A typical stress-strain curve of remaining strength, % cementitious composites shows 3 zones (as shown in figure 1a): (i) at low stresses the composite shows linear elastic behaviour, and is usually is matrix dominated (this is the as pre-cracking zone); (ii) after the first crack appears, a fine crack pattern is built (multiple cracking zone) and (iii) after the last matrix crack appears, only the fibres carry extra load (post-cracking zone).

Figure 1b shows the evolution of the tensile strength with accelerated ageing time. The strength of OPC reinforced with AR-glass decreases to 50 % of the initial strength after accelerated ageing for 90 days. In comparison, the IPC composite reinforced with AR-glass maintains 90-95 % of its initial strength. Eglass fibre reinforced IPC also shows loss of strength, but the degradation is significantly lower than for the combination of OPC and AR-glass. The pre-cracking stiffness is determined from the same stress-strain curves and from measurement of the first natural frequency of the specimens. Both techniques lead to similar results. It is found that, for each of the material combinations, the stiffness in the pre-cracking stage did not —or only slightly— change with ageing. Advantages of determination of the pre-cracking stiffness from the measurement of natural frequencies are found in the fact that it is a fast method and it is non-destructive. The post-cracking stiffness (defined by the fibres only) is also determined from the stress-strain curves. No evolution of this stiffness is measured when IPC matrix is reinforced with E-glass or AR-glass. When OPC matrix is combined with AR-glass, the composite initially loses post-cracking stiffness. If ageing proceeds (after more than 28 days), the composite can't even resist loading into the post-cracking zone. If OPC is used, the fibres are thus degraded or the formation of hydration products leads to loss of ductility.

Two methods are used to determine the evolution of the matrix-fibre interface shear stress. The saturation crack spacing (average distance between matrix cracks, once the composite is loaded into the post-cracking zone) is measured after failure of the specimens occurred due to tensile testing: this is a widely well-known and applied method2,3. Whereas the determination of the saturation crack spacing is an easy and fast method to obtain information on the matrix-fibre interaction, it is not always useful: in case the specimen has been subjected to a loading (environmental or mechanical) sequence, or if the specimen fails before full matrix multiple cracking has been developed, it will lead to misinterpretations. This was indeed the case (see figure 2, OPC and AR-glass, 90 days): the saturation crack spacing of OPC with AR-glass initially decreases slightly (indicating a slight increase of the matrix-fibre interface shear stress), but after 90 days of accelerated ageing the combination AR-glass and Portland cement fails before multiple cracking could develop fully. Therefore, the measurement of the saturation crack spacing cannot be used.

Interpretation of limited cyclic loading4, based on earlier work concerning modelling of cyclic loading of brittle matrix composites5,6, is used as an alternative method to determine the matrix-fibre interface shear stress. This method is also useful if unloading is applied in the multiple cracking zone. The value found for matrix-fibre interface shear stress is similar (±1MPa) for both discussed methods (limited cyclic loading and saturation crack spacing determination). It was found that for IPC with E-glass or AR-glass the matrix-fibre interface shear stress does not change with ageing. Conclusively, it is clear that the alkalinity has a considerable influence on the evolution of the fibre efficiency with ageing time. The composites with IPC matrix hardly lose strength or stiffness, while OPC composites show considerable loss of strength and post-cracking stiffness (indicating loss of fibre efficiency). These conclusions are confirmed by application of several measurement methods.

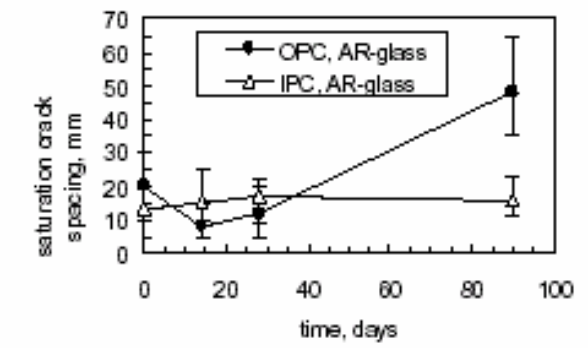

Figure 2. Evolution of saturation crack spacing with accelerated

References

1. A.J. Majumdar, V. Laws, "*Glass Fibre Reinforced Cement",* London, BSP Professional Books (1991)
2. Aveston, J., Cooper, G.A. and Kelly, A., "*Single and multiple fracture, The Properties of Fibre Composites*", IPC Science & Technology Press Ltd. London, 15-24 (1971)
3. Purnell, P., Short, N.R., Page, C.L., Majumdar, A.J., Walton, P.L., "*Accelerated ageing characteristics of glassfibre reinforced cement made with new cementitious matrices,*" Composites Part A, **30**, 1073-1080 (1999)
4. Cuypers, H., "*Analysis and Design of Sandwich Panels with Brittle Matrix Composite Faces for Building Applications*," Phd. Thesis VUB (2002)
5. Ahn, B.K. and Curtin, W.A, "*Strain and hysteresis by stochastic matrix cracking in ceramic matrix composites,"* J. Mech. Phys. Solids, **45** (2), 177-209 (1997)
6. Pryce, A.W. and Smith, P.A., "*Matrix cracking in unidirectional ceramic composites under quasi-static and cyclic loading*," Acta metall. mater., **41**, 1269-1281 (1993)

SESSION 5 – FULL FIELD TECHNIQUES I

Chair: Prof.Fabrice Pierron
ENSAM, France

Wednesday 22 September
08.30-10.35

FULL-FIELD OPTICAL METHODS FOR MECHANICAL ENGINEERING: ESSENTIAL CONCEPTS TO FIND ONE' WAY

Yves Surrel
Techlab

During the recent years, low-cost image acquisition and processing have very much impulsed the development of optical full-field measurement techniques (OFFMTs). However, the user is faced to a large variety of techniques among which it is difficult to make a choice. Moreover, the "historical" name given to some techniques is sometimes oddly chosen and confusing. As an example, almost all the words in "electronic speckle pattern interferometry" can be criticized, and "moiré interferometry" has only a remote connection to moiré. In order to make things clearer, we propose to sort OFFMTs on a basis of conceptual and functional criteria. We can list the following ones (non exhaustive).

A first aspect is the nature of the encoding, that is, whether the measurand is encoded into a deterministic (periodic) or random (noise) carrier. This will influence the metrological capabilities of the technique, because the phase detection of a modulated sinusoid is an efficient and perfectly mastered process. On the other hand, noise-based encoding will be easier to implement but will have lower measuring characteristics.

A second aspect is whether this encoding is a volume or a surface encoding. As an example, stereocorrelation works differently depending on whether the random pattern is linked to the surface (surface coding) or simply projected onto it (volume coding). The latter case can be related to profilometry by structured light method ; however, the volume encoding in the structured light technique has a richer quantitative content, allowing to use only one camera.

A third aspect is whether the coding process is interferometric or not. This allows to separate between "geometrical" and "interferometric" methods. As a striking example, speckle methods can be sorted into two families. In the first one the speckle is necessary and will carry the information (speckle correlation). In the other one, the speckle is just unwanted noise, and in fact the equations are the same as in corresponding non-speckle methods (speckle interferometry, shearography, etc). In the latter case, presentation books often confuse the reader by presenting the speckle as the heart of the technique, whereas it has nothing to do with it.

A fourth aspect in interferometric methods is the essential notion of sensitivity vector, with which all existing methods can be systematically and very easily presented. The key point is simply to identify the two interfering beams, and whether these beams have smooth (reflected, diffracted) or random (diffused) wavefronts. Interfering beams may be

- an object beam and a reference beam (e.g. out-of-plane speckle);
- two object beams having existed at different times (holographic interferometry);
- two object beams having different illumination directions (moiré interferometry, in-plane speckle) ;
- two object beams coming from two neighbouring points (shearing interferometry).

Having in mind the essential concepts and the necessary requirements (vibration isolation, surface preparation, etc), and knowing the sensitivity and resolution of the different techniques, it is possible to make a sensible choice among all available approaches.

EXPERIMENTAL INVESTIGATION OF COMPOSITE PATCHES WITH A FULL-FIELD MEASUREMENT METHOD

Jean-Denis Mathias, Xavier Balandraud, Michel Grédiac
LaRAMA, French Institute for Advanced Mechanics, Campus des Cézeaux, BP 265, 63175 Aubière Cedex
LERMES, Blaise Pascal University, 24, avenue des Landais, 63174 Aubière Cedex

Extending the service life of aircraft requires suitable solutions, among which composite patches have proved to be reliable. Baker pioneered researches on the mechanical response of structural components repaired with composite patches [1]. In most cases, patches are used for repairing cracked structures. In these cases, patches are bonded onto the cracks and behave like bridges which reduce their propagation. The key issue in this case is to compute the stress intensity factor and to deduce the crack growth rate. Many studies show that this stress intensity factor is notably reduced by a bonded composite repair [2].

The present work is a part of a project dealing with the reinforcement of metallic structures with composite patches. It must be emphasised that the aim is somewhat different of repairing metallic structures. The objective is indeed to design suitable patches in such a way that the stress flow in metallic components deviates from the initial path, thus leading areas where cracks are expected to appear to be relieved. The crack appearance is therefore delayed. A previous work has shown that defining optimal composites patches in terms of stacking sequence and shape led to some significant stress level reductions in the areas to be relieved [3]. This study was carried out with finite element calculations and genetic algorithms. The shapes of these optimal composite patches were somewhat unexpected and could not be guessed *a priori*.

This experimental study is an investigation of the mechanical response of various composite patches used for this stress flow deviation. Different important issues are addressed among which the load transfer between metallic structure and composite patch. Indeed it is well known that a transverse shear stress takes place in the glue near the free edge of the patch [4]. Studying this shear stress peak is important because it often causes the composite plate to peel out. Some well known theoretical models are available for describing the load transfer mechanism between structure and reinforcement [5]. To the knowledge of the authors, all these approaches are however unidimensional and cannot take into account different particular phenomena like the influence of the curvature of the patch boundary, possible coupling between directions because of the Poisson's ratio or in-plane shear for instance.

The above issues have been investigated here with a full-field measurement method. The grid method and its companion programme "Frangyne" developed by Surrel [6] have been used to reach this goal. A grid is first bonded onto the surface where displacements are to be measured [7]. A CCD camera captures this grid before and after loading. Both images are stored on a computer and processed with Frangyne to provide the displacement field onto the surface. The resolution is about 1E-06 m and the spatial resolution (the shortest distance between two independent measurements) about 360E-06 m. Unidirectional or bidirectional displacement fields can be measured, depending on the nature of the bonded grid. The strain field can also be deduced but spatial filtering for averaging out the noise and numerical differentiations are required in this case. Such a full-field method has been successfully used in the past for investigating composite structures [8] but it seems that it has never been used until now in the case of composite patches.

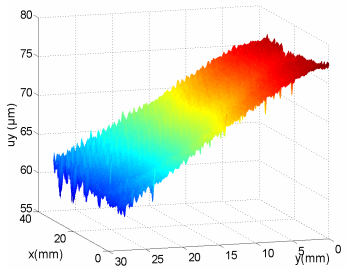

Figure 1: longitudinal displacement field

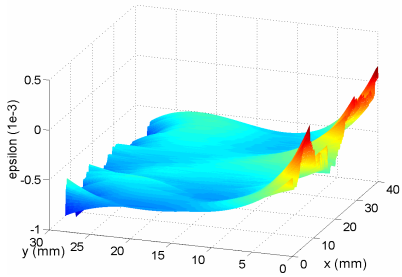

Figure 3: longitudinal strain field.

Figure 1 shows a typical longitudinal displacement field measured with this method onto a rectangular patch bonded onto an aluminium tensile specimen (see Figure 2). As can be seen, the displacement field is approximately linear apart from near the free edge of the patch (top part of the field). Filtering and differentiating the displacement field provide the longitudinal strain field (see Figure 3) which is first linear and then tends to zero near the free edge, as expected. The decrease rate is directly related to the shear peak in the glue.

The main features of the full-field measurement method used in this study will first be recalled in the paper. Various results will then be discussed: influence of the stacking sequence, length of the transfer zone, influence of some geometrical parameters of the patch (shape, thickness of the glue), comparison with theoretical unidirectional models and numerical bidirectional models, amplitude of the shear stress peak in the glue which is directly related to the length of the transfer zone.

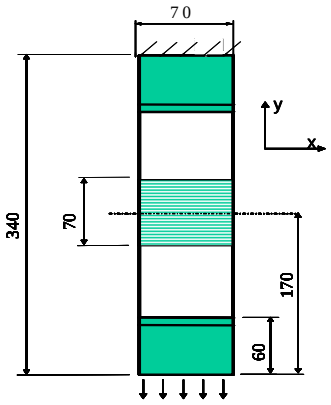

Figure 2: Schematic view of the specimen under test

[1] Baker A.A., Jones R., Bonded Repair of Aircraft Structures, Baker A.A., Jones R. eds, Martinus Nijhoff Publ., 1988
[2] Baker A.A. Repair of Cracked or Defective Metallic Aircraft Components with Advanced Fibre Composites - an Overview of Australian Work, *Composite structures*, vol. 2, pp. 153-164, 1984
[3] Mathias J. D., Balandraud X., Grédiac M., Applying a genetic algorithm to the optimization of composite patches, *Computers and Structures*, Elsevier, submitted, 2003
[4] Tsai M.Y., Morton J., An experimental investigation of nonlinear deformations in single-lap joints, *Mechanics of materials*, vol. 20, pages 183-194, 1995.
[5] Tsai M.Y., Oplinger D. W., Morton J., Improved theoretical solutions for adhesive lap joints, *International Journal of Solids and Structures*, vol. 35, no. 12, pages 1163-1185, 1998.
[6] Yves Surrel, Moiré and grid methods: a 'signal processing' approach. Photomechanics, pages 118-127, 1994.
[7] Piro J.L., Grédiac M., Producing and transferring low-spatial-frequency grids for measuring displacement fields with moiré and grid methods, *Experimental Techniques*, Society for Experimental Mechanics, in press, 2004
[8] Grédiac M., Pierron, F., Surrel Y., Novel procedure for complete in-plane composite characterization using a T-shaped specimen, *Experimental Mechanics*, vol. 39, no. 2, pp. 142-149, Society for Experimental Mechanics, 1999

QUANTITATIVE THERMOELASTIC STRESS ANALYSIS OF LAMINATED COMPOSITE COMPONENTS

J.S. Earl and J.M. Dulieu-Barton
School of Engineering Sciences, Ship Science, University of Southampton, Highfield, Southampton,
(email: janice@ship.soton.ac.uk)

Thermoelastic Stress Analysis is a well-established, non-contacting, full-field stress measurement technique [1-3], which has potential for optimization of composite components [4-5] and damage characterisation [6-7]. The technique uses an infra-red detector to measure the small surface temperature changes produced when a component undergoes cyclic loading. These temperature changes can then be related to the sum of the principal stresses by means of a calibration constant, which is a function of the infra-red detector characteristics and the material being tested. For an isotropic material, this relationship is straightforward, however, for orthotropic materials the relationship is more complex [2]:-

$$\Delta\sigma_{11}\alpha_{11}^{P} + \Delta\sigma_{22}\alpha_{22}^{P} = A'S \qquad (1)$$

where α^{P}_{11} and α^{P}_{22} are the principal coefficients of thermal expansion of the surface layer, σ_{11} and σ_{22} are the changes in surface direct stress in the two orthogonal material directions (i.e. longitudinal and transverse to the fibres in orthotropic composites), and

$$A' = \frac{DRG}{Te}\rho C_p \qquad (2)$$

where A′ is the calibration constant, which is a function of the detector responsivity, D, an amplification factor, G, the temperature correction factor, R, the emissivity of the material, e, the absolute temperature, T, the mass density, ρ and the specific heat at constant pressure, C_p. The validity of equation (1) depends on a number of assumptions that must be assessed with regard to the particular material under test before quantitative analysis can proceed. Some of these assumptions have been dealt with for the material used in this study and the findings are reported in a recent publication [8]. A key issue in the authors' research concerns materials with identical surface properties but different sub-surface configurations and if is equation (1) can be considered valid in this situation.

In this paper a detailed investigation is carried out which covers:

- A representation of theory in both stress and strain terms,
- The effect of the laminate on the surface lamina thermoelastic response, and
- A means of deriving the calibration constant $A^{/}$ given in equation (2).

Test specimens have been manufactured with identical surfaces but with different laminate properties. A range of tests is carried out so that the stress in the surface ply is identical in all cases and the calibration constants derived from each loading case. It is shown that $A^{/}$ is not the same for identical surface stress conditions and that the surface lamina cannot be treated in isolation. Reasons for this are provided and discussed in detail. An alternative approach for calibration is suggested.

References

[1] J.M. Dulieu-Barton: *Introduction to thermoelastic stress analysis.* Strain. Vol. 35, (1999), pp. 35-39.
[2] J.M. Dulieu-Barton and P. Stanley: *Development and applications of thermoelastic stress analysis.* J. Strain Analysis. Vol. 33, (1998), pp. 93-104.
[3] P. Stanley and W.K. Chan: *Quantitative stress analysis by means of the thermoelastic effect.* J. Strain Analysis. Vol. 20, (1985), pp. 129-137.
[4] J.M. Dulieu-Barton, J.S. Earl and R.A. Shenoi: *The determination of the stress distribution in foam cored sandwich construction.* J. Strain Analysis, Vol. 36, (2001). pp. 545-561.
[5] J.S. Earl, J.M. Dulieu-Barton, and R.A. Shenoi: *Determination of hygrothermal ageing effects in sandwich construction joints using thermoelastic stress analysis.* J. Comp. Sci. Tech., Vol 63, (2003), pp 211-223.
[6] Santulli, C., Dulieu-Barton, J.M. and Cantwell W.: *Thermoelastic investigation of impact damaged woven GRP composites.* Proc. 4th Int. Conf. on Modern Practice in Stress and Vibration Analysis, (2000), Nottingham, 285-296.
[7] Cunningham, P.R., Dulieu-Barton, J.M., A.G. Dutton and R.A. Shenoi: *Thermoelastic characterisation of damage around a circular hole in a GRP component.* Proc. 4th Int. Conf. on Damage Assessment of Structures (DAMAS 2001), Key Engineering Materials **204-205**, 2001, 453-463.
[8] Cunningham, P.R., Dulieu-Barton, J.M., A.G. Dutton and R.A. Shenoi: *The effect of ply lay-up on the thermoelastic response of laminated composites.* Proc. 5th Seminar on Experimental Techniques and Design in Composite Materials, Key Engineering Materials, Vols. 221-222, (2002), pp 325-336.

USE OF FULL FIELD STRAIN MEASUREMENTS TO MODEL THE BEHAVIOR OF CFRP WOVEN PLY LAMINATES

Cyril Bordreuil[1], Christian Hochard[2], Noël Lahellec, Fredéric Mazerolle
LMA/CNRS, 31 chemin Joseph Aiguier, 13402 Marseille, France

Rupture in composite material is due to numerous mechanisms acting at different scales. Models to describe the evolution of the overall mechanisms are complex [4]. Small cracks distributed homogeneously in the ply thickness can be described by the continuum damage mechanic approach. Large cracks (transverse rupture, delamination) are complicated to model. To follow the evolution of such cracks, the models must be numerical and three-dimensional. These models lead often to mesh dependence.

Woven ply laminates [3] show good resistance to delamination and are not sensitive to transverse rupture due to weaving. So, computations are simpler in this case. The mechanism of degradation to take into account are :
- Fiber rupture.
- Progressive degradation in shear with damage and plasticity coupled.

Modelling of the behaviour is mainly focused on studying coupling existing between fiber stretching and its influence on plasticity and damage.

The local behavior is characterised by homogeneous tests [*±45°*], [*±30°*]] on manufactured specimens. Due to the high rigidity of carbon fibers in respect to the resin, the shear behaviour is shown for tensile loading. A model is then presented to take into account the influence of tensile loading in fiber direction on plasticity and damage.

Structural tests on plate with an open hole [*±30°*]] and [*±45°*] are presented. Experimental strain maps coming from digital image correlation and maps coming from simulations [1] are compared in order to validate the non-linear behaviour in shear. The experimental strain levels [2] agree with those coming from computation [3] (Figures 1 and 2).

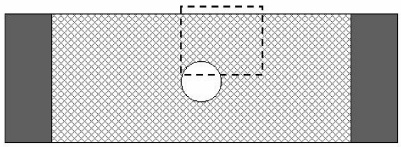

FIG. 1. Zone of study

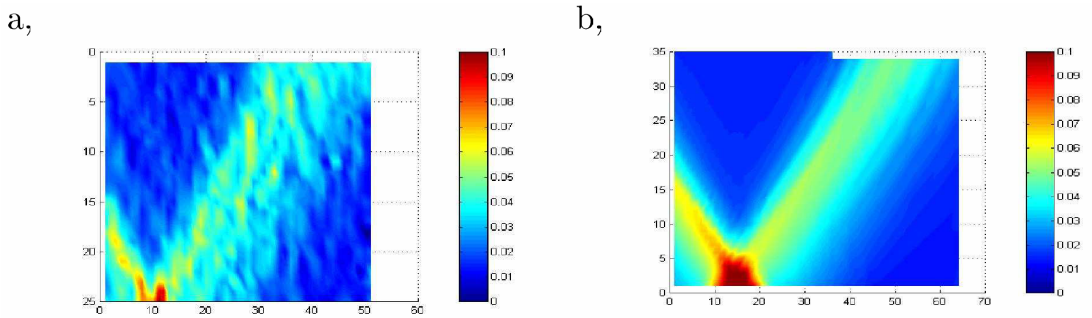

FIG. 2. a, strain field measurement ε_{11} measured with Correli [2] and b, Simulation for [±45°]

Behaviour in the fiber direction is characterised with [0°] test. It is shown that the behaviour is elastic until deadly rupture occurred. A local criteria in stress is expressed in the fiber direction.

To validate and enrich models, structural tests are developed. First, tests on a quasi isotropic laminate [0°*;* 90°*;* 45°*;¡*45°]*s* are done. This sequence is chosen in order to limit the non linear effects due to the behaviour. The macroscopic behaviour of the laminate is elastic with brittle rupture. Different specimens are chosen :
- Plates with an open elliptical hole.
- Plates with an open hole but with size effects.

To validate the behaviour just before rupture, full field strain measurements are used to show that the laminate is purely elastic until rupture occurs. It is shown that a non local criteria [5] better predict rupture for structure with high stress gradients. Woven ply are used in helicopter blade due to their good resistance (and easy lay-up). These structures are submitted to both static and fatigue loadings. To analyse the different mechanisms involved in such loadings, a test on a plate with an open hole [±45°] is performed, see Figure 3.

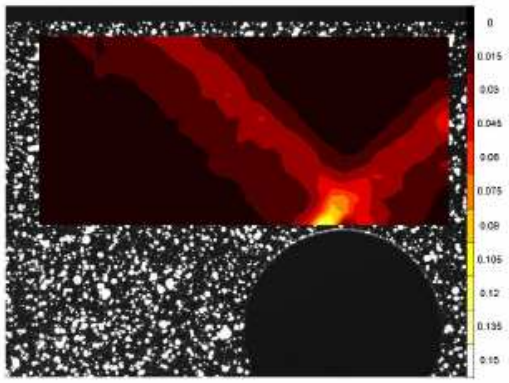

FIG. 3. Full field strain measurements on $[\pm 45°]$ after around 30000 cycles for 0-550kN cycle (rupture at 50000 cycles)

REFERENCES

[1] Bordreuil Cyril and Hochard Christian. Finite element computation of woven ply laminated composite structures up to rupture. Applied composite materials, accepté, 2004.
[2] Hild François, Périé Jean-noel, and Coret Michel. Mesure de champs de déplacements 2d par corrélation d'images numériques : *correli2D*. rapport interne LMT, 230, 1999.
[3] Hochard.Ch. Design and computation of laminated composite structures. Composites and Structures, 33 :159_165, 2004.
[4] Ladevèze P and Le Dantec E. Damage modelling of the elementary ply for laminates composites. Composites Science and Technology, 43 :257_268, 1992.
[5] Withney and Nusimer. Strain gradient in composite laminate structure. Journal of composite material, 35 :733_745, 2003.

POSTER SESSION 3

A CONTINUUM DAMAGE MODEL FOR THE SIMULATION OF DELAMINATION UNDER VARIABLE-MODE RATIO IN COMPOSITE MATERIALS

A. Turon* , P.P. Camanho**, J. Costa*, C.G. Dávila***
*AMADE, Escola Politècnica Superior, Universitat de Girona, 17071 Girona, Spain
**DEMEGI, Faculdade de Engenharia, Universidade do Porto, 4200-465 Porto, Portugal
***Analytical and Computational Methods Branch, NASA Langley Research Center, Hampton VA 23681, U.S.A.

Interlaminar damage (delamination) is one of the predominant forms of failure in many laminated composites systems, especially when there is no reinforcement in the thickness direction. The simulation of delamination in composites includes delamination initiation and delamination propagation. Delamination initiation analyses are usually based on stresses and use criteria such as the quadratic interaction of the interlaminar stresses [1]. Delamination propagation is often studied using a fracture mechanics approach, evaluating energy release rate for self-similar delamination growth. The Power-Law and the Benzeggagh-Kenane (BK) criterion are two criteria used for mixed-mode delamination growth [2]. In a recent study [3] it has been shown that BK criterion provides a better correlation with the experimental data than the Power-Law criterion.

The objective of the current work is to formulate a thermodynamically consistent damage model for the simulation of delamination under variable mode ratio. The meso-modelling approach [4] is used, considering only energy dissipation at the interface. The interface is modelled using decohesion elements [3]. The constitutive equation proposed combines the initiation and propagation criteria for delamination simulation. The formulation of the decohesion elements is based on the concept of strong discontinuities with a discrete framework approach: by using discrete constitutive equations (tractions vs relative displacements) to describe the cohesive behaviour of the interface between two adjacent layers. The formulation must be able to change between different mode ratios in a thermodynamically consistent way. A new expression for the delamination initiation criterion is developed. The proposed expression and the formulation of the damage evolution assure a perfect transition between the initiation to the propagation surface as shown in Figure 1.

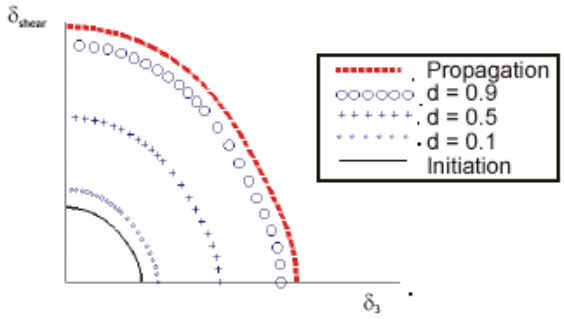

Figure 1: Damage evolution surface in the relative displacement's space

The model is developed in the framework of the continuum damage mechanics (CDM). A scalar damage model based on the work of Simo and Ju [5] and Lemaitre and Mazars [6] is formulated.

A bilinear constitutive equation is defined by a penalty parameter, the damage evolution law, the mixed mode damage initiation and the total decohesion parameter obtained from the propagation criterion. The formulation of the free energy, ø, prevents the interfacial penetration of the two adjacent layers after complete decohesion:

$$\psi\left(\delta_i, d\right) = \left(1-d\right)\psi^0\left(\delta_i\right) - d\psi^0\left(\bar{\delta}_{i3}\left\langle-\delta_i\right\rangle\right) \qquad (1)$$

where ψ^0 is a convex function in the relative displacements' space, $\langle\bullet\rangle$ is the McAuley bracket and $\bar{\delta}_{ij}$ is the Kronecker delta.

The model is compared with experimental data obtained at different mode ratios to test the accuracy of the method. As shown in Figure 2, the cases analyzed are in good agreement with the test results and they indicate that the proposed model can predict the strength of composite structures that exhibit progressive delamination.

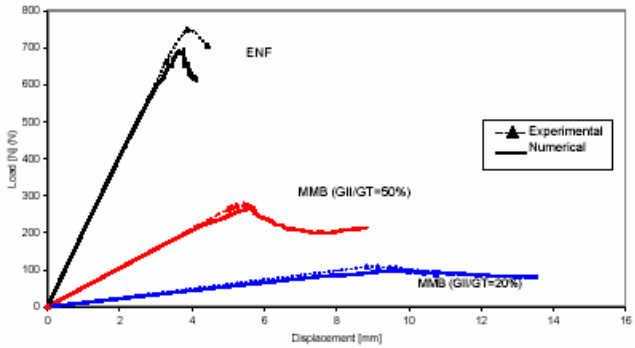

Figure 2: Comparison between numerical and experimental results

References

[1] Ye, L., "Role of Matrix Resin in Delamination Onset and Growth in Composite Laminates", Composites Science and Technology, 33, 257-277, 1988.
[2] Benzeggagh, M.L., Kenane, M., " Measurement of Mixed-Mode delamination Fracture Toughness of Unidirectional Glass/Epoxy Composites With Mixed-Mode Bending Apparatus." Composites Science and Technology,49,439-49, 1996.
[3] Camanho, P.P., Dávila, C.G., de Moura, M.F., "Numerical simulation of mixed-mode progressive delamination in composite materials", Journal of Composite Materials, 37, 1415-1438, 2003.
[4] Allix, O., Ladevèze, P., " Interlaminar interface modelling for the prediction of delamination", Composites Science and Technology, 22, 235-242,1992.
[5] Simo, C., Ju, J., " Stress and Strain Based Continuum Damage Models. Part I and II", Int. J. Solids and Structures, 23, 821-840, 1987.
[6] Mazars, J., "Mechanical Damage and Fracture of Concrete Structures". Advances in Fracture Research (Fracture 81), 4, 1499-1506. Pergamon Press, Oxford, 1982.

ANALYSING THE FLEXURAL STRENGTH PROPERTIES OF UNIDIRECTIONAL CARBON / EPOXY COMPOSITES

Zs. Rácz Ph.D. student – Z. L. Simon Ph.D. student – L. M. Vas **A**ssociate Professor
Department of Polymer Engineering, Faculty of Mechanical Engineering,
Budapest University of Technology and Economics,
H-1111 Budapest, Muegyetem rkp. 9., Hungary Tel: +36 (1) 463 2462
(E-mail: racz@pt.bme.hu)

Unidirectional (UD) composite materials are commonly used in a number of important applications, such as helicopter blade, hovercraft propeller, and a great variety of industrial fans and compressors, where specific strength and stiffness are the properties sought. Bending and tension are both major forms of loading for this type of components. The ability to predict the strength of components subjected to bending, tension, compression and shear or a combination of these is, therefore, of significant practical interest.

As it is well known the bending test provides a simple and convenient way of measuring the strength of unidirectional composite materials and gives very repeatable results. Flexural deformation is a particularly versatile method of testing composite materials because it combines tensile, compression and shear responses.

The aim of this research work was to study and analyze the strength properties of unidirectional reinforced carbon fiber/epoxy specimens produced as impregnated continuous tow bundle subjected to flexural loading using different span-to-thickness (*L/h*) and width to thickness (*b/h*) ratios.

The effect of span-to-thickness ratio (*L/h*) by measuring the flexural strength was examined. Results have shown that unidirectional composites exhibit a transition in the failure mode from shear delamination to fiber yield as the span-to-thickness ratio (*L/h*) in flexural testing is increased.

The composite used in this study was unidirectional (UD) carbon fiber-reinforced epoxy resin composite. The carbon fiber was PANEX 35 from ZOLTEK and the epoxy resin system was ARALDITE LY556 – ARADURE 2954 from CIBA. The continuous carbon tow was impregnated and laid in the open-ended compression moulds. The cross-linking was taken place at elevated temperature (at 80°C for 1h and postcured at 150°C for 4h) under pressure. The thicknesses of the UD specimens were 2, 4, 6 and 8 mm, while they were 10 mm in width.

Flexural tests were carried out using a three-point loading apparatus changing the span-to-thickness ratio (*L/h*) from 5 to 25, where *L* [mm] and *h* [mm] are the support span and the thickness of the specimen, respectively. Flexural tests were performed with a Zwick Z020/TH3A universal tensile testing machine equipped with bending fixtures and CCD camera system. Crosshead speed of 1 mm/min was used.

Most of the explanation of the decrease in strength with increasing specimen size are based on Weibull strength theory. Fitting Weibull distribution to the results measured at different given span-to-thickness (*L/h*) and width-to-thickness (*b/h*) ratios the Weibull parameters, that is the scale- and modulus parameters have been determined and the size effects as the ships between them and the ratios in question have been analyzed.

References

[1] Wisnom, M.R.: Relationship between strength variability and size effect in unidirectional carbon fiber / epoxy. *Composites* **22** 1 (January 1991) pp. 47-52

[2] Wisnom, M.R.: The effect of specimen size on the bending strength of unidirectional carbon fiber-epoxy. *Composite Structures* **18** (1991) pp. 47-63

[3] Marom, G. and Rosensaft, M.: Evaluation of bending test methods for composite materials. *Journal of Composite Technology Research* **7** 1 (1986) p 12

[4] Timoshenko, S.: Strength of Materials – Part 1, Van Nostrand, New York, 1955, Chapter IV.

[5] Standard test methods for flexural properties of unreinforced and reinforced plastics and electrical insulating materials, ASTM D 790-99, *American Society for Testing Materials* (2001)

INTRALAMINAR FRACTURE IN CFRP LAMINATES

N Vrellos, S L Ogin and P A Smith
School of Engineering, University of Surrey
N Balhi, F J Guild and B W Drinkwater
Department of Mechanical Engineering, University of Bristol

Matrix ply cracking is the most common damage to form when a laminate is loaded, and is of considerable significance for the integrity of a composite structure. The overall aim of the present work is to provide validated constitutive relations for crack accumulation in off-axis plies under mixed mode loading. Our work includes experimental investigations to describe the development of the cracking, ultrasonic characterisation of cracked laminates and the development of finite element-based models of cracked laminates.

Shear tests on $(\pm 45)_{4s}$ CFRP specimens have been carried out to measure basic elastic properties and to determine the shear stress/shear strain response. Tensile tests on $(0/90)_{4s}$ and $(02/904)_s$ CFRP specimens (with polished edges) were carried out to gather base-line cracking data. Data were obtained for the crack density as a function of applied stress/strain and the corresponding reduction in laminate stiffness properties (longitudinal modulus, Poisson's ratio) were measured. As expected, the crack density of the specimens increased as the stress increased, and for the same strain, decreased as the inner ply thickness increased. Both modulus and Poisson's ratio decrease with increasing crack density. Crack initiation and propagation in the central 90° layers of the $(02/904)_s$ lay-up have been distinguished by testing "notched" specimens and comparing the cracking data with the laminates having polished edges. The notch consisted of a 3 mm deep hole, drilled into the 90° ply, without damaging the adjacent 0° plies. When notches were present, the applied strain for transverse crack formation in the $(02/904)_s$ coupons was reduced significantly. Figure 1 shows the measured crack density with increasing stress for the different cross-ply laminates; the effect of the notch is clearly shown.

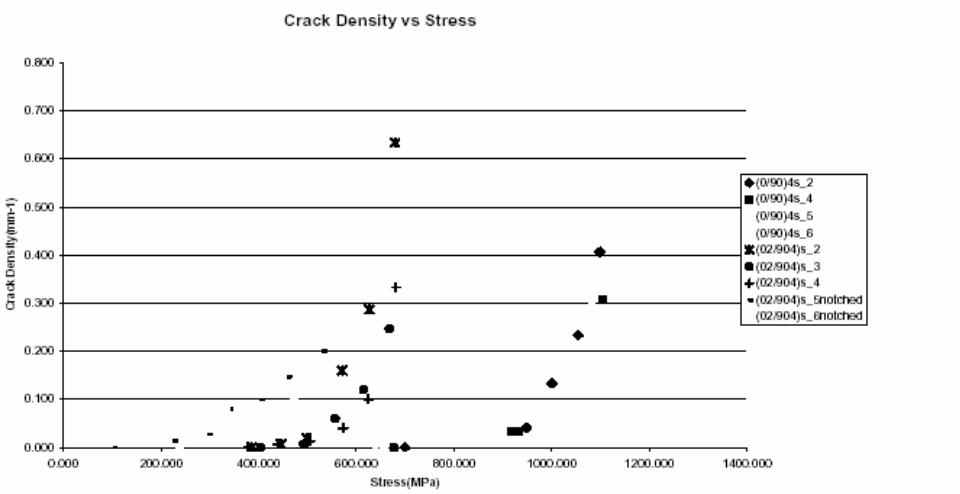

Figure 1 Crack Density against stress, showing the effect of the notch

Highly damaged CFRP specimens were investigated ultrasonically using normal incidence while a cracked $(0/90)_{4s}$ CFRP was tested at oblique incidence to image transverse cracks. It was possible to detect delamination on thin CFRP specimens using the double through transmission method. This method was better than back face reflection monitoring for delamination detection. Front face and back face echoes are close to one another on thin specimens, making it harder to set appropriate data collection gates to monitor their amplitudes. Matrix cracks on the other hand are difficult to observe with normal incidence because they are located in a plane parallel to the wave path. Oblique incidence testing was performed on a 16-layered CFRP $(0/90)_{4s}$ specimen that was shown to contain 23 through width cracks using dyepenetrant enhanced X-ray radiography. Several incidence angles were tried and 20º gave the best imaging of the transverse cracks. Signal gating was found to be crucial and very good agreement with X-ray results was finally achieved. The results from both methods of characterisation are in excellent agreement, as shown in Figure 2.

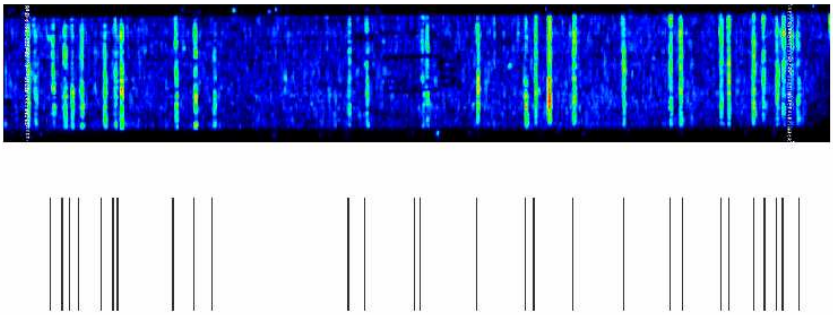

Figure 2 Comparison of X-ray radiograph and ultrasonic polar backscattering scan

The influence of through-width and through-thickness ply cracks on the residual stiffness of quasi-isotropic $(0/90/-45/+45)_s$ CFRP laminates was modelled using the FEA software ABAQUS. Two-dimensional Generalised Plane Strain elements were used. Cracking in the 90° plies only and both 90° and +45° plies was considered. The additional presence of +45° plies cracks was shown to degrade the longitudinal stiffness further than 90° plies cracks alone both in quasi-static and fatigue loading.

Strain energy release rates G associated with various crack spacings were also calculated with energy balance considerations for a quasi-isotropic $(0/90/-45/+45)_s$ laminate cracked in the 90° layers. The FE models make it possible to calculate the compliance of the specimen in the non cracked and in the cracked state, where the cracks in the 45° and/or 90° plies are assumed to have grown across the entire width and thickness of the plies. Identical results were obtained with the compliance method and the energy method. For small crack spacings, the energy release rate drops because of cracks interactions, whereas for larger crack spacings, G is constant.

The results of these simulations can be compared with the experimental observations of cracking, which can be well characterised both by x-ray radiography and ultrasonic testing. This work should lead to determination of the constitutive relations to describe crack accumulation for a wide range of loading conditions.

DEFORMATION AND FRACTURE OF UNIDIRECTIONAL GFR COMPOSITES AT HIGH STRAIN RATE TENSION

G. Makarov, W. Wang & R. A. Shenoi
School of Engineering Sciences, Ship Science, University of Southampton, SO17 1BJ, UK

Present paper deals with experimental investigation of the high strain rate behaviour of unidirectional (UD) glass fibre-reinforced (GFR) composite materials. The related experiments were performed with a high rate test machine to determine the mechanical properties of UD E-glass/epoxy composites. The specimens were tested separately under quasi-static and high-speed conditions with loading rates of up to 20 m/s. All specimens were tested to failure in order to characterise the effect of high strain rate on failure strength of the material. The results show that high strain rates have a significant effect on the properties of UD GPR composites. The increment of an ultimate strength with high strain rate is proportional to the strain rate in a given range with remaining elastic modulus.

Composite materials are widely used in civil and military engineering, aerospace, marine and automotive industries. In some cases, the loading on these structures is dynamic. Up to now, most structural designs are based on the material properties obtained through quasi-static tests at low strain rates. However, there is some evidence that in many cases the mechanical properties of composite materials are significantly dependent on the strain rate. For example, the ultimate strength or modulus of elasticity for composites could increase compared with the value under quasi-static loading conditions. Although the behaviour of the fibre-reinforced composite materials at high strain rates has been experimentally studied in many aspects, mostly under impact compression load by the Split Hopkinson Pressure Bar (SHPB) method, only a few works are provided for detailed experimental analysis of dynamical tensile loading of composites. Towards this objective unidirectional E-glass/epoxy composite specimens are specially manufactured and tested on an Instron high strain rate machine to investigate the effect of strain rate on the tensile strength of the UD composites.

The main experimental feature of this investigation was to use exactly the same coupon configuration specimen and strain gauges both for quasi-static and dynamic tests to be sure that geometrical sizes and ends fixing conditions do not affect to tensile load and strain measurement results. To achieve this and also to prevent the crushing of composite specimen due to sidekick from jaw faces of “FastJaw” grips of an Instron high strain rate machine at the initial moment of clamping and subsequent failure from edge effect a special adapter was designed. This adapter provided a rigid connection between the composite specimen and disposal mild steel stripe, which was loaded first and transferred tension from actuator to the composite specimen.

The analysis of experimental results shows that high strain rates have a significant effect on the properties of unidirectional GPR composite. The most important of this are:

- the behaviour of material under quasi-static and dynamic loading conditions is linear elastic up to the failure and its character does not change;
- a significant increment of ultimate strength within high strain rate is proportional to the strain rate in a given range with remaining elastic modulus;
- the dynamical properties of unidirectional glass-fibre reinforced composite are determined by the fibres properties and not the matrix.

A DIGITAL IMAGE ANALYSIS FOR DETERMINIG MODE I AND MODE II STRESS INTENSITY FACTORS

S. M’Guil, N. Bahlouli , C. Hisson & S. Ahzi
Institut de Mécanique des Fluides et des Solides, UMR 7507 Université Louis Pasteur / CNRS
2 rue Boussingault - 67000 Strasbourg-France
siham.mguil@ipst-ulp.u-strasbg.fr

A digital image correlation method is used to measure mode I and mode II stress intensity factors. This non-contact technique could be used for all application which needs the knowledge of displacement and strain fields. Like the speckle method, it uses the digital image correlation principle, but it is much simpler to perform. In fact, a set of pixels, called pattern, in an initial image is directly compared to the pixels of the final image (figure I). The accuracy of displacement measurement could reach $1/60^{th}$ of a pixel. Treatment of two images with large strain (≅ 100 %) is possible. Very accurate cartography of strain field is obtained. The covered field can range

from few square millimetres to few square metres. Comparison of fracture is performed between experimental data obtained for an industrial polymer with or without fibbers. Specimens used are represented in figure II. The symmetric specimen permits the determination of mode I stress intensity factors and the non symmetric specimen the mode II. A finite element and analytical analysis were performed using plasticity model (figure III). Cartography obtained by both methods are compared and showed the influence of fibbers on K_{IC} and K_{IIC}. Results were compared with experimental data obtained by a strain gage technique.

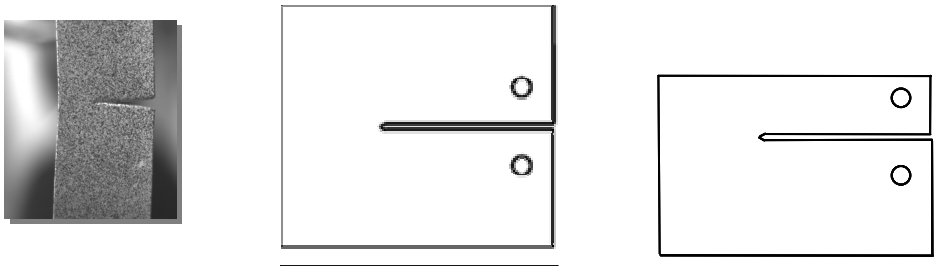

Specimen with speckle aspect | *Compact tension test specimen for mode I* | *Compact tension test specimen for mode II*

Figure I: Tensile test for an initially notched specimen with speckle aspect

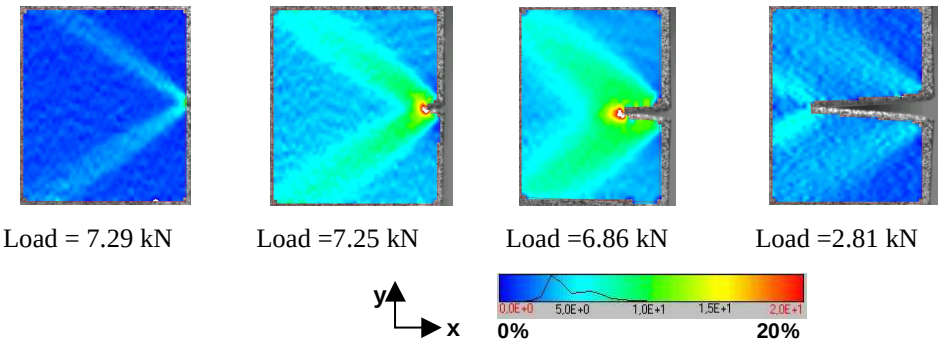

Load = 7.29 kN | Load =7.25 kN | Load =6.86 kN | Load =2.81 kN

Figure II Evolution at the creep cracking and plastic zones

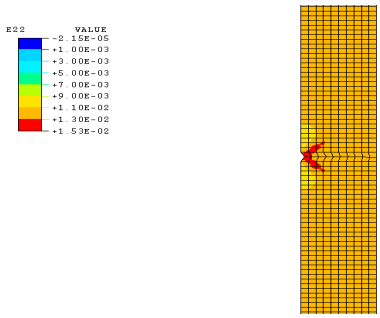

Figure III: Finite Element Analysis

REFERENCES :

[1] Bidimensional deformation measurement using digital images, Vacher, Dumoulin, Morestin & M'Guil-Touchal, Proc Instn Mech Engrs, Vol 213 part C I MechE, 1999

[2] A two-strain-gage technique for determining mode I stress-intensity factor, J. Wei & J.H. Zhao, Theoretical and Applied Fracture Mechanics 28, pp. 135-140, 1997

[3] Strain gage methods for measurement of opening mode stress intensity factor ,Levend Parnas and Omer G. Bilir & Erding Tezcan, Engineering Fracture Mechanics, Vol 55, N° 3, pp. 485-492, 1996

[4] A single strain gage method for KI measurement, J.H. Kunag & L.S. Chen, Engineering Fracture Mechanics, Vol 51, N° 5, pp. 871-878, 1995
[5] Discrete averaging effects of a strain gage at a crack tip, N.T. Younis and J. Mize, Engineering Fracture Mechanics, Vol 55, N° 1, pp. 147-153, 1996
[6] Strain–gage methods for measuring the opening–mode stress intensity factor, KI, J.W. Dally, R.J. Sanford, Exp Mech. 27, pp. 381-388, 1987

SQUARE GRID ANALYSIS FOR INTRAPLY SHEAR IN THERMOFORMED THERMOPLASTIC COMPOSITES

G. F. Nino, O.K. Bergsma, H.E.N. Bersee
Delft University of Technology, Faculty of Aerospace Engineering
Design and Production of Composite Structures, Kluyverweg 1, 2629 HS Delft. The Netherlands.

In the design of new composites parts, it is necessary to have a good understanding of the behavior of the material during its manufacturing stage. During the thermoforming process of advanced thermoplastic composites, the laminate must deform to meet the complex geometric requirements of the component. Among the most important deformation mechanisms involve, the intraply shear or Trellis effect is responsible for the formability of a given material over certain geometry in the forming process. The shear deformation of woven fabrics is limited by the so-called locking angle; the smaller the locking angle, the better the deformation possibilities of the fabric. Excessive shearing angles imply manufacturing difficulties, and the fibers may not keep the desired orientations; So, the study of this topic on the real product during the R&D stage is a necessity in order to reduce the develop cost associated with the trial-and-error approach.

With the aim of study the intraply shear phenomenon, a Square Grid Analysis (SGA) tool, adapted from the traditional metal applications, was created using Matlab®. This tool is being used and integrated with drapability and finite element analyses in the Aerospace Faculty at the TU Delft, in order to analyze the final deformations in thermoformed products, and in develop and evaluation of diaphragm foils for diaphragm forming process.

The SGA technique is a well-known experimental method used in strain analysis in metal forming processes, where an array with a good contrast is placed or attached to the sample prior to the deformation. In contrast with metals, the composite thermoplastic matrix is melted due to the high process temperature, so the array will be subject to distortion. For that reason, it is inadvisable to use inks or any other kind of superficial marks. Therefore, in order to visualize the deformations, the most suitable arrangement for woven composites is incorporating a plain weave pattern in the laminate using two kinds of fibers to improve the contrast like carbon and glass fibers. In the case of high temperature test for diaphragm foils, special inks can be used in order to warranty its geometrical stability and adherence to the foil. After the thermoforming, the user can select a region of interest in the piece to analyze, and takes a series of pictures of the formed shape from different perspective views with a digital camera. From the photos, the array position is localized and with two or more images the global 3D co-ordinates are computed using photogrammetric methods. The stereo reconstruction can be performed manually or automatically defining the shape of the deformed sample. The relationship between the global co-ordinate system and the local-image co-ordinate system is obtained by camera calibration using a known pattern.

In the post-processing, the shearing angle for each square is computed. The deformed grid is compared with a geometrical drapability analysis performed by Drape (Software developed at TU Delft). On this stage, it is possible to superimpose both results and compare visually and numerically the fidelity of the simulation versus the experimental test in order to calibrate the simulation tool. Also, it is possible to compare those results directly with the data obtain from commercial finite element software like Pam Form from ESI Group.

The main objective of this SGA tool is the automatic integration between the experimental tests with the simulation environment in order to obtain some feedback from the real process, providing important information about the intraply shear phenomenon in thermoforming of thermoplastic composites.

1 Corresponding author: Giovanni Nino. Email: g.f.nino@lr.tudelft.nl
Office Phone Number: +31(0) 15 278 9740, Fax Number: +31(0) 15 278 1151.

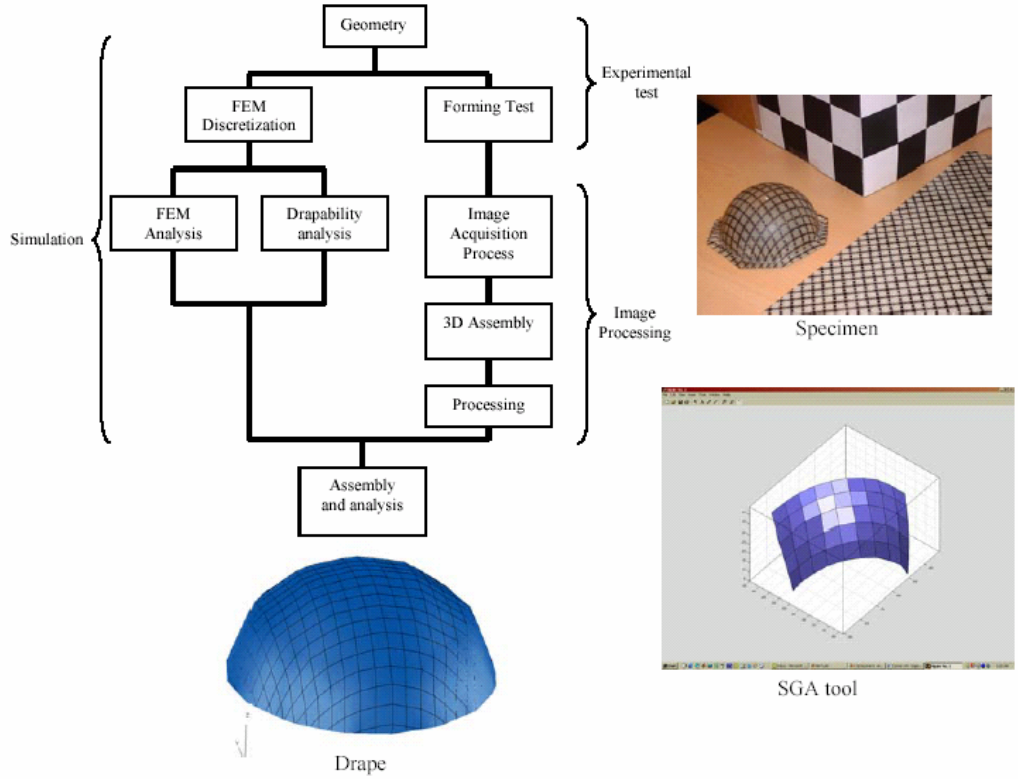

Figure 1. Scheme of the Square Grid Analysis tool integrated with the simulation software for thermoplastic thermoformed composites.

A MIXED NUMERICAL-EXPERIMENTAL IDENTIFICATION METHOD FOR EVALUATING THE CONSTITUTIVE PARAMETERS OF COMPOSITE LAMINATED SHELLS

Joël Cugnoni, Thomas Gmür* & Alain Schorderet
School of Engineering (STI), Swiss Federal Institute of Technology (EPFL),1015 Lausanne, Switzerland
*e-mail: thomas.gmuer@epfl.ch

Fibre-reinforced composites are being increasingly used as alternatives for conventional materials primarily because of their high strength, specific stiffness, light weight and adjustable properties. However, before using this type of material with confidence in industrial applications such as marine, automotive or aerospace structural components, a thorough characterization of the constituent material properties is needed. Unfortunately, with laminates resulting from a stacking of layers, the constitutive properties can not be accurately estimated by performing experimental tests on one lamina and by extrapolating the results to a multilayered composite according to the fibre orientation and the stacking sequence of the laminae. An elegant way to circumvent this lack consists in using mixed numerical-experimental methods which constitute powerful tools for estimating unknown constitutive coefficients in a numerical model of a composite structure from static and/or dynamic experimental data collected on the real structure. Starting from the measurement of quantities such as the displacements, stresses, or natural frequencies and mode shapes, these methods allow, by comparing numerical and experimental observations, the progressive refinement of the estimated material properties in the corresponding numerical model. In this domain, dynamic mixed techniques have gained in importance owing to their simplicity and efficiency.

In this paper, a mixed numerical-experimental identification method based on the modal response of thick laminated shells is presented. This technique is founded on the minimisation of the discrepancies between the eigenvalues and eigenmodes computed with a highly accurate composite shell finite element model with adjustable elastic properties and the corresponding experimental quantities. In the case of thick shells, the

constitutive parameters that can be identified are the two in-plane Young's moduli E_1 and E_2, the in-plane Poisson's ratio ν_{12} and the in-plane and transverse shear moduli G_{12}, G_{13} and G_{23}. To determine these six parameters, a typical set of 10 to 15 measured eigenfrequencies and eigenmodes is selected, and the over-constrained optimisation problem is solved with a nonlinear least square algorithm.

In order to maximize the quality of the identification, free-free boundary conditions and a non- contacting modal measurement method are chosen for the experimental determination of the eigenparameters. To obtain optimal experimental conditions, the specimens are suspended by thin nylon yarns and excited by a calibrated acoustic source (loudspeakers) while the dynamic response is measured with a scanning laser vibrometer. The measured frequency response functions are then treated in a modal curve fitting software to obtain a high quality set of modal data (mode shapes and frequencies). Unfortunately, due to the sound propagation phenomena, the phase of the acoustic pressure on the specimen is not constant, implying that the modal excitation resultant strongly depends on the mode shape, so that not all the modes may be sufficiently excited and thus measured. Hopefully, this problem can be solved by optimizing the positions and phases of the loudspeakers, with the aim of exciting the greatest number of modes. A simple but effective acoustic source optimization method is also discussed and experimentally verified.

As the accuracy of this inverse method directly depends on the precision of the finite element model, a family of very efficient thick laminated shell finite elements based on a variable p-order approximation of the through-the-thickness displacement with a full 3D orthotropic constitutive law has been developed. It is shown that for thick and highly orthotropic plates, the formulation exhibits a good convergence on the eigenfrequencies with p=3 and a nearly exact solution for p=7. In comparison to other 3D solid or thick shell elements, such as layerwise models, the presented elements show an equivalent precision of the computed eigenfrequencies and are computationally less expensive for laminates with more than 8 plies.

A classical Levenberg-Marquardt nonlinear least square minimisation algorithm is used to solve the inverse problem of finding the elastic constitutive parameters which are best matching the experimental modal data. Original multiple objective functions are used for comparing the computed and measured values. They are based upon the relative differences between the eigenfrequencies, upon the diagonal and off-diagonal terms of the so-called modal assurance criterion norm on the mode shapes, and upon geometrical properties of the mode shapes such as the nodal lines or the curvature of the isolines. As for other iterative minimisation methods, the derivatives of the objective functions must be computed precisely and with a minimum of computational cost in order to accelerate the convergence of the procedure and to reduce the total computation time. In the present work, these derivatives with respect to the identification parameters require the computation of the eigenfrequencies and eigenmodes derivatives, which is carried out by an optimized direct finite difference method. Moreover, the convergence properties as well as the identification residuals of the minimisation algorithm are also investigated. It can be observed that usually the minimisation requires 5 iterations to reach a residual error of less than 0.1 percent. The minimization algorithms have been tested on both purely numerical and experimental data, showing excellent accuracy and convergence speed. Typically, if the measurement quality is sufficient, the identification algorithm converges in ess than five iterations within a tolerance 0.1% on the eigenfrequencies and 2% on the in-plane tensile or shear moduli. The in-plane Young's moduli and inplane shear moduli can be identified within a tolerance of 2%. The in-plane Poisson's ratio and the transverse shear moduli may however be less accurate, with a usual uncertainty of 5% and 10%, for relatively thick and thin specimens respectively.

Finally, two real identification examples are presented, one for a thin unidirectional AS4-PPS plate and another for a thick industrial-grade carbon-epoxy specimen. An estimation of the errors and uncertainties on the final estimated parameters as well as a comparison with standard characterization tests is also presented. It can be concluded that overall the present identification method can accurately determine the in-plane Young's and shear moduli and to a lesser extent the transverse shear moduli and the in-plane Poisson's ratio. It is also seen that the stability of the method is excellent as long as the number of measured modes is much larger than the number of parameters to be identified.

FLEXURE TESTS FOR DETERMINING TENSILE AND COMPRESSIVE MODULUS

F. Mujika[1] and I. Mondragon[2]

[1] Mechanical Engineering Department. **e-mail**: impmugaf@sp.ehu.es

[2] Chemical and Environmental Engineering Department

[1,2] EUP, Universidad del País Vasco/Euskal Herriko Unibertsitatea, Plaza de Europa 1, 20018 San Sebastián/Donostia, Spain

In a unidirectional composite material tensile and compressive modulus are different, mainly in longitudinal direction. Tensile and compressive tests are needed for determining both modulus. This work proposes a way for determining tensile and compressive modulus by flexure tests.

Supposing that tensile and compressive moduli are different, neutral surface position must be determined. Figure 1 shows the distances *h1* and *h2* from the neutral surface to the outer and the inner faces, respectively.

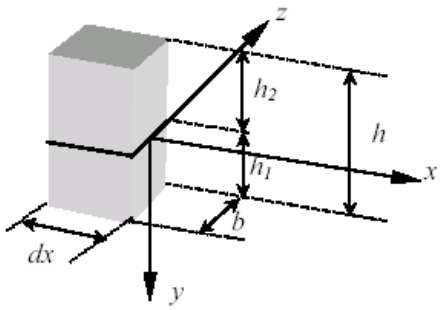

Figure 1. Reference system in the neutral surface and dimensions

According to hypothesis of classical beam theory, longitudinal strains are:

$$\varepsilon_x = \frac{y}{\rho} \tag{1}$$

Stresses at tensile and compressive sides are respectively:

$$\sigma_t = E_t \frac{y}{\rho} \qquad \sigma_c = E_c \frac{y}{\rho} \tag{2}$$

Due to normal force is 0 and taking into account $h_1 + h_2 = h$ results:

$$h_1 = \frac{h}{1+\sqrt{\lambda}} \qquad h_2 = \frac{h\sqrt{\lambda}}{1+\sqrt{\lambda}} \tag{3}$$

where $\lambda = \frac{E_t}{E_c}$

Then, according to Equation (1) maximum strains at the outer and the inner faces are respectively:

$$\varepsilon_t = \frac{h_1}{\rho} \qquad \varepsilon_c = \frac{h_2}{\rho} \tag{4}$$

And the ratio between them:

$$\frac{\varepsilon_c}{\varepsilon_t} = \frac{h_2}{h_1} = \sqrt{\lambda} = \sqrt{\frac{E_t}{E_c}} \tag{5}$$

Otherwise, as long as bending moment is the resultant moment of normal stresses results:

$$M = \frac{E_f I}{\rho} \tag{6}$$

where:

$$E_f = \beta E_t \qquad \beta = \frac{4}{\left(1+\sqrt{\lambda}\right)^2} \tag{7}$$

For calculating moduli the following procedure is proposed:

1. A specimen with a strain gage is tested twice for loads lesser than failure load. In the first test strain gage is on the tensile side and in the second test is on the compressive side. In both cases load-strain curve slope is determined. The test can be repeated to ensure specimen has not damage. Being *mt* the slope corresponding to tensile side and *mc* the one corresponding to compressive side, their ratio is:-

$$\frac{m_t}{m_c} = \frac{\varepsilon_c}{\varepsilon_t} = \sqrt{\lambda} \tag{8}$$

2. The same specimen is tested in 3-point flexure or 4-point flexure for determining *Ef*, using a span-to-depth ratio that warrants shear effects have not influence. Knowing the value of ë from Equation (8), *Et* can be calculated from Equations (7) and finally *Ec* is calculated from Equation (8).

Tests have been carried out in 3 specimens of different carbon fibre/epoxy matrix materials from Hexcel Composites manufactured by compression, with 55% fibre percentage in volume.

Table1. Experimental results obtained for 3 carbon fibre/epoxy matrix materials

Material	Strain gage position	P/ε (N)	E_f (MPa)	E_t (MPa)	E_c (MPa)
AS4/3501-6	Tension	44,922	117,900	123,300	103,400
	Compression	41,134			
AS4/8552	Tension	94,394	131,200	137,600	113,800
	Compression	85,864			
IM7/8552	Tension	188,916	150,000	157,100	131,100
	Compression	172,595			

References

1. Jones, R.M. (1976). Apparent Flexural Modulus and Strength of Multimodulus Materials, *Journal of Composite Materials*, **10**: 342-354.
2. Zhou, G. and Davies, G.A.O. (1995). Characterization of Thick Glass Woven Roving/Polyester Laminates: Part 2: Flexure and Statistical Considerations, *Composites* **26**: 587-596.

COMPARISON OF MOIRÉ INTERFEROMETRY AND IMAGE CORRELATION DEFORMATION MEASUREMENT TECHNIQUES

D. Mollenhauer[1α] and J. Tyson[2]
[1] U. S. Air Force Research Laboratory, AFRL/MLBC, Wright-Patterson AFB, OH 45433, USA
[2] Trilion Quality Systems, 200 Barr Harbor Drive, West Conshohocken, PA 19428, USA

An advanced image correlation technique was used to measure deformation on the surface of a complicated composite joint. The joint consisted of a combination of tape layup, cloth, and 3D woven architectures. Phase-shifting moiré interferometry was used as a reference for comparison of in-plane deformation. The image correlation and the moiré interferometry measurements both used digital cameras that had similar number of

pixels in the region of view. Initial comparisons between the two sets of data consisted of a direct comparison between full resolution moiré and image correlation. The image correlation methodology produced fewer displacement data points than did moiré. As a result, the moiré interferometry data shows better spatial resolution of the complex variations in strain. Displacement and strain magnitudes, in general, matched very well. However, regions of very fine detail and high strain were missed by the image correlation method. Subsequent comparisons of data consisted of examining the moiré results at a data point resolution exactly the same as the image correlation technique. These displacement and strain data were extremely close in both magnitude and distribution. The image correlation methodology appears to be a viable and robust method for deformation analysis, especially when considering reduced specimen preparation time.

[α] Corresponding author, tel.:01-937-255 9728, e-mail: david.mollenhauer@wpafb.af.mil

DEVELOPMENT OF DESIGN SYSTEM FOR FRP GEARS FOR POWER TRANSMISSIONS

Toshiki Hirogaki[1], Eiiichi Aoyama[1], Tsutao Kataua,a[1]
Kazuya SUGIMURA[2], Yoshinori YAGURA[3]
1. Faculty of Engineering, Doshisha University Japan
2. Ishida Co., Ltd., Japan
3. Graduate student, Doshisha University Japan

Plastic gears have thus far been used only under low torque conditions of rotational transmission. Fiber reinforced plastic (FRP) gears are now attracting attention because of their high strength and material rigidity. In recent years, FRP gears have begun to be used under severe conditions as mechanical elements in automobile engines. However, there are few reports dealing with FRP gears. Therefore, the construction of a design system for FRP gears used for power transmission elements is the aim of this research.

In this research, a laminate material (a phenolic resin reinforced by plain woven cotton cloth) was used for the gear material. The gear was produced by hobbing. This material was used because of its excellent heatproof and impact characteristics. Mechanical characteristics are also good.

Table 1 shows the dimensions of the gears used in this research. The material is also anisotropic because of the plain woven cotton cloth reinforcement. Therefore, we investigated the influence of the material anisotropy on strength and fracture toughness of the gear teeth. Thus, a gear made of a phenolic resin reinforced by paper laminate material, which was isotropic, was produced for comparison. We also investigated the difference strength conferred by reinforced fiber on strength and fracture. Therefore, gear made of a phenolic resin reinforced by plain woven glass fiber cloth laminate material was produced.

In this report, we addressed the bending strength of gear teeth in the basic design progress.

First, to examine bending fractures in teeth, a line load was applied to the tooth root fillet and tooth breakage in this area during bending was investigated. Figure 1 shows the results. A difference in bending fracture strength according to the fiber angle of each tooth was found, as shown in the figure. Moreover, from photograph 1, it was found that the crack progresses along the fiber distribution and breakage beginning position rises compared with an isotropic gear.

Second, to investigate the repetition fatigue strength of teeth, a fatigue test was conducted. Figure 2 shows the obtained result.

Third, a tension test, a uniaxial compression test, 3-point and 4-point bending tests, and a shearing test were performed for the gear material used to investigate destruction strength in the gear shape and the primary factors in the destruction form. Here, in the bending test, the 4-point bending test and the 3-point bending test were used to investigate influence of shearing stress on bend strength.

As a result, it was found that compressive strength and the bending and shearing stress greatly influence the bending strength of teeth.

Table 1 Dimensions of gears

		Cotton Reinforced Gear					Glass Reinforced Gear	Paper Rein forced Gear
Laminate Configuration		[0/90]					[0/90]	
Module		3		4		5	3	4
Standard Pressure Angle	[deg]	20						
JIS Class		4						
Face Width	[mm]	25						
Tooth Depth	[mm]	6.75		9		11.25	6.75	9
Number of Teeth		49	65	49	39	49	49	
Diameter of Standard Pitch Circle	[mm]	147	195	196	195	245	147	196
Refarence Diameter	[mm]	153	201	204	205	255	153	204

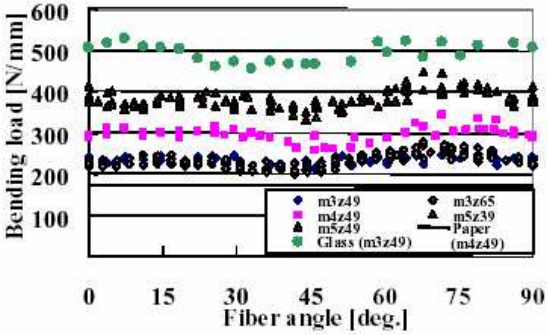

Fig.1 Result of bending fracture test

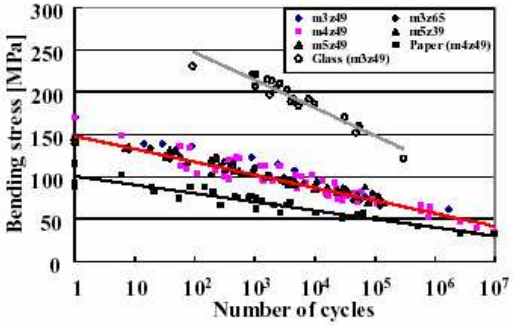

Fig.2 Result of bending fatigue test

(a) 0 Degree of cotton (b) 45 Degree of cotton (c) 75 Degree of cotton (b) Paper gear

Photo 1 Fractured gear teeth by bending load

IMPACT DAMAGE AND CAI STRENGTH OF MR50K/PETI5 CARBON/TOUGH-POLYIMIDE COMPOSITE MATERIAL

Hisaya Katoh[1], Toshiyuki Shimokawa[2], Akira Ueda[2], and Yasumasa Hamaguchi[1]

[1] Advanced Composites Evaluation Technology Center (ACE-TeC), Japan Aerospace Exploration Agency (JAXA)

[2] Department of Aerospace Engineering, Tokyo Metropolitan Institute of Technology (TMIT)

PETI5 is recently developed by NASA as a high heat-resistant and tough polyimide-resin for use in HSCT structures. CAI strength is frequently used for the structural design criteria because of the low CAI strength of general laminated CFRPs. A tough resin CFRP is practically attractive and scientifically interesting, because such a resin is expected to show improved mechanical properties and different behavior from those seen in common epoxy CFRPs. However, there is no report on the CAI behavior of a CFRP of PETI5, a typical tough resin.

The objective of this study is to experimentally investigate the CAI behavior of a CFRP laminate of a typical tough resin, i.e., the impact damage and CAI strength of MR50K/PETI5 composite material, with a stacking

sequence [45/0/-45/90]4S. MR50K is a carbon fiber having medium-elastic modulus and high strength produced by the Mitsubishi Rayon Co. This fiber is considered to be matched well with PETI5.

The test contents are as follows. (1) The impact damage was given to a MR50K/PETI5 specimen at room temperature. Load and energy were measured during impact loading. (2) The impacted specimens were observed by an ultra sonic C-scanner and a 3-D ultra sonic inspection system. (3) The CAI strength at room and high temperatures was obtained. (4) The cross-sectional area cut from the CAI failure specimens was observed to study the failure mode. (5) A part of test results were compared with those of T800H/PMR-15, a typical carbon/ brittle-polyimide composite material.

Examples of Test Results

Figure 1 indicates the typical response curves of the load and energy during a 6.67 J/mm impact test, including those of a T800H/PMR-15 specimen. The impact load as a function of time shows a trapezoidal shape for the MR50K/PETI5 specimen, though it is a parabolic shape for the T800H/PMR-15 specimen.

Figure 2 shows an image of damage inside of the MR50K/PETI5 specimen obtained at impact energy 4.45 J/mm. This picture was taken by a 3-D ultrasonic inspection system. Small damage area is expanded between laminae and the helical pattern of damage progress is confirmed. The typical features shown in Figs. 1 and 2 are due to the high interlaminar fracture toughness.

Figure 3 presents the CAI strength of MR50K/PETI5 at room temperature and 180°C, including those of T800H/PMR-15 obtained by Fuji Heavy Industries Ltd. at room temperature. Moreover, the static compressive strength is plotted at the impact energy 0 J/mm. The CAI strength of MR50K/PETI5 is much higher than that of T800H/PMR-15, though the compressive strength is reversed.

Major Concluding Remarks

(1) Small delamination area was observed for MR50K/PETI5 and considered to be dependent on the high toughness of PETI5. (2) Typical and fundamental compressive-failure behaviors of a CFRP using a tough resin were clarified after impact tests. (3) The CAI strength of MR50K/PETI5 as a function of the impact energy was approximately linear with a negative slope up to 8.90 J/mm. (4) The observation of the cross-sectional area cut from the CAI failure specimens elucidated that the shear failure mode was macroscopically dominant with a little amount of delamination cracks for the low impact energy, although with numerous small delamination cracks for the high impact energy. (5) If a highly tough resin such as PETI5 was introduced, the weak out-of-plane strength of CFRP structures could be greatly improved.

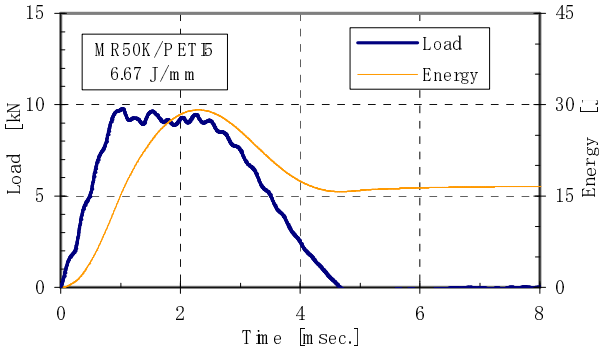

MR50K/PETI5 (Max Load = 9.79 kN)

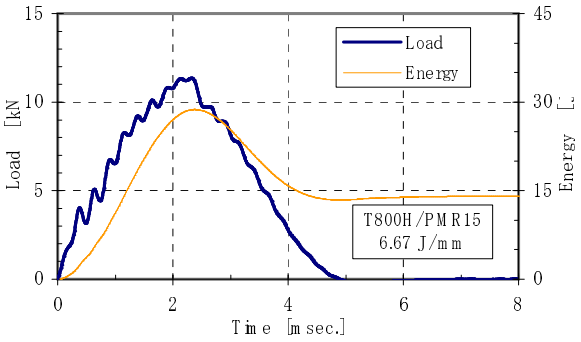

T800H/PMR-15 (Max Load = 11.35 kN)

Figure 1 Load and energy during an impact test (IE = 6.67 J/mm).

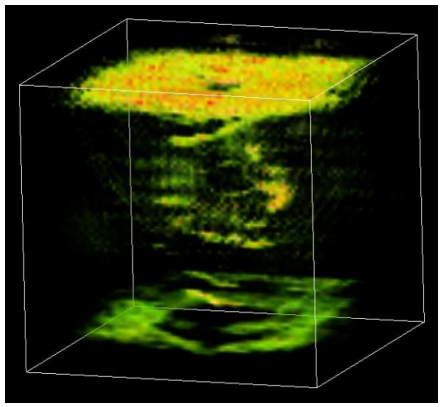

Figure 2 A three dimensional view of the impact damage and delamination formed in MR50K/PETI5 observed by a 3-D ultrasonic inspection system (IE = 4.45 J/mm).

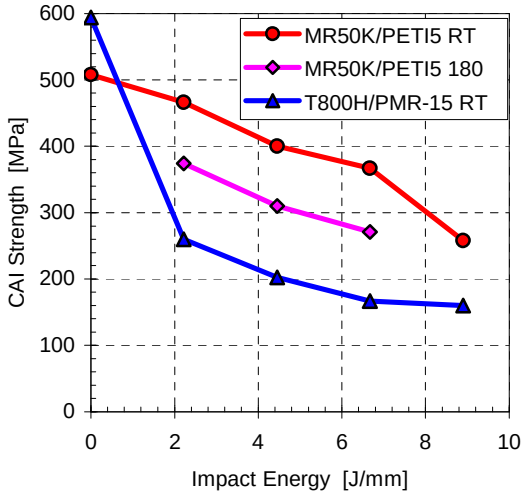

Figure 3 CAI strength vs. impact energy for MR50K/PETI5 and T800H/PMR-15, including static compressive strength plotted at IE=0 J/mm.

THE APPLICATION OF THE INTERPHASE MODEL FOR THE DESCRIPTION OF THE FILLED COMPOSITE PROPERTIES WITH NANOPARTICLES. IDENTIFICATION OF THE PARAMETERS OF THE MODEL.

S. A. Lurie, N. P. Tuchkova, V.I. Zubov,
Dorodnicyn Computing Centre of the Russian Acad. of Scs, Vavilov st.40, 119991 Moscow GSP-1, Russia, E-mail: lurie@ccas.ru

The nano-particles themselves and composite materials obtained on their base are objects of the investigation. It is assumed that the following physical objects and appropriate local effects may determine the uncommon properties of the composites: cohesion fields, and a zone of an internal interaction determined by them; adhesion interactions, which determine the peculiarity of the interaction of contacting bodies. These effects may be significant and can define of the mechanical properties of the mediums possessing developed interface surface.

It is assumed that the following physical objects and appropriate local effects may determine the uncommon properties of the materials: cohesion fields, and a zone of an internal interaction determined by them; surface tension; adhesion interactions, which determine the peculiarity of the interaction of contacting bodies. The correct consistent mechanical model is constructed with the aid of new variant of the kinematics variation principle [1,2] and satisfies the following requirements: i). The model describes the behavior of the deformed media taking into accounts the scale effects. ii). The total deformation energy depends not only on the volume deformation density, but also on the surface density of deformation. This requirement is due to the necessarily of accounting for the surface effects and scale effects determined by the phase interfaces. iii). The model of deformation takes into account the scale effects, is not contradict to the classical models, and have to include them as a limiting case.

The algorithm of the model constructing consists in the following steps: 1). The kinematics restrains for the particular medium are formulated. The list of arguments is determined. 2) In accordance with the assumption of the integrability of bilinear variation form the potential energy is formulated taking into account tensor's dimensions of the arguments and constitutive equations are constructed. 3) The constitutive equations allow to obtain particular expressions for the potential energy, which defines the mathematical statement of the model as a whole.

As the result the closed mathematical formulation of the interphase model is given, as variant of the a Cosserat model for a medium with non-free deformations and symmetric stress tensor. The offered model contains new physical constant in comparison with the classical theory of elasticity, which allows to describe the cohesion type interaction. This constant has other dimension, than dimension of the Lame's coefficients, and differs from them on a square of length. In framework of the offered model also surface effects are described with the aid of two physical constants in the superficial parts of potential energy, which determine the surface effects associated with the normal to the surface of the body and the superficial effects in the tangent plane. Their account leads to appearance in boundary conditions additional members, modeling adhesive properties of a surface of contact.

Within the framework of the cohesion field model, a theoretical model of an interphase layer is obtained. The approximated analytical dependences of the properties of interphase layer in a composite near the border between an inclusion and matrix on the characteristics of cohesion fields of phases are established. For modelling periodic structures definition the micro- and nano-mechanical descriptions are given on the basis of comparison of the sizes of inclusions with geometrical characteristics of cohesion fields and interphase layers produced by them. The approximated analytical estimations of thickness and rigidity of an interphase layer for micro-and nano-mechanical models are given. It is shown that the interface layer occupies part of the volumes of both phases; its mechanical properties changes exponentially in the vicinity of the phases contact surface within the limits of values of moduli of the inclusion and the matrix. It is shown that the effect of increase of effective rigidity can be modeled within the framework of the suggested model. This effect depends on the size and quantity reinforced particles at the fixed volume part of the reinforced material.

The algorithm of identification of parameters of the model was considered. It was shown in particular that parameter determined the cohesion type interactions can be established based on the fracture mechanics problem. The relation of the new physical constant to the parameters of the fracture mechanics (critical crack disclosing, the Barenblatt's zone of length, and specific superficial energy) is established. The treatment of a local field as the Barenblatt's cohesion fields is given. The problem of the model parameters identification on the base of the experimental data [3] was solved firstly for spherical inclusions in the frame of the simplified micromechanical model (according to the suggested classification) when characteristic lengths of phases in the composite were considered significant and considerably exceeding the characteristic size of an interphase layer.

It is shown that micromechanical modeling gives the good description of a composite with microinclusions if concentration of inclusions is not present exceeds 30 %. Then, the identification problem is considered for more common nano-mechanical model. The results calculation showed that the model constructed on the base of nano-mechanical description of the composite is more flexible then the previous model. The diapason of parameters (concentration and sizes of the inclusions) for which the model agrees well with experimental data of the new model is much wider then the previous model also. The problem of finding model parameters to fit theoretical data to experimental data from mathematical point of view is solved as inverse problem. This problem is formulated as variation problem to find such set of parameters to minimize cost function: $\Phi = \sum_{i=1}^{K} \frac{1}{K} \cdot \left[E_i^t - E_i^e \right]^2$, where K points with coordinates $\left(E^e, f^e, R^e\right)_1$, $\left(E^e, f^e, R^e\right)_2$, … , $\left(E^e, f^e, R^e\right)_K$, $2R$ is the diameter of reinforcing element; f - volume fraction of inclusions; E is effective modulus of composite which depends from matrix Young's modulus- E_M, reinforcing material Young's modulus E_D, and model parameters determined cohesion and adhesion interactions - a. The problem of identification model parameters may be formulated as follows: to find the parameters a in such a way, that the "distance" between experimental set of points with coordinates $\left(E^t, f^e, R^e\right)_1$, $\left(E^t, f^e, R^e\right)_2$, … , $\left(E^t, f^e, R^e\right)_K$ and theoretical set of points to be minimum. The minimization of cost function was carried out numerically with the aid of conjugate gradient technique. The parameters a of used mathematical model were determining for two kinds of composite materials: the composite material based on epoxy resin reinforcing by glass fraction and the composite material based on non-saturated polyester reinforcing by glass fraction.

The algorithm of estimation of average mechanical properties for composites reinforced by the nanofibers is also obtained based on the proposed theoretical model of an interphase layer. *(The work is supported by the European Office of Aerospace Research and Development, Int. Grant N2154p and Grant 01-03-00165).*

REFERENCES

1. Lurie S., Belov P., Volkov-Bogorodskii. Multiscale Modeling in the Mechanics of Materials, in: book "Lecture Notes in Applied and Comp. Mechanics", Analysis and Simulation of Multifield Problems, vol. 12, Springer, (2003), 101-110
2. Lurie S.,Belov P., Volkov-Bogorodskii, Tuchkova N. Nanomechanical Modeling of the Nanostructures and Dispersed Composites // Int. J.l "Computational Materials Science", Volume 28, Issues 3-4 , 2003, Pages 529-539.
3. Miva M. Influence of the diameters of particles on the modulus of elasticity of reinforced polymers, Kobunshi Ronbunshu, 1978, Vol. 35, 2, p.p. 125-129.

THERMAL FATIGUE BEHAVIOR OF SICP/ AL COMPOSITE SYNTHESIZED BY METAL INFILTRATION

C. M. Lawrence Wu[1] and G. W. Han[1,2]
[1]Dept. of Physics and Materials Science, City University of Hong Kong, Hong Kong SAR, P.R. China
[2]Dept. of High Temperature Mater. Res., Central Iron & Steel Research Institute
Beijing 100081, P.R. China

The combination of the properties such as high stiffness, low coefficient of thermal expansion, high thermal conductivity, high toughness and low density from ceramic reinforcement and metallic matrix enables the metallic matrix composites (MMCs) with high volume fraction of reinforcement to find potential applications in aerospace, automobile and support structures for electronic devices. There have been many routes developed to synthesize such composites. In comparison, the pressureless spontaneous liquid metal infiltration is a cost-effective technique to manufacture such composites with complex shape to near net shape in mass production.

Thermal fatigue, much in common with creep and mechanical fatigue, is produced basically by cyclic or periodic temperature changes and complete or partial restriction of thermal deformation due to external or internal factors. External constraints produce forces that act on a component with alternating heating and cooling, leading to fatigue cracking at the location with stress concentration caused by restriction of thermal

deformation. Internal constraints may be resulted from temperature gradients, structural anisotropy and different coefficient of expansion in adjacent grains or phases, including the matrix and the reinforcement in composites, and would possibly result in cracking of interfaces. The particulate reinforced composites with high volume fraction of reinforcement employed for such components may undergo thermal fatigue in service due to the internal and external restriction of thermal deformation. Therefore, the resistance to thermal fatigue should be an important property of such composites. However, there has not been adequate research yet on thermal fatigue behavior of this kind of composites synthesized by pressureless melt infiltration. This paper is aimed at presenting the thermal fatigue behavior of a SiC particulate reinforced aluminum matrix composite synthesized by pressureless melt infiltration route.

SiCp/Al composite plates of 3mm thick containing about 65vol% SiC particulate reinforcement were prepared by pressureless melt spontaneous infiltration of molten Al-10Si-3Mg alloy into SiC particulate perform at 850°C in nitrogen atmosphere. Thermal fatigue specimens with V-shape notch were cut from the synthesized composite plates by electrical discharge cutting. Thermal fatigue tests were carried out by quenching the notch part of the specimen from 300°C to ambient water cyclically after the specimen was kept at the temperature in a furnace for 15 minutes. The initiation and propagation of crack from the notch root was examined using an optical microscope every 5 cycles. The characteristics of crack initiation and propagation as well as fracture surface features were examined using a scanning electron microscope.

It was found that thermal fatigue crack initiation and propagation of this kind of composite is very dependent on fracturing of large particulate reinforcement in the composite by thermal shock. So the reduction of the size of the particulate reinforcement and employing the particulate reinforcement with low expansion coefficient should increase the resistance of this kind of composite to thermal fatigue.

SESSION 6 – FULL FIELD TECHNIQUES II

Chair: Dr. Bill Broughton
National Physics laboratory, UK

Wednesday 22 September
11.15-12.55

NON-HOMOGENEOUS CFRE STRAIN FIELD MONITORING WITH THE ELECTRONIC SPECKLE PATTERN INTERFEROMETRY TECHNIQUE.

Pascal, J-P. Bouquet[1] and Albert, H. Cardon[2]

[1]SABCA LIMBURG n.v. , Belgium, Development, studiebureau, Dellestraat 32, B-3560 Lummen
e-mail: Pascal.Bouquet@sabca-limburg.com

[2]Vrije Universiteit Brussel (VUB), Belgium, Department Mechanics of Materials and Constructions (MeMC), Pleinlaan 2, B-1050 Brussels. *e-mail: mbourlau@vub.ac.be*

The matrix of a polymer-based composite laminate is time dependent and is sensitive to the environmental conditions. Polymer matrix composites therefore behave as viscoelastic-viscoplastic anisotropic continua. This concerns not only the stiffness but also the strength characteristics. Various models for the lifetime prediction are considering the changes in stiffness properties as an expression of damage superposed to a viscoelastic model. These models based on the viscoelastic behaviour propose an accelerated characterisation procedure for composites that would allow the prediction of long term properties from short term experiments including time-stress-superposition procedures and non-linear viscoelastic behaviour as well as models to predict delayed failures such as creep ruptures. Creep measurement data obtained from different load levels of test specimen provided with strain gages and/or extensometers were not conclusive.

The question arises on how to detect the failure initiation on the test specimen and the ability to measure the non-homogeneities in mechanical response of the unidirectional composite material. Digital imaging methods like the Electronic Speckle Pattern Interferometry are techniques to determine in situ properties at a local scale commensurate with the continuum modelling procedure. The success of the experimental techniques with a macromechanical approach on the strain behaviour of isotropic materials is inadequate to be extrapolated to the composite material behaviour description. A survey of various optical measurement techniques was performed from which the ESPI method showed to be the most suitable for the given strain range for the given creep experiments. The resolution of the ESPI method combined with the area of inspection drastically improves the monitoring of the strains on the outer surface. It has to be emphasised that the ESPI measurement doesn't allow in depth measurement like e.g. ultrasonic inspection, however it presents some promising features. Pristine CFRE test beams were subjected to creep loads. It has been observed that the area of increased strain at the initiating failure is hardly detectable with the strain gage technique due to its limited measurement base and the averaging of the measurement over it's measurement area.

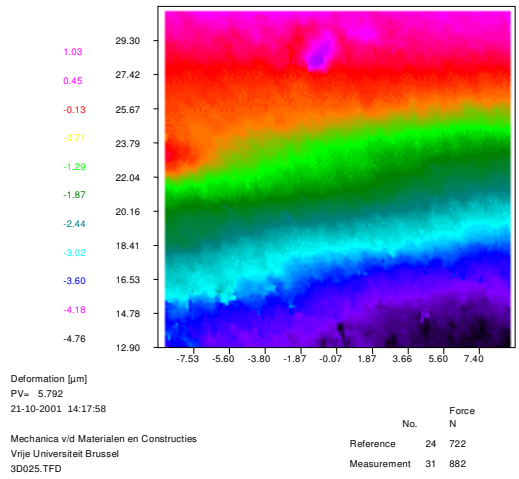

Figure 1: out of plane deformation $[90°]_{10}$ laminate prior to rupture 35MP a->40MPa

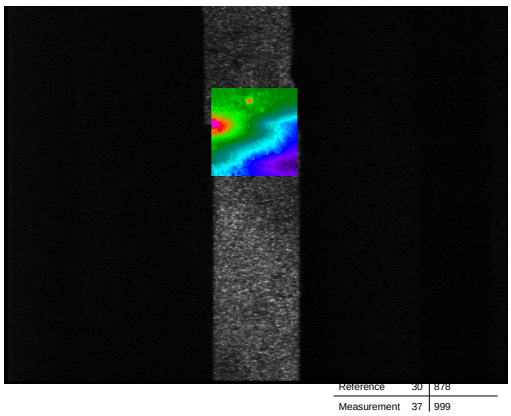

Figure 2: out of plane deformation (833N)$[90°]_{10}$ laminate prior to rupture 40MPa creep (30min.), with underlay of the ruptured sample

On the $[90°]_{10}$ unidirectional laminates considered sudden failure will occur as a result of small defects or redistribution of the stress. A closer look on different fibre orientations is however to be considered as to evaluate the strain field and its redistribution as a function of time.

USE OF PHASE-STEPPING PHOTOEASTICITY TO MEASURE INTERFACIAL SHEAR STRESS IN SINGLE FIBRE MODEL COMPOSITES

F.M. Zhao[1] S.A. Simon[1] E.A. Patterson[2], R. J Young[3] and F.R. Jones[1]
[1]Department of Engineering Materials, University of Sheffield, Sheffield S1 3DJ UK
[2]Department of Mechanical Engineering, University of Sheffield, UK
[3]Manchester Materials Science Centre, UMIST, Manchester M1 7HS, UK

The interface of a composite plays an important part in determining its mechanical properties and reliability. In order to evaluate the interfacial properties between fibre/polymer matrix and to investigate stress transfer at the interface, some experimental micro-mechanical techniques and methods, such as Raman and fluorescence spectroscopy, fibre fragmentation or pull-out, have been used commonly. The analysis has to be based on certain mechanical models and assumptions which are used for calculating an interfacial shear strength or related parameter. Therefore the results obtained are sometimes shown to be contradictory because the assumptions are invalid [1]. Furthermore, the application of Raman and fluorescence spectroscopy is limited to the certain type of fibres, such as high modulus carbon and polymer fibres. The fragmentation test requires the polymer matrices with high failure strain. On the other hand, fracture events, such as interfacial debonding and transverse matrix cracking, occur at a fibre-end or a fibre-break, and then the debond propagates along the bonded interface with increasing load. These make the measurement of the interfacial shear stress at the debond front quite difficult. The mechanical properties of the matrix resins have been found to have an obvious influence on the interfacial shear strength obtained from the fragmentation test [2-3]. So far, the stress field in the resin near the debonded and the bonded interface has not been considered experimentally. Therefore, it is still necessary to measure directly the interfacial shear stress and the stress field in the matrix nearby.

A phase-stepping automated polariscope has been used to measure the stress field in the matrix around a fibre-end or near a fibre-break, combined with a mini-loading frame and microscope used for fragmentation test [4]. The instrument can capture simultaneously the four images needed to produce maps of isochromatic and isoclinic parameters over a full field of view at various levels of applied load. The automatic polariscope allows real-time data to be obtained during fibre fracture, from which stress contour maps can be constructed on the micro scale. In this case interfacial debonding and matrix cracking cab be readily identified and quantified.

A two-dimensional model composite specimen consisting of a high modulus Al_2O_3 fibre embedded in an epoxy resin has been used. A load is applied to the specimen along the fibre direction. Figure 1 gives the contour map of the isochromatic fringe order in the resin around the fibre-end showing local stress concentrations. The continuous isochromatic pattern is shown using twelve colours from blue to white. The twelve colours also have the relevant numerical scale indicating the value of the fringe order. The result suggests that the stress was transferred effectively to the fibre from the matrix by the locally enhanced matrix shear stress. The adhesion of the face-end of the short fibre, and the debond at the interface have been found to have a large influence on the stress concentration zone and shear stress distribution at the interface. The models commonly used for fragmentation test ignore the effect [5-6]. We can now experimentally measure the matrix stress field and the distributions of interfacial shear stress in the coexistence of a matrix crack and debond at the interface under various loads. Particularly, photoelastic images can been collected rapidly and accurately using the present technology. This can avoid the stress relaxation of the matrix, which occurs during the fragmentation test and the measurement of the Raman spectroscopy. Automated photoelasticity with phase-stepping technology has proved to be a useful tool for the detailed examination of the stress field in an epoxy matrix in which a short fibre is embedded.

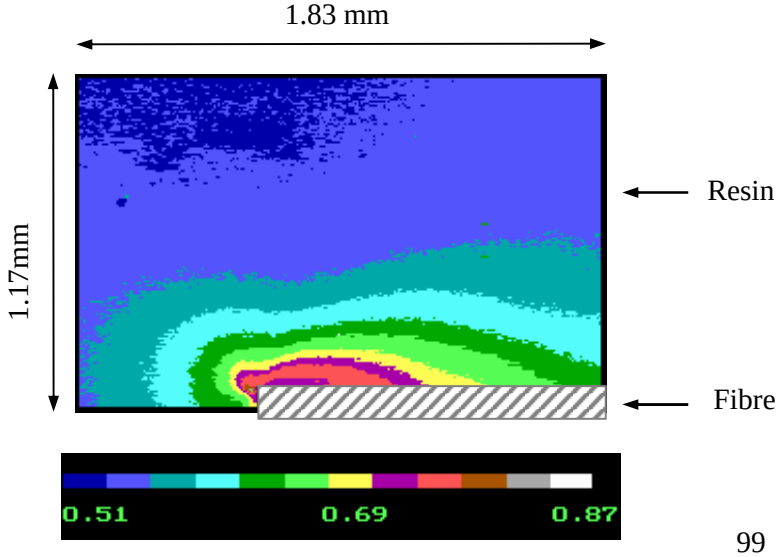

Fig 1. Contour map of isochromatic fringe order in the resin around a high modulus Al_2O_3 at applied matrix stress.

References

1. Tripathi D, Jones FR. Measurement of the load-bearing capability of the fibre/matrix interface by single-fibre fragmentation test. Composites Sci Technol 1997; 57:925-935.
2. Andrews MC, Young RJ. Fragmentation of aramid fibres in single-fibre model composites. J Mater Sci 1995;30:5607-5616.
3. Zhao FM, Okabe T, Takeda N. Effect of matrix properties on fragmentation behavior of single fibre composites. Composite Interface 2002;9:289-308.
4. Zhao FM, Hayes SA, Patterson AE, Young RJ, Jones FR. Measurement of micro stress fields in epoxy matrix around a fibre using phase-stepping automated photoelasticity. Composites Sci Technol 2003;63:1783-7
5. Cox HL. The elasticity and strength of paper and other fibrous materials. Br J Appl Phys 1952;3:72-79.
6. Kelly A, Tyson WR. Tensile properties of fibre-reinforced metal: copper/tungsten and copper/molybdenum. J Mech Phys Solids 1965;13:329-350.

IDENTIFICATION OF THE THROUGH-THICKNESS ELASTIC CONSTANTS OF THICK LAMINATED TUBES USING THE VIRTUAL FIELDS METHOD

Raphaël MOULART, Stéphane AVRIL, Fabrice PIERRON
LMPF-ENSAM
Rue Saint Dominique, BP 508, 51006 Châlons en Champagne, FRANCE.

Composite materials structural components are usually composed of thin plates or shells for which the knowledge of the in-plane ply moduli and strengths are enough to design the structure. However, the extension of composite applications in several industrial sectors such as the naval or ground transportation industry requires the use of less costly materials such as glass reinforced polymers, for which increased thicknesses are usually necessary to fulfil the structural function. For this type of applications, it is necessary for the designer to know not only the in-plane but also the through-thickness ply moduli and strength. This is for example the case of tubes used for offshore applications, which have to be relatively thick to withstand the large external pressures when underwater. Because of the new development of such structures, the measurement of their through-thickness properties remains difficult. Usual standard test methods such as the Iosipescu shear test or the direct tension test are not adapted to this situation.

Alternative approaches have been proposed in the literature for addressing this problem [1,2]. A promising one is based on the determination of through-thickness stiffnesses from testing configurations which give rise to heterogeneous stress fields inside the specimen [2]. Strain fields measured with an optical method are processed through the Virtual Fields Method (VFM) for identifying the four unknown stiffnesses [3]. The basic idea is to apply the principle of virtual work to the tested specimen with some explicit and independent virtual displacement fields. Each virtual field provides a linear equation where the unknown stiffnesses are involved. This leads to a linear system. Inversion of this linear system yields the unknown stiffnesses.

In order to validate this procedure, tests have been carried out on a PMMA ring tested in diametric compression (Fig. 1). The ring has been cut in a thick tube used in offshore applications. Strain fields are measured thanks to an original optical method called the *grid method* [4]. It is a white-light non-interferometric method, easy to implement and well suited for the investigation of in-plane full-field strain measurements. The rings are instrumented on their lateral surface with a pattern of crossed straight lines bonded onto the material. The pitch of this grid is 610 µm. The spatial phase shifting method is used to detect with a high accuracy the apparent displacement of the grid lines. Thus, longitudinal and vertical displacement fields are measured by the *grid method* with a resolution of 3 µm. Strain fields are derived from displacements by numerical differentiation. They are obtained with a resolution of 2.10^{-4}.

Strain fields are then processed through the Virtual Fields Method, providing Young's modulus and Poisson's ratio of the tested ring. The values obtained here for PMMA are 3.29 GPa for Young's modulus and 0.46 for Poisson's ratio. These values are consistent with the reference properties of PMMA, although Poisson's ratio seems less accurately determined, as it is usually the case in such tests because its influence on the strain state is smaller than Young's modulus. This is quite promising for future applications of the procedure.

Other tests are currently under progress, carried out on laminated glass-epoxy rings. The constitutive equations for this material are orthotropic and thus involve four independent parameters. Their identification is harder than

for isotropic constitutive equations. Numerical studies have been achieved for determining the regions of interest over the specimen where the influences of each unknown are approximately balanced to ensure its identifiability. An algorithm has also been programmed for selecting virtual fields which lead to a well-conditioned system and which minimize the effects of noise.

Once obtained, strain fields measured over the predefined area of the laminated glass-epoxy rings will be processed with the algorithm. Results of the identification procedure will be exhibited at the conference.

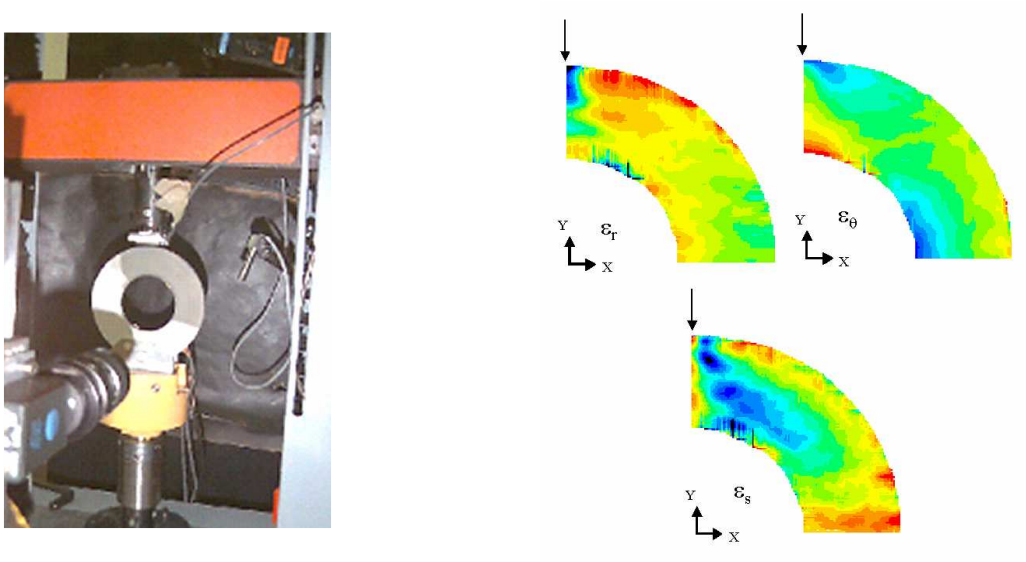

Fig.1. Experimental set-up of the diametric compression test on a thick ring using the grid method and strain fields measured over the whole area of a PMMA ring.

References

[1] W.R. BROUGHTON, G.D. SIMS. « An overview of through-thickness test methods for polymer matrix composites », NPL Report DMMA(A) 148, National Laboratory, UK, 1994.
[2] F. PIERRON, S. ZHAVORONOK, M. GRÉDIAC. « Identification of the through-thickness properties of thick laminated tubes using the virtual fields method », *International Journal of Solids and Structures*, **37**, 4437-4454, 2000.
[3] M. GRÉDIAC. « Principe des travaux virtuels et identification/Principle of virtual works and identification », *C. R. de l'Académie des Sciences*, **II-309**, 1-5, 1989.
[4] Y. SURREL. « Moiré and Grid Methods in Optics : a Signal-Processing Approach », *SPIE*, **2342**, 213-220, 1994.

APPLICATION OF THE OPEN HOLE TENSILE TEST TO THE IDENTIFICATION OF THE IN-PLANE CHARACTERISTICS OF ORTHOTROPIC PLATES

J. Molimard [1,2], R. le Riche [1,2,3], A. Vautrin [1,2]
SMS/MeM (1), GDR CNRS 2519 (2), URA CNRS 1884 (3), Ecole des Mines de St Etienne, 158 Cours Fauriel, 42000 Saint Étienne, France

The characterization of in-plane anisotropic elastic properties of composite laminated plates classically requires various types of specimens and mechanical tests, such as tensile tests performed on strips cut in different directions versus a given material direction. However, since more 15 years optical full-field measurement methods (OFFM) applied to mechanical characterization show that a huge amount of data can be supplied from one single test and make it possible to characterize material properties from a limited number of both specimens and tests [1].

As a matter of fact, OFFM can be combined with algorithms and analytical models or FEA to settle new efficient hybrid methods to solve the inverse problem and identify the mechanical properties of the materials. Those methods are based on criteria to compare experimental to simulated displacement or strain fields.

Reasonable criteria, algorithms and mechanical models are necessary to start the identification process. Extracting the material parameters from the full-field maps requires the use of algorithms such as model updating iteration which will be used in the following [2]. The parameters are adjusted in such a way that value computed with the model match the corresponding experimental data, which are generally displacement or strain field in OFFM-based tests. The final values converged with certain criteria are regarded as the identified parameters.

The present paper deals with a particular application leading to the identification of material *and* structural properties. The open hole specimen under uniaxial tension is considered since this test is used as routine test in aeronautics, analytical approaches result in well-controlled reference solutions and it gives rise to interesting stress-strain gradients that can be used to perform identification. The link between the experimental and identified results is still complicated and a refined study, focusing on the utilization of the metrological content of experimental data, has been necessary.

The contribution introduces the identification method applied to an open hole orthotropic NC2/epoxy resin specimen under uniaxial loading along orthotropic axis, the special merit of the approach being to identify *material* properties, such as the elasticity moduli and Poisson's ratio, and *structural* properties such as: radius and coordinates of the hole as well. It presents the experimental set up and the OFFM (moiré interferometry), the optimization strategy and finally focuses on the analysis of the difference between experimental and simulated results from the *analytical solution* (table 1) [3].

	E_{xx}	E_{yy}	G_{xy}	ν_{xy}
Reference value	59.5 GPa	55.8 GPa	4.26 GPa	0.049
Identified value	57.1 GPa	58.1 GPa	4.48 GPa	0.062
Difference (%)	4.1%	4.0%	5.2%	26.5%

Table 1. Identified values from the analytical model.

The point is how to improve the quality of the identification of Poisson's ratio, that is a problem people usually has to face. The new approach will be now based on a refined analysis of the structure by *FEA*, taking account of the finite width of the specimen. This second method, now based on a *numerical solution* leads to a significant improvement of the identified results, still based on the same experimental data (table 2).

	E_{xx}	E_{yy}	G_{xy}	ν_{xy}
Reference value	59.5 GPa	55.8 GPa	4.26 GPa	0.049
Identified value	57.6 GPa	55.3 GPa	4.48 GPa	0.046
Difference (%)	4.1%	4.0%	5.2%	6.1%

Table 2. Identified values from FEA.

The sensitivity of the identified results to the boundary conditions is finally tackled.

In conclusion, the paper gives first guidelines to utilise the well-known open hole tensile test as reference test to identify material and structural properties. This type of approach seems to be very efficient since it is based on existing test usually performed by industry.

[1] M. Grédiac, A. Vautrin, 'A new method for determination of bending rigidities of thin anisotropic plates', Mechanical Identification of Composites, edited by A. Vautrin and H. Sol, Elsevier Applied Sciences, pp. 91 – 98, 1990.
[2] F. Guyon, and R. Le Riche, "Least squares parameter estimation and the Levenberg-Marquardt algorithm: Deterministic analysis, sensitivities and numerical experiments," Technical Report INSA de Rouen, No. 041/99, November 20, 2000.
[3] S. Lekhnitskii, 'Theory of Elasticity of an Anisotropic Body', Moscow, MIR Publishers, 1977.

SESSION 7 – IDENTIFICATION OF DAMAGE MODELS

Chair: Dr. Kevin O'Brien
U.S. Army Research Laboratory

Wednesday 22 September
14.00-15.40

EXPERIMENTAL IDENTIFICATION OF A DAMAGE MODEL FOR COMPOSITES USING THE GRID TECHNIQUE COUPLED TO THE VIRTUAL FIELDS METHOD

H. Chalal, F. Meraghini S. Avril, F. Pierron
Laboratoire de Mécanique et Procédés de Fabrication, Ecole Nationale Supérieure d'Arts et Métiers (ENSAM).
Rue Saint-Dominique - BP 508 - 51006 Châlons-en-Champagne Cedex, France.

The present paper addresses the direct identification of mechanical parameters governing a non-linear behaviour law for composite materials. All the parameters of constitutive equations can be identified simultaneously with experimental tests giving rise to heterogeneous strain/stress fields in the specimen. Indeed, strain fields measured with a suitable full-field optical technique can be processed through the Virtual Fields Method (VFM). It consists in applying the principle of virtual work with as many virtual fields as there are unknown parameters. Unknown parameters are then the solutions of a linear system of equation [1].

For composite materials, the VFM has been successfully used to determine the in-plane [2,3] and the through thickness [4,5] moduli.
Numerical studies have shown the suitability of the VFM for characterising non-linear orthotropic behaviour, where the nonlinearity is due to the damage inherent to the in-plane shear response [6,7]. The damage model adopted was the one developed by Ladevèze [8, 9] using the strain energy. Constitutive equations write:

$$\begin{pmatrix}\sigma_1\\ \sigma_2\\ \sigma_6\end{pmatrix}=\begin{pmatrix}Q_{11} & Q_{12} & 0\\ Q_{12} & Q_{22} & 0\\ 0 & 0 & Q_{66}(1-\alpha\gamma_6^2)\end{pmatrix}\begin{pmatrix}\varepsilon_1\\ \varepsilon_2\\ \gamma_6\end{pmatrix} \quad (1)$$

Five parameters are unknown: the four in-plane stiffness components and the damage parameter governing the nonlinearity. A preliminary study [7] has proved that an unnotched specimen tested according to the Iosipescu configuration (figure 1) is a suitable test for identifying the five parameters simultaneously.

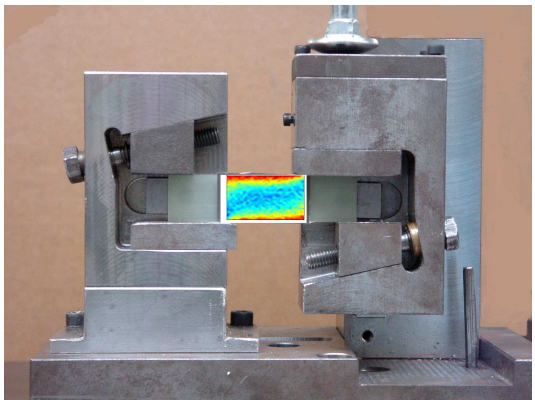

Figure 1. Bending-shear test based on the Iosipescu configuration

In the present paper, tests have been carried out to validate this identification procedure. Displacements fields over the front face of the composite coupon are measured with the grid technique. The pitch of the cross-grid transferred onto the surface of the specimen is 100µm. Image grabbing and processing are achieved using the *Frangyne 2000* software [10] and a CCD camera. In-plane strain fields in the central part of the specimen are derived form displacement fields by numerical differentiation. It can be seen from figure 2 that the tree strain components are not well balanced and that the shear strain is predominant. The parameters identified from these full-field measurements are reported in Table 1. The high values of Q_{11} and Q_{22} show that there is a considerable sensitivity to the noise related to the fact that both normal strains are much lower than the shear strain. As expected, it seems that the stiffness (Q_{12}) remains difficult to identify correctly (negative value) due to its small contribution to the overall material response. However, the identified shear modulus agrees well with that determined by the off-axis tensile test. Finally, the identified value of the damage parameter remains underestimated compared to the expected value. Further experimental aspects of the procedure, in terms of noise sensitivity, will be examined in the final paper. Also, results on off-axis unnotched Iosipescu test specimens will be presented. Relevant values of the off-axis angle enable to balance the three strain components and therefore improve identification.

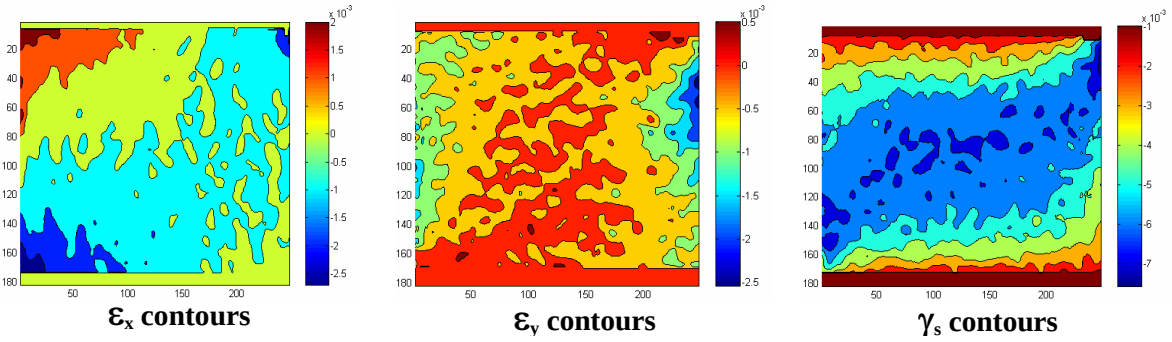

Figure 2: Experimental strain fields measured in the central part of the specimen

	Q_{11}	Q_{22}	Q_{12}	Q_{66}	$K=Q_{66}$.
Reference values obtained by experimental uni-axial tests (GPa)	44.65	12.03	3.729	3.863	2275
Identified stiffness from full-field measurements	55.77	26.65	-	3.582	1480
Relative difference (%)	24.90	121	-	-7.27	-34.9

Table 1 : Identified stiffness for the nonlinear behaviour of a glass/epoxy composite from full-fields strain measurements

References

[1] Grédiac M. Principe des travaux virtuels et identification. *Comptes Rendus de l'Académie des Sciences (In French with abridged English version),* II (309): 1-5, 1989.

[2] Grédiac M., Pierron F. A T-shaped specimen for the direct characterisation of orthotropic materials. *Int. J. Num. Meth. in Engng*., 41:293-309, 1998.

[3] Grédiac M., Toussaint E., Pierron F. Special virtual fields for the direct determination of material parameters with the virtual fields method. Part 1- principle and definition. *Int. J. Solids and Struct.,* 39:2691-2705, 2002.

[4] Pierron F., Zhavaronok S., M. Grédiac. Identification of the through thickness properties of thick laminates using the virtual fields method. *Int. J. Solids and Struct.,* 37(32):4437-53, 2000.

[5] Pierron F., Grédiac M. Identification of the through thickness moduli of thick composites from whole-field measurements using the Iosipescu fixture: theory and simulations. *Compo. Part A,* 31(4):309-18 2000.

[6] Grédiac M., Auslender F., Pierron F. Applying the virtual fields method to determine the through-thickness moduli of thick composites with a nonlinear shear response. *Compo. Part A*, 32: 1713-1725, 2001.

[7] Chalal H., Meraghni F., Pierron F., Grédiac M. Direct identification of damage behaviour of composite materials using the virtual fields method. *(in press) Compo. Part A*, 2004.

[8] Ladevèze P. Sur la mécanique de l'endommagement des composites. *Comptes Rendus des JNC5. Paris : Pluralis Publ.* pp 667-683, 1986.

[9] Ladevèze P., Le Dantec E. Damage modeling of the elementary ply for laminated composites. *Comp. Sci. & Tech.,* 43(3):257-67, 1992.

[10] Surrel Y. Moiré and grid methods in optics: a signal-processing approach. *Proceedings of SPIE, 2342:213-220, 1994.*

IDENTIFICATION OF A DELAY-DAMAGE MESOMODEL FOR THE LOCALIZATION AND RUPTURE OF COMPOSITES: FEASIBILITY AND IDENTIFICATION STRATEGY

P. Feissel*, O. Allix* et P. Thévenet+
*Laboratoire de Mecanique et Technologie, ENS Cachan, 61 avenue du Pdt Wilson 94230 CACHAN
+ EADS-CCR, Suresnes

The purpose of this study is the prediction of the crash behavior of multi-layered composites, that are used in aircraft crash absorbers. In order to avoid numerous and costly experiments, *EADS Suresnes* wishes to develop a reliable numerical tool. Such a tool must include properly identified material models capable of capturing the physics of the deterioration and dissipation phenomena which take place during a crash.

For the static part of such a model, the key-point is to choose a scale small enough to describe the phenomena that is in accordance with the numerical capacities. The choice here is to use the more and more used approach of the damage mesomodel, introducing the damage mechanisms through internal damage variables which are constant throughout the thickness of each ply [1],[2]. It allows a good prediction in the case of complex loading [3] and, furthermore, this static model can be identified from basic tests.

The idea followed here in order to describe the dynamic effects up to rupture has been to extend the previous static mesomodel by introducing a delay effect in the damage evolution laws, [4]. This delay effect allows a consistent description of rupture. Modifying the evolution laws introduces two delay parameters, that have to be identified.

The central point of this study is a discussion about the identification of these delay parameters. Two main questions are addressed:

1. is the identification possible and what kind of tests and measurements should be considered?
2. since some data in the dynamic experiments the identification should be based on can be very corrupted, how can one take into account uncertain measurements in an identification approach?

A first study of the model response is conducted in order to propose answers to the first question. By comparing the dissipated energy with the other energies implied in a quasi-static test up to failure, the delay parameters can be significant in term of energy. Then a discussion is proposed about the measurements needed for the identification, by studying a *SHPB* test. The sensibility of the measurements to the delay parameters is observed by a numerical analysis.

The second point of the study is motivated by the fact that dynamic tests up to rupture often have uncertain measurements. In such a case, classical inverse methods [5] may not lead to a relevant identification. The taking into account of corrupted experimental data is addressed by proposing a mechanical filtering of the measurements within the identification process itself. The guiding principle of the proposed method, which was directly inspired by studies on model updating in vibration [6], is the exact verification, during the identification process, of the properties which are considered to be reliable. Then, the uncertain quantities are taken into account by minimising a modified constitutive relation error [7]. The formulation has been developed in a first time, [8], in the framework of elasticity in order to test the method. Its robustness has been proven on various examples where the perturbations on the measurements are extremely severe. Furthermore, it has been shown that the method is robust, because it takes the whole experimental information in one calculation and it introduces a distance between the measurements and the calculation.

Further examples have been proposed in order to deal with more complicated problems, such as the identification of heterogeneous properties or of the size of heterogeneity figure 1. One of the applications that should be presented at *Comptest* is the case of displacement fields measurements.

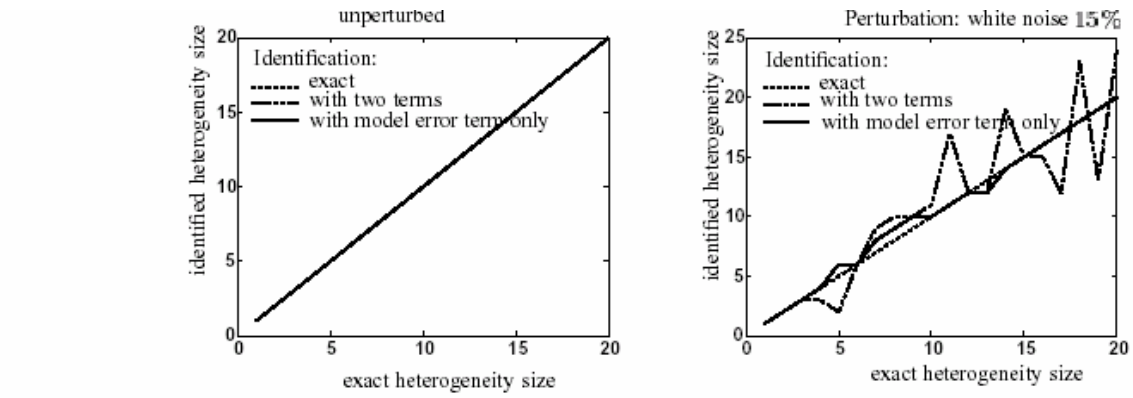

Figure 1: Identification of the heterogeneity size

References

[1] P. Ladeveze, E. Le Dantec. *Damage modelling of the elementary ply for laminated composites.*Composite Science and Technology, 257–267, (1992).
[2] O. Allix, P. Ladeveze. *Interlaminar interface modelling for prediction of laminates delamination.*Composite Structures, 22, 235–242, 1992.
[3] O. Allix, D. Guedra-Degeorges, S. Guinard, A. Vinet *Analyse de la tenue aux impacts faible itesse ´energie et faible ´energie des stratifi´es composites par la m´ecanique de l'endommagement* M´ecanique et Industrie, 1, 27–35, 2000.
[4] O. Allix, J.-F. De¨u. *Delay-damage modelling for fracture prediction of laminated composites under dynamic loading.* Engineering Transactions, 45, 29–46, 1997.
[5] L. Rota, *An inverse approach for identification of dynamic constitutive equations*, Int. Symposium on Inverse Problems, Ed A.A.Balkema, 1994.
[6] P. Ladeveze and A. Chouaki, *Application of a posteriori error estimation for structural model updating*, Inverse Problems, 15, 49-58, 1999.
[7] P. Ladeveze, *A modelling error estimator for dynamical structural model updating*, in Advances in Adaptive Computational Methods in Mechanics, P. Ladeveze, J.T. Oden eds, Ed Elsevier, 1998.
[8] O. Allix, P. Feissel, *A delay damage mesomodel of laminates under dynamic loading: basic aspects and identification issues*, Computers and Structures, 81-12, 1177-1191, 2003.

EXTRACTING MATRIX CREEP PARAMETERS FOR MODELLING THE CONSOLIDATION OF MATRIX-COATED FIBRE COMPOSITES

H. X. Peng * and M. R. Wisnom
Department of Aerospace Engineering, University of Bristol, Bristol, BS8 1TR, UK.
F. P. E. Dunne [a], P. S. Grant [b] and B. Cantor [c]
(a) Department of Engineering Science, Oxford University, OX1 3PJ, UK.
(b) OCAMAC, Department of Materials, Oxford University, OX1 3PH, UK.
(c) Vice-Chancellor Office, York University, YORK, YO10 5DZ, UK.

Titanium matrix composites (TMCs) reinforced by continuous silicon carbide fibre are being developed for applications in the aerospace industry, such as compressor bladed rings (BLINGS). TMCs manufactured by the matrix-coated fibre (MCF) method offer optimum TMC properties because of the resulting uniform fibre distribution, minimum fibre damage and fibre volume fraction control. Despite the many investigations of the consolidation behaviour of MCFs, the effect of matrix properties on the dynamic consolidation behaviour is not well understood, in part because of the complex matrix microstructure formed during the processing of these MCFs.

In this paper, the consolidation of Ti-6Al-4V matrix-coated fibres during vacuum hot pressing has been investigated by using a combined experimental and theoretical approach. In order to determine the fibre

coating properties, customised compression testing was performed on single matrix-coated fibres under transverse loading at elevated temperatures. A special finite element model (FEM) was developed to simulate the single fibre compression process where power-law creep (PLC) behaviour was assumed for the matrix. The parameters in the PLC equation were optimised by fitting the FEM results to the experimental data. Fig.1 shows a micrograph of a deformed MCF with superimposed FE mesh showing best-fitted FE prediction for single MCF compression test at 900°C and 30 MPa for 10 min. These optimised parameters were then used in the modelling of the consolidation process of MCF composites with regular fibre arrays. Experiments were carried out on multi-ply MCFs under vacuum hot pressing. In contrast to most of existing studies, the fibre arrangement has been carefully controlled either in square or hexagonal arrays throughout the consolidated sample. This has enabled the dynamic consolidation behaviour of MCFs to be demonstrated. The experimental results were compared with the FEM predictions and show excellent agreement (Fig.2).

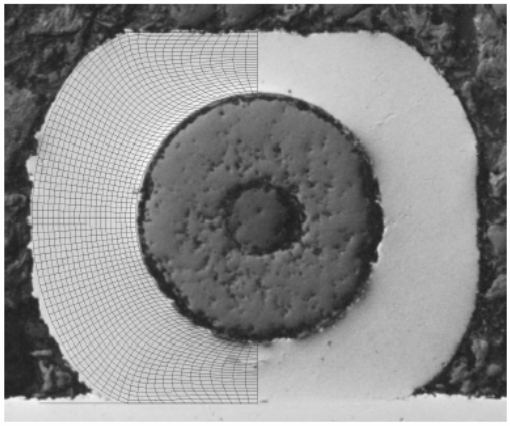

Fig.1 Micrograph of a deformed MCF with superimposed FE mesh showing best-fitted FE prediction for single MCF compression test at 900 ^{o}C and 30 MPa for 10 min.

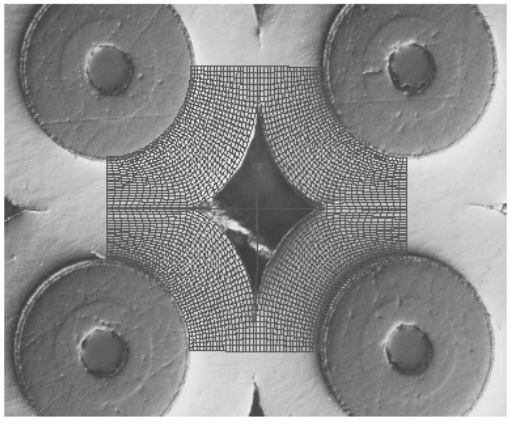

Fig. 2 Corresponding FE predicted mesh geometry superimposed on partially densified multi-ply square fibre array.

IDENTIFICATION OF PARAMETERS IN NONLINEAR VISCOELASTIC, NONLINEAR VISCOPLASTIC MATERIAL MODEL

Janis Varna and Lars-Olof Nordin
Lulea University of Technology, SE 971 87 Lulea, Sweden
Janis.Varna@ltu.se, fax +46-920-491084

Wood fiber composites made from paper have become an attractive candidate for applications in load bearing structures. Due to complex microstructure and inelastic constituent behavior the wood fibers composites have complex time dependent stress-strain response. For example, in tensile tests laminates made from phenol-formaldehyde impregnated kraftliner paper show nonlinear behavior in slow loading and hystheresis loops in unloading [1]. Compressive creep and strain recovery tests on phenol-formaldehyde impregnated paper composites show [2] large nonlinear viscoelastic strains and irreversible strains. It has been observed [1,2] that stiffness degradation in tension and compression is negligible which excludes micro damage evolution as a possible reason for nonlinearity.

The objective of this study is to develop methodology to determine stress and time dependence of viscoplastic strains and to develop nonlinear viscoelastic and viscoplastic material model. The material model is given also in incremental form implemented in computational scheme and used in simulations.

Schapery's non-linear viscoelastic and viscoplastic constitutive law [3] is used. For the strain transverse to the main fiber orientation it may be written as [2]

$$\varepsilon_T = \varepsilon_T^{el} + b_T \int_o^{\psi} \Delta S_{TT}(\psi - \psi') \frac{d}{d\psi'}(a_{42T}\sigma_T) d\psi' + \varepsilon_T^{pl}(t, \sigma_T) \qquad (1)$$

The viscoelastic time dependence is given by functions $\Delta S_{ik}(\psi)$ which are chosen in form of Prony series

$$\Delta S_{ik}(\psi) = \sum_m C_{ik}^m \left(1 - \exp\left(-\frac{\psi}{\tau_m}\right)\right) \qquad (2)$$

Functions b_T , a_{42T} and ψ are dependent on stress invariants. Creep and strain recovery tests have been performed for different levels of stress to identify the stress dependent functions b , a_{21}, a_{42} and the plastic strains [2]. The time and stress dependence of viscoplastic strains is described by Zapas et al model [4].

$$\varepsilon_T^{pl} = \left\{ \int_0^t [\sigma_T(\tau)]^N d\tau \right\}^n \qquad (3)$$

Parameters are identified measuring the irreversible strains after strain recovery of different length at the same stress and doing the same for creep tests of a fixed length but at different stress. Fig.1a) demonstrates that plastic strains obey power law with respect to time. The stress dependence is also according to power law. The model of viscoplasticity is validated in tests with a sequence of steps with increasing stress level, see Fig.1b). Then, the determination of nonlinear viscoelastic stress dependent parameters is performed. In the nonlinear case the method for data reduction based on one-step load application and removal is sensitive to the time interval during which the load increases to the plateau value and also to the length of the load removal interval [5]. The perturbations are considered negligible after sufficiently large time.

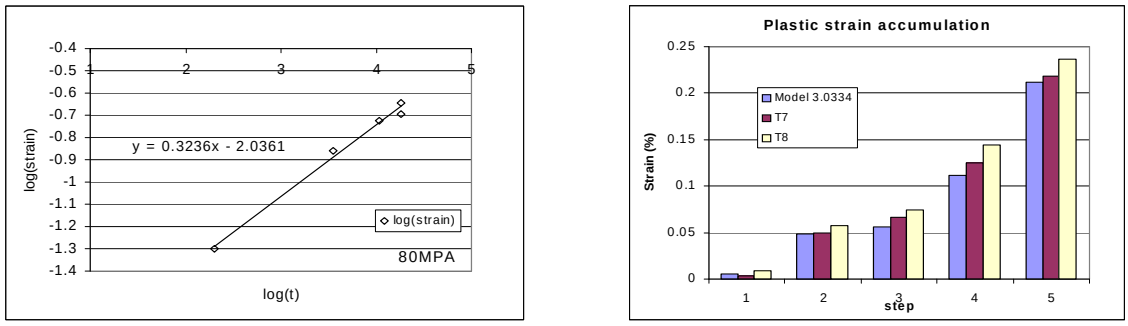

Figure 1 Plastic strains in compression: a) time dependence; b) accumulation in creep steps with increasing stress level.

However, it was shown in [5] that these changes affect very strongly the accuracy of nonlinearity parameters. Therefore, here a two-step loading approximation of the creep test is employed [5] which leads to more reliable results. Fig. shows that model is in a good agreement with tests.

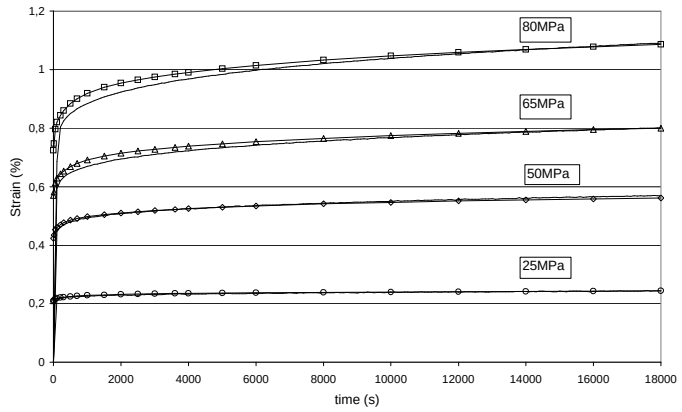

Figure 2. Model prediction (lines with dots) and experimental data (lines) in creep tests

References

1. Nordin LO, Varna J, 'Nonlinear viscoelastic behavior of paper fiber composites', Submitted to *Composites Science and Technology*, 2004.
2. Nordin LO, Varna J, "Nonlinear viscoplasticity and viscoelasticity of paper fiber composites: material model", Submitted to Mechanics of time-dependent materials, 2004
3. Schapery R.A., "Nonlinear Viscoelastic and Viscoplastic Constitutive Equations Based on Thermodynamics", *Mechanics of Time-Dependent Materials*, **1**: 1997, 209-240.
4. Zapas L.J., Crissman J.M., "Creep and recovery behavior of ultra-high molecular weight polyethylene in the region of small uniaxial deformations", Polymer 25, 1984, 57-62.
5. Nordin LO, Varna J, "Methodology for parameter identification in nonlinear viscoelastic material model" Submitted to Mechanics of time dependent materials", 2004.

POSTER SESSION 4

MICROSCOPIC OBSERVATION OF TOW DEFORMATION FOR CARBON FABRIC- PVC FOAM SANDWICH STRUCTURES DURING FORMING

Seung Hwan Chang*
School of Mechanical Engineering College of Engineering, Chung-Ang University 221, Huksuk-Dong, Dongjak-Ku, Seoul 156-756, Korea

Sandwich structures composed of fibre reinforced composites and polymer foams are widely being used in many application fields such as automobile and aeronautics because of their high specific stiffness and specific strength. Among many different kinds of core materials, polymer foams like PVC foams and polyurethane foams are widely used for their good machinability and formability as well. At the beginning stage of development of sandwich structures their geometries were relatively simple but recently the required geometries of composite sandwich structures have become more and more complex. Draping fabric composites onto elastic foundations is therefore needed to make complex 3-D sandwich structures. During the draping process fabric prepregs fit to the mould by means of shear deformation, which makes tow structure deform. The deformation of tow structures affects the mechanical properties of final products so that finding out the exact deformation pattern of tow structure during draping or forming process is essential to estimate the performance of the products.

This paper aims to investigate the micro-mechanical behaviour of tow geometry with forming pressures and foam densities during the curing process of plain weave carbon fibre fabric prepregs onto PVC foams. In order to find out and compare with deformation patterns between different forming conditions, tow parameters such as Y-directional tow interval, amplitude and crimp angle etc. are investigated. To observe the micro-deformation of the fabric structure with respect to the forming pressure and foam density, carbon fabric-PVC foam sandwich structures are fabricated by using vacuum bag degassing moulding method and appropriate specimens are cut from the cured sandwich structures and observed under the digital microscope. From the observation results, it is found that the crimp angle of longitudinal tow strongly depends on the polymer foam density (the crimp angle decreases sharply as the foam density increase). On the other hand, the crimp angle increases slightly with respect to the forming pressure but it has peaks at a certain pressure level in the cases of low-density foams. This phenomenon could be related to foam properties in higher temperature environment under certain pressures. It is known that the variation of crimp angles of fabric materials are related to the compressive strength of fabric structures because the excessive crimp angle may cause low compressive strength due to ‘micro-buckling’ of longitudinal tows in fabric structures.

For the amplitude of longitudinal tow the results show that it increases with the increment of foam density but for the stiffest foam (HT110) of this test, this value decreases or saturates. These micro-deformations are fully dependent on the foam densities which cause different mechanical and thermal properties. And these phenomena should be explained by mechanics between foam and carbon fabric during forming. In order to explain the behaviour of foam and tow geometry the stress-strain relations of various PVC foams with respect to environmental temperature are also measured. Test specimens are prepared for the compressive test based on ASTM D 1621 and the size of the specimen is 50(W) × 50(L) × 30(t). A universal testing machine (STATIC 4206, INSTRON, USA) which is equipped with a heating chamber was used for the test. The testing temperatures are room temperature (approximately 25°), 80° and 125° considering the curing cycle of carbon fabrics, which has dwelling temperatures (at 80° and 125°) during forming. From the compressive tests plateau stress, yield stress and compressive modulus of various foams were measured. The test results show that the yield stress abruptly decreases as the testing temperature increases and at the highest testing temperature (125°) little differences in the yield stress (approximately 0.5MPa) between various foams were observed.

In this paper, the microscopic tow behaviour during forming is estimated and explained by using the above observation results and foam properties with respect to temperature. It is expected that the mechanical properties of final composite sandwich products could be estimated using those results. And those results may give useful data for designer to make complex 3-D sandwich structures using fabric composites with foams.

EXPERIMENTAL DETERMINATION OF COMPOSITE IN-PLANE SHEAR PROPERTIES

L. Niklas Melin and Jonas M. Neumeister
Dept. of Solid Mechanics, KTH - Royal Institute of Technology, SE - 100 44 Stockholm, Sweden

The Iosipescu (or V-notched) shear test (ASTM D-5379) is well established for measuring composite in-plane shear properties. It prescribes V-notches with 90° opening angle. Particular to many composite panels are their anisotropic properties, elastic as well as strengths etc. One important consequence of this is that the stress- and strain fields depend on both the material and its orientation
in a specimen (i.e. its anisotropic properties). This implies that testing conditions, performance and thus evaluation must vary from one material tested to another. It was demonstrated, experimentally and numerically, that using a modified specimen geometry copes effectively with many of these problems. In an orthotropic material, the recommended modifications depend in a simple manner on the two principle Young's moduli, E_x and E_y, see Figure 1. For a sharp notch in an isotropic material no singular mode II stresses (shearing) are present with a notch opening angle $\theta_{iso} > 102.6°$ while in practice, $\theta_{iso} = 110°$ is used. For an orthotropic material, the corresponding angle depends (mainly) on the ratio of orthotropy, i.e. Ey/Ex. By a simple rescaling operation of the notch opening angle θ, the resulting elastic fields of an isotropic specimen can be essentially recreated. Thus, using a notch opening angle θ defined by

$$\tan\left(\frac{\theta}{2}\right) = \frac{1}{\sqrt[4]{\lambda}}\tan\left(\frac{\theta_{iso}}{2}\right), \text{ where } \lambda = \frac{E_y}{E_x} \qquad (1)$$

gives much more homogeneous and controlled testing conditions. The validity of eq. (1) was numerically demonstrated for a material with an orthotropic ratio $\lambda = 16$ (or 1/16). In addition to the recommended notch angles from eq. (1), both wider and narrower θ (including the ASTM standard $\theta = 90°$) where evaluated for the two material orientations. Further, the effects of the notch root geometry were investigated by modelling one sharp and one rounded notch. Resulting normalized stress fields are shown in Figure 2. With the stiff material orientation aligned with the test region (cf. Figure 1), the shape of the notch root proved to be much more decisive for the stress profiles.

In-situ whole field strain measurements were performed with digital speckle photography (DSP) on several materials confirming that a notch angle modified according to eq. (1) consistently produced the most uniform strain profiles in the test region. In Figure 3, such profiles are shown for the material and the specimens numerically investigated in Figure 2. Note that these are recorded at high loads and at different magnitudes, thereby substantially exceeding the elastic limit of the material.

Further, using the modified specimen geometry substantially improved the capability of measuring complete stress-strain curves in shear and thus also giving more reliable strength data.

Even with the effects of varying anisotropy among the tested materials taken into account by a careful specimen design, shear testing of composites remains an intricate issue. The clamping forces required to securely hold the specimen throughout a test are of the same magnitude as the transferred shear forces. These may induce additional and unwanted stress states in the test region due to Poisson effects. Moreover, as test performance and attained stress levels are improved, the combined effects of clamping and loading results in very high contact stresses outside the test region. Such can lead to local crushing or other undesired excessive deformation, loss of symmetry, failure initiation etc. all impairing test performance. Some of these issues can be addressed by an improved fixture function whereas others are inherently related to damage localization occurring at high loads. Thus, a new Iosipescu fixture which specifically addressed clamping function, alignment of fixture halves and their suspension was designed and built, it can be seen in Figure 4.

All deviations from nominal conditions, such as non-symmetric deformation, local damage, rotation and twisting of specimen, bending and out-of-plane motion of the fixture, cause undesired stress states in the specimen test region but can never be completely avoided in an experimental situation. therefore, also other deformations and strains were monitored using the DSP equipment. For example, Figure 5 shows the twisting of the central region of a specimen which occurred at high load.

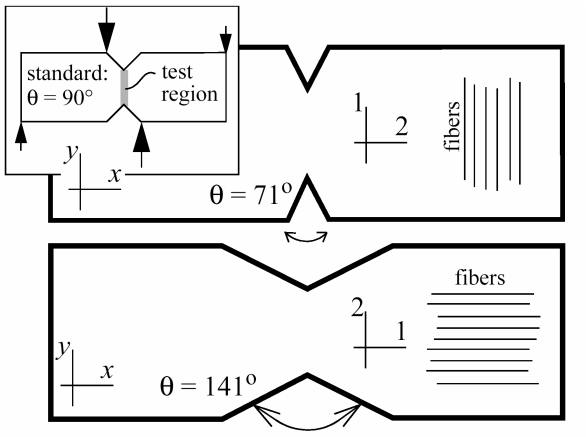

Figure 1. Two orientations of the Iosipescu test

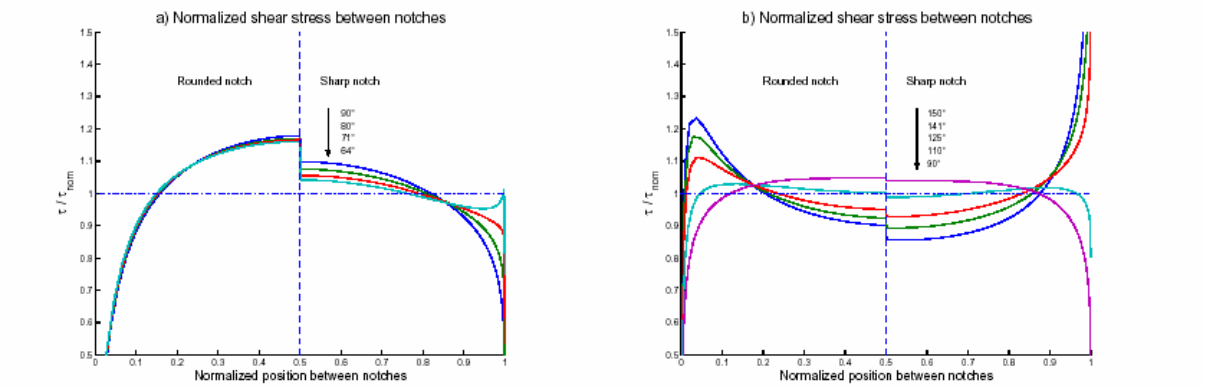

Figure 2.Shear stress profiles (normalized for each half of the test region) for different notch opening angles for a) the stiff material direction along test region, and b) with stiff direction across.

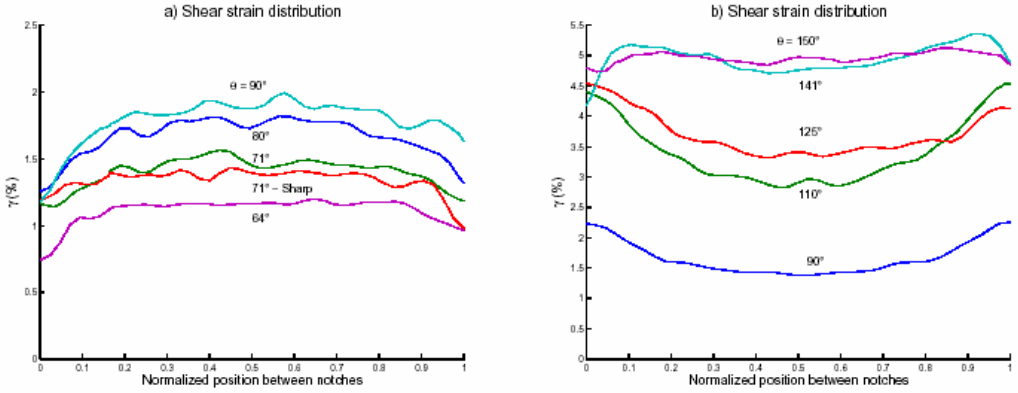

Figure 3.DSP measured strain profiles along the test region for specimens close to failure/first cracking for a) fibers oriented aligned the test region and b) oriented crossing the test region.

Figure 4. New Iosipescu fixture with DSP camera

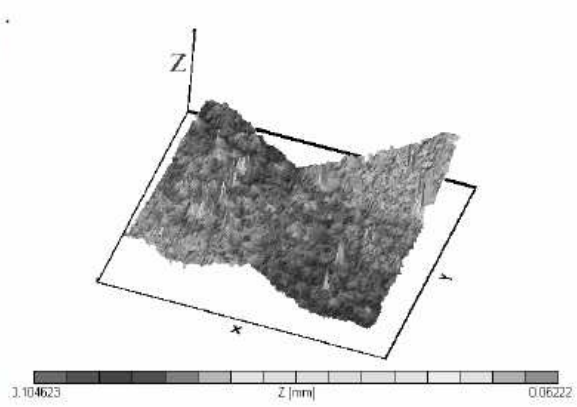

Figure 5. DSP-recorded specimen twisting

AN INVESTIGATION OF THE PULL-OUT AND SHEAROUT PROCESSES IN Z-PIN REINFORCED LAMINATES

Marcin Fert, Dr. Paul Robinson, Mr. Dennis Hitchings
The Composites Centre & The Department of Aeronautics, Imperial College London

The structural properties of laminated polymer matrix composites are usually characterised by excellent strength in the plane of the composite (X-Y plane) but by low strength in the through-thickness, Z direction. Z-Pins were developed to provide designers with a means to increase through-thickness properties. As shown in a number of works and papers, the use of Z-Pins as interlaminar reinforcement has proved to be very effective in improving the crack propagation resistance under mode I, II and mixed mode loading conditions. Z-Pin reinforcement is based on the insertion of strong, stiff rods through the thickness of a composite laminate before curing. The Z-Pin provides extra strength in the Z-direction (perpendicular to the plane of structure) by making a real 3D fibre reinforced structure after curing. The study reported in this paper consists of experimental and numerical parts and is aimed at characterising the action of Z-Pins bridging an already existing crack under Mode I (pull-out), Mode II (shear-out) and Mixed Mode I/II loading conditions.

Experimental Study

For the experiments IM7/8552 carbon-epoxy prepreg and carbon-epoxy Z-Pins were used. Z-Pins in diameters of 0.28mm and 0.51mm were inserted into 48-ply (6mm) unidirectional (UD, $[0°]_{48}$) or quasi-isotropic (QI, $[[0°{\pm}45°/90°]_S]_6$) laminates to form specimens containing either a single pin or a group of four pins. Three different insertion methods were investigated to produce the required pinning pattern:

- The pins that were not required were removed from the preform that holds the pins in a standard square array. The standard ultrasonic method was then used but this produced a high percentage of faulty insertions, due to highly dispersed z-pin distribution (approximately 1 pin for every 200mm²).
- Fully pinned preform was used in with the ultrasonic method to insert the pins in the panel. The unwanted pins were then removed manually from the panel before cure.
- The prepreg assembly was preheated to 50°C and the prepreg was then perforated in the required locations using a steel needle. Pins were then inserted manually into these holes.

A 20µm PTFE release film was located in the mid-plane of each in order to introduce a crack. Cured panels were cut into 16x16mm square specimens. In a number of specimens Z-Pins were drilled from one side to a desired depth in order to test the influence of the pinning depth on the properties pinned composite.

Specimens were tested with a specially designed universal testing rig (Figure 1). The tests performed were as follows:

- Mode I (pull-out): 0.51mm & 0.28mm diameter (singly & grouped) Z-Pins in QI & UD laminates, 1.0mm & 2.0mm pinning depths.

- Mode II (shear-out): 0.51mm & 0.28mm diameter (singly & grouped) Zpins in QI & UD composite (shearing along and across fibres), 1.0mm & 2.0mm pinning depth. In Mode II tests, springs were used in the test jig to control the tendency of the sliding surfaces of the specimen to move apart. Three sets of springs of different stiffnesses were used, from very weak springs (with only a slight influence on the shear-out process) to very stiff springs.
- Mixed ModeI/II (combined pull/shear out): 0.51mm & 0.28mm diameter (singly & grouped) Z-Pins in QI & UD composite (shearing along and across fibres), with loading at angles of 30°, 45°, 60°, 70°, 80° to the pin axis. Typical load displacement plots of these mixed mode tests are shown in Figure 2.

Finite Element Analysis

Based on the microscopic observations of the Z-Pins embedded into the composite structure a finite element model was built. The model consists of the orthotropic composite body and a single Z-Pin surrounded by the isotropic resin pocket. The objective of this model is the simulation of the phases of the pull-out process. The results from this model will be used to build a link-element tool representing Z-Pins bridging a crack. (This model may also be used as a Unit Cell in various applications such as investigating the stiffness characteristics of z-pinned laminates.)

The first stage of the FE analysis has indicated that the pin will dis-bond in a stable manner from the surrounding laminate. Further work is underway to investigate the subsequent behaviour and to relate this to the experimentally observed characteristics.

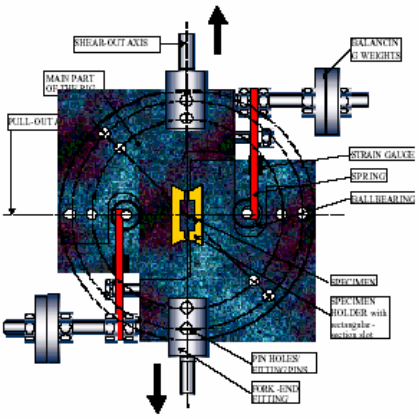

Figure 1

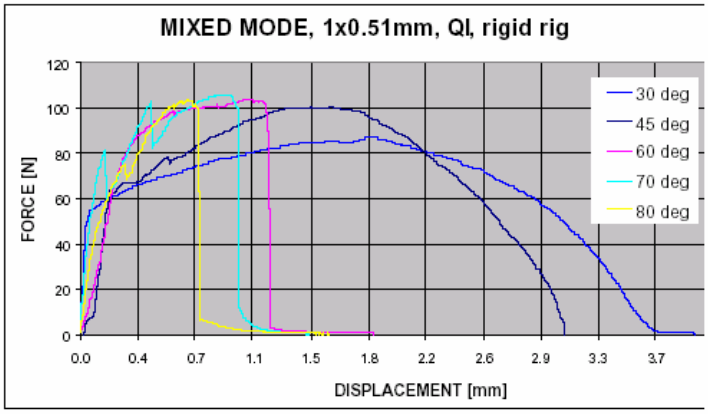

Figure 2

OFF-AXIS CREEP RUPTURE BEHAVIOR OF UNIDIRECTIONAL CFRP LAMINATES AT ELEVATED TEMPERATURE

M. Kawai [1], Y. Masuko [2] and T. Sagawa [3]
1 Institute of Engineering Mechanics and Systems, University of Tsukuba, Tsukuba 305-8573, Japan.
2 Graduate School of Systems and Information Engineering, University of Tsukuba, Tsukuba, Japan.
3 Graduate School of Science and Engineering, University of Tsukuba, Tsukuba, Japan.

INTRODUCTION

Deformation and fracture of polymer matrix composites (PMCs) are usually governed by the shear responses of matrix materials along reinforcing fibers and between stacked plies. The inelastic deformation, damage and fracture of polymers significantly depend on temperature. Moreover, they are governed by complicated interactions between viscoelastic and viscoplastic responses and by the change in mechanical properties due to physical aging. Such a matrix-dominated behavior is crucial to the high-temperature durability of PMCs [1]. To understand properties for PMCs and to correctly evaluate their performance and reliability under service stress

conditions at elevated temperatures, therefore, it is one of the most important issues to elucidate by experiment the time- and rate-dependent deformation and fracture behaviors. Furthermore, a realistic and rational modeling is prerequisite to making reliable evaluations of the ultimate capacity of high temperature composite structures and to establishing accurate design methods based on local stress analysis. Due to the limited amount of attempts [2-4], however, understanding and modeling for the creep rupture behavior of PMCs at high temperature are still limited.

In the present study, the creep behavior of unidirectional carbon/epoxy laminates is examined, with a particular emphasis on the effects of fiber orientation and stress level on the creep rupture behavior under off-axis stress conditions at high temperature. An attempt is also made to develop a phenomenological damage mechanics model for the creep deformation and rupture behaviors of unidirectional PMCs. The validity of the proposed model is evaluated by comparing with experimental results.

EXPERIMENTAL PROCEDURE

The material used in this study is a unidirectional fiber composite fabricated using the autoclave method from the T800H/Epoxy prepreg. The lay-up of the laminate is [0]12. Five kinds of plain coupon specimens with different fiber orientations (θ = 0, 10, 30, 45, 90°) were cut from 400 mm by 400 mm unidirectional laminate panels. The shape and dimensions of the off-axis specimens are based on the testing standards JIS K 7087 and ASTM D2990.

Off-axis constant-stress creep tests in tension were carried out at 100°C. In principle, three different stress levels
were selected for every fiber orientation. Relatively large magnitudes were specified so that the creep rupture data were obtained within the time range shorter than 10 hours. To reduce the end-constraint effect on the strain distribution over the off-axis specimens, the oblique-shaped end tabs proposed by Sun and Chung [5] were adopted. The off-axis specimen with oblique tabs is illustrated in Fig.1.

RESULTS AND DISCUSSION

Comparisons between the longitudinal strains measured with the 2 mm strain gauges at the center of specimen and evaluated on the basis of the displacement for the 100 mm gauge length are shown in Fig. 2, for the 10° specimens with rectangular and oblique tabs, respectively. The agreement between the longitudinal strains obtained as such is much better of the specimen with oblique tabs over the tested strain range. Similar improvements by means of oblique tabs were also achieved for other off-axis specimens. These observations indicate that the oblique shaped end tabs have successfully reduced the inhomogeneous strain distribution due to
the end constraint in off-axis coupon specimens with a low aspect ratio.

The off-axis creep curves for θ = 10° are shown in Fig. 3. The creep strain becomes larger at a higher creep stress, and the creep rate rapidly decreases with time in an early stage of the creep response. The steady-state creep response in a classical sense is not substantially followed with the load duration, and the transition to tertiary stage is not observed. Thus, the transient creep is dominant for the off-axis fiber orientations and the off-axis creep rupture occurs in a brittle manner. Similar results have also been observed for other fiber orientations. The decay of the creep rate under a constant stress condition can be described using a viscoplastic model based on the overstress concept.

The log-log relationships between the creep stress and creep rupture time are presented in Fig. 4 for all fiber orientations. The tensile creep strength becomes lower as the off-axis angle increases. As far as the log-log plots are concerned, the creep-rupture data can be approximately described using straight lines with negative slopes over the range of rupture time up to 10 hours, regardless of the fiber orientations. Also note that the fitted straight lines extrapolate back to the static tensile strengths plotted on the vertical axis in Fig. 4.

The creep rupture behavior predicted using the Dillard-Morris-Brinson criterion [2] is shown by solid and dashed lines in Fig. 4. The creep rupture curve implies that the anisotropy of the off-

axis creep rupture strength is similar to that of the static strength. This supports a modified Tsai-Hill failure criterion of the following form:

$$\frac{\sigma_1^2}{\{X(t_c)\}^2} - \frac{\sigma_1\sigma_2}{\{X(t_c)\}^2} + \frac{\sigma_2^2}{\{Y(t_c)\}^2} + \frac{\tau_{12}^2}{\{S(t_c)\}^2} = 1 \qquad (1)$$

where the longitudinal and transverse strengths X, Y and the shear strength S in the original Tsai-Hill criterion are replaced with the time-dependent strength functions $X(tc)$, $Y(tc)$, and $S(tc)$, respectively. This simple phenomenological failure model has succeeded in adequately describing the characteristics of the off-axis creep rupture behavior observed. A comparable accuracy has been achieved by applying the damage mechanics model [4]. A coupled analysis of the off-axis creep deformation and rupture behavior of UD PMCs is also addressed.

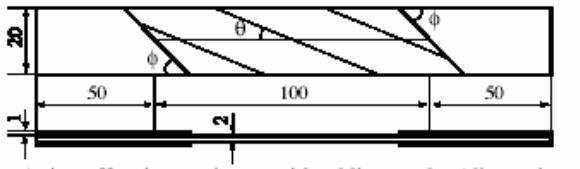

Fig 1 An off-axis specimen with oblique tabs (dimensions in mm)

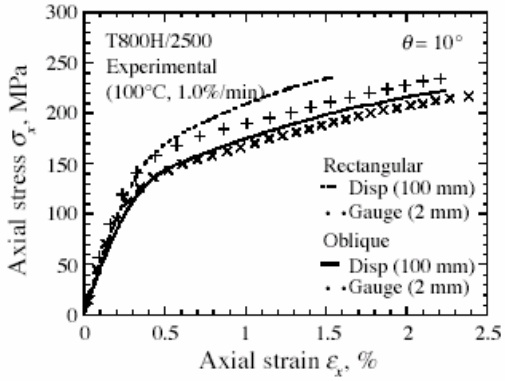

Fig 2 Off-axis stress-strain curves for $\theta = 10°$

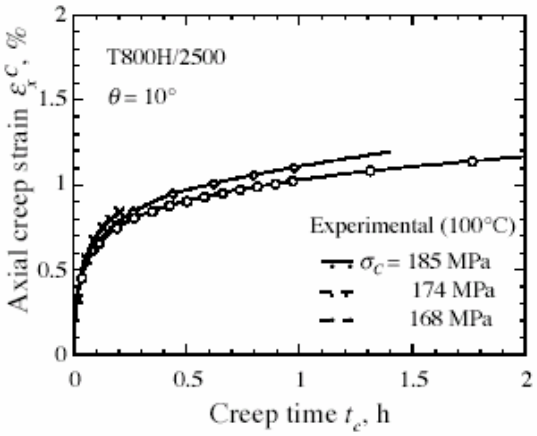

Fig 3 Off-axis creep curves for $\theta = 10°$

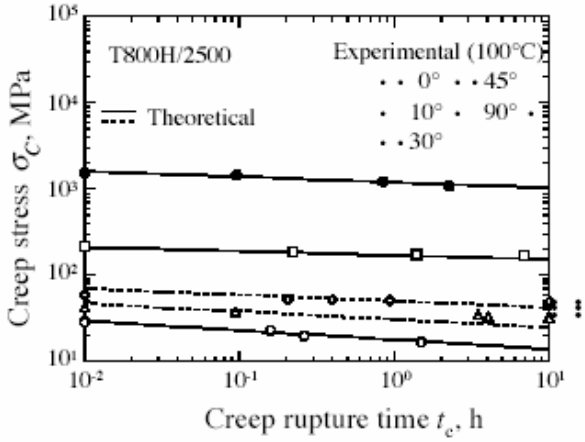

Fig 4 Off-axis creep rupture behavior at 100 ïC

REFERENCES

[1] Brinson H.F. Matrix dominated time dependent failure predictions in polymer matrix composites. Composite Structures 1999; 47: 445-456.
[2] Dillard D.A., Morris D.H. and Brinson H.F. Predicting viscoelastic response and delayed failures in general laminated composites, ASTM STP 1982; 787: 357-370.
[3] Kawai M. Off-Axis Creep behavior of unidirectional polymer matrix composites at high temperature, Proceedings of IUTAM Symposium on Creep in Structures 2001, pp. 469-478, Kluwer Academic Publishers.
[4] Kawai M. Coupled inelasticity and damage model for metal matrix composites. International Journal of Damage Mechanics 1997; 6: 453-478.
[5] Sun C.T. and Chung I. An oblique end-tab design for testing off-axis composite specimens. Composites 1993; 24(8): 619- 623.

EXPERIMENTAL ANALYSIS OF RC BEAMS IN FLEXURE REINFORCED WITH CFRP SHEETS

Z. J. Wu, M. Xylouri and P. Nedwell
Manchester Centre for Civil and Construction Engineering, Manchester, M60 1QD

Strength, stiffness (deformation) and the load carrying capacity of reinforced concrete (RC) beams are always the primary topics which have been specified in many existing design codes and guidelines[1].

There is no doubt that such considerations should also be given to RC beams when retrofitted with advanced fibre reinforced plastics (FRP) particularly when incorporated into existing structures [2]. Because of the many combinations of material and geometric configuration for reinforcement selection, it is very difficult to have a single design code to cover all eventualities. Experimental investigation is therefore still a reliable basis with which to check innovation design. This is particularly true in the case of FRP application in civil and structural engineering. This paper reports the test results of strength and deformation for a set of 6 flexural beam specimens with a clear span of 1.2 m and a cross-section of 125mm x 75mm. All beams were externally reinforced (wrapped) with carbon fibre reinforced plastic (CFRP). The research had two objectives. The first was to study the effectiveness of three different fibre orientations on the loading capacity of the reinforced concrete beams. The second was to investigate the suitability of structural deformation analysis based on the modelling of classic Bernoulli composite beam theory which has been widely used in engineering[3].

Materials and Specimens

Each beam was 1300mm long by 125 mm deep and 75 mm wide, longitudinally reinforced by 2 no 10mm high yield steel bars (Young's modulus E=210GPa and strength 300MPa) at 110 mm depth. The concrete had the mix proportions 0.73:1:2.92:4.38 (water : cement : sand : coarse aggregate {max 10mm}). Standard 100 mm cubes showed the average 28 day strength to be 27 MPa. The beams, having a reinforcement ratio (ρ) of 0.019 were designed to be under reinforced as specified by Eurocode 2 ($0.0033<\rho<0.022$). Unidirectional CFRP sheets and strips were then used to poststrengthen the structures. All CFRPs had a thickness of 0.165mm, tensile strength 3.43MPa with an elastic modulus along fibre direction of 230GPa.

Strengthening Configuration

CFRP was bonded to concrete surfaces using a two-component epoxy adhesive according to the manufacturer specifications. Three types of layout (configuration) of CFRP were selected, as shown in Fig.1.

(1) Vertical U-wrap continuous (angle of fibres to the longitudinal axis of the beams is 90°);
(2) 45° continuous sides only wrap and
(3) Vertical U-strips at an interval of 80mm between the adjacent strips.

Experimental Procedure

In addition to the recording of load and the mid-displacement of each beam, eight linear otentiometers were installed on both shear spans of the beam as shown in Fig.2. These were used to measure the relative elongation along the 450 direction. The potentiometers, having effective length 150mm, were placed at a spacing a =100mm. The load was applied continuously via support displacement control at the rate of 0.01mm/s.

Results and Conclusions

(1) The table shows the increase of the loading capacity comparing with the average ultimate load (24.6kN) of the similar beams without CFRP strengthening[4].
(2) U-strip configuration is a preferable and effective selection of strengthening.
(3) The measurement of the variation of the relative displacement along 45° direction in shear spans does not support the analysis of the classic Bernoulli composite beam theory. More refined modelling analysis is required.

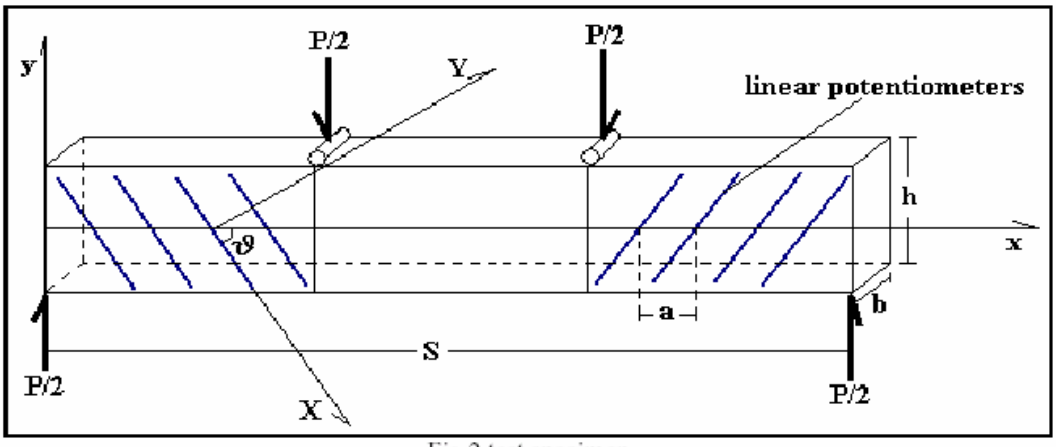

Fig.2 test specimen

Beam No.	Ultimate Load (kN)	Loading Capacity Increase(%)	Failure mode
C1--U-wrap	40	62.6	concrete crushing
C2--U-wrap	42	69.9	concrete crushing
C3--45^0-wrap	36	46.3	Shear failure
C4--45^0-wrap	38	54.5	Shear failure
C5--U-strip	39	58.5	Shear failure
C6--U-strip	35	42.3	Shear failure

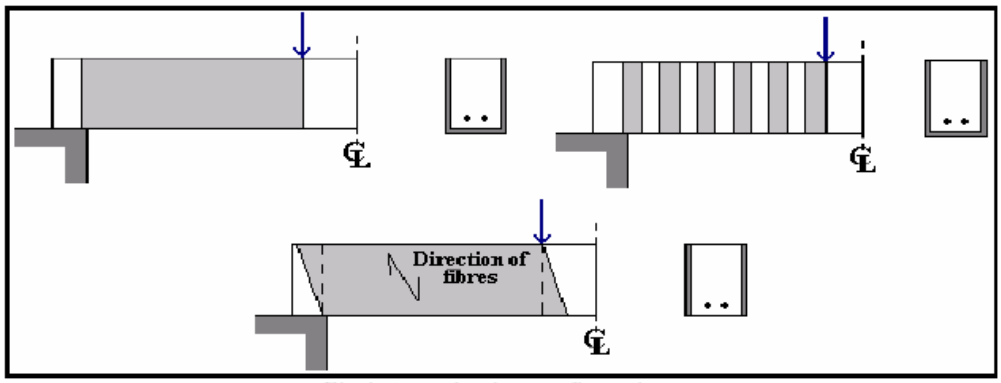

Fig.1 strengthening configurations

References

[1] Tan K H ed., Fibre -reinforced polymer reinforcement for concrete structures, Vol.1, World Scientific, 2003, Singapore.
[2] Khalifa A and Nanni A, Rehabilitation of rectangular simply supported RC beams with shear deficiencies using CFRP composites, Construction and Building Materials, **16**, 2002: 135-146.
[3] Wu Z J and Davies J M, Mechanical analysis of a cracked beam reinforced with an external FRP plate. Composite Structures, **62**, 2003: 139-143.
[4] Xylouri M, Shear strengthening of reinforced concrete beams using externally applied composite fabrics. MSc dissertation, Manchester Centre for Civil and Construction Engineering, UMIST, 2003.

THE BEHAVIOUR OF UNCURED PREPREG

Cary Langer and Kevin Potter
Aerospace Engineering Department, University of Bristol, UK

It has become increasingly apparent that, when considering the manufacturing processes and conditions for composite materials, an understanding of the behaviour of the material in its uncured state is required. The responses of the material itself and the interactions between the material and the tooling during cure can greatly influence the properties of the cured component.

This work is addressed at improving the understanding of the behaviour of uncured UD prepreg material. Specifically, the behaviour of this uncured material under tension is investigated. The insight gained is considered particularly relevant to tool-part interaction, which induces tensile strains while the composite material is transformed from its uncured to its cured state.

The experiments were performed using Hexcel unidirectional AS4/8552 0.25 mm thick prepreg in 600 x 40 mm strips. Both ends were reinforced by sandwiching them between two 50 x 40 mm pieces of prepreg. The ends of each strip had to be cured to ensure they would not slip out of the grips of the Instron 1341 testing machine. A series of samples was tested for the following variables:

- Strain and modulus values
- The actual load-carrying area of each sample
- Incremental removal of tows
- Comparison of testing in uncured and cured state
- Effects of hand lay-up on the properties of the sample
- Effect of bending during storage on the properties of the sample
- Strain along the length and across the width of a sample

On the whole, the samples tested during this work tended to fail one tow at a time, revealing a consistent failure mode for strips of uncured prepreg under tension. The position of the tow initiating failure was random. In addition, the 'hairy' appearance of the samples after failure indicates some fibre failure before the whole tow broke. This behaviour suggests that there were fibres of different lengths in the tows, in addition to different initial tow lengths.

A considerable level of variability was encountered in all results; the test procedure was developed to give consistent test conditions, so this variability seems to be inherent to the material. It also appears to be reflected in the results given for the strain measurements taken along the length and across the width of one sample.

Once the samples were under a certain level of tension for an extended period of time, the tows separated from each other along their length. This clearly shows that there must be some contraction along the width of each tow when the material is under tension. On the one hand, this result indicates that the Poisson's Ratio of this material may not be negligible, as is conventionally assumed; on the other hand, this time-dependent phenomenon seems more akin to a flow process rather than a contraction induced by a conventional Poisson's Ratio.

On average the moduli values encountered in this work were about 10 % lower than that given by the material property specification (135 GPa). Concerning the experiments where tows were incrementally removed, this could have been due to damage caused by repeated testing of the sample.

The discrepancy could also be due to the fact that there are broken fibres in the material. This can occur quite easily during the production of the prepreg; it is irrelevant once the material has been cured, since the critical fibre length to transfer loads from one fibre end to the other is very short because the fibres are very thin. In the

uncured state, however, the modulus of the resin is negligible; therefore, according to the Rule of Mixtures, say 10% broken fibres would result in a 10 % reduction of material strength in the fibre direction. It is shown that the modulus of samples tested in the uncured and cured state increases once they had been cured; however, the increased values remained short of the assumed 135 GPa.

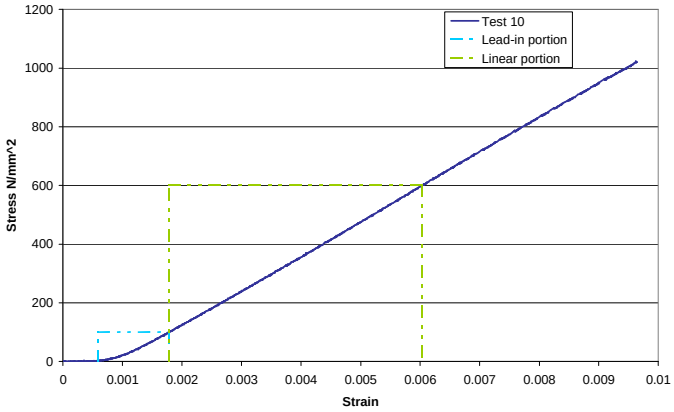

The manufacture and storage methods used for prepreg induce some fibre waviness. It is assumed that a low level of load should straighten this level of fibre waviness out. This work shows that there is still a considerable discrepancy between the modulus measured below 100 N/mm² - a region where the fibres are assumed to be straightening out - and between 100 N/mm² and 600 N/mm² – a region where the fibres are assumed to have all straightened out. These two moduli only approach each other in value for the last experiment of those samples from which the tows were removed incrementally; that is to say, when there is only one tow left. Fibre waviness seems to have a greater impact on the material properties than one might initially anticipate.

The material also appears to be very sensitive to the conditions it is stored in. The specimens which were bent during storage showed a considerable reduction in strength, including one extreme which failed upon removal from the freezer and an attempt to straighten it out by hand.

OPTIMISATION OF THE MECHANICAL TEST PROCEDURE FOR TESTING OF UNIDIRECTIONAL CARBON FIBRE/ PEEK SPECIMENS

John Kilroy, Pat McDonnell, Conchúr O'Brádaigh
Composites Testing Laboratory, Údarás Industrial Estate, Baile an tSagair, An Spidéal, Co. Galway, Ireland.
jk@ctlcomposites.com

Mechanical testing of unidirectional high strength thermoplastic composites such as Carbon Fibre/ PEEK has traditionally proven to be difficult using conventional test methods. Two important areas of testing in which problems are encountered are tensile and compression tests of unidirectional 0° lay-up specimens and there are a number of reasons for this. Due to a combination of high strength in the longitudinal direction and low friction on the surface of the thermoplastic specimen, successful end-tabbing of the material proved impossible. Following numerous trials involving various adhesives, end-tabbing of the material could not be achieved which would result in valid failures in the gauge length. A new approach in specimen testing and specimen preparation was necessary to overcome these problems. In conjunction with Irish Composites (specialists in thermoplastic composites manufacture), Composites Testing Laboratory carried out a unique series of tensile and compression tests in an effort to establish test procedures which would give valid mechanical properties.

Tensile tests to EN 2561 on batches of six specimens were examined. Tensile tests were carried out using a Zwick 250kN testing machine with hydraulic grips on specimens without end tabs attached first. It was found that the gripped section of the specimen was flattened in the hydraulic grips under the pressure required to grip the specimens. This caused premature failure of the specimens and the corresponding tensile strength was low. Tests were then carried out on UD specimens with moulded on end-tabs and fibres in the end-tabs running at 90° to the longitudinal directional. The tabs were moulded on at the autoclaving stage and the 90° fibres were used to achieve the needed support for the 0° fibres and prevent specimen flattening during testing. The strength results were higher than in the previous test but were still less than the expected ultimate strength of the material. It was thought that the premature failure obtained using this type of test was due to a slight buckle of the specimen induced during the moulding of the end-tabs. Because of this, failure of each specimen occurred at this region and the desired mode of failure (full delamination) did not occur.

Tensile tests were then carried out on un-tabbed specimens using mechanical wedge grips. With wedge action grips, grip pressure is proportional to the tensile load applied and thus the grip pressure is minimised. This prevented specimen flattening during the test and full delamination occurred throughout the full gauge length of the specimens tested. Tensile strengths were higher than for the previous two cases and were as expected. See Fig. 3 for the average tensile strengths achieved using the various test techniques.

Compression tests to EN 2850 were then carried out (see Fig.1). The first tests carried out were on specimens with moulded on end-tabs. The tabs were moulded on during the autoclave process using caul plates and spacer plates. On examination after moulding, it could be seen that there was a slight buckle of the specimen just outside the gauge length in the tabbed area. As with the moulded tensile tabbed specimens, it was thought that the problem arose due to slight movement of the caul plate during the moulding process. The batch of specimens was tested and as expected, the buckle caused a much larger drop off in strength than in the case of the tensile specimens. Following this, a 6 mm thick sheet of material was autoclaved and the 10 mm gauge length necessary for EN 2850 was milled into the material. This left a gauge length of 2.3 mm of unidirectional material in the centre of the specimen and the batch was then tested. The strength results achieved were higher than in the previous test but were still not as high as the expected compressive strength of the material. It was thought that the drop off in strength on this occasion was caused by damage to the fibres caused in the milling performed on the laminate.

The difficulty of using end-tabs – either glued or moulded had been proven. As with the tensile tests, an attempt was made to test compression specimens without end-tabs attached. Tests were carried out on flat specimens to ASTM DD641, a test that incorporates a combined loading compression (clc) fixture (see fig.2). The fixture, which subjects the specimen to combined end- and shear-loading is itself loaded in compression between flat plates in the test machine. Tests were carried out and the mode of failure was delamination in the gauge length as was desired. Compression strengths were higher than for the previous two cases and were as expected. See Fig. 4 for the average compression strengths achieved using the various test techniques.

Fig. 1 Celanese Compression Fixture

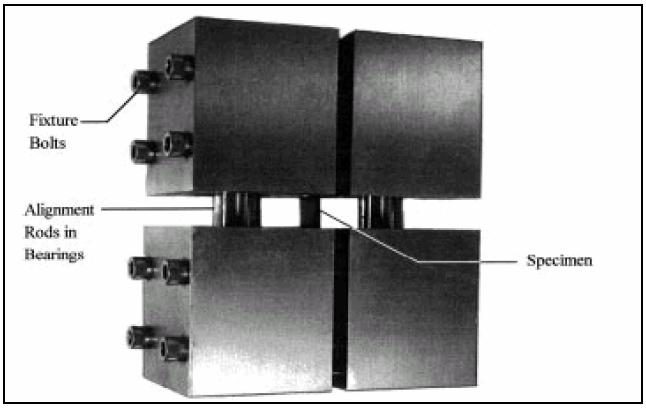

Fig. 2 Combined Loading Compression (CLC) Fixture

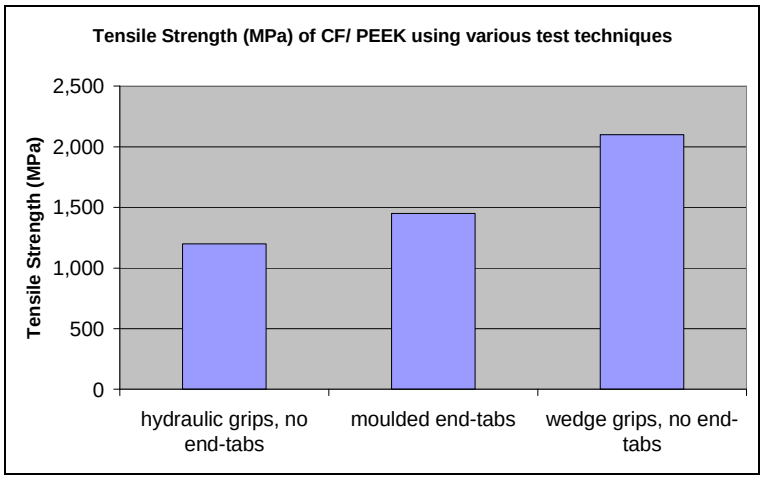

Fig. 3 Tensile Strengths of CF/ PEEK achieved using various test techniques

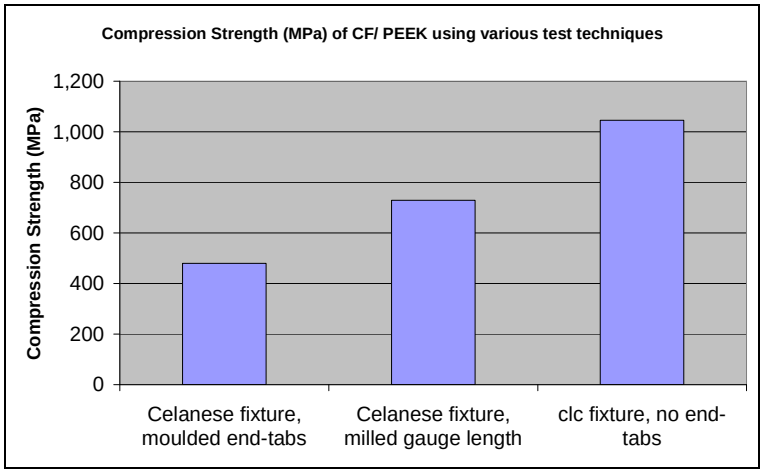

Fig. 4 Compression Strengths of CF/ PEEK achieved using various test techniques

MODELLING THE THERMOELASTIC PROPERTIES OF SHORT FIBRE COMPOSITES WITH ANISOTROPIC PHASES

P.J.Hine*, C.D.Price*, A.M.Cunha#, I.M.Ward*
* - IRC in Polymer Science and Engineering, University of Leeds, Leeds, LS2 9JT, UK
# Department of Polymer Engineering, Universidade Do Minho, Campus Azurem, 4800-058, Guimaraes, Portugal.

In a number of recent joint papers with the group of Andrei Gusev at ETH Zurich, we have combined their finite element approach (PALMYRA) with a mixture of structural characterisation (using image analysis) and mechanical measurements to formulate the best analytical route for predicting the thermoelastic properties of short fibre composites based on isotropic matrices [1-3]. For the analytical route, the prediction of the properties of a misoriented reinforced material can be broken into two components: firstly the prediction of the properties of the fully aligned 'unit' and then including the effects of misorientation using tensor averaging. The recent research has confirmed the following points when the matrix is isotropic (the fibre can be either isotropic or anisotropic):

- The best model for the prediction of the unit properties is that based on the original ideas of Eshelby and Mori and Tanaka as modified by Tandon and Weng [4] for isotropic phases and as reported by Qui and Weng [5] for anisotropic fibre reinforcement.
- The best approach for predicting the thermal expansion properties of the unit uses the explicit treatment of Levin [6] which is identical to that of Christensen [7] and Rosen and Hashin [8].
- If the fibres are discontinuous the best measure is the number average fibre length [9].
- The best approach for predicting the properties of the misaligned composite is to use the tensor averaging approach [10,11] and a constant strain prediction [3].

While the modelling of short fibre reinforced composites with isotropic phases has been extensively researched and reported, there is much less in the literature regarding modelling procedures when either or both of the phases are anisotropic. The purpose of this paper is to describe the validation of a modelling route for predicting the thermoelastic properties of a short fibre composite where both phases are anisotropic, that is a liquid crystalline polymer (LCP) reinforced with carbon fibres. Injection moulded dumbbell samples were produced at The University of Minho, in three materials of different combinations of isotropy: carbon fibre filled nylon (anisotropic fibre and isotropic matrix), glass fibre filled LCP (isotropic fibre and anisotropic matrix) and carbon fibre filled LCP (both phases anisotropic). In addition to the filled materials, samples were also produced from the pure matrix materials in order to determine the appropriate matrix properties for the modelling.

To provide the greatest test of the modelling procedure, four different measures of the thermoelastic properties of the central cylindrical section of the injection moulded composite dumbbells were measured: the longitudinal modulus, E_{11}: the transverse modulus E_{22}: the longitudinal thermal expansion α_1 and the transverse thermal expansion α_2 (the 1 direction is the main axis of the central portion of the dumbbell). In addition, the fibre orientation distribution was also measured in the central dumbbell section using image analysis techniques developed at Leeds. The orientation was measured to be transversely isotropic so it could be specified by only 2

orientation parameters, $\langle\cos^2\theta\rangle$ and $\langle\cos^4\theta\rangle$, where θ is the angle a fibre makes with the dumbbell (1) axis. For modelling the LCP matrix materials, an anisotropic form of the Eshelby matrix tensor was determined from the work of Mura [12].

a) ***Carbon fibre filled aromatic Nylon***:

Phase data (E and G in GPa, α K^{-1}.)				Carbon/Nylon	
				Theory	Measured
Carbon Fibre	E_{11}	230	E_{11}	21.8	23.9
	E_{22}	14	E_{22}	4.02	3.6
	ν_{12}	0.26			
	ν_{23}	0.38	α_1	7.2e-6	5.5e-6
	G_{12}	17.5	α_2	67e-6	60e-6
	α_1	-4e-7			
	α_2	26e-6			
Nylon	E	2			
	ν	0.4	$\langle\cos^2\theta\rangle$	0.856	
	α	70e-6	$\langle\cos^4\theta\rangle$	0.830	
Volume fraction				0.21	
Aspect ratio				25	

This composite material was used to check the modelling scheme described above for an isotropic matrix. The challenge with modelling when using carbon fibres is obtaining the values of all the elastic constants. The values here are our best estimates from our previous work and the literature.
Within this constraint the agreement between theoretical prediction and measurements is seen to be good.

b) ***Glass and carbon fibre filled LCP***

Phase data (E and G in GPa, α K^{-1}.)				Glass/LCP		Carbon/LCP	
				Composite	Measured	Composite	Measured
LCP matrix	E_{11}	25.6	E_{11}	29.1	25.6	51.7	43.2
	E_{22}	1.45	E_{22}	2.86	1.95	2.54	2.45
	ν_{12}	0.48					
	ν_{23}	0.71	α_1	-1.2e-6	-0.43	-5e-6	-1e-6
	G_{12}	1.13	α_2	55e-6	60e-6	58e-6	49e-6
	α_1	-5e-6					
	α_2	80e-6					
Glass fibre	E	72.5					
	ν	0.2	$\langle\cos^2\theta\rangle$	0.904		0.929	
	α	5e-6	$\langle\cos^4\theta\rangle$	0.865		0.87	
Volume fraction				0.19		0.24	
Aspect ratio				25		25	

For the LCP matrix composites, the agreement between experiment and theory is still good but not as good as when the matrix is isotropic. The weak-point in the proposed modelling scheme is the tensor averaging component, where the assumption has to be made that the fibre and matrix have the same orientation: it is likely that the LCP matrix has a different orientation to the fibres. Further modelling work is in progress to allow the two phases to have different orientations.

REFERENCES

1. Gusev, A. A.; Lusti, H. R.; Hine, P. J. Advanced Engineering Materials 2002, 4, 927-931.
2. Gusev, A.; Heggli, M.; Lusti, H. R.; Hine, P. J. Advanced Engineering Materials 2002, 4, 931-933.
3. Hine, P. J.; Lusti, H. R.; Gusev A. Composites Science and Technology 2004, in press,
4. Tandon, G. P.; Weng, G. J. Polymer Composites 1984, 5, 327-333.
5. Qiu, Y. P.; Weng, G. J. International Journal of Engineering Science 1990, 28, 1121-1137.

6. Levin, V. M. Mech. Tverd. tela 1968, 88, 25.
7. Christensen, R. M., Mechanics of Composites Materials. 1991, Malabar FL: Kreiger Publishing Company.
8. Rosen, B. W.; Hashin, Z. International Journal of Engineering Science 1970, 8, 157-173.
9. Hine, P. J.; Lusti, H. R.; Gusev, A. A. Composites Science and Technology 2002, 62, 1445-1453.
10. Brody, H.; Ward, I. M. Polymer Engineering and Science 1971, 11, 139-151.
11. Camacho, C. W.; Tucker III, C. L. Polymer Composites 1990, 11, 229-239.
12. Mura, T., Mechanics of Elastic and Inelastic Solids. 1982, The Hague: Nijhoff.

COMPOSITE DEFORMATION CONTROLLED WITH A SOURCE OF HEAT

H. Drobez [a,b], G. L'Hostis [b], F. Laurent [a], B. Durand [b], G. Meyer [a].
[a] Cetim Cermat, B.P. 2278, F 68068, Mulhouse Cedex,, tel : +33 (0)3 89 32 72 20, fax : +33 (0)3 89 59 97 87
[b]Laboratoire de Physiques et de Mécanique Textile, CNRS FRE2636, 11 rue Alfred Werner, F 68 093, Mulhouse Cedex, tel : +33 (0)3 89 33 60 53, fax : +33 (0)3 89 33 63 39,
e-mail: herve.drobez@cetim-cermat.fr g.lhostis@uha.fr

An actual problem for composite structures is their control and the shape adaptation for a given application. To solve this problem piezoelectric elements, alloys of memory-shape, electro or magnetostrictif elements are commonly used. They are integrated in or on the surface of the structure, but these solutions induce generally, stress concentrations which involve damage phenomena. The process proposed in this paper, in order to substitute these classical actuators, consists in using the anisotropic behavior of the composite structure. During a given temperature elevation, the difference between the thermomechanical properties of the constitutive layers, generates internal stresses which cause the deformation. So the whole structure becomes the actuator, the useful power is higher and the problems of stress concentration are reduced. The structure deformation depends on the kind of the reinforcement (woven, non woven and knitting fabrics), on the properties of the fibers (dilatation coefficients, thermal conductivity) used to make the reinforcements and on the active layer inside the composite, which drive the thermal distribution. This active layer is an electrical conductor made of carbon or metallic fibers connected to a current generator.

In order to characterise this new type of actuator, we have manufacture and test various models of plates (laminates, sandwiches) to analyse the influence of the different parameters.

The experimental procedure consists in measuring the bending deflection at the plate center versus time for a given constant voltage applied to the active layer. During the experiment the temperature is measured on the surface of the skins. Then, the efficiency is evaluated from the electrical and mechanical powers. So the weight which generates the same deflection is measured.

A numerical specific model is developed by using homogenization methods and classical laminate models : This model of different computational routines, depending of the plate structure (thin plates, sandwich plates) which involve different assumption for the thermo mechanical calculation. Thermal distribution is calculated from finite difference methods, and the plate deflection is obtained with the classical lamination theory.

An exemple of tested sample is a sandwich plate (about 100×500 mm^2 and 6.7 mm of thickness) with a core in PVC foam and two skins. Each one is composed by two layers of non woven glass fibers and one layer of woven glass. In one of the skins the active layer is inserted, its resistance is 7.8 Ω. The applied voltage is 15.3 and 20.4 V.

The figures (1) and (2) show respectively the experimental deflection and the temperature vs. time for the two voltages. Figure (3) shows the measured and calculated values. We obtain a good correlation between the different results.

Finally, the results show the validity of this new process of control. Now heating cyclic tests are carried out to study the durability of these plates.

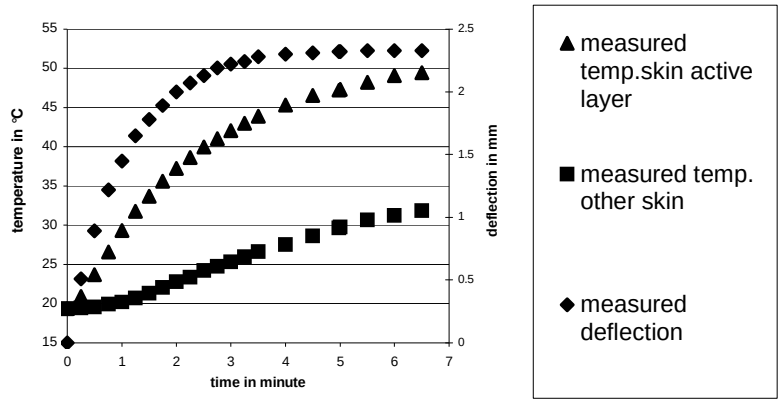

Figure 1: deflection and temperature for U = 15.3 V

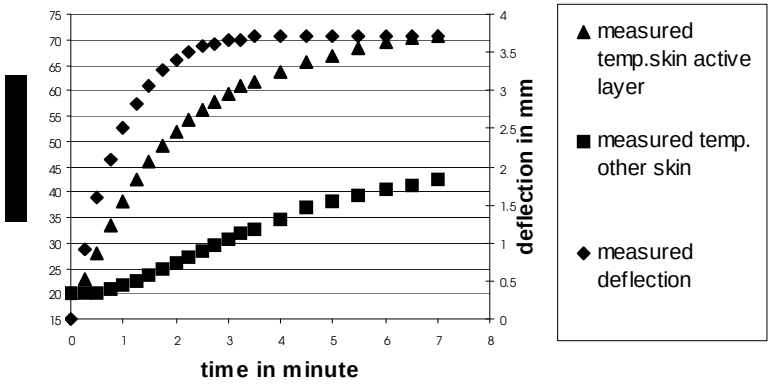

Figure 2: deflection and temperature for U = 20.4 V

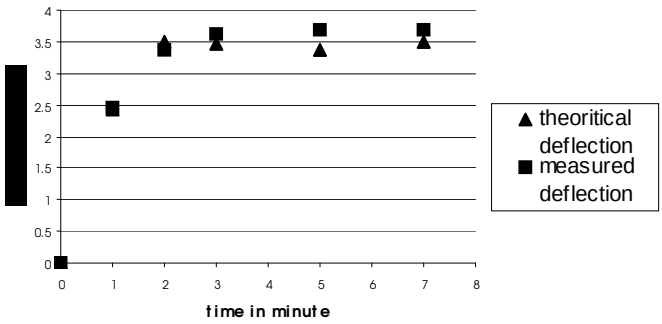

Figure 3: theoretical and measured deflection for U=20.4 V

MULTISCALE MODELLING OF THE STRAIN RATE DEPENDENT DAMAGE IN SHEET MOULDING COMPOUND COMPOSITES

F. Meraghini, Z. Jendli, J. Fitoussi, D. Baptiste
*LMPF JE 2381, ENSAM CHÂLONS EN CHAMPAGNE, rue Saint Dominique,
BP 508. 51006 CHÂLONS EN CHAMPAGNE, France.
LM3 UMR-CNRS 8006, ENSAM Paris, 151 bd de l'Hôpital 75013 Paris, France.

Discontinuous fibre reinforced composites have a growing interest in the transport industry since they are commonly used as a substitute for steels in structural components in order to reduce vehicle weights. Nevertheless, their mechanical responses under low and high-speed loadings are not well understood. In spite of recent advances [1-2], obtaining dynamic experimental data is still complex to achieve for composite materials. This is one of the most aspects that inhibit their widespread use in the industry although such composite materials are characterised by a high-energy dissipation. Accordingly, this stresses further the need for research aimed at analysing and modelling the mechanical behaviour of composite materials and structures under dynamic loadings in relation with material microstructure variability. In fact, mechanical response of composites depends widely on the conjunction of the material microstructure and the involved complex damage processes.

The present paper addresses the theoretical development and the experimental validation of a multi-scale model predicting damage accumulation in sheet moulding compound composites (SMC-R26). The developed model is intended to set up a reliable predictive analysis of the strain rate effects on the 3-D overall dynamic behaviour of SMC composites subjected to rapid accelerations. The developed micromechanical modelling relies upon an experimental methodology performed according to an incremental operating strategy [3]. The latter was devoted to the micro and macroscopic characterisation of composites mechanical behaviour under high-speed loadings. Notable in the experimental findings is that SMC-R26 exhibits a visco-damaged nature of the non-linear behaviour under dynamic loadings. In fact, damage onset and kinetic are widely sensitive to the strain rate whereas there is an insignificant load rate effect, if any, on the elastic properties. Experimental results have established that the damage is strain-rate dependent and the fibre-matrix interface debonding is the major degradation process [3]. The viscodamage aspect of the SMC mechanical behaviour is modelled using the generalised Mori-Tanaka scheme and Eshelby's equivalence theory coupled to a probabilistic approach [4-6]. An evolutionary interfacial particle-debonding criterion is subsequently considered in accordance with the Weibull's statistical function to describe the varying probability of damage. In this work, a quadratic damage criterion is used to describe interfacial debonding whose the formulation required the calculation of the interface stress state at the microscopic scale. The interfacial debonding process is controlled by the internal interfacial strengths and the Weibull parameter. These damage parameters are sensitive to the strain-rate and were experimentally identified through an inverse approach using the microscopic damage assessment obtained by interrupted high-speed tensile tests (figure 1).

The developed multi scale model allows predicting 3-D stiffness reduction brought about by the high-speed loading achieved at different crosshead velocities. The strain-rate dependent damage model was experimentally validated for strain rates up to $150s^{-1}$ on SMC-R26 composite. As illustrated in figure 2, a good agreement between numerical and experimental results has been obtained for high-speed tensile tests.

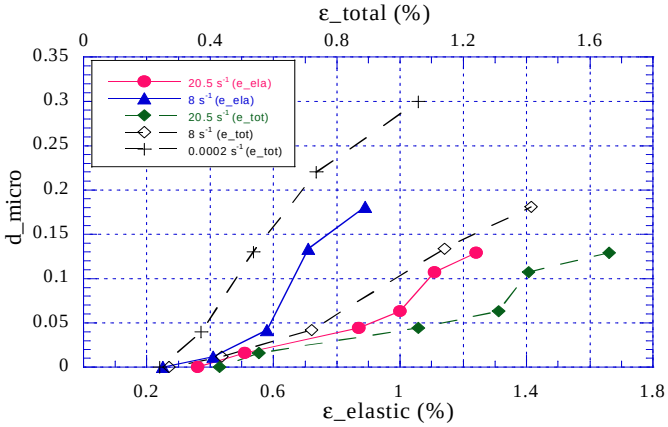

Figure 1: Experimental assessment of the overall microscopic damage evolution vs strain for different strain rate

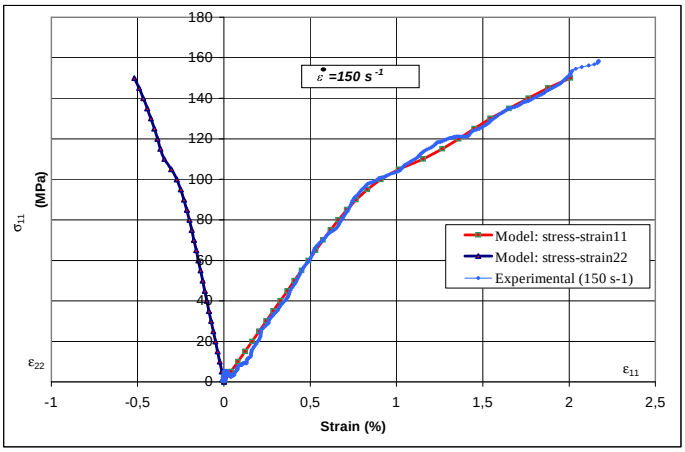

Figure 2. Comparison of experimental and predicted tensile stress-strain curves for SMC composite at strain rate of $150s^{-1}$.

References

[1] Okoli OI. The effects of strain rate and failure modes on the failure energy of fibre reinforced composites. Composite Structure 2001; 54: 299-303;

[2] Dear JP, Brown SA. Impact damage in reinforced polymeric materials *Composites. Part A: Applied Science & Manufacturing*, 34(2003) 411-420.

[3] Jendli Z., Meraghni F., Fitoussi J., Baptiste D. Micromechanical analysis of strain rate effect on damage evolution in Sheet Molding Compound composites. (In press) *Composites. Part A: Applied Science & Manufacturing, 2004*

[4] H.K Lee and S. Simunovic. A damage mechanics model of crack-weakened, chopped fiber composites under impact loading, Composites Part B: Engineering 2002; 33: 25-34.

[5] Desrumaux F, Meraghni F., Benzeggagh ML. Generalised Mori-Tanaka Scheme to Model Anisotropic Damage Using Numerical Eshelby Tensor. Journal of Composite Materials 2001; 35(7):603-624.

[6] Meraghni F., Desrumaux F., Benzeggagh ML. Implementation of a constitutive micromechanical model for damage analysis in glass mat reinforced composites structures. Composites Science and Technology 2002; 62: 2087-2097.

NEURAL NETWORK METAMODELLING FOR OPTIMISATION OF NEGATIVE POISSON'S RATIO CHIRAL HONEYCOMB

T. L. Lew, F. Scarpa and K. Worden
Dynamics Research Group, University of Sheffield, S1 3JD Sheffield

Negative Poisson's ratio (auxetic) materials expand in all directions when pulled in only one, acting therefore in an opposite fashion compared to classical material. Cellular centresymmetric structures (i.e., having two in-plane axis for translational symmetry) constitute a consistent part of auxetic materials (re-entrant honeycombs, microporous PTFEs and foams to a certain extent). A novel concept of non-centresymmetric honeycomb has been proposed recently [1] as potential core material for sandwich composite structures. The honeycomb (Figure 1) present chiral symmetry and an in-plane negative Poisson's ratio around –1. The negative Poisson's ratio feature can lead to a sinclastic curvature behaviour ("dome" shaping) when the material is bent. The characteristics could be used to shape curved sandwich panels with reduced in-plane cell buckling. The transverse shear modulus of the chiral honeycomb is carried almost completely by the cell walls, while the cylinders provide essentially the compressive strength of the cellular material [2].

A recent metamodelling technique [3] has been proposed by the authors to reduce the computational effort in Finite Element homogenisation calculations when stochastical variations of several geometric and material parameters of the unit cell of the periodic composite have to be considered. The metamodelling (or reduced order modelling) consists of surface envelopes embedding the possible solutions space generated by neural networks trained using FE analysis. The reduced order models allow decreasing greatly the computational effort when it is requested to optimise the configuration of the unit cell of the composite. In this work we use a Multi Layer Perceptron Neural Network (MLP) to generate the surface envelopes on chiral unit cells (Figure 2), also making use of Voigt and Reuss bounds for the transverse shear properties. For the latter in particular, a

technique suggested by Grediac [4] and successfully used also for re-entrant auxetic honeycombs [5] allows identifying the transverse shear modulus in function of the gauge thickness of the honeycomb.

The honeycomb unit cells are optimised for compressive and shear strength with constraints imposed on minimum weight and stochastically variations given by the manufacturing process chosen. Honeycomb structures of this type can be successfully produced using rapid prototyping facilities like Fusion Mould Deposition (FMD) or synthered powder procedures. Honeycomb samples are produced and tested using ASTM standard for flatwise compressive strength and shear loading.

References

1. Paulhac, A. D. Perrott, F. Scarpa and J. R. Yates. Flatwise compressive behaviour of novel chiral honeycomb concept. Proceedings of DFC-7, Sheffield, April 2003.
2. Paulhac, A. F. Scarpa, D. Perrott and J. R. Yates. The linear transverse mechanical properties of hexagonal chiral honeycombs. Submitted to International Journal of Mechanical Science.
3. T. L. Lew, F. Scarpa and K.Worden. Homogenisation metamodelling of perforated plates. Strain. In press.
4. M. Grediac. 1993. A Finite element study of the transverse shear modulus in honeycomb cores. International Journal of Solids and Structures, 30, pp. 1777-1788
5. Scarpa and P. J. Tomlin, 2000. On the transverse shear modulus of negative Poisson's ratio honeycomb structures, Fatigue and Fracture in Engineering Materials and Structures, 23, 717-720.

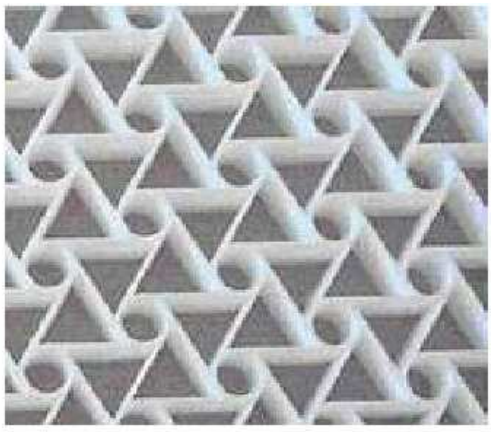

Figure 1. Chiral honeycomb structure

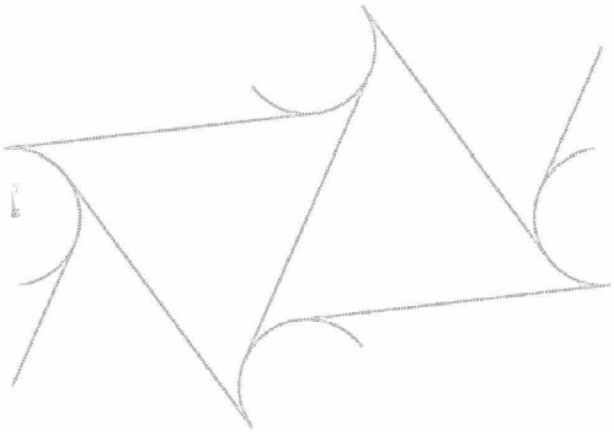

Figure 2. FE chiral unit cell for neural network training

DAMAGE EXTENSION AND FAILURE BEHAVIOR OF CFRP SPECIMENS IN OPEN HOLE COMPRESSION TESTS AND ANALYTICAL SIMULATION

Tetsuji Kato[+], Takashi Ishikawa[+],Yasumasa Hamaguchi, Naoya Shikata[++], and Goichi Ben[++]
+ Advanced Composite Evaluation Technology Center, Japan Aerospace Exploration Agency (JAXA-ACETeC)
++ Production Engineering Department, Nihon University

In order to estimate the critical strength in composite structural design, open hole compression (OHC) tests are carried out similarly to compression after impact (CAI) tests. OHC test is simple and low cost test method as compared with CAI test. Therefore, importance of OHC tests is enhanced in present manufacture of composite structures. Although the results of OHC tests are regarded as one of the most important evaluation for the critical strength of laminates, the failure process of a specimen in OHC test is not yet understood well due to the complexities of its mechanics caused by lamination.

In this paper, detailed observation of the failure process of the OHC specimens was carried out to understand the failure sequence of ply damage and delaminations. Several kinds of quasi-isotropic CFRP laminates ($[(45/0/-45/90)_2]_{sym}$) were used in OHC tests and SACMA 3R-94 and NAL-III test method were adopted in OHC tests. NAL-III test method (see Fig.1) that is newly developed by JAXA-ACE TeC bring test cost reduction due to its short size of specimen. A comparison in test results between de-facto SACMA 3R-94 and NAL-III was also made for justification of the latter.

The results obtained by NAL-III method are in good agreement with the results obtained by SACMA method (see Fig.2), even in statistical diagnosis which is not shown here. Therefore, these results are important information about the validity for NAL-III OHC test method. We also obtained some important features of mechanics of damage growth in OHC tests by using fiber-optic micro scope. Fig.3 shows the pictures of the specimens around the hole and these figures show the failure sequence of ply damage and delaminations. The buckling-like damage is observed in hole edge area of 0° lamina at low level of applied compression load as initial phase. With the increase of the load, the buckling-like damage occurred in 0° lamina near the specimen surface. The initial damage at the hole edge of the specimen is the most probable onset of delamination extension. Second phase of the failure process is that the delaminations occurred in interface between 0° lamina and 45° lamina near the specimen surface with the increase of the load. As can be seen in Fig.2, the surface delamination failure is observed with about 80% of OHC strength. The final failure process is that the delaminations propagate transversely to the applied load. These features of the failure process of the specimen in OHC test can be seen in both SACMA test method and NAL-III test method with several kinds of laminates.

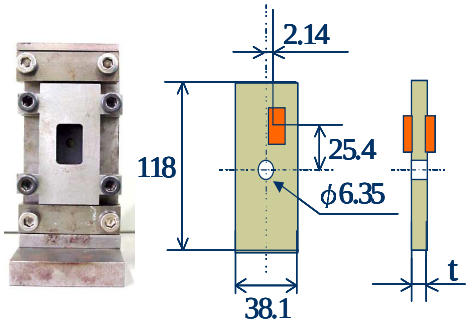

Fig.1 NAL-III OHC test method

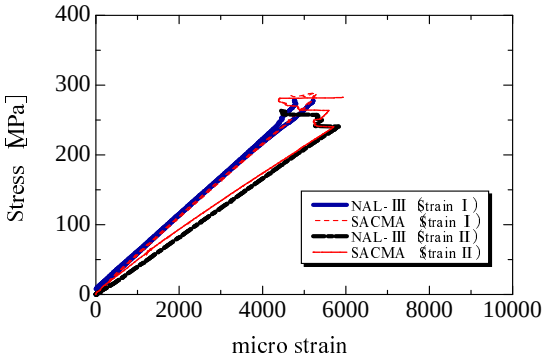

Fig.2 Stress-strain curves

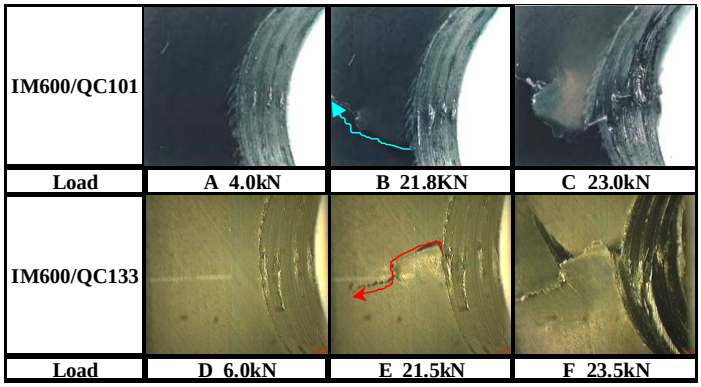

Fig.3 Typical failure process of OHC test

Furthermore, an analytical finite element method is developed to investigate the damage extension and failure behavior of laminates. For developed method, the ply damage initiation and extension is judged by using stress criterion and the extension of delamination is judged by using energy release rate that is calculated by virtual crack closure integral method (VCCM). The failure growth such as the initiation and extension of the ply damage and the delaminations is modeled by using the response of stiffness reductions of elements. Therefore, finite element models of the laminates have normal elements in interfaces between laminates and these interface elements have thickness.

The analysis of failure process of OHC specimen was carried out and some early results are shown in this paper. The analytical model is in the shape of the NAL-III OHC test specimen (see Fig.1). The early analytical target is the cross-ply CFRP laminates (IM600/QC133-$[0/90]_{sym}$) and its elastic properties and critical energy release rate are listed on advanced composites database, JAXA-ACDB (www.jaxa-acdb.com). Figure 4 shows the initiation and extension of the ply damage and Figure 5 shows the extension of the delaminations. The initial ply damage is observed in hole edge area of 0° lamina where will be the highest stress concentration area. With the increase of the load, the ply damage area extends to load applied direction. The initial delamination extension occurs in the hole edge area which is shifted from the most highest stress concentration area to the applied load direction.

With the increase of the load, the delaminations propagate transversely to the applied load. All delamination extension behaviors have the features of mode II fracture in present results. The early analytical failure process is similar to the results obtained by the OHC tests although the laminate construction is quasi-isotropic laminates in the OHC test.

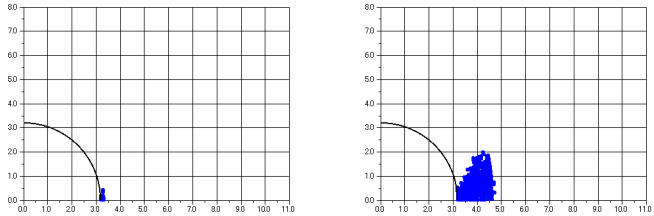

(a) Ply damage (0°Ply) - Load 150 MPa (b) Ply damage (0°Ply) - Load 320 MPa

Fig.4 Ply Damage initiation and extension

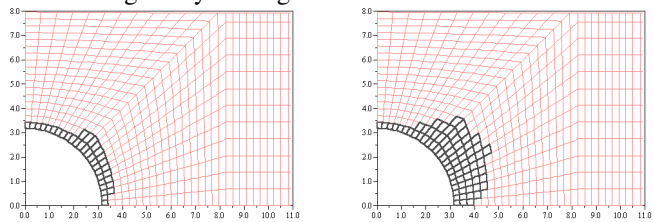

(a) Delamination (0°-90° interface) - Load 150 MPa (b) Delamination (0°-90° interface) - Load 390 MPa

Fig.5 Delamination extension

MODELING OF LEFT OVER STRENGTH IN DRILLING OF COMPOSITE LAMINATES:

S.K.Malhotra, R.Krishnamurthy and J.Ramkumar*
I.I.T., Madras, Chennai - 600 036, India
*I.I.T., Kanpur - 208016, India

Fibre Reinforced Plastics (FRP) composites occupy an important place as high performance engineering materials. Although in most of the fabrication processes used for composites, machining is avoided, sometimes machining of FRP is essential and cannot be avoided. Out of various machining processes used for FRP, drilling is the most common machining operation used. The drilling of holes in FRP composites presents problems different from those encountered in drilling metals. Problems encountered in drilling of FRP composites include:-

- crack formation
- damage of surface layers (delamination)
- surface roughness
- deviation of hole diameter from nominal diameter (hole shrinkage)
- roundness error.

In the present work, a new concept of Left Over Strength (LOS) is introduced. A centre hole is drilled in a flexural test specimen and flexural load at failure is determined. The LOS is expressed as percentage of load which specimen with a drilled centre hole can carry as against the specimen with first hole. LOS depends upon the quality of hole in the specimen. As number of holes drilled using a particular drill increases, quality of hole deteriorates and value of parameters such thrust, torque and temperature monitored during drilling also increase.

Modeling of LOS using Multiple Regression Analysis is carried out to correlate LOS with thrust, torque and temperature.

$$LOS = K_1(\text{thrust})^{n1}\,(\text{Torque})^{n2}\,(\text{Temperature})^{n3}$$

Significance of the mode of drilling on LOS can be assessed by referring to the exponents of thrust, torque and temperature in the above equation. After study with different drill materials and drill geometry, it was observed that LOS is influenced maximum by thrust followed by temperature and torque.

SESSION 8 – FABRIC COMPOSITES

Chair: Prof.Stepan Lomov
Katholieke Universiteit Leuven, Belgium

Wednesday 22 September
16.20-18.00

3D FINITE ELEMENT DAMAGE ANALYSIS
OF A TWILL-WEAVE LAMINA SUBJECTED TO IN-PLANE SHEAR

G. Baruffaldi, E. Riva, G. Nicoletto
Dipartimento di Ingegneria Industriale - Parco Area delle Scienze 181/A
Università di Parma, 43100 Parma, Italy, e-mail: riva@me.unipr.it

Use of textile preforms is one of the most important developments in the composite material sector for structural applications. Woven composite laminates are characterized by such advantages as balanced in-plane mechanical properties, improved impact resistance and easy handling and shaping, [1]. They are also now competitive in terms of cost with respect to unidirectional laminated composites. However, an enhanced use of woven composite materials depends primarily on the availability of reliable predictive methods of the mechanical behavior. Predictive methods should account for the complex geometry of the reinforcing phase, the widely different architectures, the wide selection of constituent materials and the variety of damage mechanisms.

In the last decade computational approaches adopting mainly the finite element method have been extensively used to model the mechanics of woven composite laminates, see for example [2] for a review. Due to their role in critical structural applications, the relatively simple plain-weave texture, the carbon fiber reinforcement (CFR) and the mechanical response in the fiber direction have been mostly considered in the computational studies. Factors such as such as yarn curvature, number of plies, stacking sequence etc., on the global stiffness of fabric laminates were quantified, [2], the role of twill weave texture in [3]. Computational procedures for modelling the damage and strength response of such materials have also been proposed and applied but not yet completely validated, [4-6].

This paper deals with the application of the finite element based approach to the prediction of the stiffness and strength of a CFR woven composite lamina subjected to in-plane shear. A preliminary detailed mesostructural characterization of material texture by optical microscopy helps in identifying a idealized yarn geometry of the representative volume element (RVE), Fig. 1a. A parametric 3D finite element model, see Fig. 1b, which allows a systematic investigation of the role of mesostructural features, is then developed using solid (8 nodes) finite elements and the mapped meshing format. The computational procedure, originally developed for the modeling of damage development in woven laminates under direct traction, [3], is then outlined and the appropriate boundary conditions defined and applied to the RVE [7]. The carbon fiber yarns were modeled as a transverse isotropic, linear elastic material having homogenized properties while a nonlinear matrix was assumed. The nonlinear procedures of the ABAQUS finite element code were used to include the global geometric nonlinearity. The damage accumulation process was modeled according to the Blackketter's strategy, [4].

As an example of typical results are shown in Fig.2. The superposed undeformed and deformed FE meshes of Fig. 2a show the global homogenized shear strain applied to the RVE and the periodic nature of the displacement component. The in-plane shear stress distribution of the RVE due to a global in plane shear load of Fig. 2b demonstrates the degree of stress non-uniformity within the single yarn and between yarn and matrix. Stress nonuniformity is influenced by architectural features, such as texture, yarn crimp ratio, etc. and it is responsible of the development of the various damage mechanisms involved in material degradation.

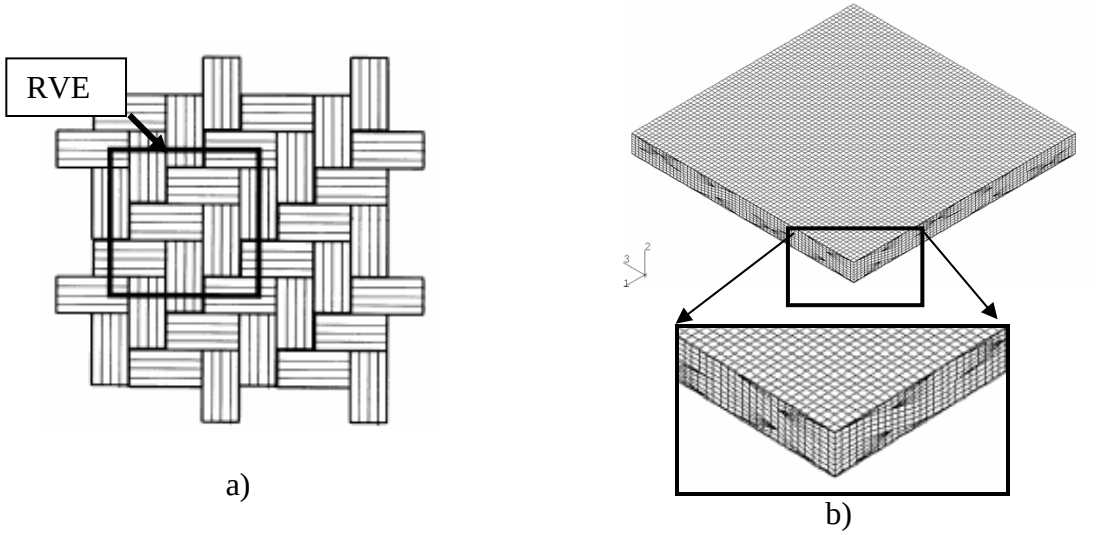

Fig. 1- a) twill-weave texture and RVE; b) finite element model of the RVE

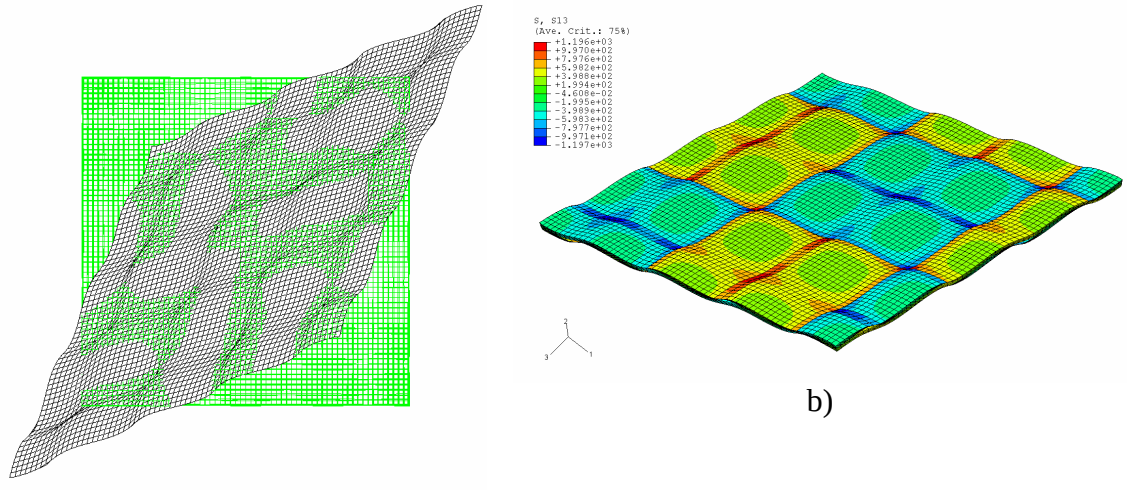

Fig. 2 – a) Top view of underformed and deformed RVE under in-plane shear, b) in-plane shear stress distribution in the RVE

Selected References

1. Naik, N.K., Woven Fabric Composites, Tecnomic Pub., 1994
2. E. Riva, G. Nicoletto, "Modeling and prediction of the mechanical properties of woven laminates by the finite element method", In: M. Guagliano and M.H. Aliabadi, editors, *Fracture and Damage composites,* WIT Press, Southampton UK, 2004 (In press).
3. Nicoletto, G., Riva, E., "Failure Mechanisms in Twill-Weave Laminates: FEM Predictions vs Experiments", *Composites Part A*, 2004 (in press).
4. Blackketter, D., Walrath D., Hansen A., "Modeling Damage in a Plain Weave Fabric-Reinforced Composite Material", *Journal of Composites Technology & Research*, Vol. 15, No. 2, 1993, pp. 136-142.
5. Guagliano M; Riva E, "Mechanical behaviour prediction in plain weave composites", The Journal of Strain Analysis for Engineering Design, vol. 36, no. 2, 2001, pp. 153-162
6. Zako M., Y. Uetsuji, T. Kurashiki, "Finite Element Analysis of Damaged Woven Fabric Composite Materials", *Composite Science and Technology*, Vol. 63, 2003, pp. 507-516.
7. Carvelli, V., Poggi, C., (2001), "A homogenization procedure for the numerical analysis of woven fabric composites", *Composites: Part A* , 12, 1435-1433.

FAILURE AND IMPACT MODELLING OF BRAIDED FABRIC REINFORCED COMPOSITES

M. Fouinneteau and A. K. Pickett
Department of Advanced Materials, SIMS, Cranfield University, Bedfordshire, MK43 OAL.

In recent years cost effective advanced composites have received increasing attention as a possible replacement material for traditional metals. Amongst these the application of textile braided composites for automotive, and other applications, is of particular interest. Today these textile forms can be cheaply manufactured using fast braiding machines to give a wide variety of fibre architectures and preform shapes. Furthermore, the availability of new low cost carbon fibres and the use of flexible resin injection processes are helping to encourage industrial interest, particularly in niche (low volume) applications.

The particular application considered here is braided composite sections for potential automotive structures. Experimental work has shown that braided composites offer high stiffness and strength-to-weight ratios; high impact resistance and can absorb significantly greater specific energy compared to equivalent metal structures[1]. Furthermore, braiding machines are adaptable and can produce a wide range of fibre architectures that can be tailored to meet these, and other, criteria.

Most analytical constitutive models for advanced composites have been specifically developed for unidirectional (UD) plies and a large number of stiffness and failure models are to be found in the literature[2]. Under impact and crash loading, methods using damage mechanics are usually preferred but, again, most

models concern UD composites. This paper presents the adaptation of a UD composite ply damage model for analysis of stiffness, failure and impact of braided composites.

The simulation code used in this work is the explicit Finite Element code PAM-CRASH[3] which has over the past five years developed promising new composites delamination and ply failure models[4]. For the basis of this work the PAM-CRASH Ladeveze UD composite ply model[5] is used. This model uses continuum damage mechanics to treat fibre and transverse matrix failure and elasto-plastic with damage to model shear failure. The plane stress orthotropic constitutive law with damage parameters is given by

$$\begin{Bmatrix} \varepsilon_{11} \\ \varepsilon_{22} \\ \varepsilon_{12} \end{Bmatrix} = \begin{bmatrix} 1/E_1(1-d_1) & -\upsilon_{12}/E_1 & 0 \\ -\upsilon_{12}/E_1 & 1/E_2(1-d_2) & 0 \\ 0 & 0 & 1/G_{12}(1-d_{12}) \end{bmatrix} \begin{Bmatrix} \sigma_{11} \\ \sigma_{22} \\ \sigma_{12} \end{Bmatrix} = [\mathbf{S}]\{\sigma\}$$

where the compliance matrix [**S**] comprises of four undamaged elastic constants E_1, E_2, G_{12} and υ_{12} and damage parameters d_1, d_2 and d_{12} for the two principle fibre and shear directions. Usually d_1 and d_2 are uncoupled, but there is an interaction between d_2 and d_{12}.

Work presented here shows that this model, with some simple modifications, can be realistically used to represent the important failure modes observed in braided composites. Special attention has been paid to check validity of the model under various loading conditions and for braids having different fibre architectures. The presentation gives the Finite Element modelling methodologies used to represent the braid and details of the testing and parameter identification procedures used to fully characterise the failure model. These tests include conventional tensile and compressive testing to failure and more unorthodox shear cyclic testing to determine the evolution of elasto-plasticity and shear damage. The application of these test and analysis methods to simple coupons and more complex structures are described.

[1]Beard S.J. Energy absorption of braided composites tubes, PhD, Stanford University, Stanford, 2001.
[2] Hinton M J, Kaddour A S, Soden, P D. A comparison of the predictive capabilities of current failure theories for composite laminates, judged against experimental evidence. Composite Science and Technology, Vol. 62, Issues 12-13, September-October 2002, p. 1725-1797.
[3] Pam-Crash. ESI Software (2002) Engineering Systems International, 99, rue des Solets, SILIC 112 94513 Rungis Cedex France.
[4] Johnson A F, Pickett A K and Rozycki P. Computational Methods for Predicting Impact Damage in Composite Structures. Composites Science and Technology 61, p. 2138-2192, 2001.
[5] Ladeveze, P. and Le Dantec E. (1992), 'Damage modelling of the elementary ply for laminated composites', Composites science and technology, Vol. 43, pp. 257-267.

PROGRESSIVE DAMAGE CHARACTERIZATION OF STITCHED, BI-AXIAL, MULTI-PLY CARBON FABRICS COMPOSITES

M.Vettori1, T. Truong Chi[2], S. V. Lomov[2], I.Verpoest[2]
1 Dipartimento di Ingegneria Industriale, Università degli studi di Parma.
Parco Area delle Scienze, 181/A – 43100 Parma e-mail: vetto@me.unipr.it
2 Material Engineering Department – Katholieke Universiteit Leuven

Introduction and Materials

The main aim of the present work is the damage characterization and damage evolution analysis of laminates made by innovative textile composites due to quasi-static loads. The main characteristic of these fabrics is the geometry, created in order to reduce the bending effects due to fiber crimping of standard textiles [1]. The identification of the damage mechanisms and the analysis of the evolution of the damage at different strain levels are the results of the study.

The material studied is a non-crimp fabric [2], obtained by superposing layers of unidirectional material oriented in different directions and maintained together by a stitching PES (?) yarn through the thickness. In particular, the bi-axial fabric studied, is made of two UD plies stacked in a 0/90° sequence, and stitched with a tricot-warp pattern (Fig.1). The specimens [3] are obtained from a laminate plate of 8 fabrics (16 plies), with a [(0/90)/(90/0)/(0/90)/(90/0)]S lay-up, made by RTM. The final volume fraction of the laminate is about vf =47%.

Experimental Set-Up

The material has been subjected to tensile loading along its characteristic directions (0°, ±45°, 90°), while recording acoustic emissions (A.E.) in order to follow the damage evolution. Observation of the events vs. strain diagrams shows three different regions (Fig.2), where the damage evolves at different rates; inside each region a characteristic strain level was chosen (cfr. Fig.2). In order to characterize damage, other tensile tests up to the predefined strains were conducted (Fig.2). Then, the damaged specimens have been analyzed with ultrasonic (US) and X-ray Non-Destructive techniques. The extension of the damage, its pattern and distribution were evaluated. The influence of the fabric geometry, of the stitching yarns, and of the holes induced by the needle has been taken into account as a possible cause of damage.

Electrical resistance methodology has been also used on new tensile tests, to gain more information about damage effects, and to complement A.E. information.

Results

The results of the non-destructive investigations are presented in figure 2. The evolution of the damage due to a tensile load along 0° direction is represented (similar analysis has been done along ±45° and 90° dirs.). As revealed by X-Ray radiography, the damage initiation starts at very low strains (lower than 0.2%) near the edge of the specimen [4]. Then it evolves going through the width of the specimen, along the transversal-to-load direction inside the matrix-dominated layers. When higher strains are reached, and the transversal cracking process tend to saturate, the longitudinal cracking process initiates (in the load direction). Damage in the fibre-dominated plies consists of yarns splitting and fibre debonding leading to final failure of the specimen due to fibres cracking. Furthermore, histogram and threshold analysis were carried out on US images, revealing the extent of progressive damage and its different modes.

Lastly, the position of the damage has been evaluated and compared to the stitching dimensions: it seems that somehow the damage follows a pattern during its evolution. The possibility to have correlation between stitching and damage pattern is quite high.

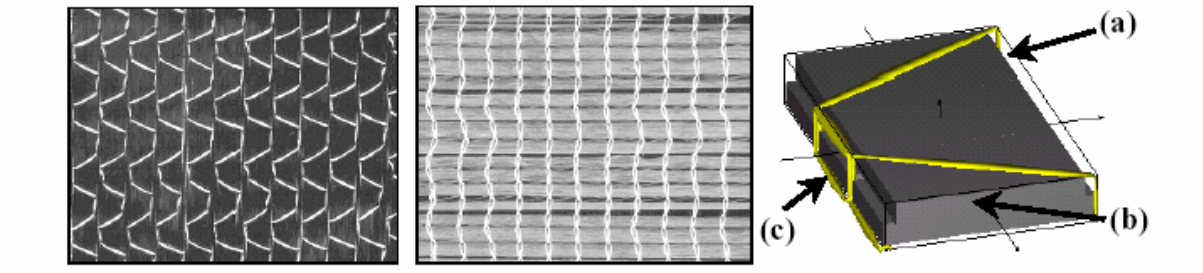

Fig.1: Biaxial textile composite: from left to right: upper surface (0° lamina), bottom surface (90° lamina) and the elementary unit cell, made by a 0° (a) and a 90° (b) UD layer maintained together by a PES stitching yarn, with a tricot-warp pattern.

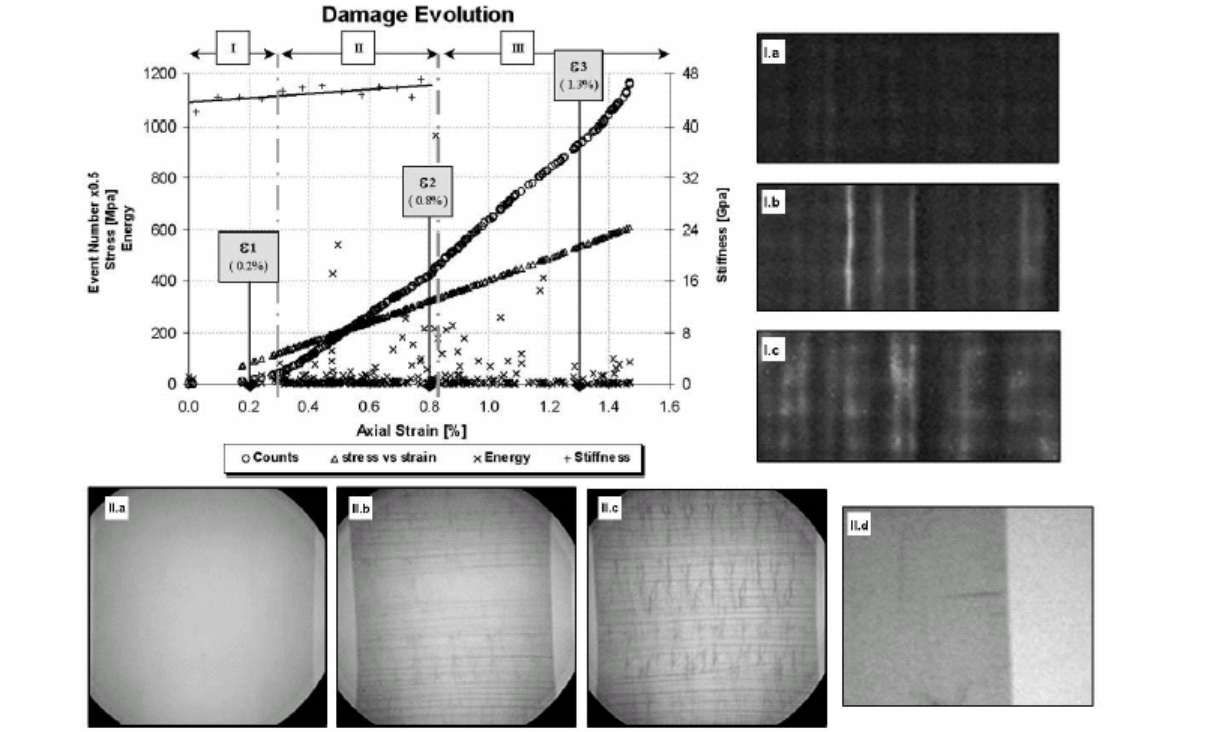

Fig.2: results of the study along the Machine direction (MD - 0° dir.). On the graph are reported the stress-strain and the stiffness-strain points, AE counts vs strain and event's energy. C-scan images (I.a, I.b, I.c) and X-ray images (II.a, II.b, II.c, II.d) are included. It is visible (II.d) that the initially transverse crack, observed at ε_1=0.2% , starts from the edge of specimen.

References

[1] Rafael Avila-Dominguez, "Composites manufacturing using non-crimp fabrics (NCF)", Structures and Materials Centre, DERA Farnborough;
[2] S.V.Lomov, E.B.Belov, T.Bischoff, S.B.Ghosh, T. Truong Chi, I.Verpoest, "Carbon composites based on multi-axial multi-ply stitched preforms. Part 1: Geometry of the perform" , *Composites:Part A*, 33 (2002) pg. 1171–1183;
[3] AA.VV., "Tensile properties of Fiber Resin Composites", ASTM Standard D 3039 – 00;
[4] T. Truong Chi, M. Vettori, S. Lomov, I. Verpoest, "Multi-axial multi-ply carbon fabric reinforced epoxy composites: mechanical properties and investigation of initial damage" *Proceedings of the 14th International Conference of Composite Materials*, (ICCM-14), San Diego (CA).

MEASUREMENT OF MESO-SCALE DEFORMATIONS FOR MODELLING TEXTILE COMPOSITES

Prasad Potluri and David A Perez Ciurezu
Textile Composites Group, UMIST, PO Box: 88, Manchester M60 1QD
Email: Prasad.Potluri@umist.ac.uk

Geometry of Textile Composites

While traditional short-fibre and unidirectional long-fibre composites are treated at micro- and macro-scales, textile composites have an additional level, meso-scale, to consider. Woven textiles are constructed by interlacing two orthogonal sets of tows in a variety of weave topologies as show in figure 1. Tow waviness, which in turn depends on degree of interlacement - lowest for sateen to highest for plain weave, has a direct influence on both physical and mechanical properties of composites.

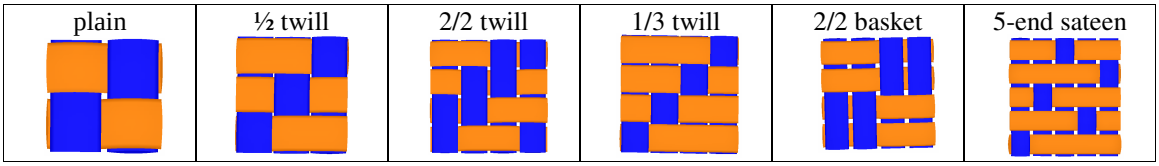

Figure 1: Topology of weave interlacements

Textile preforms undergo complex deformations during processes such as RTM and thermoforming; biaxial tensile deformation, in-plane shear deformation, transverse compaction and out-of-plane bending deformations. Figure 2 shows the meso-scale, i.e. tow level, representation of a typical plain weave. Tensile deformations lead to changes in the dimensions of unit cell 'ABCD' due to a combination of crimp interchange and tow flattening. The unit cell distorts into a parallelogram due to in-plane shear deformation and as a result, an idealised Repeating Unit Cell (fig 2) can no longer be used. Relatively large in-plane shear deformations, as a result of draping on a mould surface with a large Gaussian curvature, may also lead to tow narrowing, 3D buckling and slippage. Transverse compaction results in tow flattening, reduction in crimp and a slight increase in tow spacing. Crimp levels may also change slightly due to out-of-plane bending deformations.

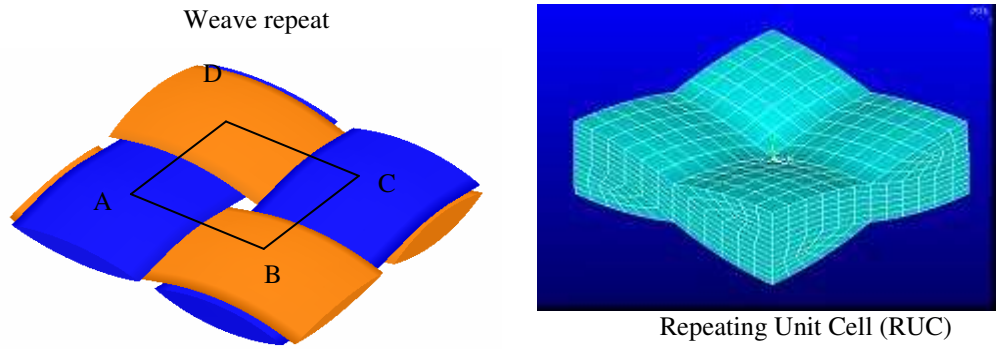

Figure 2: Meso-scale representation

As a result of complex process-induced tow deformations, an idealised orthogonal RUC can no longer be used. Additionally, unit cell geometry varies significantly from place to place at macro level, i.e. component level. While there has been a computational effort in the area of fabric mechanics [1,2], tow deformations are too complex to predict accurately. The present paper looks at an experimental technique to map global or whole-field tow deformations.

Whole-field mapping of in-plane tow deformations

Tow deformations during processing are relatively large and hence cannot easily be measured with techniques such as speckle-interferometry. In the present work, an inexpensive optical technique, based on image processing has been developed. A textile preform is subjected to in-plane stresses (tensile and/or shear) and the resulting deformed image is scanned with a flatbed scanner for each deformed state. The resulting tensile and shear deformations are computed for each unit cell over the entire sample area. In the initial work, points of tow interlacements were marked for ease of image processing. Further work is in progress to compute the strain data directly from the weave details. Figure 3 shows the measured shear angles (shear deformation) and tow width during a bias extension test.

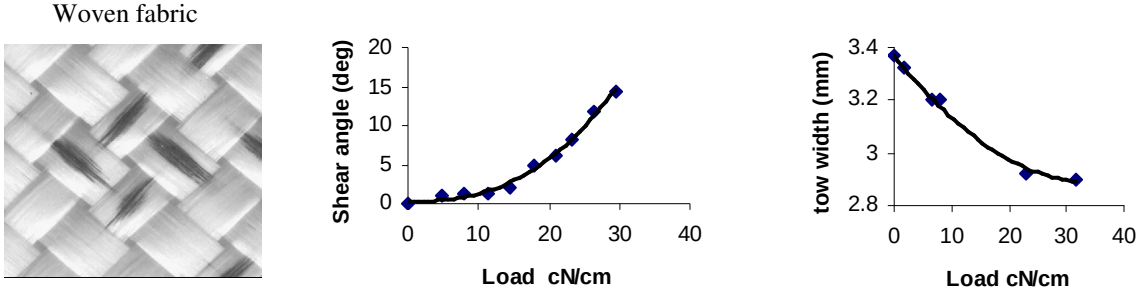

Figure 3: Measurement of tow-deformations

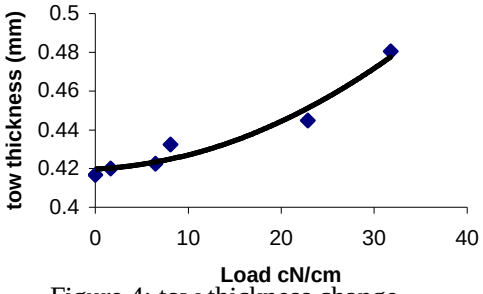

Figure 4: tow thickness change

Transverse tow deformations

Tow thickness can be computed from the measured tow width, assuming a lenticular geometry and an empirical value for the fibre-packing ratio within a tow. However, it is important to measure through-the-thickness details, i.e. tow cross-sectional shape, weave angle and tow length between crossover points, in order to generate more accurate 3D models. A stress-freezing technique, reported earlier for transverse compaction [3] is used here. Two additional techniques, 3D profilometry and tomography are currently being explored.

Model identification

Idealised RUC (shown in figure 2) used by many researchers [4] is only applicable to orthogonal structures. For components subjected to in-plane shear, we identified a new RUC as shown in figure 5. With the new RUC, one can divide a component into a number of elements with each element having a unique RUC. This is a significant improvement over using one idealised RUC for the entire component. Figure 5 shows micro-mechanical analysis of $+65^{o}$ and -65^{o} tows (resin elements not shown for clarity).

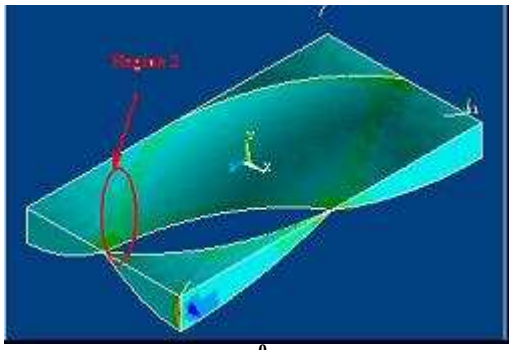
$+65^{0}$ tow

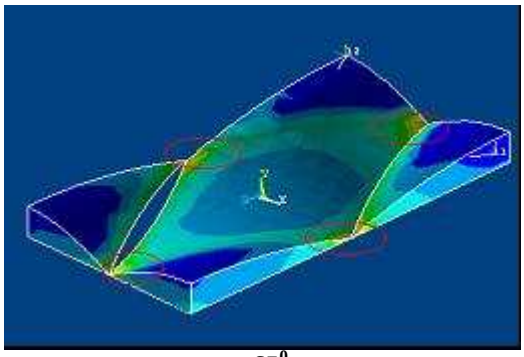
-65^{0} tow

References:

1. T Sagar, P Potluri and JWS Hearle, Mesoscale modelling of interlaced fibre assemblies using energy method, *Computational Material Science*, *28 (1), 2003, 49-62.*

2. P. Potluri, S. Sharma and R. Ramgulam, Comprehensive drape modelling for moulding 3D textile preforms**,** *Composites Part A, 32(10), 2001, 1415-1424.*

3. P Potluri, M A Wilding and A Memon, A novel stress-freezing technique for studying the compressional behaviour of woven fabrics, Textile *Research Journal*, 72 (12), 2002, 1073-1078.

4. J D Whitcombe, Three-dimensional stress analysis of plain weave composites in '*Composite Materials: fatigue and fracture' (ed. T K O'Brien). ASTM STP 1110,* 1991: 417-438.

SESSION 9 – NOVEL METHODS AND RESIDUAL STRESSES

Chair: Prof.Anoush Poursartip
University of British Columbia, Canada

Thursday 23 September
08.30-10.35

NOVEL METHODS FOR TESTING AND MODELING COMPOSITE MATERIALS AND LAMINATES

C. T. Sun
School of Aeronautics and Astronautics, Purdue University
West Lafayette, Indiana, U.S.A.

Fiber-reinforced composite materials are usually treated as homogeneous and orthotropic solids. Because the matrix in a composite often exhibits nonlinear behavior, the composite also has nonlinear stress-strain relations, except for the fiber direction. Laminates of these composites, besides being anisotropic and nonlinear, are also nonhomogeneous in the thickness direction and multiple failure mechanisms may be present in coupon specimens Because of these unique anisotropic and nonhomogeneous properties, testing and modeling of composites often require special methods that are different from the traditional methods used for homogeneous and isotropic materials.

In this talk, a number of special testing and modeling methods for fiber-reinforced composites or laminates, which were developed by the present author, are reviewed. Included are: 1) an oblique end tab suitable for testing off-axis coupon specimens, 2) a method for delaying premature free edge failure in testing notch strength in composite laminates containing a circular hole, 3) a simple method for testing and modeling anisotropic rate-dependent nonlinear behavior and compressive strength of composites using off-axis specimens, and 4) testing dynamic interlaminar fracture toughness of polymeric composites using static loading setups.

CHARACTERIZATION OF MANUFACTURING RESIDUAL STRESSES IN WOUND COMPOSITE TUBES

P. Casari, F. Jacquemin, P. Davies*
GéM Laboratoire de Génie Civil et Mécanique de Nantes – France
2, rue de la Houssinière BP 92208 44322 Nantes Cedex 03 - France
*IFREMER Centre de Brest – France
BP70, 29280 Plouzané, France

This paper will present a method for the characterisation of residual stresses in thick filament wound tubes. Such tubes are widely used for a range of industrial applications. Residual stresses are known to affect mechanical behaviour of composites, e.g.[1,2], but little work has been performed on the influence of residual stresses on tube performance.

The aim of the present work is to evaluate a simple method to measure internal stresses and to compare results with predictions from a residual stress model.

The three materials considered are wet wound epoxy composite tubes, of 55mm inner diameter and 6 mm wall thickness, based on E glass, R glass and T700 carbon fibres. Three winding angles are considered, [±55], [±35] and [±85] with respect to the tube axis. Tubes were cured at 125°C.

The experimental technique involves sectioning the tubes and measuring the change in strains. Figure 1 summarizes the steps of stresses release due to machinings.

Residual stresses correspond to the induced strains or displacements due to the two cutting steps. Then strains on the external and internal surfaces of the tube are measured with biaxial strain gages and recorded during these operations. The first order of magnitude of residual stresses is obtained by means of the classical laminate theory. This leads to a simple technique which allows the quick identification of the effects of manufacturing or eventually moisture on the internal multiaxial stress level.

A model is associated with the experimental assessment, which predicts the normal and shear stress level in the constitutive plies of the tube [3,4]. The residual stresses, induced by the temperature differential (between cure and room temperatures), for every ply at any time, are calculated by using the classical equations of solid mechanics: constitutive laws of thermoelastic orthotropic materials, strain-displacement relationship, compatibility and equilibrium equations and boundary conditions. An example of a predicted stress distribution in a [±55] E glass/epoxy tube due to cooling from 125°C to 20°C is shown below.

This shows that shear stresses are not negligible and must be taken considered at the design stage. The paper will describe the experimental technique, present results from residual stress measurements and model predictions for the 9 cases (three fibres, three winding angles) described above, and discuss the implications of the results for the optimisation of tube manufacturing.

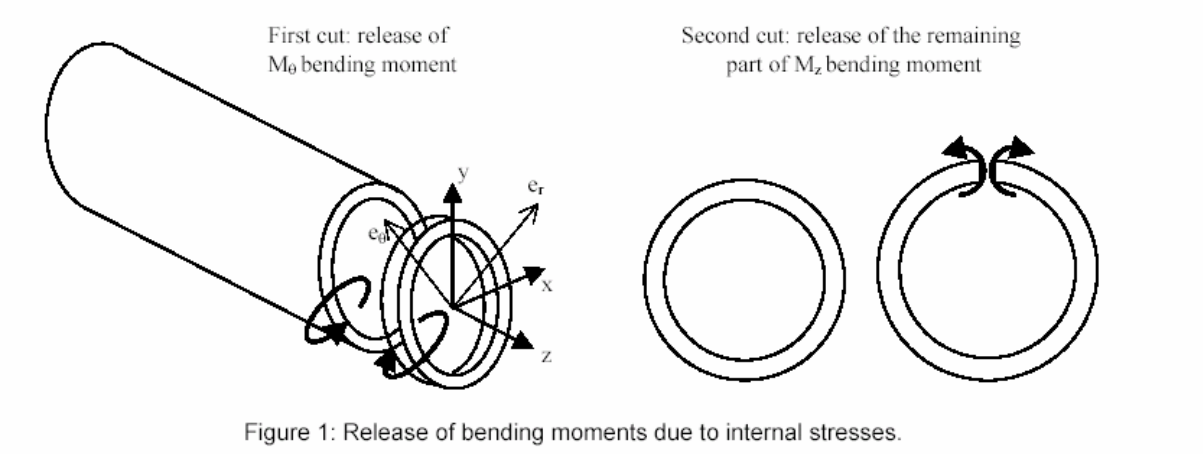

Figure 1: Release of bending moments due to internal stresses.

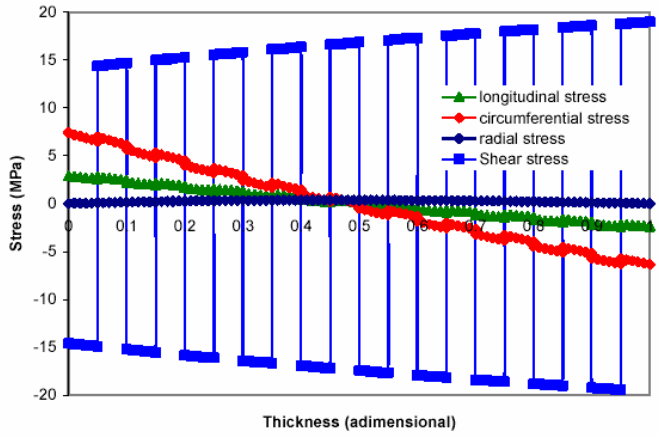

References

[1] Ersoy N., Vardar O. "Measurement of Residual Stresses in Layered Composites by Compliance Method" Journal of Composite Materials **2000**; 34: 575-598

[2] Manson J.E., Seferis J.C. "Process Simulated Laminate (PSL): A Methodology to Internal Stress Characterisation in Advanced Composite Materials" **1992**; 26: 405-431

[3] Paul D, Vautrin A, Transient hygrothermal stresses in laminated cylinders, Proc DURACOSYS **1996**, p281.

[4] Jacquemin F, PhD thesis, Modelling of internal stresses in thick tubular composite structures, Ecole des Mines de St Etienne, **2000**.

TESTS TO MEASURE THE MATERIAL PROPERTIES RELEVANT TO THE MODELLING OF PROCESS INDUCED DEFORMATIONS OF COMPOSITE PARTS

Nuri Ersoy, Tomasz Garstka, Kevin Potter and Michael Wisnom
Department of Aerospace Engineering, University of Bristol, Bristol, UK

Modelling of the manufacturing deformations in composite parts has attracted considerable research effort in recent years. The motivation behind this effort is to have a reliable analytical method to predict the deformations in order to make necessary tool corrections to obtain the dimensional fidelity required by aerospace industry. The reliability of the predictive methods highly depends on the reliability of the material data used in modelling. This paper summarizes the state of the current experimental research to measure some of the material properties relevant to the modelling of composites processing. Cure kinetics of the resin, points of gelation and vitrification and cure shrinkage behaviour of a carbon fibre thermosetting composite are investigated experimentally.

The cure kinetics of the resin is important information to determine the evolution of degree of cure, □, glass transition temperature, T_g, as well as the gelation and vitrification points. DSC test are performed to simulate the Manufacturer's Recommended Cure Cycle (MRCC), and the evolution of ∝ and T_g. Fig. 1 shows the development of ∝ and T_g. From the graph it can be seen that there is a sharp rise in degree of cure during the second ramp, where the resin transforms from a viscous fluid to a rubbery solid, and vitrification occurs at about 30 min. at the 180°C hold.

Gel point of the curing resin is determined in a separate test where, two layers of prepreg were pulled out from between another two layers, while they were cured between two heating plates according to the MRCC. Fig. 2 shows the shear stress required to pull the layers of prepregs against each other. The gel point of the resin exhibits itself as a sharp rise in the force required and is measured to be at around 160°C during the second ramp, and this corresponds to a degree of cure of a=0.30.

Through-the-thickness cure shrinkage of AS4/8552 composite was measured using a novel technique where, unidirectional and crossply stacks of prepregs were placed in between two heating plates, and the whole assembly was placed in a die-set. The MRCC was replicated and the through-thickness strain is measured using a non-contact video extensometer.

A typical strain versus time graph throughout the MRCC is plotted in Fig. 3 for a cross-ply sample together with the recorded temperature profile. It can be noted that several regions where different mechanisms are effective can be distinguished. At Region I the resin is expanding as a result of increasing temperature, however at about 60°C, the thickness starts to reduce due to consolidation, trapped air rejection and resin flow, which continues in Region II, up the onset of second ramp. Cure kinetics indicate that there may me some cure shrinkage as well. However in Region III, at the first part of the second ramp, there are three mechanisms competing each other, consolidation, cure shrinkage, and thermal expansion in liquid state, where the latter is believed to be dominant. The peak coincides with the onset of gelation, though that should be considered as a mere coincidence. In Region IV, the consolidation mechanism ceases to be effective; since the resin is gelled, there cannot be any void migration of resin flow. The cure shrinkage becomes dominant over the thermal expansion and an overall reduction in thickness is recorded. The total through-the-thickness strains after the onset of gelation is an important parameter in terms of residual stress modelling, and this is measured to be 0.5±0.05% for unidirectional and 1.0±0.05% for cross-ply composites.

The relevance of the above measurements to the modelling of the processing is discussed.

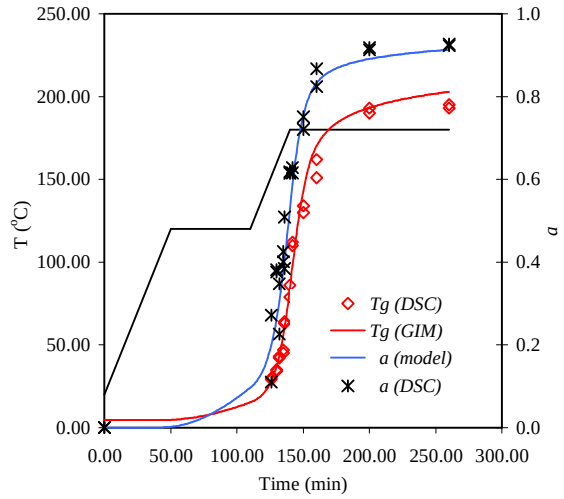

Fig. 1 Development of □ and T_g during the MRCC

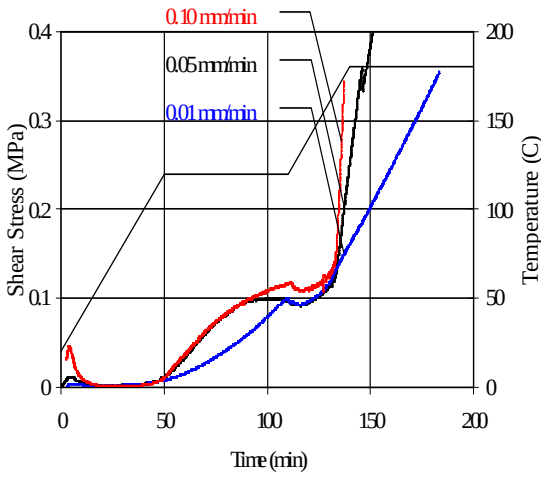

Fig. 2. Development of pull-out stress during the MRCC

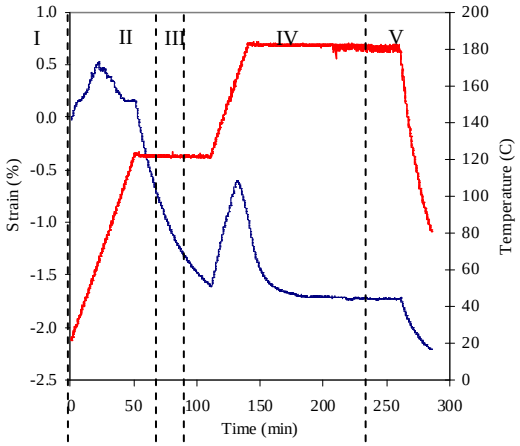

Fig. 3 Development of the through-the-thickness strain during the MRCC

RESIDUAL STRAIN DEVELOPMENT IN LAMINATED THERMOPLASTIC COMPOSITES MEASURED USING FIBRE BRAGG GRATING SENSORS

Larissa Sorensen, Thomas Gmür and John Botsis
Laboratory of Applied Mechanics and Reliability Analysis
Swiss Federal Institute of Technology, Lausanne, Switzerland (larissa.sorensen@epfl.ch)

In processing of polymer composite parts, residual stresses develop due to the differences in material properties of the matrix and reinforcement and their dependence on temperature. They are normally generated by several interacting mechanisms including thermal contraction, crystal growth and their level depends on the cooling path, fiber content and other processing parameters. In the case of polyphenylene sulphide (PPS) matrix composites, these parameters can influence the initial strain state to such an extent that consolidated laminates may exhibit microcracking solely due to the residual strains induced during processing. This is an extreme case; however, it clearly indicates the need for a reliable method for determining the residual strain state of a laminated composite.

Ideally, a sensor could provide internal strain measurements without compromising the composite structure or laminate properties. A fibre optic sensor, when embedded parallel to the reinforcing fibres, is minimally disruptive and generally causes no degradation of macroscopic properties. It is also possible to use this type of sensor to follow the strain development in a composite during the fabrication process, and afterwards in a completed structure.

This research utilizes fibre Bragg grating (FBG) sensors to follow the strain development inside carbon fibre-PPS (AS4/PPS) laminates throughout the consolidation process. The FBG sensor's response to a strain and temperature field (ε_x, ε_y, ε_z-, ΔT) is characterized by a change in its Bragg wavelength. When the transverse strains ((ε_x, ε_y,) are equal and the strain field remains uniform along the fibre, only a single Bragg wavelength peak is present. In the case where (ε_x is sufficiently different from ε_y,, two Bragg wavelength peaks appear, and the measured spectra are dependant on the polarization axis of the light sent into the sensor. Finally, if the axial strain, ε_Z, is not constant along the fibre length, then different Bragg wavelengths are reflected from different locations along the sensor. This produces a measured spectrum with more than one peak.

When FBG sensors are placed between the 0° plies of unidirectional and cross-ply AS4/PPS laminate, the consolidation process can be monitored by following the form of the measured spectra and the value of its Bragg wavelength. These measurements are significantly modified by changes in the state of the material by the cooling and by the load applied via the press platens. For example, the initial transverse load of the press platens at room temperature creates both birefringence and non-uniform contact resulting in shifted multi-peak spectra. After the glass-transition temperature (Tg ~ 90°C), the laminate plies become rubbery, creating relatively uniform contact between the plies and the sensor. As a result, the measured spectra become more regular, while keeping a double-peak due to the transverse load-induced birefringence. At Tg, the evolution of the temperature

compensated Bragg wavelength also reacts by changing its slope, as observed on the heating portion of the $\Delta\lambda_b$ curve in Figure 1. This figure also shows that measured wavelength evolution further changes its slope upon melting, (~ 280°C). Evidence of melting is also observed through the spectral form, which turns into a single peak, indicative of an axi-symmetric strain state due to the redistribution of the loading pressure by the now viscous polymer matrix.

During cooling and solidification, the FBG sensor is assumed to have perfect adhesion with the surrounding composite and its response follows the thermal contraction of the surrounding material. The magnitude of the effective thermal contraction of each specimen is proportional to the slope of the cooling portion of the $\Delta\lambda_b$ curves in Figure 1. Since the cross-ply specimens exhibit larger slopes than the unidirectional specimens, it is evident that the 0° direction in the cross-plies has a larger effective coefficient of thermal expansion (CTE) than does the 0° direction in the unidirectional specimens. It is the influence of the matrix-dominated 90° plies, which have a relatively high CTE, that creates the difference in the residual strain development in a cross-ply as compared to in a unidirectional laminate.

Although both of the cross-ply specimens display the same slope during cooling, there is an offset between their absolute . $\Delta\lambda_b$ values. This is likely due to the lay-up procedure, wherein the fibre optic is placed between the curved prepreg plies and then only held in place by the weight of the mould lid. This procedure allows the fibre to be initially free; however, the fibre may be displaced or pinched as a result of the stack of curved plies and the lack of pretensioning. The inconsistent jumps in $\Delta\lambda_b$ for specimen C2 are likely a result of some initial compression in the fibre, that was then released during melting.

During cooling, both the cross-ply and unidirectional specimens exhibit spectral form returns to a double peak due to the load-induced birefringence in the fibre optic sensor in the solid composite. Further, some spectra evolve into multi-peak forms indicative of non-homogeneous axial strains along the sensors. At room temperature, when the platen pressure is released and when the mould is removed, the Bragg wavelength jumps, but the spectral form does not change. The final Bragg wavelengths are tensile for the unidirectional specimens and compressive for the cross-ply specimens. The difference between the two types of specimens means that the addition of 90° plies into a laminate has added approximately 600µm/m of compressive residual strains in the centre of the laminate.

Post-fabrication measurements of the FBG spectra for all specimens show a significant polarization dependence of their reflected spectra. This indicates differences in the transverse strains (åx, åy) on the FBG sensor. In addition, the spectra suggest potentially non-linear distributions of the axial strain on the fibre sensor. It is difficult to decouple the two aforementioned effects using available tools; however, a technique allowing for the measurement of the relative contribution of the birefringence effects and the non-linear axial strains is under development.

To provide a complete picture of the actual strain distribution in the composite laminate, a finite element model of the actual lay-up configuration is constructed and used to provide a comparison with the experimental data. It accounts for the variation of the material properties with temperature and allows for the strains in the fibre optic sensor to be related to those in the surrounding plies.

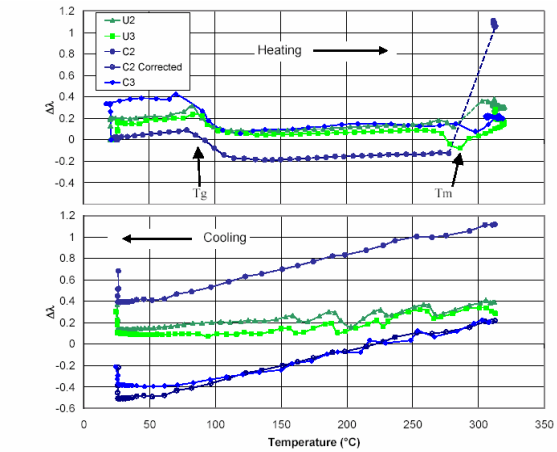

Figure 1 Temperature compensated change in Bragg wavelength during the heating and cooling portions of the consolidation cycle for unidirectional (U) and cross-ply (C) specimens. (In case of split spectra, the rightmost peak value is used)

Acknowledgement: The authors would like to acknowledge the financial support of the Swiss National Science Foundation , Grant no. 20-68279.02/1.

POSTER SESSION 5

DAMAGE MONITORING IN WOVEN COMPOSITES LAMINATES USING THE D.C. ELECTRICAL METHOD

E. Riva, M. Vettori, G. Nicoletto
Dipartimento di Ingegneria Industriale - Parco Area delle Scienze 181/A
Università di Parma, 43100 Parma, Italy

Woven fabric composites laminates are probably the most commonly used textiles in structural applications, [1]. The mechanical properties of woven fabric composites, such as strength and stiffness, are strongly influenced by the weave parameters. Although woven fabric composites have optimal in-plane mechanical properties compared to other textile fabric composites, their in-plane mechanical properties are inferior to those of classical unidirectional laminates. The prediction of the interaction between the mechanical behavior and structural parameters is very difficult. This leads to a gap in the knowledge about properties, damage mechanisms and failure criteria.

To achieve the full potential of these materials, various techniques for monitoring degradation mechanisms detection, especially the status of the load-carrying fibers, and for assessing the structural integrity have been investigated. The electrical resistance method is one such method, [2]. It is based on the idea that the carbon fibers act as electric resistors when a d.c. current is applied. Upon tensile loading the fibers stretch in the longitudinal directions and contract in the transverse direction due to the Poisson's ratio effect and the measured electrical resistance varies accordingly i.e. increases proportionally. If fibers suddenly fail the resistor cross-sectional area reduces and the measured electrical resistance suddenly increases. Progressive failure processes, such as fatigue damage development, can therefore be monitored, [2-4]. Previous studies demonstrated the high sensitivity of the d.c. electric method when applied to unidirectional fiber reinforced composite laminates both under static and fatigue conditions, [2-5].

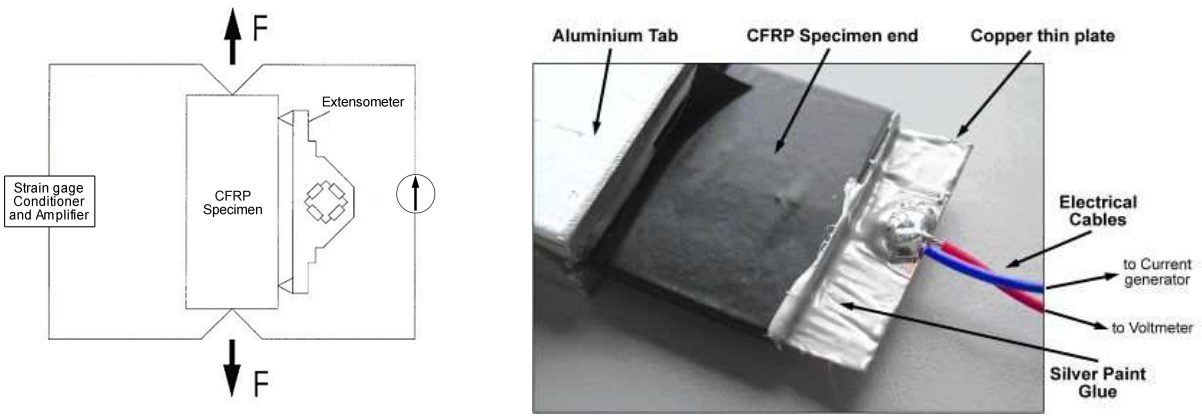

(1.a) (1.b)

Fig.1. a) System scheme b) electric contact at specimen end.

The present work considers unidirectional and woven fabric composite laminates and it is aimed at presenting the set-up and the technique along with damage observation under static and cyclic loading. Tensile specimens with geometry according to ASTM D3039-76 and ASTM D 3479M-96 were cut with tow yarns at 0° to the loading direction. Aluminium tabs were bonded to the specimen sides to transfer load from the grips and to assure electrical insulation. In figure 1 is presented the electrical circuit used during tests and a detail of the contacted specimen, obtained on abraded outermost sections with a special silver glue and thin copper plates. A constant electric current was applied to the specimen, the voltage V continuously monitored during the test and the variation of the electrical resistance calculated according to Ohm's law. Both an extensometer and strain gages were attached to the specimen to provide continuous strain monitoring during static and cyclic tests at room temperature. Stress-strain curves were recorded and elastic constants along the warp and fill direction were determined. Figure 2 present a typical stress vs strain and resistance vs strain curves, obtained with biaxial non-crimped fabrics. Additional tests and discussion will be included in the presentation.

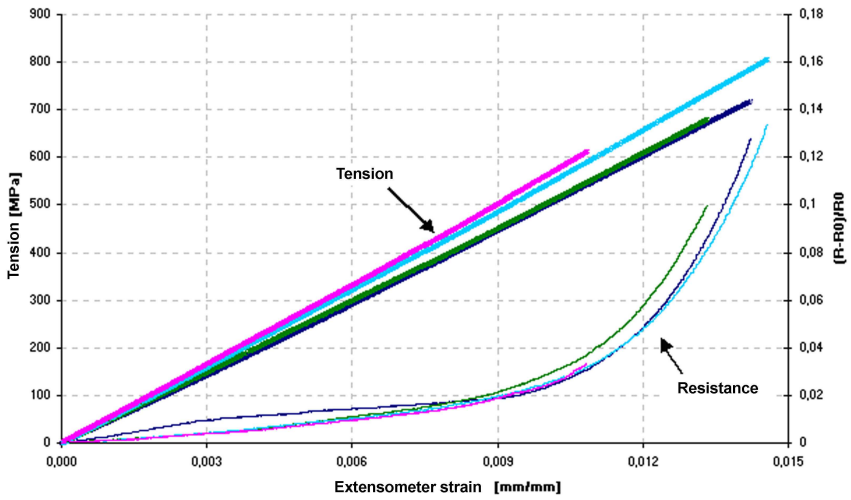

Fig.2: Stress-strain and ER-strain plots for 4 biaxial non-crimped laminated specimens subjected to monotonic traction (displacement rate 0,8 mm/min).

References

[1] N. K. Naik, 1994, *Woven fabric composites*, Technomic.

[2] K. Shulte, Ch. Baron, 1989, "Load and Failure analysis of CFRP laminates by means of electrical resistivity measurements", *Composite Science and Technology*, Vol. 36, 63-76.

[3] M. Kupke, K. Shulte, R. Schuler, 2001, "Non- destructive testing of FRP by d.c. and a.c. electrical methods", *Composite Science and Technology*, Vol. 61, 837-847.

[4] Akira Todoroki, 2001, "The effect of number of electrodes and diagnostic tool for monitoring the delamination of CFRP laminates by changes in electrical resistances", *Composite Science and Technology*, Vol. 61, 1871-1880.

[5] J.C. Abry, Y.K. Choi, A. Chateauminois, B. Dalloz, G. Giraud, M. Salvia, 2001, "In-situ monitoring of damage in CFRP laminates by means of AC and DC measurements", *Composite Science and Technology*, Vol. 61, 855-864.

[6] M. Martinelli, 2002, "Damage detection of CFRP laminates using electrical resistance measurement", *Laurea Thesis in Mech. Eng.*, Università di Parma (in Italian).

INDUSTRIALISED SHEAROGRAPHY TESTING ON AIRCRAFT COMPOSITES IN COMBINATION WITH 3D IMAGING AND DEFECT LOCATION

Roman Berger, Project Manager Shearography, Steinbichler Optotechnik GmbH, r.berger@steinbichler.de
Joerg Collrep, Product Manager Interferometry, Steinbichler Optotechnik GmbH, j.collrep@steinbichler.de

Continued development and improvements to laser shearography measurement techniques have led to greatly improved performance and acceptance of this technique for primary aircraft structure nondestructive inspection and is now fully industrialised. With improvements in sensor portability and reduced sensitivity to environmental disturbances, especially ambient vibrations, it is now practical to use laser shearography with a stationary measurement set-up for quality control in production and NDI technique qualification, as well as for in-service-testing with a robust hand-transportable mobile measuring system suitable for use in hangars and remote locations for routine inspection of commercial aircraft structures. With developments in data acquisition, software tools for image processing as well as for test documentation it is now a total user-friendly system. By combining this technology with the experience from Steinbichler in the digitising business we can now map defects on 3D model created by fringe projections systems or laser triangulation scanners.

By combining the Steinbichler exclusive use of spatial phase shift technology with the Steinbichler GUI "ISIS" the technology has reached now the level of an simple, effective and fast measurement technology capable solving many existing problems in composite production, quality control and in-field inspection. Beside the very robust measurement the technology gives also full-field, non-destructive inspection capabilities including low-cost laser diodes, one-man operation, optimised weight and handling. Steinbichler is one of the only system suppliers offering an in-house software solution to exchange data from digitising, CAD or libraries.

Superimposing defects on a CAD data file or an actual 3D model is already realised and will help the operator to identify, categories and allocate defects on the test object.

The paper will discuss the development of hardware, software and handling features and will include results from practical measurements on composite aircraft structures, including commercial aircraft, and other structures.

MECHANICAL RESPONSE OF A FIBER BRAGG GRATING SENSOR IN A NON-UNIFORM STRESS FIELD

P. Casari, X. Chapeleau*, D. Leduc* , GéM Laboratoire de Génie Civil et Mécanique de Nantes – France
*LPIO Laboratoire de Physique des Isolants et d'Optronique, 2, rue de la Houssinière BP 92208 44322 Nantes Cedex 03 - France

A Fiber Bragg Grating sensor is a periodical modulation of refractive index along an optical fiber. The refractive index is specified by three parameters:
• The average value of the modulation of the induced refractive index,
• The ratio of reflected signal versus the transmitted one,
• The grating period along the fibre axis.

A measurement technique of these three parameters has been established and validated [1,2]. It consists in using low coherence reflectometry in order to measure the complex reflective coefficient. An inversion algorithm is then used to get back to the three above-mentioned parameters of the grating. Once these parameters have been identified along the grating, a corresponding evolution of the strain can be deduced. This technique is used for measuring some mechanical properties in composite materials which can not be measured by means of classical tests on coupons.

As a first step, a FBG sensor has been embedded in a resin coupon in order to assess its intrusive effect on the strain field normally existing in the material without sensor. The coupon is a parallelepipedal sample moulded in epoxy resin in which an optical fiber of optic has been inserted during manufacturing. Two sets of tests have been run:
• The first one was a tensile test on the coupon in order to validate the measurement technique without any stress concentration.
• The second one consisted in running the same tensile tests on the same coupon in which two holes have been drilled symmetrically beside the sensor (see Figure 1).

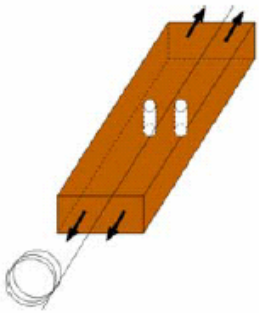

Figure 1: sketch of the tensile coupon equipped with an optical fiber

The measured reflective index for this second set of tests in shown in Figure 2.

From these results, strain along the grating can be deduced.

A Finite Element model has been prepared in order to predict the strain evolution along the grating. Thanks to the symmetries, a quarter of the sample is sufficient to model the full strain field. It shows that strains follow the same kind of evolution as the ones measured with the FBG sensor (Figure 3).

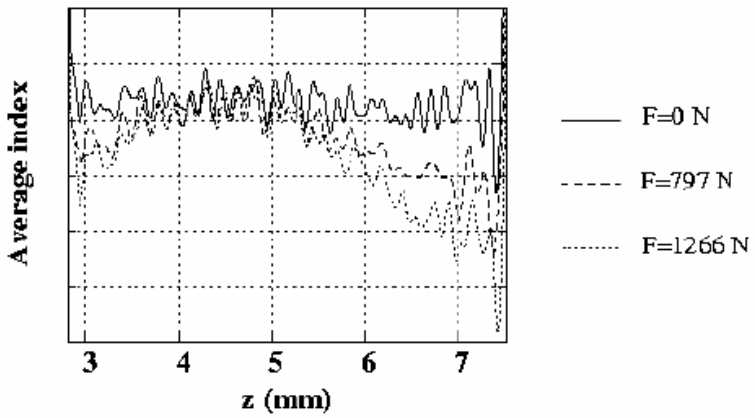

Figure 2: Refractive index measured along the grating for three load levels.

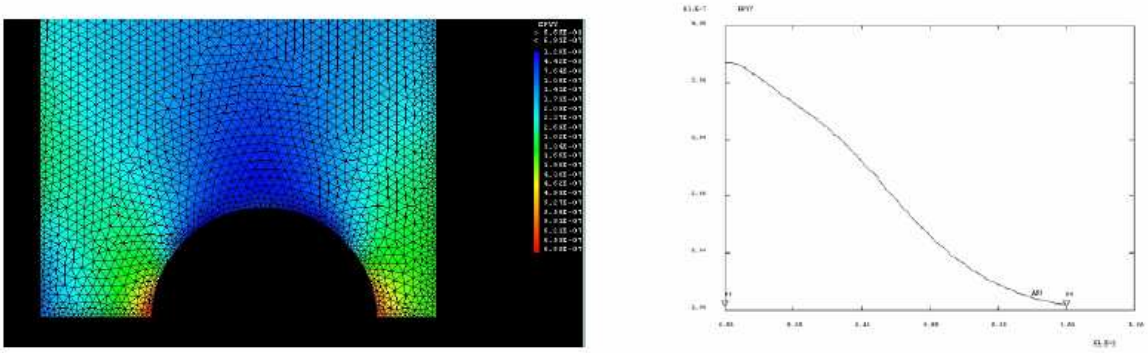

Figure 3: strain field in the vertical direction and strain evolution along the FBG direction

This strain field will be compared and explained in the final article to assess the intrusivity of the sensor. Some more tests should be available on composite laminates with FBG sensors placed through the thickness in order to characterize elastic properties as shear moduli or Poisson ratios.

REFERENCES

1 X. Chapeleau, D. Leduc, C. Lupi, R. Le Ny, M. Douay, P. Niay and C. Boisrobert, Experimental synthesis of fiber Bragg gratings using optical low coherence reflectometry, Applied Physics Letters, 82(24), pp. 4227-4229, 2003.

2 X. Chapeleau, D. Leduc, C. Lupi, R. Le Ny, M. Douay, P. Niay and C. Boisrobert, Mesure du profil d'indice de réseaux de Bragg, JNOG 2003, Valence (France), Nov. 2003.

EFFECT OF LOCAL CONSTRAINT ON MEASURED BEARING STRESS IN CARBON/EPOXY LAMINATE

R Ferguson
Composite Research, Airbus UK, Building 07C, Golf Course Lane, Filton, Bristol BS99 7AR

Over the last 25 years, the use of composite materials on Airbus aircraft has become steadily more widespread. Early uses such as fairings, spoilers and rudders for the A300/A310 have been steadily expanded and in-service applications for the A320 family, A330 and A340 now include primary structure such as the fin, horizontal tailplane, rear pressure bulkhead and keel beams.

One of the key material properties used in the design of composite structures is bearing strength. Various studies have looked at the significance of the relationship between measured bearing strength and local constraint, i.e. clamping due to bolt torque, but information across a range of constraint conditions for a typical aerospace carbon/epoxy material is not readily available. This paper describes work carried out at Airbus UK to quantify the influence of local constraint on failure load and mode for a typical high strength carbon fibre / toughened

epoxy material. The results will be used to support calculation of bearing strength allowables used in analysis of aircraft structure.

TESTING PROGRAMME

The philosophy of the test programme was to keep the material, layup, loading configuration, coupon geometry, operator, test rig and load frame constant so that the effects changing the local constraint could be evaluated. The material used was a typical aerospace grade unidirectional high strength carbon fibre / toughened epoxy prepreg tape, laid up to give a 4mm thick quasi-isotropic laminate. The specimen design and loading configuration was based on prEN6037, which uses a double lap shear loading arrangement with a single 6.35mm diameter steel fastener to apply bearing load to a 4mm thick composite coupon. The test matrix consisted of 6 coupons at each of the following local constraint conditions:

Pin bearing:	0.5mm gap each side of the composite coupon.
Pin bearing:	0.1mm gap each side of the composite coupon.
Clamped:	0.6Nm torque applied to the fastener.
Clamped:	1.3Nm torque applied to the fastener.
Clamped:	2.4Nm torque applied to the fastener.
Clamped:	3.5Nm torque applied to the fastener.
Clamped:	7.0Nm torque applied to the fastener.

All clamped specimens had a 12.7mm diameter washer positioned on each side of the composite coupon.

Specimens were loaded at 1mm/min using a standard load frame, with load and hole deformation data recorded for each coupon. Bearing Stress vs. Hole Deformation plots were constructed and the bearing strength calculated at various Hole Deformation values.

RESULTS

All coupons had a valid failure mode (i.e. failed in bearing or offset compression). Although the observed failure mode was consistent within each specimen configuration, the different local constraint conditions gave differences in the local failure surfaces, ranging from unconstrained local out-of-plane crushing/brooming at the loaded surface (bearing failure) for pin bearing coupons to unconstrained out-of-plane brooming at the circumference of the washer for torqued coupons (offset compression failure) for clamped coupons. Local bearing damage appeared to initiate at the end of the linear region of the Bearing Stress vs Bearing Strain curve, though all specimens continued to carry load (at various levels depending on the configuration) after damage initiation. A typical Bearing Stress vs Bearing Strain curve for each local constraint condition is shown in Fig 1.

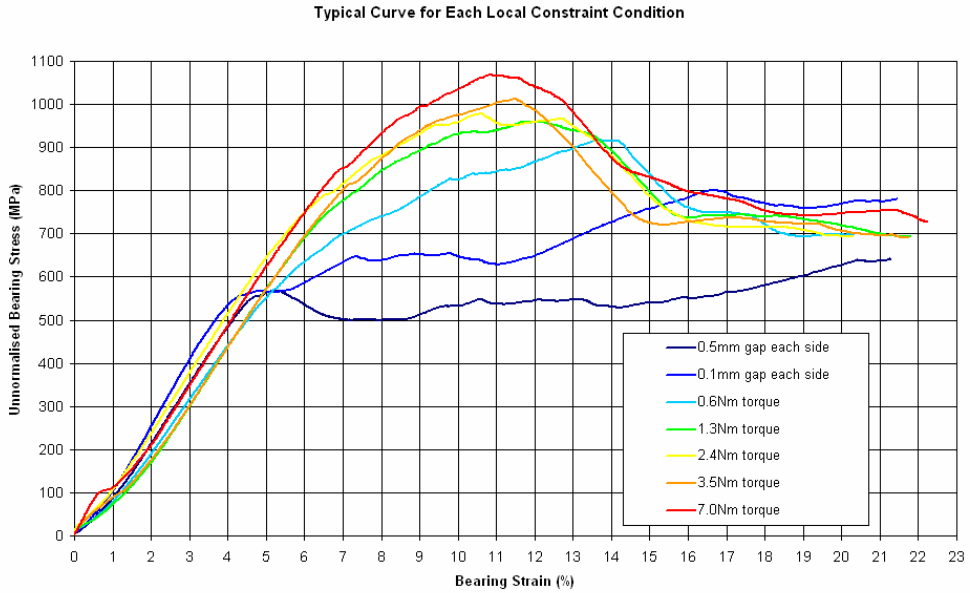

Taking the data for 0.1mm gap specimens (as per prEN6037) as a baseline, the following factors were calculated for Bearing Strength at 2% Hole Deformation and Bearing Strength at Peak Load:

Constraint	Bearing Strength	
	2% Hole Deformation	Peak Load
0.5mm gap	0.81	0.70
0.1mm gap	1.00	1.00
0.6Nm torque	1.33	1.12
1.3Nm torque	1.49	1.18
2.4Nm torque	1.52	1.17
3.5Nm torque	1.59	1.22
7.0Nm torque	1.72	1.28

CONCLUSIONS

The effect of local constraint on the measured bearing strength of a typical aerospace grade carbon/epoxy laminate has been determined. Failure strengths for constraint conditions ranging from 0.5mm gap each side to 7Nm applied torque have been measured, and the failure modes corresponding to these different levels of constraint have been identified.

For pin bearing specimens, increasing the gap each side of the specimen from 0.1mm to 0.5mm has a significant influence on the measured Bearing Strength and the failure mode. For clamped specimens, the level of applied torque has a significant influence on the measured Bearing Strength.

EXPERIMENTAL INVESTIGATION INTO THE USE OF PENETRANT ENHANCED X-RAY TECHNIQUES FOR THE EVALUATION OF FATIGUE DAMAGE AROUND AN OPEN-HOLE IN 4MM THICK CARBON FIBRE COMPOSITE PANELS

N.J. Rooney and T.M. Young
Composites Research Centre, Department of Mechanical and Aeronautical Engineering,
University of Limerick, Ireland

The use of X-rays has long since been established as a method of identifying damage in metallic aerospace structures. However the use of this technique to uncover defects in composites remains very much a trial-and-error process, due to a lack of substantive data and standardised procedures governing parameters such as film speeds, voltage and time settings, and type of penetrants used. Because of their relative transparency to X-rays carbon fibre composites require the use of low voltage X-rays to detect damage. Furthermore, an X-ray opaque penetrant is required to uncover flaws, cracks and delamination in the material.

Recent work [1] has focused on the use of this technique for the resolution of defects in impact-damaged areas where there is a clear indication of surface breaking defects for the penetrant to infiltrate. Where the damage present is not as immediately apparent, it is questionable as to whether Penetrant-Enhanced-Radiography-Techniques (PEXR) is capable of resolving the defects, such as is the case around open-hole type situations. Traditionally ultrasonic methods have been used to good effect to evaluate the effect of low-level damage around fastener holes and other such stress raisers: fatigue induced damage is typically hard to resolve, and the use of ultrasonic testing can prove time consuming, while being quite accurate in the detection of such damage as matrix cracking and delamination, which are generally indicated by the reduction or elimination of a back wall signal from the material.

To date, studies [2] have focused on the assessment of fatigue damage using PEXR in relatively thin sections (<2mm) using inorganic penetrants. Inorganic penetrants suffer from the drawback that they remain in the damaged area after the inspection has taken place, whereas organic penetrants, such as iodomethane, evaporate without causing any recognisable damage to the fibres or matrix. In the current study iodomethane 99% was used as the penetrant since it has been found to evaporate out of the material within 5 hours of its first application. Using a large number of different damage scenarios ranging from minute intra-ply damage to large delaminations a complete analysis of the usefulness of this chemical for the detection of defects in thicker laminates was carried out.

The study carried investigated the effects of three different load levels on the progression of damage in ~ 4mm thick open-hole tension-tension fatigue specimens. The lay-up considered was a carbon/epoxy 32 ply quasi-isotropic laminate of dimensions 300mmx 36mm, with a centrally located 6mm diameter hole, which was based on ASTM D5766[3]. Upon the establishment of static, tensile ultimate load values, three different load levels (i.e. 70%, 80% and 90% of this value) were utilised at a stress ratio of R = 0.1. Six specimens were tested at each load level and the progression of damage was monitored up to 1 million cycles, at which point the tests were terminated in order to observe the effect of this loading on the residual strength and stiffness of the material. Both Ultrasonic and PEXR techniques were used to inspect the area of interest around the open hole. Initially damage was monitored up to 100,000 cycles in order to look at the early damage mechanisms (e.g. fibre breakage, matrix cracking, delamination) that were in action. Further non-destructive evaluation of the damage took place up to the limit of 1 million cycles. Another set of specimens were stopped at six different stages during the testing to investigate, with the aid of optical microscopy, the exact damage that was present at the different load levels (Fig. 1).

The evolution of matrix and fibre damage can clearly be seen to extend outwards from the open hole in a pattern that confirms the relative attributes of both PEXR and ultrasonic techniques for the resolution of small defects near a free edge, such as that around an open hole. In some cases the damage extended outwards from the hole to reach the free edge of the sample, where microscopy was used to assess the type of damage.

Before PEXR could be used to detect the damage close to the holed region a series of tests with three different types of radiographic film — of varying speeds — was carried out to determine the effects of: (1) tube voltage on final film density; and (2) exposure times on the film contrast. It was concluded that slower films, such as Agfa D2, are impractical due to the long exposure times and apparent sensitivity to small voltage variances. Faster films such as Agfa D4 and D7 proved more successful; clear agreement with the damage found in the UT volume scans and hole region microscopy images was obtained using exposure times of less than 5 minutes (Fig.2).

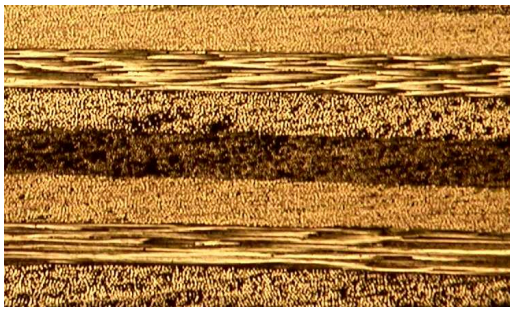

Fig. 1: Optical micrograph of undamaged surface in hole region after sectioning

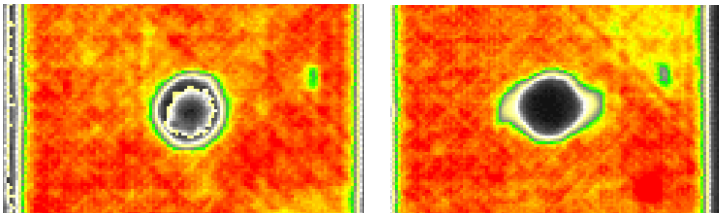

(a) **(b)**

Fig. 2: UT C-scans show early fatigue induced damage progression from non-damaged state(a) to damage present after $5x10^5$ cycles at 70% UTS load level using UT method.

REFERENCES

[1] E. A. Birt. The applicability of X-radiography to the inspection of composites. *Insight Magazine*, Vol. 42, No. 3, March 2000.
[2] F. Aymerich and M. S. Found. Response of notched carbon/PEEK and carbon/epoxy laminates subjected to tension fatigue loading. *Fatigue and Fracture of Engineering Materials and Structures.* Vol. 23, Iss. 8, Aug 2000, pp. 675–683.
[3] American Society for testing and Materials, ASTM D 5766: Standard Test Method for Open Hole Tensile Strength of Polymer Matrix Composite Laminates, Book of Standards, Vol. 15.03.

IDENTIFICATION OF THE ELASTIC CONSTANTS OF COMPOSITE MATERIALS USING DEFLECTOMETRY

S. Avril[a], M. Grédiac[b], F. Pierron[a], Y. Surrel[c] and E. Toussaint[b]
[a] : LMPF, École Nationale Supérieure d'Arts et Métiers, rue Saint Dominique BP 508, 51006 Châlons-en-Champagne, France, stephane.avril@chalons.ensam.fr, fabrice.pierron@chalons.ensam.fr
[b] : LERMES, Université Blaise Pascal Clermont II, 24, avenue des Landais, BP 206, 63174 AUBIERE Cedex, France, grediac@lermes.univ-bpclermont.fr, toussaint@lermes.univ-bpclermont.fr
[c] : CNRS-LM3 École Nationale Supérieure d'Arts et Métiers, 151, boulevard de l'Hôpital, Paris, France, surrel@cnam.fr

In this work, the problem of determining the flexural stiffnesses of composite plates is addressed. A brief review of literature shows that modal analyses are commonly used for tackling this problem [1]. However, modal analyses have to face several difficulties: experimental boundary conditions must be modeled faithfully, the solution is found iteratively and modal analyses are limited to linear elastic constitutive equations.

An alternative to modal analyses can be the use of full-field optical methods for investigating the response of thin plates under static flexural loading. Indeed, full-field data provided by optical methods can be processed through the Virtual Fields Method [2, 3], which allows the identification of several material parameters from a single heterogeneous mechanical test. The method is direct, that is, it does not require numerical modeling and iterative computations. A precise knowledge of the boundary conditions is not required either. Thus, it appears as a promising alternative to modal analyses for flexural stiffness identification.

For validating this procedure, tests have been carried out on a PMMA plate and on a glass-epoxy plate. It is supported horizontally by three supports located at three corners of a square plate (Fig. 1). A load is hanged up to the center of the plate, causing heterogeneous curvature fields.

Curvature fields (Fig. 1) are measured thanks to an original optical method based on deflectometry. It is a white-light non-interferometric method, easy to implement and well suited for the investigation of flexural tests on plates. The plate surface must allow some amount of specular reflection. A pattern of crossed straight lines is observed by reflection at the surface of the reflective plate. Curvatures induce a deformation of the pattern, according to the principle of deforming mirrors. The spatial phase shifting method is used to detect with a high accuracy the apparent displacement of the grid lines, proportional to local slopes. Thus, slope fields over the whole area of the specimen are obtained with a resolution of 7.5 µrad. Curvature fields are derived from slopes by numerical differentiation. They are obtained with a resolution of 1 km^{-1}.Curvature fields are then processed through the Virtual Fields Method, providing the unknown stiffnesses of the tested plate. The values obtained for glass-epoxy are: E_{xx}=36.1 GPa, E_{yy}=9.26 GPa, ν_{xy}=0.43 GPa and G_{xy}=4.01 GPa. These values are consistent with the reference properties of glass-epoxy identified with standard tests. This is quite promising for future applications of the procedure.

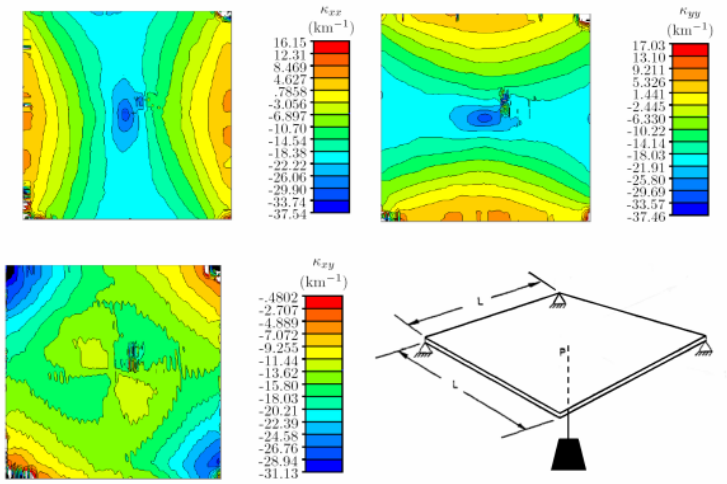

Fig. 1. Curvature fields measured over the whole area of a PMMA plate and scheme of the mechanical test carried out for causing those curvature fields.

BIBLIOGRAPHY

[1] S.-F HUANG AND C.-S. CHANG. « Determination of elastic constants of materials by vibration testing », *Composite Structures*, **49**, 185-190, 2001.

[2] M. GRÉDIAC. « Principe des travaux virtuels et identification/Principle of virtual works and identification », *C. R. de l'Académie des Sciences*, **II-309**, 1-5, 1989.

[3] M. GRÉDIAC. « The use of heterogeneous strain fields for the characterization of composite materials », *Composites Science and Technology*, **56**, 841-846, 1996.

IDENTIFICATION OF ELASTIC PROPERTIES OF A CERAMIC-BASED JOINT USING KINEMATIC FIELDS DETERMINED BY DIGITAL IMAGE CORRELATION

Matthieu Puyo-Paina, Francois Hildb and Jacques Lamona
a LCTS, UMR 5801 CNRS / Snecma / CEA / Universite Bordeaux 1
b LMT-Cachan, ENS Cachan / UMR 8535 CNRS / Universite Paris 6

1 INTRODUCTION

Joining of materials is a well-known and widely used technique to make structures from simple elements. In the typical case of ceramics and ceramic matrix composites (CMC) that operate under severe conditions of temperature and environment, ceramic-based adhesives, called BraSiC [3], are required. Data on the mechanical behavior and properties of joints are a prerequisite to the design of reliable parts [5]. Determination of joint properties is generally difficult because of the small size of the joints (around 100 μm in the present paper) and because test specimens of the bulk BraSiC material are not available. This paper aims at first evaluating the digital image correlation technique for joint behavior investigations. Then the elastic constants (Young's modulus and Poisson's ratio) of the joint were determined using 4-point bend, tensile and o_-axis compressive tests on SiC/joint/SiC samples. Testing materials are made of two SiC parts joined using a silicon-based braze (BraSiC). An optical microscope was mounted on the testing machine and coupled with a 12-bit digital camera. At various load levels, a numerical image is shot and a correlation algorithm was used to extract the local displacement and strain fields. The joint is examined at various scales: 1 pixel = 1.66 μm and 1 pixel = 0.33 μm. At these scales, quality of images is of primary importance since strains do not exceed 10^{-3} in ceramic [4].

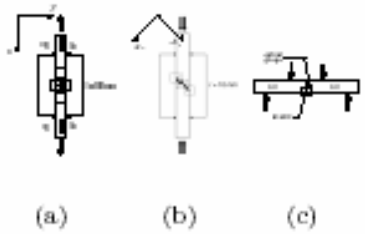

Figure 1. Testing configurations

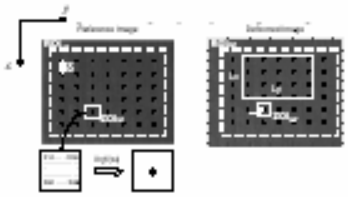

Figure 2. Schematic diagram of the DIC method

2 DIGITAL IMAGE CORRELATION TECHNIQUE

The digital image correlation method is based on the construction of a mesh from a digital image of the surface of materials [1]. Construction of the mesh depends on the distribution of gray levels. In the present case, the distribution is given by the natural texture of the material microstructure, which must display a random pattern so that groups of pixels can be matched at different load levels. Displacements and strains are then evaluated from the locations of these groups of pixels referred to as Zone of Interest shifted by δ pixels (ZOI within a larger area that was selected for the analysis referred to as Region of Interest (ROI) [2] see Figure 2). In Figure 2, xij represents the gray level data associated to each pixel within a ZOI, *N* is the number of pixels and X is the center of gravity of the ZOI. Successive locations of X gives the displacements. Strains are then calculated on a Lx × Ly pixel gauge.

Several experiments were designed to evaluate the resolution and accuracy of the system. Images from the surface of the materials are numerically shifted by a constant vector *U*. The DIC system response, and the prescribed displacement are compared. The displacement resolution by the DIC system is here equal to 10^{-2} pixel associated with a standard deviation of 20%. Furthermore, successive images are taken on a specimen that was subjected to a constant load, to determine the minimum strain error at each scale of magnification for

different gauge sizes. The minimum strain that can be measured at a magnification of 1 pixel = 0,33 μm is 7.8 × 10-5 in tension for a gauge length of 128 pixels.

3 EXTRACTION OF DATA AND RESULTS

In the case of tensile tests, elastic properties of BraSiC joint are derived from the comparison of the analytical and experimentally measured strain fields. Equation 1 relates the Young's modulus E_i and strain $\varepsilon_{xx,i}$ where F is the applied load and S the cross sectional area.

$$E_i = \frac{1}{S\frac{\epsilon_{xx,i}}{F}} \tag{1}$$

The subscript i refers to the BraSiC joint or to the SiC substrate. This expression of E_i in terms of $k_{xx} = \frac{\varepsilon_{xx,i}}{F}$ is very convenient. Consequently, k_{xx} is determined from $\varepsilon_{xx,j}$ (Fj) data linear regression. The accuracy on this coefficient can be expected to be quite good with a wide sample of data. The Poisson's ratio is given by $\nu = \frac{-\varepsilon_{yy}}{\varepsilon_{xx}}$.

For 45° off-axis compression test, strain components in the local co-ordinate axes are given by Equation 2.

$$\begin{cases} \epsilon_{x'x'} &= \frac{1-\nu_i}{E_i}\frac{\sigma}{2} \\ \epsilon_{y'y'} &= \frac{1-\nu_i}{E_i}\frac{\sigma}{2} \\ \epsilon_{x'y'} &= \frac{1+\nu_i}{E_i}\frac{\sigma}{2} \end{cases} \tag{2}$$

The Young's modulus of the joint can be extracted from the analysis of $\epsilon_{y'y'} + \epsilon x'y' = \frac{F}{SE}$.

The Poisson's ratio is derived from $\frac{\epsilon_{y'y'}}{\epsilon x'x'}$ since $\nu = \frac{\epsilon x'y' - \epsilon_{y'y'}}{\epsilon x'y' + \epsilon_{y'y'}}$.

In 4-point bending tests, the description of stress and strain states in the joint is not straightforward. Finite element computations were used to estimate the displacement in an area identical to the experimental ROI. Elastic properties of the joint were then derived from the minimization of J (see Figure 3).

$$J = \sum_F \sum_{(\overline{x},\overline{y})} \left[\bar{\mathbf{U}}_{\exp}(\overline{x},\overline{y}) - \bar{\mathbf{U}}_{\mathrm{EF}}(\overline{x},\overline{y}, \frac{E_{\mathrm{joint}}}{E_{\mathrm{SiC}}}, \nu_{\mathrm{joint}}, \nu_{\mathrm{SiC}}) \right]^2 \tag{3}$$

The results are summarized by Figure 4.

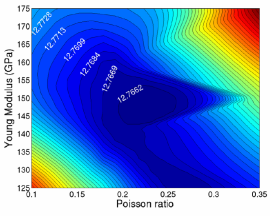

Figure 3: Norm of $\mathcal{J}$ as a function of the unknown elastic properties of the joint

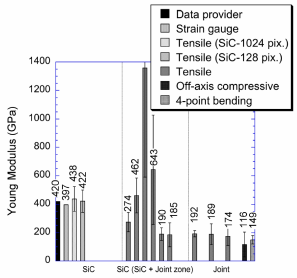

Figure 4: Evaluations of the Young's modulus by using different tests

4 SUMMARY

A direct and an inverse analysis of the determination of elastic constants in a ceramic joint have both been set up. It was based on a digital image correlation technique. It was applied to SiC/BraSiC/SiC test specimens subject to tensile, o_-axis compressive and 4-point bending loading conditions. It allowed strain and displacement fields to be measured and elastic properties to be estimated. The SiC elastic modulus estimates were found to be similar to values available or measured using an extensometer or strain gauges (see Figure 4). The BraSiC elastic properties were estimated to be E_{joint} = 164 GPa and ν_{joint} = 0.23 for the 4 point bending configuration. However a certain scatter between Poisson's ratio values in tensile and o_-axis compressive tests were obtained and further analysis is under way.

The digital image correlation technique is a powerful method for measuring displacement and strain fields. This is well suited for specimens such that joints even for low strain levels ($< 10^{-4}$).

REFERENCES

[1] F. Hild. CorreliLMT : A software for displacement field measurements by digital image correlation. Internal Report 254, LMT-Cachan, January 2002.
[2] F. Hild, B. Raka, M. Baudequin, S. Roux, and F. Cantelaube. Multiscale displacement field measurements of compressed mineral-wool samples by digital image correlation. Applied Optics, 41(2):6815–6827, 2002.
[3] F. Moret, P. Sire, and A. Gasse. Brazing of sic based materials using the brasic process chemical and thermal applications. In International Conference on Joining of Advanced Materials, Rosemont (USA), October 1998. ASM Materials Solutions.
[4] M. Puyo-Pain and J. Lamon. Determination of elastic properties of a ceramic-based joint using a digital image correlation method. In Ceramic Engineering and Science Proceedings, volume In press,
Cocoa Beach (USA), January 2004. The American Ceramic Society.
[5] M. Singh and E. Lara-Curzio. Design, fabrication, and testing of ceramic joints for high temperature SiC/SiC composites. Journal of Engineering for Gas Turbines and Power, 123:288–292, April 2001.

NON-DESTRUCTIVE EVALUATION OF PROSTHETIC CARBON FIBER FEET

Rúnar Unnþórsson
Engineering Department of University of Iceland, Hjarðarhaga 2-6, 107 Reykjavík, Iceland.
Tel:+354 525 5882, Email: runson@hi.is.

Engineered materials are derived by combining reinforcement individual materials with the intent of achieving properties over the ingredients. Carbon reinforced composites contain carbon fibers as reinforcement supported by binder, i.e. matrix. Carbon reinforced composites are used extensively in products that require; superior strength, flexibility, and quality. These requirements, and the fact that such products are generally expensive, necessitate good fault detection procedures. In this project a literature study of methods for fault detection of carbon-fiber composites, will be presented. The project is collaboration between the Mechanical and Industrial Engineering Department, University of Iceland and Össur hf, a leading innovator and manufacturer of prosthetics devices. This study is a part of a larger project which goal is to design a fault detection method for the evaluation of Össur's Flex-foot product line.

In order to stay ahead of the competition, Össur hf. must invest in research and development. The aim with such research is mainly to create or improve manufacturing processes that will cut down production costs, develop new products, or improve existing ones. Improvements may include better reliability and performance. When the design of prosthetic carbon fiber feet is being optimized, prototype models are built, evaluated, and improved to meet the design criteria. This results in a series of evaluations, one of which is endurance test which this discussion is limited to. The fatique test is performed, according to the ISO 10328 specifications, in a test system at Össur's testing facilities. One foot at time is placed in the system, and actuators are used to flex the foot for 2.000.000 cycles. During each evaluation, which takes about 23 days to complete at 1Hz, the deflection is monitored. At the end of the evaluation period a visual test is performed, on those feet that haven't failed, to see if flaws can be detected. For production testing, due to the long evaluation time, only few samples undergo this endurance evaluation. Therefore, by shortening the required time, products can be; designed and developed in less time and at a lower cost than previously possible. Shorter evaluation time means that larger number of samples at the production line can be tested resulting in an improved quality assurance for customers. The study

will cover evaluation methods for fiber composites which include; X-ray, thermography, laser shearography, eddy current, infrared and ultraviolet, ultrasonic and acoustic systems. Acoustic Emission (AE) is very well suited to detect the progression of flaws in composite material. AE-analysis measurements are recorded using piezoelectric receivers which are placed on the surface of the foot.

For speeding up the evaluation process, ultrasound sensors can be placed on the feet during testing. The sensors are used to monitor the high-frequency sound waves generated in the material. These high frequency sound waves can be used to detect flaws much earlier than possible by visual inspection. This is based upon the idea that degradation occurs before failure, and incipient faults change the properties of the sound waves. The evolving flaws that the sound waves can help identify are; matrix cracking, fiber matrix de-bonding, delamination, air/porosity, and fiber breakage.

In order to be able to detect flaws, the monitoring system must know how to distinguish them from normal conditions, i.e. a flawless specimen. However, for detection, it is not practical to compare the measured signal from one flawless leg against other legs to be classified. This is mainly because the properties of the signal measured for each leg differs, due to variations in; the production process, the placement of each leg in the test system, and the placement of the sensors on the leg. It is therefore intuitive to use only measurements obtained from each individual leg to classify it. By doing so the classification task becomes a one-class classification problem . One-class classification problems differ from conventional classification problems in the way how the classifier is trained. It is trained by using only the normalities, and never sees flaws. By using only normalities the classifier must; estimate the boundary that separates the two classes, and minimize misclassifications.

This means that the classifier must start fresh with each new leg placed in the test system and learn the distribution of normalities. The measured signal at the start of the evaluation period can be assumed to represent the class of normalities. If a foot starts to degrade, during the endurance evaluation, the signal's characteristics change and the classifier must classify the foot as faulty.

In this study, we will take a look at different types of classifiers that are suitable for one-class classification problems. Examples of such classifiers are; rule based classifiers, nearest-neighbor classifiers, Bayes classifiers and Neural Networks. Many types of neural networks exist such as; Multi Layer Perceptron, Radial Basis Function (RBF), Self Organizing Map (SOM), Support Vector Machines (SVM) and Principal Component Analysis (PCA). Sometimes some of these classifiers are used together. One of the most popular classifier has been the MLP trained with backpropagation however, in the recent years kernel based classifiers, such as the SVM, have been used to match or even improve earlier results obtained by MLP classifiers.

MULTI-INSTRUMENTED TECHNOLOGICAL DEMONSTRATOR: A MULTISCALE STUDY OF COMPOSITE STRUCTURES

M. Mulle*/**, F. Collombet*, B. Trarieux*, J.-N. Périé*, Y-H Grunevald**
*LGMT, PRO^{2}COM team - IUT Paul Sabatier -31077 Toulouse Cedex 4- France
email: firstname.surname@ iut-tlse3.fr
**D.D.L. Consultants, Pas de Pouyen, 83330 Le Beausset- France

Composite materials have the great advantage to allow the embedment of instrumentation. Optical fibre Bragg gratings (FBG) appear to have a promising potential in way of contributing to an optimal health monitoring of composites over all the life cycle: starting from the manufacturing stage up to the mechanical behaviour during life service. The efficiency of such monitoring, regarding performances and cost reduction, can be made possible by optimising the number and placement of the embedded sensors. An instrumentation strategy concerning technological demonstrators is in hand within the framework of the AMERICO research program (Analyses Multi-Echelles : Recherches Innovantes pour les COmposites) and the collaboration of DDL Consultants Company [Grunevald, 03]. It is a question of defining a methodology that enables to specify the state of an industrial structure, taking into account the various aspects such as the processes influence (cure shrinkage, residual stresses), [Kang, 01], design singularities, real boundary conditions.

Figure 1: a) lay up and FBG instrumentation; b) demonstrator after the autoclave curing process; c) demonstrator waterjet cut.

Our technological demonstrator integrates several conceptual choices, which are representatives of aeronautical structures (drop off, holes, important thickness and over all dimensions, cf. Figure 1c). It is manufactured using HexPly® pre-preg UD M21 / 35% / 268 / T700 GC (carbon fibre / epoxy resin, specific lay-up, autoclave cure, cf. Figure 1b). The FBG's optical sensors are embedded between the plies during the lay-up operation. They have the advantage of not being much intrusive (compared to the over all structure dimension, cf. Figure 1a), to resist at high temperature (autoclave cure), not to require any recalibration, and of being electromagnetic field proof [Esquer, 02]. Surface metrologies are used such as digital image correlation or conventional strain gauges in order to be confronted to embedded optical measurements [Mulle, 04)]. The complementarity of the gathered experimental allows fine and interesting comparisons between tests and calculations.

Our approach consists in identifying behaviour relations between the different scales, while considering more particularly the part played by the structural scale: meso to structure (RB), macro to structure (displacement field measurements), and processes to structure (material properties in the structure depend on the manufacturing process). Two specific zones are studied: one in the reinforced part and another in the ply growth.

Figure 2: three point bending test with an INSTRON machine; strain measurement systems: HAMAMATSU C4742-95 numerical cameras for image stereo correlation (VIC2D®/VIC3D® software), si 425 MICRO N OPTICS wave length analyser, VYSHAY 2100 gauge unit.

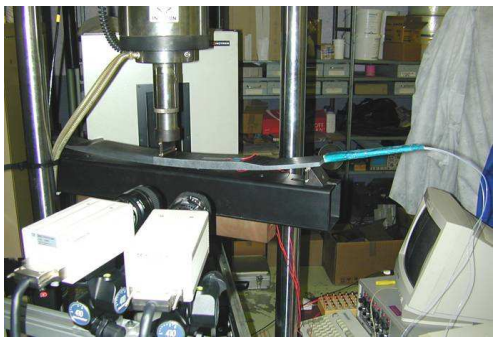

The presented methodology leans at the same time on an experimental phase and a numerical modelling analysis. The technological demonstrator is modelled with volumic elements of degree 1 (17100 elements) using SAMCEF software (cf. figure 3). The numerical definition takes into account the real lay-up of each zone and boundary conditions in order to simulate a three point bending test (two linear supports and fixed nodes).

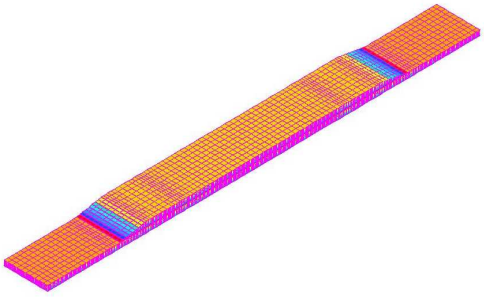

Figure 3: FEM model of the technological demonstrator

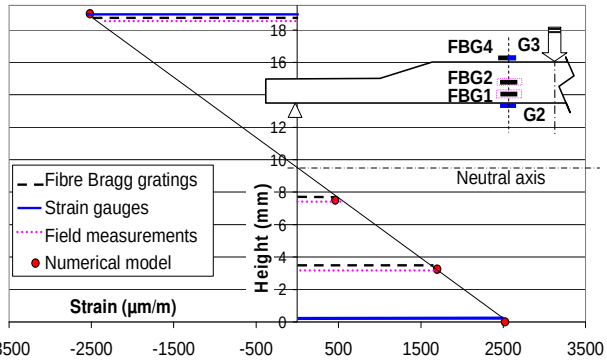

Figure 4: strain measured with 4 metrologies on the same cross section – loading of 8000 N on a 3 pt bending test.

The results presented on figure 4 relate to the reinforced zone of the technological demonstrator. All in all, they show a very satisfactory correlation between calculation and experimental measurements. In detail, we will discuss the influence of the parameters variability such as thicknesses, real ply distributions or material properties within the structure.

REFERENCES

[Grunevald, 03]; Y.-H. Grunevald, F. Collombet, M. Mulle, P. Ferdinand; *Global approach and multi-scale instrumentation of composite structures in the field of transportation*; proceedings of 8th Japan Int. SAMPE, Tokyo (Japan); Nov. 2003.
[Mulle, 04]; M. Mulle, J.-N. Périé, F. Collombet, L. Robert, Y.-H. Grunevald; *Mesures de champs sur éprouvette technologique instrumentée par réseaux de Bragg : comparaison et validation de métrologies*; Photoméca Colloquium Albi (France) (accepted for oral presentation); 2004.
[Kang, 01]; Kang et al; *Monitoring of fabrication strain and Temperature during composite cure using fiber optic sensor*; SPIE Vol 4336; 2001.
[Esquer, 02]; P.M Esquer, Lence F.R., Menendez J.M.; *Fibre optic sensor in AIBUS Espana*; Structural Health Monitoring, Paris (France); July 2002.

Acknowledgements
The authors make a point of thanking Laurent Robert from the EMAC (CROMeP) for his contribution to the displacement field measurements, the DGA/STTC for its financial support through the AMERICO research program supervised by ONERA, and also HEXCEL Composites Company for the provision of HexPly® pre-preg necessary to this study.

GENERATION OF DESIGN ALLOWABLES FOR COMPOSITE MATERIALS AT AIRBUS UK

S J Hallett
Composite Stress Engineering, Airbus UK, New Filton House, Filton, Bristol, BS99 7AR, UK

INTRODUCTION

Over the last 25 years, the use of composite materials on Airbus aircraft has become steadily more widespread. Early uses such as fairings, spoilers and rudders for the A300/A310 have been steadily expanded and in-service applications for the A320 family, A330 and A340 now include primary structures such as the fin, horizontal tail plane, rear pressure bulkhead and keel beams.

An important but often overlooked process is the derivation of design allowable values from raw test data. This process must provide data for design that satisfies regulatory requirements whilst giving the designer the best value available.

This paper describes in outline this process as used by Airbus UK, using a specific allowable, bearing strength, as an example.

REQUIREMENTS REGULATORY

In order for an aircraft to gain its Certificate of Airworthiness, the manufacturer must demonstrate that the relevant Airworthiness Requirements are met. For design allowables, the key requirement is JAR 25.613 *Material Strength Properties And Design Values*, which specifies the level of statistical confidence required for any design allowable value used, as well as stating that all design allowable values must take into account the effects of temperature and environment.

TEST MATRIX

Before a material can be accepted for use on aircraft structure, it must be qualified against the relevant material specification issued by Airbus UK. The material specification includes the types of test that must be carried out, laminate configurations, test methods, environmental conditions and the number of coupons required. Table 1 provides an example of a typical test matrix for bearing strength testing; each square of the matrix specifies the number of batches to be tested at a particular combination of layup and environment. In this example each batch contains 6 specimens giving a total of 150 test coupons.

Laminate Construction (%age 0° fibres / %age ±45° fibres / %age 90° fibres)	Number of Batches to be Tested (six specimens per batch)				
	Dry		Wet (Conditioned at 70°C / 85% RH)		
	-55°C	RT	120°C	70°C	90°C
25 / 50 / 25 (Quasi-isotropic)	-	5	1	1	5
40 / 40 / 20	1	5	1	1	5

Table 2: Extract from material specification test matrix for bearing strength properties

STATISTICAL REDUCTION

Once all the tests have been completed, data processing and statistical reduction are carried out on the results. This takes place in several stages, the first of which is to normalise the results to a nominal cured ply thickness if appropriate. The statistical mean and coefficient of variation for each batch of specimens is then calculated and, where multiple batches have been tested for a single condition, a statistical test is carried out to check that the all batches are from the same population. Further statistical calculations are then performed to establish the confidence limits specified in the regulatory requirements. The method used by Airbus UK for this process is based on that defined in US Department of Defense Military Handbook 17 (MIL-HDBK-17).

For the bearing example, a mean value and a reduced value including the calculated confidence limit are then calculated for each combination of layup, temperature and condition.

ENGINEERING JUDGEMENT

Once the mean and reduced values have been established for each square in the test matrix, carpet plots and temperature/condition envelopes can be created for each material property. The values for each material property are assessed using engineering judgement and, where appropriate, modified to provide a coherent dataset for use in structural analysis. For the bearing example, the maximum operating temperature of the structure might be determined and a single design allowable defined for use at any temperature below this, giving one design allowable value for each layup (if the values for each layup are similar, a single design allowable value might be provided for use at all layups within a specified envelope).

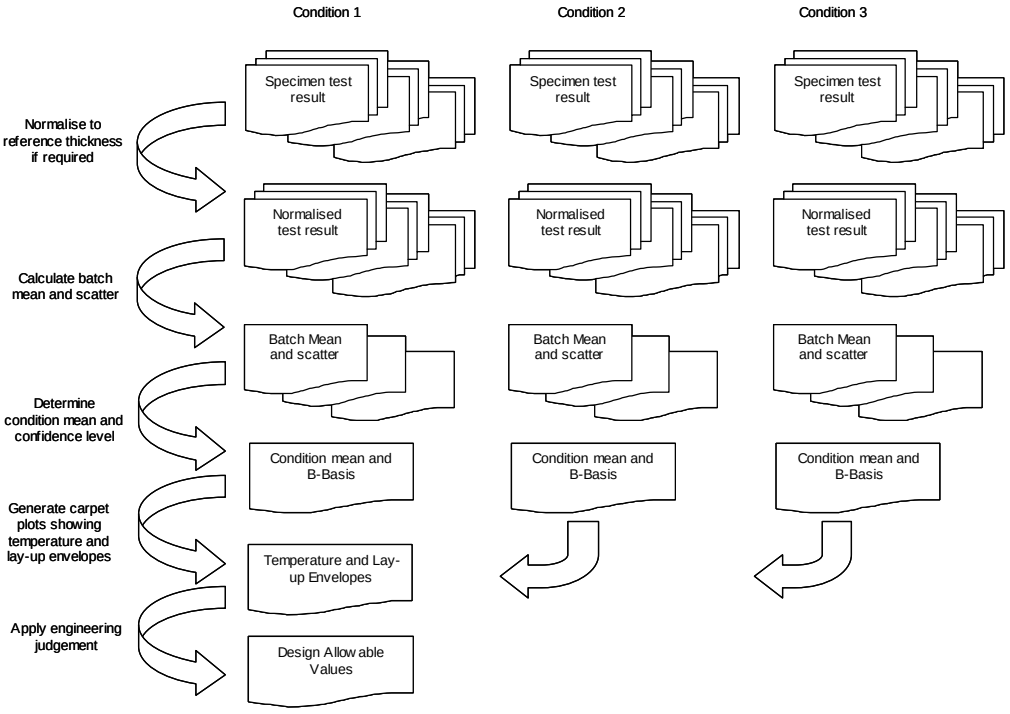

Figure 1: Summary of AUK process to generate a design allowable from test results

Once a design allowable is established it may, of course, be subject to further modification within different analysis methods and tools. For example, the bearing strength allowable may be factored to allow for use with countersink fasteners or single lap joints. Figure 1 summarises the information flow from individual test results to structural analysis design value.

STRAIN MONITORING OF SMART CONCRETE CYLINDERS WITH OVERWRAP COMPOSITE MATERIALS USING FIBRE OPTIC SENSORS

J. S. Leng [a] D. Winter [b] R. A. Barnes [b] G. C. Mays [b] and G. F. Fernando [b]
[a] P.O. Box 2147, Centre for Composite Materials, Harbin Institute of Technology, Harbin, 150001, P.R.China
[b] Engineering System Department, Defence Academy of the United Kingdom, Cranfield University, Shrivenham, Wiltshire, SN6 8LA, UK
E-mail: lengjinsong@yahoo.com

Structural health monitoring (SHM) in-service is very important and definitely demanded for safely working of engineering structure such as composite and concrete structures. It is very difficult to carry out by using conventional methods. A unique opportunity is provided to real-time monitor the health status by using embedded fibre optic sensors (FOSs). In this paper, fibre optic sensors including Extrinsic Fabry–Perot Interferometer (EFPI), Fiber Bragg Grating (FBG) sensors are employed to monitor the static and dynamic strain of the composite wrapped concrete structures. The static compression tests of concrete cylinders with overwrap composite materials embedded EFPI and FBG sensors have been performed, as shown in Figure 2. The dynamic strain measurements also have been achieved as shown in Figure 3. The results indicate that the fibre optic sensors given a very good strain accordance in both of vertical and hoop direction to comparing with the results of related reference electrical resistance strain (ERS) gauges on the surface of the concrete structures. It is also note that dynamic measurement capability of fibre optic sensor is proved in this paper.

Figure 1 Compression test of GRP composite wrapped concrete cylinder with embedded EFPI and FBG sensors

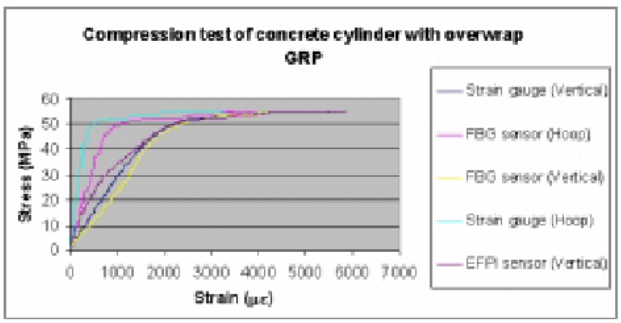

Figure 2 Static compression results of concrete cylinder with overwrap GRP composites uisng fibre optic sensor and electrical resistance strain gauges

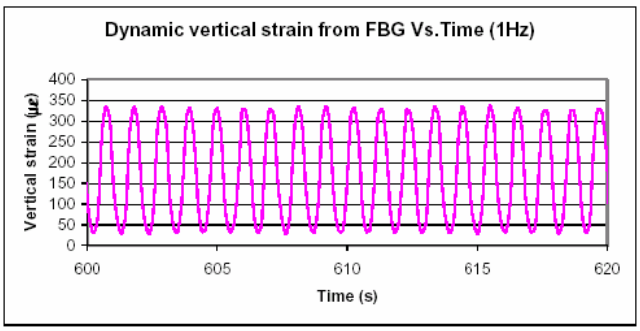

Figure 3 Dynamic measurement results using FBG sensor

INVESTIGATION OF PARAMETERS DICTATING DAMAGE CHARACTERISTICS IN COMPOSITE HONEYCOMB SANDWICH PANELS

G. Zhou[1], M. Hill[1] and N. Hookham[2]
[1] Department of Aeronautical and Automotive Engineering, Loughborough University, Loughborough, Leicestershire, LE11 3TU, UK
[2] Hexcel Composites, Duxford, Cambridge CB2 4QD, UK

Composite sandwich structures have been widely used in the aerospace and automotive industries due to their high specific bending stiffness. In recent years, they have increasingly been expected to be damage-tolerant and energy-absorbing. This has highlighted the need for a better understanding of the mechanical behaviour of such structures with particular interest in damage initiation and propagation. In particular, analytical engineering models need to be developed so that such structural performance under various loading conditions could be predicted to facilitate preliminary composite sandwich structure design.

Various composite-skinned honeycomb sandwich panels have been studied with both T700/LTM45-EL and IM7/8552 carbon/epoxy skins and each with aluminium and nomex honeycomb cores. For each given sandwich material system, three different skin thicknesses were used all with a cross ply lay-up along with two different core densities of a constant thickness. These panels were tested under both quasi-static and impact loadings, each involving two different indenter nose shapes. They were either tested to ultimate failure or terminated early so that the corresponding specimens were used for a diagnostic purpose. In addition, respective composite skin plates and honeycomb cores were also tested. The effects of varying these parameters on induced damage mechanisms were examined through load-displacement, load-LVDT and load-strain curves as well as a cross-sectioning of selected specimens.

A typical example of a load-displacement curve from a panel with 16-ply skins and 70-kg/m^3 aluminium honeycomb core is shown in Fig. 1. A three-stage deformation process is clearly characterised by initial and secondary critical loads and ultimate failure load. There was significant slope loss beyond the initial damage. Three damage mechanisms that were identified to dominate the deformation process were core crushing, delamination and fibre fracture or shear-out of the loaded compressive skins, as an example shows in Fig. 2. As the initial critical loads were less than 30% of respective ultimate loads, the permanent deformation between the two loads clearly offered the maximum amount of energy absorption. It was also interesting to note that the tensile skin remained intact after the ultimate compressive skin failure and the skin-core interfaces did not suffer from debonding before the skin fracture, indicating a good quality of the manufacturing processes.

The nose shape of the indenters was found to have an overriding effect on the damage mechanisms in the sandwich panels. The panels loaded by a hemispherical indenter exhibited the initial damage through a simultaneous occurrence of core crushing and the onset of delamination in the compressive skin, continued core crushing and delamination propagation and the ultimate failure due to fibre fracture of the compressive skin. The panels loaded by a flat-ended indenter showed the initial degradation due to core crushing and further degradation due to the onset of delamination in the compressive skin and continued core crushing, and the ultimate failure due to shear-out of the compressive skin. It was demonstrated that increasing the skin thickness of the panels loaded by a hemispherical indenter resulted in the increase in both the initial critical and ultimate failure loads and stiffness. However, with a flat-ended indenter, increasing the skin thickness has changed

damage mechanisms with delamination occurring after core crushing. Increasing core density was shown to have affected only the initial critical loads and the slopes of linear elastic region. Increasing the skin thickness and using the flat-ended indenter were much more effective in absorbing energy than increasing core density. A developed engineering model was capable of predicting the flexural rigidity of the sandwich panels for the linear elastic stage.

Such model was modified to estimate the flexural rigidity beyond the initial damage by degrading individually both the [D] matrix of composite skins and core on the basis of their effects on the damage mechanisms. Prediction of the model was useful for the estimation of energy absorption, as the initial critical loads were much less significant when compared to the magnitude of the ultimate failure loads.

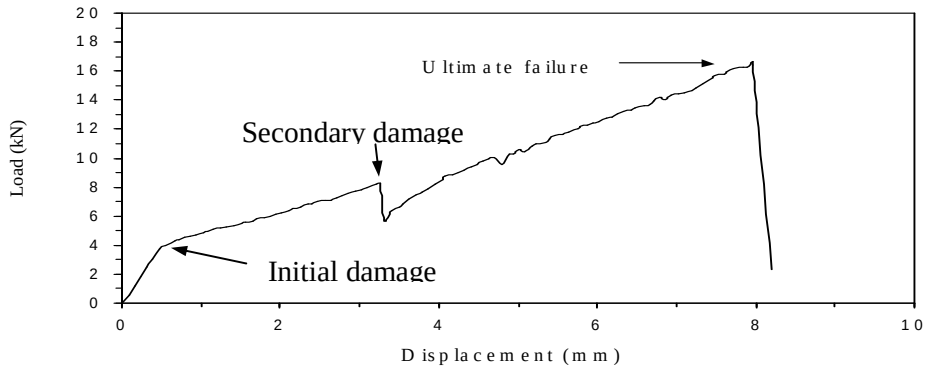

Figure 1 Load-displacement curve from a sandwich panel with 16-ply skins and 70-kg/m^3 aluminium honeycomb core quasi-statically loaded by a flat-ended indenter

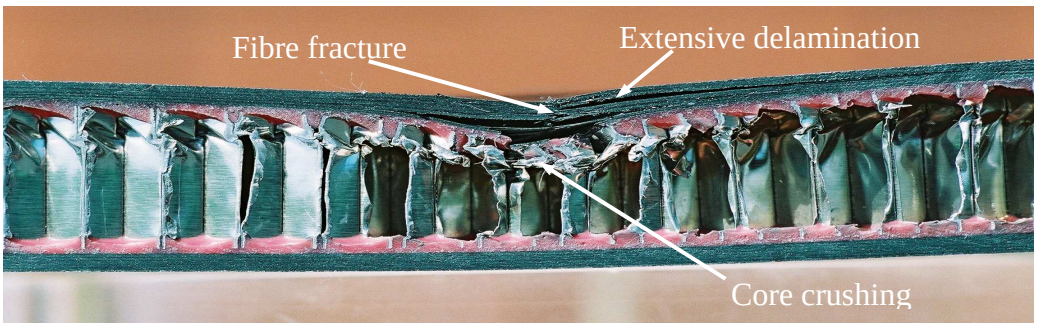

Figure 2 Cross-sectional view of a failed sandwich panel with 12-ply skins and 70-kg/m^3 aluminium honeycomb core quasi-statically loaded by a hemispherical-nosed indenter

IDENTIFICATION OF RESIDUAL STRAIN AND STRESS IN CROSS-PLY LAMINATE BY USING EMBEDDED FIBRE BRAGG SENSOR

S. Vacher[1], J. Molimard[1], H. Gagnaire[2], A. Vautrin[1]
[1]Mechanical and Materials Engineering Department, SMS Division, Ecole Nationale Supérieure des Mines de Saint-Étienne, F-42023 Saint-Étienne cedex 2, France
[2]Laboratoire Traitement du Signal et Instrumentation, Université Jean Monnet, UMR CNRS 5516, 42023 Saint-Étienne Cedex 2, France

This paper presents the experimental assessment of the residual strains occurring in a cross-ply laminate during the manufacturing process. The particular case of a $[0_6/90_3]_S$ carbon / RTM6 epoxy laminate manufactured by Resin Film Infusion process (RFI process) is considered. A Fibre Bragg Gratings (FBG) is embedded in the mid-plane of the 90 degrees dry unidirectional carbon layers NC2® in the mould before the resin infuses the preform, the direction of the FBG being that of the unidirectional carbon fibres of the ply [1].

After the resin infusion and curing at 180°C, the laminate cooling from the curing to the ambient temperature results in two reflected peaks (Fig.1) proving that accidental birefringence effect takes place, due to the shear strain within the optical fibre cross-section [1]. The directions of principal strain and principal refraction indices are along the width and the thickness of the laminate.

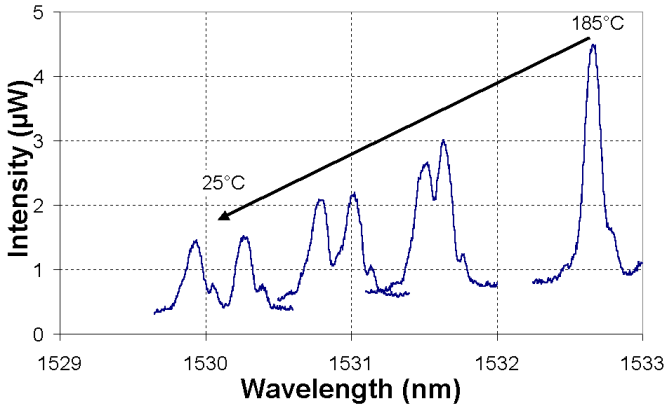

Figure 1: accidental birefringence effect during the cooling phase.

The horizontal displacement of each peak is a linear function of both the temperature and the stress within the fibre. However, it is easy to show that the difference leads to the following simple proportion between the displacement and the maximum shear strain within the fibre cross-section:

The relative displacement is due to the fact that ε_2 is different from ε_3, direction 1 is the fibre direction, 2 and 3 two orthogonal axes in the cross-section along width and thickness respectively, p_{11} and p_{12} are photoelastic constants.

Then we consider the problem of the determination of the principal strains (or stresses) along axes 1, 2 and 3 within the laminate. It is obvious we need a two-step approach, since the in-situ FBG is sensitive to the strains caused by the variation of temperature and by the presence of the optical fibre:

1.modelling of the local stresses and strains due the fibre when the medium is subjected to a given state of stress far from the fibre (i.e. at three times the fibre radius);
2.modelling the relationship between the local strains and the displacements of the two reflected Bragg peaks.

Step 1 is solved analytically by using the solution of Lekhnitskii [2], assuming the fibre cross-section to an elliptical inclusion surrounded by UD composite, and step 2 is simply based on the photomechanical relationship between peak displacement and strains. Finally, a set of two equations is obtained for three unknowns. Assuming that a laminate ply is under plane stress, the normal stress σ_3 *is* set to 0; therefore the system can be solved, leading to the residual laminate strains ε_3 *and* ε_3.

Comparison between the residual strains and stresses determined by FBG and by using the Classical Laminated Plate Theory (CLPT) leads to reasonable agreement (Table 1 below):

Strains	FBG	CLPT
ε_1	–529 με	–520 με
ε_2	–985 με	–857 με
ε_3	–5971 με	–5873 με

Table 1 : Comparison between strains derived from FNG measurements and CLPT in the case of $[0_6/90_3]_S$.

[1] S. Vacher, J. Molimard, H. Gagnaire, A. Vautrin, 'Monitoring of the RFI Process by Fibre Bragg Gratings, Euromech 453, December, 1 – 3 2003, Saint-Étienne, France.
[2] S. Lekhnitskii, 'Theory of Elasticity of an Anisotropic Body', Moscow, MIR Publishers, 1977.

SESSION 10 – FRACTURE

Chair: Dr. Pedro Camanho
DEMEGI, Portugal

Thursday 23 September
11.15-12.55

MEASUREMENT OF FRACTURE ENERGY FOR KINK-BAND GROWTH IN SANDWICH SPECIMENS

Wade C. Jackson
U.S. Army Research Laboratory, Hampton, VA 23681
James G. Ratcliffe
National Research Council, Hampton, VA 23681

Experimental observations [1] have shown that thin-skin honeycomb sandwich structure containing an open hole or a region of impact damage often fails by "kink band propagation" when loaded in compression. This type of failure is a three-stage process, beginning with the nucleation of kink bands (local micro-buckling in the applied load direction fibres) at the locations of maximum stress adjacent to the damaged region. The kink bands then propagate through the specimen in a stable manner, perpendicular to the applied load. Once the kink bands reach a critical length, growth becomes unstable, corresponding to catastrophic failure of the sandwich specimen.

An analytical technique was developed by Soutis and Fleck [2] to model similar failure mechanisms in open-hole solid laminates loaded under compression. A modified version of this method was developed for sandwich panels containing impact damage. First, the stress field surrounding the impact region is approximated to that developed around an open hole. The far field stress required to cause stable kink-band growth is calculated using the Whitney Nuismer average stress criterion [3]. The second part of the method uses a failure criterion based on linear elastic fracture mechanics (LEFM), where the kink band is modelled as a crack emanating from the open-hole edges. The onset of unstable kink-band growth (corresponding to failure of the specimen) is assumed to occur when the strain energy stored in the vicinity of the kink-band tip is equal to the through-thickness fracture toughness of the facesheet.

A specimen configuration, called the "compact compression" specimen, was designed to replicate the kink-band growth observed during compression tests. Energy required to grow the kink band is calculated from the test data using an area method. The configuration is similar to the compact tension specimen used in metals to obtain crack growth data but is loaded in compression. This paper outlines both the experimental and analytical investigations used in the development of the compact compression test specimen. Six different specimen configurations were manufactured to characterise the test method as illustrated in Figure 1. Five of the specimens used a V-type notch with varying notch dimensions. The sixth specimen used a parallel notch configuration. Finite element analyses of the specimen were undertaken to estimate the effect of kink-band length on strain energy release rate. Analyses were also run to study the influence of notch dimensions on the change of strain energy release rate with respect to kink-band length. The objectives of the analyses were to identify an optimum specimen design, yielding fracture toughness values independent of geometry (notch dimensions, kinkband length) and to determine the specimen configuration that provides stable kink-band growth. Initial testing has revealed that fracture energy is constant up to a specific kink-band length, after which the energy is seen to rise as indicated in Figure 2. Maximum kink-band lengths monitored during open-hole compression tests are observed to be in the range corresponding to a constant fracture energy. The fracture energy calculated using the area method is sensitive to kink-band length measurements. Consequently, several measurement techniques (visual observation, digital x-ray, and shadow moiré interferometry) were compared to determine the kink-band length.

Finally, a test procedure is outlined which enables synchronization of kink-band length monitoring with corresponding load displacement data.

This research was partially funded by Sikorsky Aircraft and the Aviation Applied Technology Directorate under technology investment agreement No. DAAH10-02-2-0001.

[1]. M. K. Cvitkovich and W. C. Jackson, *Compressive Failure Mechanisms in Composite Sandwich Structures*, Journal of the American Helicopter Society, Vol.44, 1999.
[2] C. Soutis and N. A. Fleck, *Static Compression Failure of Carbon Fibre T800/924C Composite Plate with a Single Hole*, Journal of Composite Materials, Vol. 24, 1990.
[3]. J. M. Whitney and R.J. Nuismer, *Stress Fracture criteria for Laminated Composites Containing Stress Concentrations*, Journal of Composite Materials, Vol.8, 1974.

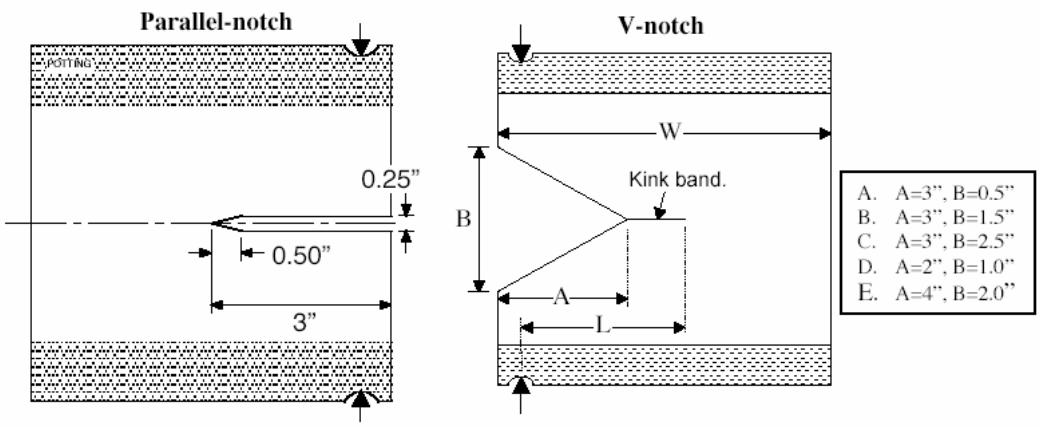

Figure 1. Specimen configurations used in compact compression test characterisation.

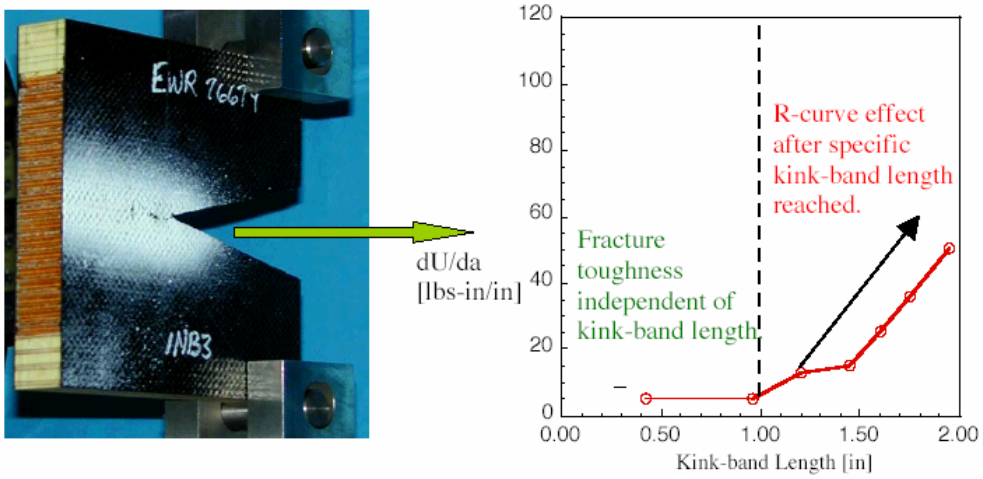

Figure 2. Fracture toughness increases after specific kink-band length reached.

AN EXPERIMENTAL STUDY OF THE FRACTURE BEHAVIOUR OF STITCHED RFI COMPOSITES – EVALUATION OF THE DAMAGE PROCESS ZONE TO CALIBRATE A STRAIN-SOFTENING MODEL

Jason Mitchell and Anoush Poursartip
Composites Group, Department of Metals and Materials Engineering
The University of British Columbia, Vancouver, Canada V6T 1Z4

This paper describes an experimental investigation of the effect of through-thickness stitching on the in-plane crack growth of Resin Film Infused (RFI) carbon fibre/epoxy laminates. Through-thickness reinforcement is a relatively recent approach to compensate for poor out-of-plane mechanical properties in laminated materials and also as a new method of joining laminated aerospace structures.

The effect of Kevlar® stitching on the fracture response of RFI laminates was successfully evaluated using an over-height compact tension (OCT) specimen. It had previously been proven that this small notched geometry allows for stable self-similar damage growth (including fibre failure) in composite laminates, under controlled loading conditions.

A detailed physical description of damage initiation and propagation in the *process zone*, (the area of discontinuous damage ahead of the notch tip) was obtained from measurements of surface displacement fields, as well as sectioning and deplying of the failed laminate. A typical set of results is shown in Figure 1. In essence, a crack propagates in a self-similar manner, with a process zone of about 10 mm in height and 5 mm in width. Within this zone the material is heavily damaged but still able to carry partial load. Behind this process

zone the material is fully separated, and ahead of the zone, the material is intact. The experimental results thus yield valuable information that can be used to calibrate a strain softening constitutive model suitable for implementation in a Finite Element Method model. In turn, such a model does a good job of predicting the observed behaviour.

The fracture response of these materials was largely unaffected by stitching, except results indicate that poor control of stitch tightness during manufacturing affects the type of damage evolved. When notched perpendicular to, but loaded parallel to the stitching, 'tight' stitching does not inhibit the natural tendency of these RFI materials to delaminate, resulting in crack blunting. However, 'loose' stitching results in a more brittle response – damage grows in a self-similar manner across the specimen width, and consists of heavy fibre breakage in plies oriented to the direction of load. Tested specimens with loose stitching also exhibit significantly less delamination.

Finally, the development and size of the process zone was examined by comparing the experimental data and specimen compliances generated from a simple finite element model.

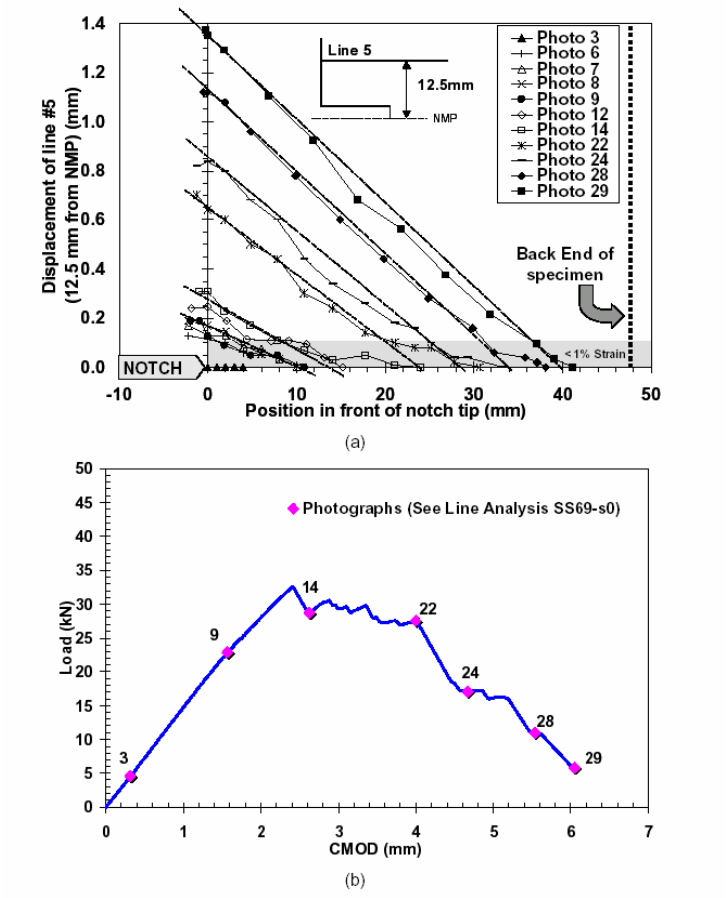

Figure 1 (a) Surface Line Analysis Plot and (b) Load-Crack Mouth Opening Displacement Plot of 5-stack stitched RFI 0° specimen (SS69-s0). Numbers on (b) correspond to profiles in (a). The dashed lines indicate how this line analysis was interpreted.

MODELLING DELAMINATION IN AN EXPLICIT FE CODE USING 3D DECOHESION ELEMENTS

Silvestre Pinho, Lorenzo Iannucci and Paul Robinson
Department of Aeronautics, South Kensington Campus, Imperial College London, SW7 2AZ, London, UK

Numerically modelling the failure of composite structures is important when designing with composite materials. In this work, interface elements are formulated and implemented into an explicit finite element code [1], to model delamination (Figure 1).

For composites, interlaminar cracks (delamination) are a common failure mode, thus requiring a detailed analysis. As delamination usually precedes final failure—rather than coinciding with it—modelling delamination cannot be restricted to predict initiation, but has also to simulate propagation, with the associated energy absorbed. A major factor that accounts for the difficulty in modelling propagation is the change in the geometry during crack growth, which usually cannot be directly modelled in commercial finite element software. For this reason, 'special' tools have been developed to model crack propagation in the last decade.

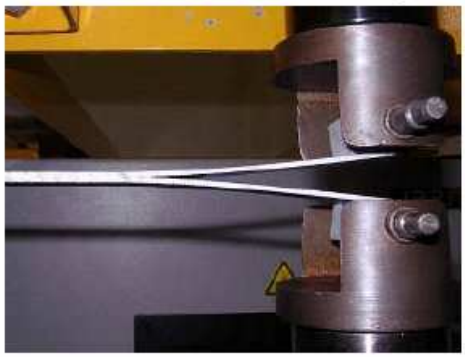

Figure 1: Mode I delamination (DCB specimen)

One such 'special' tool consists of the use of decohesion (or interface) elements. A particular advantage is that it is possible, with decohesion element formulations, to model mixed-mode delamination growth, without knowing in advance the mode ratio. For this reason, they have been chosen in this work to model delamination. The disadvantages of using decohesion elements are essentially related to the complexity added to the numerical models, the difficulty of convergence in implicit analysis, and the possible time-step reduction in explicit ones.

A new interface element with mixed-mode capabilities has been formulated and incorporated into an explicit finite element code to model delamination. For the interaction between mode I and mode II, a quadratic stress-based criterion is used for damage onset, while different energy-based criteria are implemented for propagation. This approach is based on previous works where a bilinear constitutive law (Figure 2) was used in an implicit code [2,3]. In this work, two different shapes for the constitutive law have been implemented and compared: a bilinear law (Figure 2) and a smooth curve law (third-order polynomial, Figure 3).

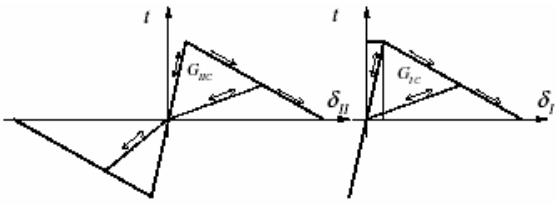

Figure 2: Bilinear constitutive law for the interface element

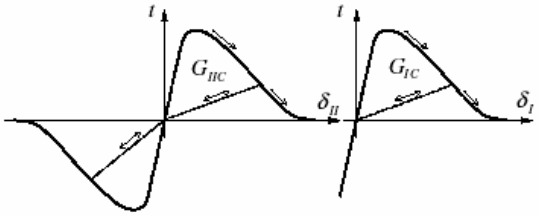

Figure 3: Curve constitutive law for the interface element (more stable)

The fracture toughness for the carbon-epoxy composite 913T300J has been determined for pure mode I, pure mode II and mixed-mode I and II. This experimental data (Figure 4) allowed the definition of an experimental parameter (a) to characterise the interaction between mode I and mode II, which is used in the mode I crack propagation (DCB test, Figures 5 and 6), mode II (4ENF test, Figures 7 and 8), and mixed-mode I and II (MMB test, Figures 9 and 10). Analytical and experimental data are shown to be in good agreement with the numerical predictions.

The use of interface elements for delamination modelling is proven to be reliable and useful. Further research on the modelling of other damage modes, and their possible interaction with the delamination process is underway and will be briefly discussed.

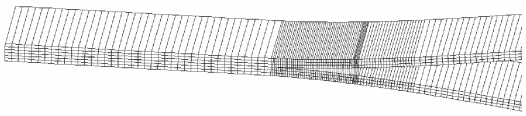

Figure 5: Deformed mesh of the DCB finite element model

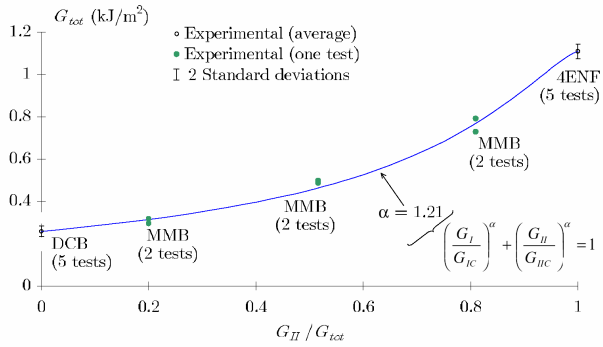

Figure 4: Experimental results for different mode ratios

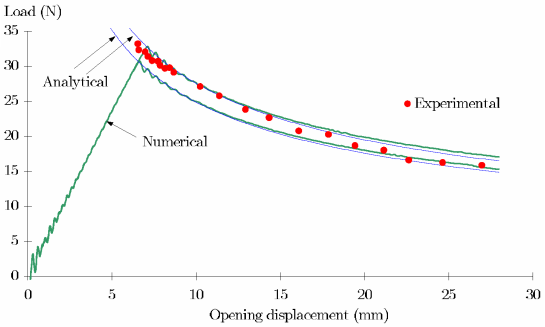

Figure 6: Numerical results for the DCB specimen (mode I delamination), compared to the corresponding numerical and experimental results

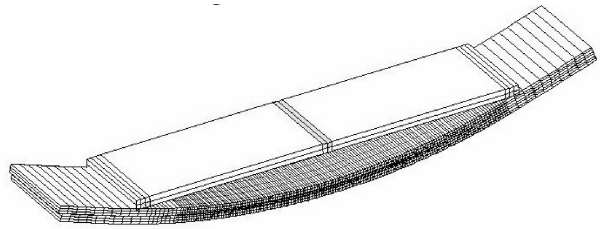

Figure 7: Deformed mesh of the 4ENF finite element model

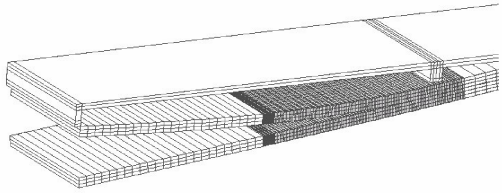

Figure 9: Deformed mesh of the MMB finite element model

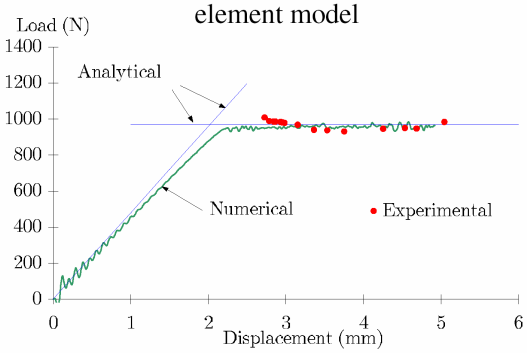

Figure 8: Numerical results for the 4ENF specimen (mode II delamination), compared to the corresponding numerical and experimental results

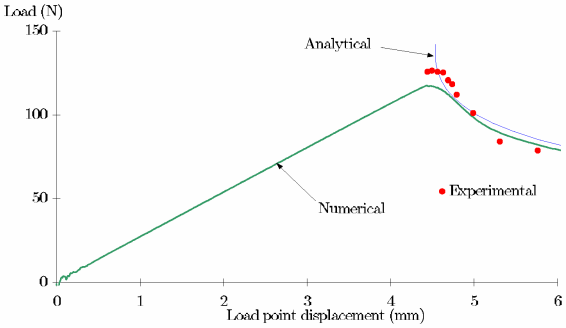

Figure 10: Numerical results for the MMB specimen (mixed-mode I and II delamination), compared to the corresponding numerical and experimental results

REFERENCES

[1] Livermore Software Technology Corporation, California, USA. LS-Dyna 970, 2003

[2] M F S F de Moura, J P Gonçalves, A T Marques, and P T de Castro. Modeling compression failure after low velocity impact on laminated composites using interface elements. Journal of Composite Materials, 31:1462-1479, 1997

[3] C G Dávila, P P Camanho, and M F de Moura. Mixed-mode decohesion elements for analyses of progressive delamination. In 42nd AIAA/ASME/ASCE/AHS/ASC Structures, Structural Dynamics, and Materials Conference, Seattle, 2001.

DEVELOPMENT AND EVALUATION OF SELF-REPAIRING CONCEPTS FOR COMPOSITE MATERIALS

Jody Pang, Ian Bond
Department of Aerospace Engineering, University of Bristol, Queen's Building,
University Walk, Bristol. BS8 1TR. UK

INTRODUCTION

Previous work [1] has shown significant restoration (~97%) of mechanical strength after damage in self-repair composite materials, as well as a demonstration of a new enhanced damage visualization method called the Ultra-violet Mapping Technique (UVMT). However, it is necessary to further investigate this new self-repair concept with respect to environmental changes, so a environmental degradation test is carried out. In addition, a quantitative test is conducted to optimize the reliability of the UVMT damage detection method.

EXPERIMENTAL APPROACH

UVMT can fulfil real-time damage detection and location simply and simultaneously. There has previously been claimed to be a lack of such simple technologies[4]. By means of pre-infiltrated fluorescent dye leaking out from the fractured hollow fibre, the internal damage area is vividly revealed under UV illumination.

The accuracy and repeatability of this new technique is now investigated. To this end, a conventional damage detection test (Ultrasonic C-scan) is used to compare and identify UVMT performance, by investigating the relationship between damage energy and the resulting dye visualization to assess its reliability for observing and measuring the damage area.

Previous workers [2,3] studied the effects of moisture on glass fibre reinforced composites, and note that polymer matrix composites are generally degraded by moisture absorption. It is thus likely that environmental degradation will occur with self-repair composite, due to using hollow glass fibre to contain the active components. Hollow shaped fibres suffer more serious environmental attack as more surface area is in contact with the environment than a solid glass fibre. The second aim of this study was therefore to investigate the environmental effect of self-repair composites with time, and to test the reliability of the new UVMT technique against ultrasonic C-scan test. Finally, the maximization of self-repair composites service life is considered.

Two groups of specimens (damaged and undamaged) were prepared for environmental testing, carried out at 6 and 9 weeks after being stored in a desiccator at room temperature condition. Damaged group specimens were immediately subjected to 1200N indentation damage after infiltration of repairing agent, then stored in a desiccator before a 4-point bending test. Undamaged group specimens were subjected to indentation 24 hours before the bending test, so that they would remain undamaged during the storage period.

In the UVMT test, specimens were subjected to five different indentation forces to create damage; 800N, 1000N, 1200N, 1400N and 1600N. The correlation of indentation energy with the size of damage area was being measured. Consequently, by identifying the size of damaged area of material, it was hoped to be possible to quantify the extent of material failure.

CONCLUSIONS

The results of the UVMT test show a promising relationship between damage energy and dye visualization. In the environmental study, flexural testing has shown in Figure 1 that the longer the curing time after damage is the better mechanical strength restoration of specimens from the damaged group, benefiting from the self-repair effect. However, undamaged group specimens seem to fail to self-repairing after being stored for 6 and 9 weeks before damage. This significant fact indicates that repairing agent might not be able to survive storage. It might be due to the viscosity and chemical nature of the repair agent changing during storage, such that specimens stored undamaged would be unable to perform repairing function. Weibull analysis is introduced to analyse the real effect on self-repair composites due to time change.

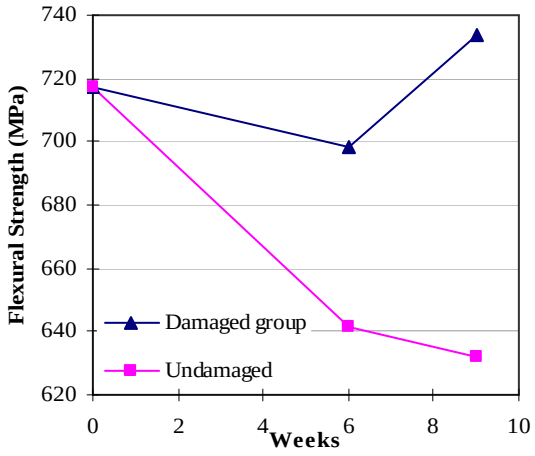

Figure 1 Environmental test results plot of the "damaged and undamaged groups" flexural strength after indentation against time.

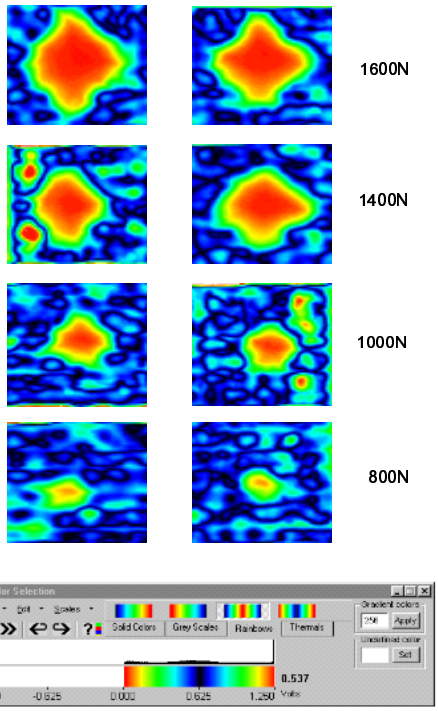

Figure 2 Defect maps of specimens under Ultrasonic C-scan test, subjected to 1600N, 1400N, 1000N and 800N impact damage.

References

1. J Pang, I Bond, "Bleeding Composites"-Damage Detection and Regeneration Using a Biomimetic Approach", *Composites*: A, 2003 (In press)
2. Y Momose, H Hira, H Miyabe, T Tanaka and S Bandoh, "Effect of Moisture on Glass Fibre Reinforced Composites", *44th International SAMPE Symposium*, May 23-27, 1999
3. M R Vanlandingham, R F Eduljee, J W Gillespie, JR , "Moisture Diffusion in Epoxy Systems", *Journal of Applied Polymer Science*, Vol. 71, 1999, pp. 787-798
4. I Sage, R Badcock, L Humberstone, N Geddes, M Kemp and G Bourhill. "Triboliminescent Damage Sensors", *Smart Mater. Struct*, **8** (1999), pp. 504-510

SESSION 11 – PROPERTIES

Chair: Dr. Jonas Neumeister
Royal Institute of Technology, Sweden

Thursday 23 September
14.00-16.05

MECHANICAL PROPERTIES BALANCE IN NOVEL Z-PINNED SANDWICH PANELS

A I Marasco, D D R Cartié and I K Partridge
Advanced Materials Department, Cranfield University, Cranfield, Bedford, MK430AL

The paper will present the test methods used and the first set of data gathered, concerning the balance of mechanical properties of X-Cor™ and K-Cor™ sandwich panels. The out-of-plane compression, in-plane shear and out-of-plane tension behaviour has been characterised for different core types. The same set of properties has been measured for Nomex and aluminium honeycomb sandwich panels, to provide suitable baseline comparisons. Fig. 1 is a photograph of a cured K-Cor™ panel with carbon fabric/epoxy skins.

Fig.1 K-Cor™ with carbon fabric facesheets

These novel composite structures are composed of composite skins separated by a layer of Rohacell foam into which carbon fibre Z-pins have been inserted at a specific angle to form a truss. For X-Cor™ the pins in the truss extend beyond each surface of the foam, for a so-called "reveal length", and enter into the surfacing prepreg plies. For K-Cor™ the pins again extend considerably beyond the foam surface but the (partially cured) pins are then folded back, flush with the foam surface prior to the adhesive bonding of the surface plies. Pre-cured composite or metallic skins can be used with K-Cor™ [1-3].

It is to be expected that the exact mechanical properties of the X/K-Cor™ products will be highly influenced by the Z-pin densities used. Changing the angle of the pins in the truss will also alter the balance between the shear and compression properties. To match typical honeycomb properties it has been found that a pin angle of 20 – 30 degrees represents a good compromise.

The presentation will include a wide range of experimental results and associated modelling, but for the purpose of this abstract we limit the description to the case of in-plane shear loading testing. Fig.2 shows examples of shear failed specimen of (a) X-Cor™ and (b) Nomex honeycomb panel respectively; the glue line indicates the connection to the steel loading plates.

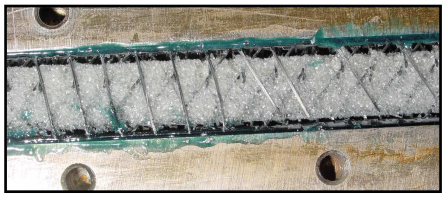

Fig.2a X-Cor™ specimen

Fig.2b Nomex specimen

Table 1 lists some of the materials tested in this study. The 'hollow' sample indicates that the foam surrounding the pins has been removed.

	Core properties					
	thickness[mm]	density[kgm^{-3}]	cell face side[mm]		stabiliser	
Nomex	12.7	64	3.18		Redux 322	
	thickness[mm]	density[kgm^{-3}]	pin Ø/fibre	pin angle θ	foam type	foam density [kgm^{-3}]
X-Cor type1	12.7	~64	0.51/ T300	22°	Rohacell	2
hollow X-Cor type1	12.7	~32	0.51/T300	22°		
X-Cor type2	12.7	~64	0.51/ T300	30°	Rohacell	2
K-Cor	12.7	~64	0.51/ T300	30°	Rohacell	2

Table 1 Core descriptions

These were all combined with carbon fabric/epoxy 6-ply skins, cured to a thickness of 0.75mm. The specimen length was 188 mm, width 50 mm and overall thickness 14.2 mm. The shear strengths and moduli of the different panels were determined by methods given in ASTM C 273, see table 2. The load is applied parallel to the sandwich in such a way that the line of action of the direct tensile force passes through the diagonally opposite corners of the sandwich, as shown in Fig. 3.

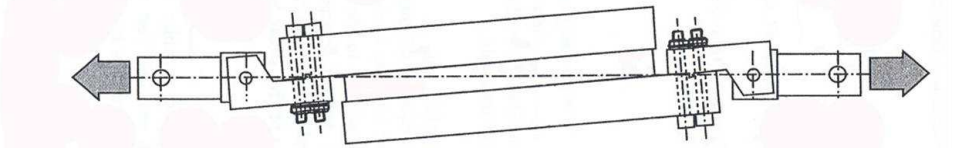

Fig. 3 Loading fixture schematic, [4]

	K-Cor (θ=30°)	X-Cor type1 (θ=22°)	hollow X-Cor type1 (θ=22°)	X-Cor type2 (θ=30°)	Nomex
max shear stress [MPa]	1.1±0.2	0.8±0.1	0.7±0.1	0.9±0.1	2.3±0.1
shear modulus G [MPa]	167±10	190±31	190±15	323±58	81±4

Table 2 Test results

It appears that in the X-Cor samples the presence of the foam enhances the shear strength by 10% whilst there is no significant effect on the modulus. Further analysis indicates that the key parameters during deformation of these sandwich structures are the pin rotation during shear and that this is strongly influenced by the physical constraint on the embedded pin end.

REFERENCES

[1] Partridge I K, Cartié D D R and Bonnington T, "Manufacture and performance of Z-pinned composites" Ch 3 in *Advanced Polymeric Materials: Structure-property relationships*, eds. S Advani and G Shonaike, CRC Press, April 2003

[2] Marasco A I, Cartié D D R and Partridge I K, "Mechanical behaviour of Z-pinned sandwich panels", Procs DFC7, University of Sheffield, 22-24 April 2003, UK

[3] Carstensen T, Cournoyer D, Kunkel E, Magee C, "X-Cor™ Advanced sandwich core material" SAMPE, Seattle WA, November 2001

[4] Zenkert D, "The handbook of sandwich construction", EMAS Publishing, 1997

FAILURE CRITERIA FOR PREDICTION OF TRANSVERSE MATRIX CRACKING IN COMPOSITES

Pedro P. Camanho
DEMEGI - Faculdade de Engenharia, Universidade do Porto, Portugal
Carlos G. Dávila
Analytical and Computational Methods Branch, NASA Langley Research Center, Hampton, VA 23681, U.S.A.

An accurate framework describing the material response caused by the evolving damage state is required for reliable structural integrity analyses of advanced composite structures. The greatest difficulty in the development of an accurate and computationally efficient numerical procedure to predict damage growth has to do with how to analyze the material micro-structural changes and how to relate those changes to the material response.

Several theories have been proposed for predicting failure of composites. While significant progress has been made in this area, there is currently no single theory that accurately predicts failure at all levels of analysis, for all loading conditions, and for all types of fiber reinforced polymer (FRP) laminates. While some failure theories have a physical basis, most theories represent attempts to provide mathematical expressions that give a best fit of the available experimental data in a form that is practical from a designer's point of view.

To the structural engineer, failure criteria must be applicable at the level of the lamina, the laminate, and the structural component. Failure at these levels is often the consequence of an accumulation of micro-level failure events. Therefore, it is also necessary to have an understanding of micro-level failure mechanisms in order to develop the proper failure theories.

The World Wide Failure Exercise (WWFE) conceived and conducted by Hinton and Soden[1-7] provides a good picture of the status of currently available theoretical methods for predicting material failure in fiber reinforced polymer composites. The recently published comparison of the predictions by the WWFE participants with experimental results indicates that even when analyzing simple laminates that have been studied extensively over the past 40 years, the predictions of most theories differ significantly from the experimental observations.[3]

The uncertainty in the prediction of initiation and progression of damage in composites has led to the undertaking of an effort to revisit existing failure theories and to develop new ones where necessary. The well-established failure criteria were revisited and their prediction capabilities were compared and their qualities were examined.

This paper describes part of a newly developed set of non-empirical criteria for predicting the different failure modes of unidirectional FRP laminates (LaRC03 Failure Criteria). All the calculations are at the lamina level with plane stress assumptions.

The proposed failure criterion for matrix failure under in-plane shear and transverse tension is based on Fracture Mechanics analyses of cracked plies. The proposed criterion can predict the increased strength of a ply when it is embedded in a laminate, and when its thickness decreases (in-situ effect).

Figure 1 shows the comparison between the predicted results and published experimental results[3] for AS4-55A carbon fiber reinforced composites. Other examples of failure envelopes for different materials under several load conditions will be presented.

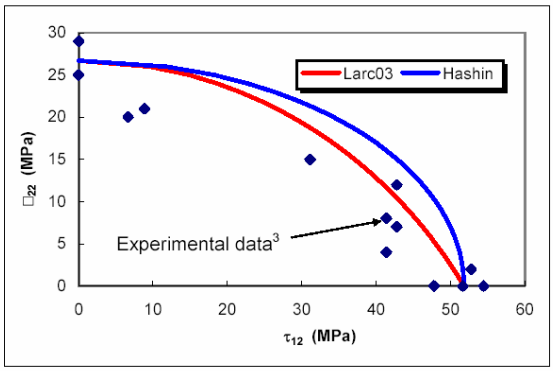

Figure 1- Comparison between LaRC03 failure criterion and published experimental data[3].

REFERENCES

1) Soden, P.D., Hinton, M.J., and Kaddour, A.S., "A Comparison of the Predictive Capabilities of Current Failure Theories for Composite Laminates," *Composites Science and Technology*, Vol. 58, No. 7, 1998, pp. 1225-1254.

2) Soden, P.D., Hinton, M.J., and Kaddour, A.S., "Biaxial Test Results for Strength and Deformation of a Range of E-Glass and Carbon Fibre Reinforced Composite Laminates: Failure Exercise Benchmark Data," *Composites Science and Technology*, Vol. 62, No. 12-13, 2002, pp. 1489-1514.

3) Hinton, M.J., Kaddour, A.S., and Soden, P.D., "A Comparison of the Predictive Capabilities of Current Failure Theories for Composite Laminates, Judged against Experimental Evidence," *Composites Science and Technology*, Vol. 62, No. 12-13, 2002, pp. 1725-1797.

4) Hinton, M.J., and Soden, P.D., "Predicting Failure in Composite Laminates: The Background to the Exercise," *Composites Science and Technology*, Vol. 58, No. 7, 1998, pp. 1001-1010.

5) Puck, A., and Schurmann, H., "Failure Analysis of FRP Laminates by Means of Physically Based Phenomenological Models," *Composites Science and Technology*, Vol. 58, No. 7, 1998, pp. 1045-1067.

6) Puck, A., and Schurmann, H., "Failure Analysis of FRP Laminates by Means of Physically Based Phenomenological Models," *Composites Science and Technology*, Vol. 62, No. 12-13, 2002, pp. 1633-1662.

7) Edge, E.C., "Stress-Based Grant-Sanders Method for Predicting Failure of Composite Laminates," *Composites Science and Technology*, Vol. 58, No. 7, 1998, pp. 1033-1041.

ANALYTICAL MODELS FOR ASSESSING ENVIRONMENTAL DEGRADATION OF UNIDIRECTIONAL AND CROSS-PLY LAMINATES

W R Broughton and M J Lodeiro
NPL Materials Centre, National Physical Laboratory
Teddington, Middlesex, TW11 0LW, UK

This paper presents an assessment of analytical and semi-empirical models that can be used for evaluating the elastic and strength properties of unidirectional and cross-ply (i.e. $[0°/90°]_{4S}$, $[0°_2/90°_2]_S$, $[0°_2/90°_4]_S$, $[0°_2/90°_6]_S$ and $[0°_2/90°_8]_S$) laminates exposed to hot/wet environments. A number of different approaches are considered. These include micromechanics, classical laminate analysis, shear-lag theory, non-dimensional temperature function, Kitagawa power-law and Arrhenius temperature dependence relationships. These different approaches have been used to determine the degree and rate of degradation of stiffness and strength properties of glass and carbon fibre-reinforced composite laminates under tensile, shear and flexure loading conditions. Consideration is given to synergistic or superimposed effects between temperature and moisture. The models are shown to be applicable to both glass and carbon fibre-reinforced composite laminates. The results of the study demonstrate that classical laminate analysis combined with micromechanics can be used to predict the elastic properties, and to a lesser degree strength properties of moisture conditioned unidirectional and cross-ply laminates (Tables 1 and 2). It also shows that simple empirical models, such as the power relationship given below (see also Figure 1):

$$\frac{P}{P_o} = \left(\frac{T_{gw} - T}{T_{gd} - T_o} \right)^n \qquad \textbf{(1)}$$

can also be used to determine matrix dominated tensile, shear and flexural properties of hot/wet aged unidirectional laminates as a function of temperature and moisture. **P** denotes a material property (e.g. transverse tensile strength) at the test temperature **T** (in K), $\mathbf{P_o}$ is the initial property value of the dry material measured at room or reference temperature $\mathbf{T_o}$ (296 K), and $\mathbf{T_g}$ is the glass transition temperature of the material (dry or conditioned).

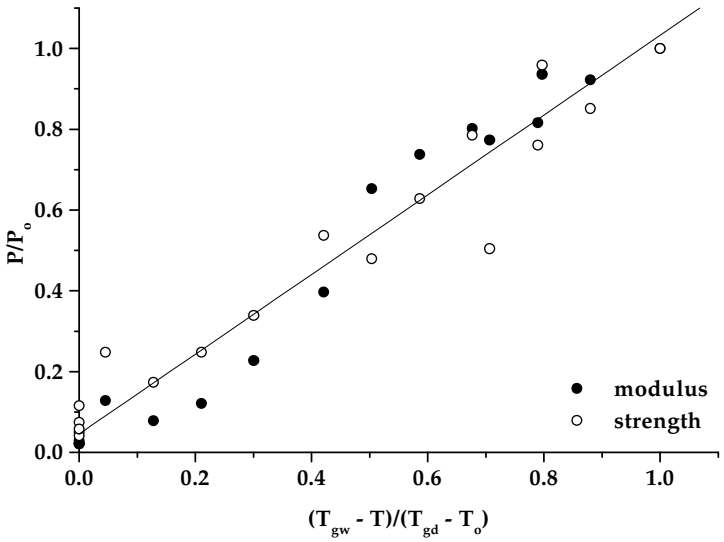

Figure 1: Transverse flexure properties of unidirectional E-glass/913.

Table 1: Measured and Predicted Tensile Properties for UD Composites
(Measured/Predicted)

Material	Tensile Strength (MPa)	Tensile Modulus (GPa)	Poisson's Ratio
E-glass/913 (dry)			
Longitudinal	1215 ± 20/1178	43.0 ± 0.9/36.6	0.30 ± 0.02/0.33
Transverse	73.1 ± 1.7/56.5	12.5 ± 0.2/10.7	0.094 ± 0.004/0.091
E-glass/F922 (dry)			
Longitudinal	1087 ± 29/1479	43.0 ± 0.9/46.0	0.31 ± 0.01/0.33
Transverse	58.6 ± 5.1/52.9	13.9 ± 1.2/15.4	0.098 ± 0.003/0.102
E-glass/F922 (wet)			
Longitudinal	797 ± 75/1475	37.2 ± 1.4/45.9	0.31 ± 0.01/0.33
Transverse	64.1 ± 6.2/36.5	14.3 ± 1.5/14.5	0.108 ± 0.007/0.096
T300/924 (dry)			
Longitudinal	1723 ± 89/2193	133 ± 2/136	0.34 ± 0.02/0.29
Transverse	92.7 ± 9.1/56.1	8.5 ± 0.2/8.7	0.020 ± 0.003/0.021
HTA/F922 (dry)			
Longitudinal	1684 ± 132/2016	126 ± 5/134	0.32 ± 0.02/0.34
Transverse	46.2 ± 9.1/53.0	9.9 ± 0.5/8.3	0.023 ± 0.003/0.020
HTA/F922 (wet)			
Longitudinal	1728 ± 132/2014	130 ± 4/134	0.33 ± 0.05/0.34
Transverse	48.6 ± 4.9/36.4	8.9 ± 0.7/7.9	0.022 ± 0.007/0.022

Table 2: Strength and Elastic Moduli of E-glass/F222 and HTA/F922 Laminates

Material	First Ply Failure Stress (MPa)		Ultimate Tensile Strength (MPa)	
	Measured	Predicted	Measured	Predicted
E-glass/F922 (dry)				
$[0_2/90_2]_S$	150	110	486	431
$[0_2/90_4]_S$	99	91	316	253
$[0_2/90_8]_S$	65	76	170	135
E-glass/F922 (wet)				
$[0_2/90_2]_S$	178	80	340	312
$[0_2/90_4]_S$	134	65	282	181
$[0_2/90_8]_S$	98	54	159	98
HTA/F922 (dry)				
$[0_2/90_2]_S$	360	455	814	972
$[0_2/90_4]_S$	135	322	516	649
$[0_2/90_6]_S$	149	255	407	484
HTA/F922 (wet)				
$[0_2/90_2]_S$	399	455	864	972
$[0_2/90_4]_S$	267	322	569	649
$[0_2/90_6]_S$	189	182	413	454

Table 2 (cont.): Strength and Elastic Moduli of E-glass/F222 and HTA/F922 Laminates

Material	Initial Modulus (GPa)		Final Modulus (GPa)	
	Measured	Predicted	Measured	Predicted
E-glass/F922 (dry)				
$[0_2/90_2]_S$	29.4	28.6	23.5	22.1
$[0_2/90_4]_S$	26.2	23.1	16.1	14.5
$[0_2/90_8]_S$	20.2	16.8	9.4	8.5
E-glass/F922 (wet)				
$[0_2/90_2]_S$	25.3	28.1	21.4	22.0
$[0_2/90_4]_S$	26.8	22.5	16.7	14.5
$[0_2/90_8]_S$	19.2	16.1	9.5	8.5
HTA/F922 (dry)				
$[0_2/90_2]_S$	64.4	70.2	60.7	66.3
$[0_2/90_4]_S$	46.7	49.8	41.9	44.4
$[0_2/90_6]_S$	37.6	39.1	31.8	32.3
HTA/F922 (wet)				
$[0_2/90_2]_S$	66.4	70.0	61.0	66.2
$[0_2/90_4]_S$	47.0	49.8	42.1	44.4
$[0_2/90_6]_S$	38.1	38.9	31.7	31.8
Material	**Initial Poisson's Ratio**		**Final Poisson's Ratio**	
	Measured	**Predicted**	**Measured**	**Predicted**
E-glass/F922 (dry)				
$[0_2/90_2]_S$	0.159	0.162	0.084	0.084
$[0_2/90_4]_S$	0.134	0.138	0.067	0.047
$[0_2/90_8]_S$	0.128	0.122	0.056	0.027
E-glass/F922 (wet)				
$[0_2/90_2]_S$	0.155	0.154	0.105	0.080
$[0_2/90_4]_S$	0.133	0.130	0.060	0.044
$[0_2/90_8]_S$	0.119	0.115	0.038	0.026
HTA/F922 (dry)				
$[0_2/90_2]_S$	0.042	0.040	0.040	0.019
$[0_2/90_4]_S$	0.042	0.031	0.027	0.010
$[0_2/90_6]_S$	0.041	0.028	0.022	0.007

FIBRE ORIENTATION MEASUREMENTS IN COMPOSITE MATERIALS

R. Blanc1Blanc, J.P. da Costa1da Costa, Ch. Germain1Germain, P. Baylou1Baylou, M. Cataldi2Cataldi
1Equipe Signal et Image, LAP - UMR 5131 CNRS - ENSEIRB, ENITAB, Univ. Bordeaux 1
1 Av. du Docteur Schweitzer, 33400 Talence - France
2Snecma Propulsion Solide, Groupe Snecma, Les cinq Chemins 33185 Le Haitian – France

In aerospace industries, carbon/carbon and carbon/ceramic composites (C/C and SiC) are well known for their high temperature resistance and high strength, associated with light weight. This kind of material is usually composed of layers of weave cloth, stacked and needled together. Each thread is composed of carbon fibers. The layers are weaved in the X and Y directions, and the needle reinforcement is carried out in the Z direction. The resulting fibrous structure is then densified with a carbon or ceramic matrix. Since the physical properties of such materials are strongly dependent on the needling operation efficiency, their characterization requires a reliable estimation of the fibre orientation.

Mlekusch describes a method for fibre orientation measurement in [1]. This method applies to circular cross-section fibres and is based on image analysis of a single polished section of the material. Miekusch proposes to use an oblique section. In such a plane, each cylindrical fibre appears as an ellipse which parameters depend on

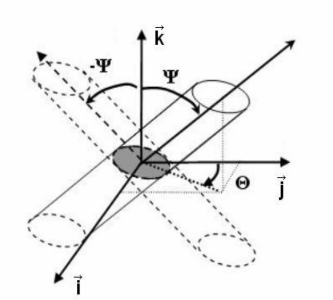

Figure 1: illustration of orientation ambiguity

the fibre orientation. Unfortunately, two fibres symmetric regarding the sectioning plane produce the same ellipse (Fig. 1). In order to solve such an ambiguity, some authors [2] [3] suggest to use the confocal microscopy. This particular technique allows optical sectioning of a material, so that fibres can be followed through the thickness, providing full orientation estimation. Nevertheless, this comes at the cost of expensive equipment and much more sample preparation.

In this paper, we propose a new approach for the unequivocal measurement of the orientation of the fibres in composite materials. Our approach operates with classical optical reflection microscope images of a single polished material section. We define an optimal section for fibre orientation measurement and propose a new segmentation algorithm which allows correcting the orientation ambiguity.

Optimal section plan

We choose the sectioning plane so that the three directions X, Y and Z, are cut with the same angle (Fig. 2a). Thus, for each direction, fibre inclination is about 35°. As the reliability of the ellipse parameters estimation depends on the ellipse elongation, this specific oblique section guarantees that the accuracy will be equivalent for each direction. Moreover, we have shown that the measurement of the surface ratio on such a section allows for volume fibre ratio estimation.

Threads segmentation

As a first step, the elliptic parameters of each fibre, orientation θ and inclination ψ (Fig. 1), are estimated. For each fibre, parameters (ψ,θ) are placed on a polar graph. The three directions X, Y and Z, clearly appear on this graph as lighter regions (Fig. 2b). Theses regions are segmented. Their mean orientations x, y and z are computed thanks to a Principal Component Analysis (PCA) of each region. As shown on Fig. 1, these mean orientations are ambiguous. Our a priori knowledge on the X, Y and Z directions allows us to solve this ambiguity. The fibres which orientation is close to the mean values x, y and z are then directly labelled to the corresponding direction.

The second step consists in the labelling of the remaining fibres. We use the fact that fibres are bundled in threads. All the fibres in a thread are necessarily in the same direction. Thus, setting a label to the threads will lead to fibre labelling. To identify the threads, we start from the fibres labelled during the first step, and then, we spread iteratively the labels to the neighbouring fibres.

Results and conclusion

Our approach leads to a reliable labelling of the fibres. Fig.3 shows an image where X fibres are red, Y fibres are green and Z fibres are blue. The layered structure of the material clearly appears. The resulting needled fibres ratio has been confirmed by other experiments. More results and details on our approach will be presented in the final paper.

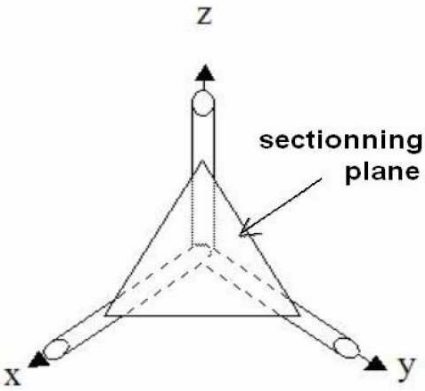

Figure 2a: definition of the sectioning plane

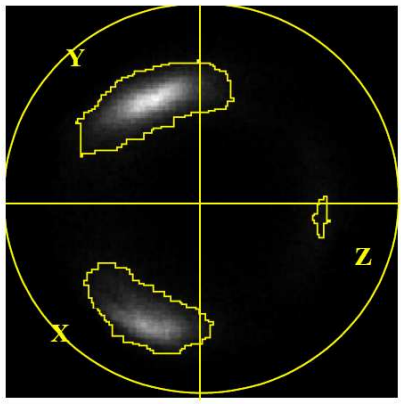

Figure 2b: polar graph, main directions

…

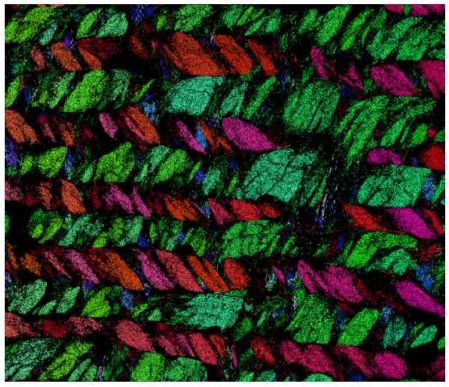

Figure 3: Labelling results

References

[1] Miekusch B. Fibre orientation in short-fibre-reinforced thermoplastics II. Quantitative measurements by image analysis. Composites Science and Technology 1999; 59-547.

[2] Eberhardt C, Clarke A. Fibre-orientation measurements in short-glass-fibre composites. Part I: automated, high-angular-resolution measurement by confocal microscopy. Composites Science and Technology 2001; 61-1389.

[3] Lee KS, Lee SW, Youn JR. Kang TJ, Chung K. Confocal Microscopy Measurement of the Fiber Orientation in Short Fiber Reinforced Plastics. Fibers and Polymers 2001, Vol.2, No.l; 41-50.

MODELLING THE THERMOELASTIC PROPERTIES OF SHORT FIBRE COMPOSITES WITH ANISOTROPIC PHASES

P.J.Hine*, C.D.Price*, A.M.Cunha#, I.M.Ward*
* - IRC in Polymer Science and Engineering, University of Leeds, Leeds, LS2 9JT, UK
# Department of Polymer Engineering, Universidade Do Minho, Campus Azurem, 4800-058, Guimaraes, Portugal.

In a number of recent joint papers with the group of Andrei Gusev at ETH Zurich, we have combined their finite element approach (PALMYRA) with a mixture of structural characterisation (using image analysis) and mechanical measurements to formulate the best analytical route for predicting the thermoelastic properties of short fibre composites based on isotropic matrices [1-3]. For the analytical route, the prediction of the properties of a misoriented reinforced material can be broken into two components: firstly the prediction of the properties of the fully aligned 'unit' and then including the effects of misorientation using tensor averaging. The recent research has confirmed the following points when the matrix is isotropic (the fibre can be either isotropic or anisotropic):

- The best model for the prediction of the unit properties is that based on the original ideas of Eshelby and Mori and Tanaka as modified by Tandon and Weng [4] for isotropic phases and as reported by Qui and Weng [5] for anisotropic fibre reinforcement.
- The best approach for predicting the thermal expansion properties of the unit uses the explicit treatment of Levin [6] which is identical to that of Christensen [7] and Rosen and Hashin [8].
- If the fibres are discontinuous the best measure is the number average fibre length [9].
- The best approach for predicting the properties of the misaligned composite is to use the tensor averaging approach [10,11] and a constant strain prediction [3].

While the modelling of short fibre reinforced composites with isotropic phases has been extensively researched and reported, there is much less in the literature regarding modelling procedures when either or both of the phases are anisotropic. The purpose of this paper is to describe the validation of a modelling route for predicting the thermoelastic properties of a short fibre composite where both phases are anisotropic, that is a liquid crystalline polymer (LCP) reinforced with carbon fibres. Injection moulded dumbbell samples were produced at The University of Minho, in three materials of different combinations of isotropy: carbon fibre filled nylon (anisotropic fibre and isotropic matrix), glass fibre filled LCP (isotropic fibre and anisotropic matrix) and carbon

fibre filled LCP (both phases anisotropic). In addition to the filled materials, samples were also produced from the pure matrix materials in order to determine the appropriate matrix properties for the modelling.

To provide the greatest test of the modelling procedure, four different measures of the thermoelastic properties of the central cylindrical section of the injection moulded composite dumbbells were measured: the longitudinal modulus, E_{11}: the transverse modulus E_{22}: the longitudinal thermal expansion α_1 and the transverse thermal expansion α_2 (the 1 direction is the main axis of the central portion of the dumbbell). In addition, the fibre orientation distribution was also measured in the central dumbbell section using image analysis techniques developed at Leeds. The orientation was measured to be transversely isotropic so it could be specified by only 2 orientation parameters, $\langle\cos^2\theta\rangle$ and $\langle\cos^4\theta\rangle$, where θ is the angle a fibre makes with the dumbbell (1) axis. For modelling the LCP matrix materials, an anisotropic form of the Eshelby matrix tensor was determined from the work of Mura [12].

a) ***Carbon fibre filled aromatic Nylon***:

Phase data (E and G in GPa, α K^{-1}.)				Carbon/Nylon	
				Theory	Measured
Carbon Fibre	E_{11}	230	E_{11}	21.8	23.9
	E_{22}	14	E_{22}	4.02	3.6
	ν_{12}	0.26			
	ν_{23}	0.38	α_1	7.2e-6	5.5e-6
	G_{12}	17.5	α_2	67e-6	60e-6
	α_1	-4e-7			
	α_2	26e-6			
Nylon	E	2			
	ν	0.4	$\langle\cos^2\theta\rangle$	0.856	
	α	70e-6	$\langle\cos^4\theta\rangle$	0.830	
Volume fraction				0.21	
Aspect ratio				25	

This composite material was used to check the modelling scheme described above for an isotropic matrix. The challenge with modelling when using carbon fibres is obtaining the values of all the elastic constants. The values here are our best estimates from our previous work and the literature.
Within this constraint the agreement between theoretical prediction and measurements is seen to be good.

b) ***Glass and carbon fibre filled LCP***

Phase data (E and G in GPa, α K^{-1}.)				Glass/LCP		Carbon/LCP	
				Composite	Measured	Composite	Measured
LCP matrix	E_{11}	25.6	E_{11}	29.1	25.6	51.7	43.2
	E_{22}	1.45	E_{22}	2.86	1.95	2.54	2.45
	ν_{12}	0.48					
	ν_{23}	0.71	α_1	-1.2e-6	-0.43	-5e-6	-1e-6
	G_{12}	1.13	α_2	55e-6	60e-6	58e-6	49e-6
	α_1	-5e-6					
	α_2	80e-6					
Glass fibre	E	72.5					
	ν	0.2	$\langle\cos^2\theta\rangle$	0.904		0.929	
	α	5e-6	$\langle\cos^4\theta\rangle$	0.865		0.87	
Volume fraction				0.19		0.24	
Aspect ratio				25		25	

For the LCP matrix composites, the agreement between experiment and theory is still good but not as good as when the matrix is isotropic. The weak-point in the proposed modelling scheme is the tensor averaging component, where the assumption has to be made that the fibre and matrix have the same orientation: it is likely

that the LCP matrix has a different orientation to the fibres. Further modelling work is in progress to allow the two phases to have different orientations.

REFERENCES

1. Gusev, A. A.; Lusti, H. R.; Hine, P. J. Advanced Engineering Materials 2002, 4, 927-931.
2. Gusev, A.; Heggli, M.; Lusti, H. R.; Hine, P. J. Advanced Engineering Materials 2002, 4, 931-933.
3. Hine, P. J.; Lusti, H. R.; Gusev A. Composites Science and Technology 2004, in press,
4. Tandon, G. P.; Weng, G. J. Polymer Composites 1984, 5, 327-333.
5. Qiu, Y. P.; Weng, G. J. International Journal of Engineering Science 1990, 28, 1121-1137.
6. Levin, V. M. Mech. Tverd. tela 1968, 88, 25.
7. Christensen, R. M., Mechanics of Composites Materials. 1991, Malabar FL: Kreiger Publishing Company.
8. Rosen, B. W.; Hashin, Z. International Journal of Engineering Science 1970, 8, 157-173.
9. Hine, P. J.; Lusti, H. R.; Gusev, A. A. Composites Science and Technology 2002, 62, 1445-1453.
10. Brody, H.; Ward, I. M. Polymer Engineering and Science 1971, 11, 139-151.
11. Camacho, C. W.; Tucker III, C. L. Polymer Composites 1990, 11, 229-239.
12. Mura, T., Mechanics of Elastic and Inelastic Solids. 1982, The Hague: Nijhoff.

AUTHOR INDEX

A

Abramovich, H 14
Adda-Bedia, EA 11
Ahzi, S 82
Akkerman, R 24
Allix, O 106
Alshaaer, M 65
Amara, KH 11
Aoyama, E 89
Avanzini, A 55
Avril, S 100, 104, 155

B

Bahlouli, N 82
Balandraud, X 70
Banks, WM 54
Baptiste, D 128
Barnes, RA 163
Baruffaldi, G 134
Baylou, P 42, 181
Ben, G 130
Berger, R 149
Bergsma, OK 84
Bersee, HEN 84
Biermann, H 23
Blanc, R 181
Bond, I 60, 173
Borbély, A 23
Bordreuil, C 73
Botsis, J 46, 145
Bouquet, PJP 98
Bourchak, M 60
Breen, C 38
Broughton, WR 179

C

Camanho, PP 78, 177
Cantor, B 107
Cardon, H 98
Cartié, DDR 176
Casari, P 142, 150
Cataldi, M 42, 181
Chalal, H 104
Chang, SH 57
Chang, SW 112
Chapeleau, X 150
Chau, N 17
Cheon, SS 57
Collombet, F 159
Collrep, J 149
Colpo, F 46
Cook, J 18
Costa, J 78
Cugnoni, J 85
Cunha, AM 124, 183
Cuypers, H 65

D

da Costa, JP 42, 181
David-West, OS 54
Davies, P 36, 142
Dávila, CG 177
Dávila. CG 78
de Bolster, E 65
Donadon, MV 13
Donzella, G 55
Drobez, H 126
Dulieu-Barton, JM 72
Dunne, FPE 107
Durand, B 126

E

Earl, JS 72
Ersoy, N 143

F

Falzon, BG 13
Farrow, I 60
Feissel, P 106
Ferguson, R 2, 151
Fernando, GF 163
Fert, M 115
Fitoussi, J 128
Fouinneteau, M 135
Fukuda, H 44

G

Gagel, A 60
Gagnaire, H 165
Galvanetto, U 48
Garstka, T 143
Germain, C 42
Germain, Ch 181
Gmür, T 85, 145
Gower, MRL 7
Grant, PS 107
Grédiac, M 70, 155
Green, B 33
Grunevald, YH 159
Guild, F 38

H

Hallett, SJ 161
Hallett, SR 30, 33
Hamaguchi, Y 90, 130
Han, GW 57, 94
Hildb, F 156
Hill, M 164
Hine, PJ 124, 183
Hirogaki, T 89
Hisson, C 82
Hitchings, D 115
Hochard, C 73
Hodgkinson, JM 13
Hookham, N 164
Horikawa, S 44
Humbert, L 46

I

Iannucci, L 13, 171

Iarve, E 34
Ishikawa, T 44, 130
Iwahori, Y 44

J

Jackson, WC 168
Jacobsen, TK 31
Jacquemin, F 142
Jang, TS 57
Järneteg, A 45
Jendli, Z 128
Jones, FR 99
Juračka, J 19

K

Kashtalyan, M 15
Kataua, T 89
Kato, T 130
Katoh, H 90
Kawai, M 63, 116
Kenesei, P 23
Khan, B 30
Kilroy, J 122
Kim, R 34
Kosmidou, ThV 55
Krakovskyb, I 52
Krishnamurthy, R 132
Kruijer, MP 24

L

L'Hostis, G 126
Lahellec, N 73
Lamona, J 156
Lange, D 60
Langer, C 121
Laurent, F 126
Lawlora, VP 4
Lawrence Wu, CM 57, 94
le Riche, R 101
Leduc, D 150
Lee, J 22
Leng, JS 163
Lew, TL 129
Lodeiro, MJ 179
Lomov, SV 12, 136
Lurie, SA 93

M

M'Guil, S 82
Makarov, G 82
Malhotra, SK 132
Marasco, AI 176
Masuko, Y 116
Mathias, JD 70
Mays, GC 163
Mazerolle, F 73
Mazzù, A 55
McCarthy, CT 4
McCarthy, MA 4
McDonnell, P 122
Meftah, SA 11
Melin, LN 113
Meraghini, F 104, 128
Meyer, G 126
Mitchell,J 169
Molimard, J 101, 165
Mollenhauer, D 34, 88
Mondragon, I 87
Moraveca, F 52
Mosselmans, G 65
Moulart, R 100
Mujika, F 87
Mulle, M 159

N

Nash, DH 54
Nedwell, P 119
Neumeister, JM 37, 113
Nicoletto, G 134, 148
Nino, GF 84
Nordin, LO 109

O

O'Brádaigh, C 122
Ogin, SL 80
Ozolinsh, O 14

P

Padhi, GS 4
Pang, J 173
Papadakis, N 26
Papanicolaou, GC 55
Partridge, IK 176
Patterson, EA 99
Pavier, M 38
Peng, HX 17, 107
Perez Ciurezu, DA 138
Périé, JN 159
Pettersson, KB 37
Phan, M-H 17
Pickett, AK 135
Pierron, F 100, 104, 155
Pinho, S 171
Potluri, P 138
Potter, K 30, 50, 121, 143
Poursartip, A 169
Price, CD 124, 183
Puyo-Paina, M 156

R

Rácz, Zs 79
Ramkumar, J 132
Ramos Gutiérrez, C 42
Ratcliffe, JG 168
Reynolds, N 26
Rikards, R 14
Riva, E 134, 148
Robinson, P 48, 115, 171
Rooney, NJ 153
Ruchevskis, S 14

S

Sagawa, T 116

Scarpa, F 129
Schorderet, A 85
Schulte, K 60
Setchell, C 50
Shenoi, RA 82
Shikata, N 130
Shimokawa, T 90
Simon, SA 99
Simon, ZL 79
Sims, GD 7
Skukis, E 14
Smith, PA 80
Sookay, NK 10
Sørensen, BF 31
Sorensen, L 145
Soutis, C 15, 22
Splíchal, J 19
Stanley, WF 4
Stoilova, T 12
Sugimura, K 89
Sun, CT 142
Surrel, Y 70, 155

T

Taniguchi, T 63
Theodosiou, TC 55
Thévenet, P 106
Tounsi, A 11
Toussaint, E 155
Trarieux, B 159
Truong Chi, T 136
Tuchkova, NP 93
Turon, A 78
Turvey, GJ 6
Tyson, J 88

U

Ueda, A 90
Unnþórsson, R 158

V

Vacher, S 165
Varna, J 109
Vas, LM 79
Vautrin, A 101, 165
Verijenko, VE 10
Verpoest, I 12, 136
Vettori, M 136, 148
von Klemperer, CJ 10
Vrellos, N 80

W

Wang, W 82
Ward, IM 124, 183
Warnet, L 24
Wastiels, J 65
Williamson, C 18
Winter, D 163
Wisnom, MR 17, 30, 33, 107, 143
Worden, K 129
Wu, ZJ 119

X

Xylouri, M 119

Y

Yagura, Y 89
Yamamoto, M 44
Young, RJ 99
Young, TM 153
Yu, SC 17

Z

Zacchè, V 55
Zhang, Y 6
Zhao, FM 99
Zhou, G 164
Zubov, VI 93